ANALYSIS OF CHROMOSOME CONDENSATION IN *SACCHAROMYCES CEREVISIAE*

Claudio D'Ambrosio

Thesis presented for the degree of Doctor of Philosophy to
University College London

2008-02-10

Chromosome Segregation Laboratory
Cancer Research UK London Research Institute
44 Lincoln's Inn Fields
London WC2A 3PX

ProQuest LLC
789 East Eisenhower Parkway
P.O. Box 1346
Ann Arbor, MI 48106-1346

Performing high quality science and art is inspirational; preserving a planet on which we can keep performing science and art is highly desirable

Claudio D'Ambrosio

This thesis is dedicated to Claire

Publications arising from this thesis

Identification of *cis*-acting sites for condensin loading onto budding yeast chromosomes

Claudio D'Ambrosio, Christine Schmidt, Yuki Katou, Gavin Kelly, Takehiko Itoh, Katsuhiko Shirahige, and Frank Uhlmann. *Genes and Development* (under review)

Condensin-dependent decatenation determines late segregation of the budding yeast rDNA locus

Claudio D'Ambrosio, Gavin Kelly, Takehiko Itoh, Katsuhiko Shirahige, and Frank Uhlmann. *Current Biology* (under review)

ABSTRACT

Eukaryotic chromosomes reach their stable rod-shaped appearance in mitosis in a reaction dependent on the evolutionarily conserved condensin complex. It is currently unknown how and where condensin associates with chromosomes. Here, we analyse condensin binding to budding yeast chromosomes by immunoprecipitation followed by hybridization on high resolution oligonucleotide tiling arrays. We observe that condensin binding sites coincide with those of the RNA polymerase III transcription factor TFIIIC and the loading factor Scc2/4 of the related cohesin complex. Both Tf3c and Scc2/4 facilitate condensin loading onto chromosomes. An isolated ectopic B box motif is sufficient to prime formation of a condensin binding site. While cohesin translocates away from these loading sites, condensin persists there. This defines the loading sites of cohesin and condensin and explains how an alternating pattern of these complexes along chromosomes is established. The findings have important implications for the fields of chromosome segregegation and nuclear structure in interphase and mitosis. The identification of SMC loading sites will allow targeted probing of eukaryotic chromosomes.

Beside condensation, mitotic chromosome segregation also depends on the chromosomal condensin complex. Without condensin, sister chromatids fail to resolve causing anaphase bridges and chromosome breakage. How condensin promotes sister chromatid resolution is unknown. We have used the budding yeast rDNA as a model locus, whose segregation depends on condensin activity during anaphase. We show that anaphase bridges in a condensin mutant are resolved by ectopic expression of a foreign (*Chlorella* virus) but not endogenous yeast topoisomerase II (topo II). This suggests that catenation prevents sister rDNA segregation, and that yeast topo II is ineffective in decatenating the rDNA in the absence of condensin. We furthermore find that expression of *Chlorella* virus topo II in wild type cells advances the normally late segregation timing of the rDNA locus. This suggests catenation is a mean for the cell to provide rDNA cohesion up to late anaphase, when condensin promotes decatenation. This provides the first direct evidence of condensin's role in the disengagement of topologically connected sister chromatids.

Acknowledgements

There are a lot of people to thank. First, I want to say thanks to Frank, my supervisor. With his inspiring approaches to science had to teach me a lot; especially I think here with Frank I learnt how to always strive for looking at a wider picture. I will try to bring this with me. And I am very grateful to have had the chance to work on such cutting edge scientific questions with high-quality tools.

Before coming back to the other professional inputs, my greatest gratefulness goes to Claire who has been always supporting me since the first time we met, in life as in work, with plenty of love and patience. I could not have lived these years comparably happy if you were not with me.
Thank you so much.

Thanks to all the people in the lab. Ethel has been very important for me in this experience- For several reasons. Thanks to Armellefor her close help in the first months in the lab. Thanks to everybody in the lab as well: John, Chris, Celine and to all of you present and past members of the lab for being such good colleagues....and friends.
I am sure with a lot of you our friendship will last for very, very long time.

There would be so many names I should mention that it will require another chapter.
Thanks to all the ones who shared with me a piece of life within and off these walls.

Lastly, I am grateful to my parents, always so "invasively" supportive in these years despite we have been living a bit more far away from each other.

Table of Contents

Table of Figures

Abbreviations

ARS (Autonomous Replicating Origins)

ATP, adenosine triphosphate

BSA, bovine serum albumin

bp, base pairs

CAR, cohesin associated sites

CDK, cyclin dependent kinases

CIP, calf intestinal phosphatase

ChIP, chromatin immunoprecipitation

DAPI, 4', 6-diaminidino-2-phenylindole

dNTP, deoxyribonucleic acid

DSB, double strand break

DNA, deoxyribonucleic acid

ssDNA, single stranded DNA

dsDNA, double stranded DNA

DNAse, deoxyribonuclease

DTT, dithiothreitol

ECL, enhanced chemiluminescence

EM, electron microscopy

FACS, fluorescence activated cell sorting

FRAP, fluorescence recovery after photobleaching

G1, G2, growth G1, growth G2

g, gram

GAL1, galactose inducible promoter 1

GFP, green fluorescent protein

HA, hemagglutinin

HEPES, 4-(2-hydroxyethyl)-1-pipeazineethansulfonic acid

HU, hydroxyurea

IP, immunoprecipitation

l, litre

ml, millilitre

MAT, mating type

min, minute

NEBD, nuclear envelope breakdown

NOC, nocodazole

OD, optical density

ORF, open reading frame

PEG, polyethylene glycol

PIPES, 1,4-Piperazinediethansulfonic acid

PMSF, phenylmethanesulfonyl fluoride

PCR, polymerase chain reaction

RNA, ribonucleic acid

RNAi, RNA interference

RNAse, ribonuclease

S, sedimentation coefficient

SDS, sodium dodecyl sulphate

SMC, structural maintenance of the chromosome

SPB, Spindle Pole Body

S phase, synthesis phase

UV, ultraviolet

µg, microgram

µl, microlitre

wt, wild type

YE, yeast extract

1 Chapter 1: Introduction

1.1 Chromosome condensation

Even before scientists understood that cellular nuclei contained the "brain" of the life unit they were fascinated by the spectacular course of chromosome formation. An apparent unorganised mass of genetic material transforming into discrete rod-shaped structures left scientists puzzling over the activities underlying such a transition. Today, we are only starting to elucidate this process in molecular terms.

What is the need, and what is driving the formation of condensed independent units of genetic information just prior cell division? The answer to the former question is that once the cell has generated a copy of the genome, it needs to physically separate the two copies. This partitioning requires the separating machinery, the spindle, to recognise and attach the two copies and pull them towards opposite poles of the dividing cell. This task becomes much more achievable by organising the genome in distinct, relatively small elements that can be recognised by the spindle. In this regard chromatin compaction performs a two-fold task: resolves the genome into distinct units (chromosomes), and axially shortens the DNA molecule pairs.

But what is the nature of the activity that re-organizes chromatin in preparation for cell division? Here, discoveries of the last two decades come to help. Several types of proteins could qualify as DNA condensing factors, including histones, topoisomerases and condensins. Strikingly, histone-like factors are absent in bacteria indicating that packaging and partitioning of the genetic information can be achieved by molecular machines other than histones. In fact, bacteria do have enzymatic activities resembling those of condensin and topoisomerases in eukaryotic cells. Condensin was first isolated by Laemmli and colleagues two decades ago (Hirano and Mitchison, 1994a; Lewis and Laemmli, 1982). High-salt extraction of mitotic chromosomes revealed what was tightly associated with DNA. They found what we now refer to as topo II and condensin, two of the most abundant components of eukaryotic chromatin. Today, several lines of evidence from bacteria to humans suggest that the multi-subunit condensin complex is the main player in chromosome condensation. Malfunctioning of this complex dramatically impinges on the

efficiency of every organism to accurately propagate the genome through generations. At this level, the link between condensin function and diseases that are fuelled, or caused by chromosome mis-segregation becomes very intimate. In fact, tumour development and genome instability are today thought to be reciprocally interdependent (Jallepalli and Lengauer, 2001). It is conceivable that functions of condensin will be shown to cause human diseases in the future. One example comes from premature chromosome condensation syndrome (PCC) in humans, where a clinical readout of the disorder is marked reduction of brain size. Mutant cells from PCC patients (Trimborn et al., 2004) show a high percentage of G2 cells with premature over-condensed chromosomes. Experiments of Condensin II knockout via siRNA in PCC human patient cells decisively reduced the condensation defects thus establishing a direct link between condensin and PCC syndrome (Trimborn et al., 2006).

Clearly, understanding the molecular basis that governs the biology of fundamental chromosomal factors like condensin would provide us with a solid foundation for the development of therapeutic agents.

1.2 The condensin complex and chromosome compaction

1.2.1 Hierarchical packaging of the eukaryotic chromosome

All eukaryotic cells have elaborate modes of packaging DNA within the size of the nuclear space. The human chromosome 22, one of the smaller chromosomes, if stretched along its entire length would be as long as 1.5 cm. However, in the cell the actual mitotic chromosome measures about 2 μm in length. Such an axial compaction ratio of nearly 10,000 fold leaves us wondering about the complexity of the task (see Figure 1.1). This is a job shared by several molecular factors that successively fold the DNA into a multilevel series of organization. Even interphase chromosomes are already 1,000 fold shorter than their linear counterparts would be. The proteins that form eukaryotic chromosomes are usually classified into two groups: histones and non-histone chromosomal proteins.

Histones are amazingly abundant factors equating the DNA itself in terms of molecular mass and they are present in a single human cell in the order of 60 million molecules. Histone binding to DNA provides the first basic level of packaging, the nucleosome. Nucleosomes have been observed as "beads on a string" of DNA under the electron microscope. Each bead is one nucleosome which consists of eight histone proteins

(two of each H2A, H2B, H3, H4) wrapped by 147 base pairs of DNA. Each nucleosome seems to be linked by roughly 60 base pairs of free DNA (linker DNA) as suggested by DNase digestion of cellular DNA (Laemmli et al., 1992).

A second level of organization whose nature is still controversial is the so-called 30 nm fibre (Laemmli et al., 1992). If nuclei are gently lysed chromatin appearance under electron microscope delineates characteristic fibres of about 30 nm in diameter. Whether this structure exists in intact nuclei is not clear but nonetheless the evidence suggests that linker histone H1 is an important player in generating and stabilizing this nucleosomal arrangement (Hansen, 2002; Konig et al., 2007)}. Organization of a subset of nucleosomal DNA into a certain geometric pattern would help the cell to create a second order of organization where each of the 30 nm fibres is interrupted by the presence of non-histone chromatin factors and/or by remodelled nucleosomes.

A chromosome packed by the 30 nm fibre would still be 100 times larger than the nucleus (0.1 cm) thus a substantial amount of further folding would be required even for the interphase chromosome. This is probably the least understood aspect of chromatin organization. It appears reasonable to envisage that nucleosomal chromatin must be folded in coils and loops perhaps by a scaffold-loop overall organization. Possibly the most apparent biological exemplification of this view is reflected in the organization of the lampbrush chromosomes observed during growth of immature amphibian oocytes. Its peculiar structure shows that there is a highly condensed DNA axis from where several loops of DNA rich in active genes emanate. Although this structure is unique to this organism, injection of non-lambrush eukaryotic DNA into amphibian oocytes transforms this DNA into a lampbrush chromosome (Lohka and Masui, 1983). Thus, although not normally observed, the fundamental features of chromatin packaging in all eukaryotes appear to be similar.

Condensation of interphase chromatin into mitotic chromosomes is tightly linked with cell cycle progression and requires the condensins, large multi-subunit ATPases able to drive compaction and disentanglement of DNA daughter molecules (see below). We are only recently beginning to elucidate this process in molecular terms. Whether condensin plays an active role in the formation or stabilization of the large interphase chromatin loops discussed above is so far unknown (see below). A summary describing the overall current view of chromatin packaging within eukaryotic nuclei can be seen in Figure 1.1.

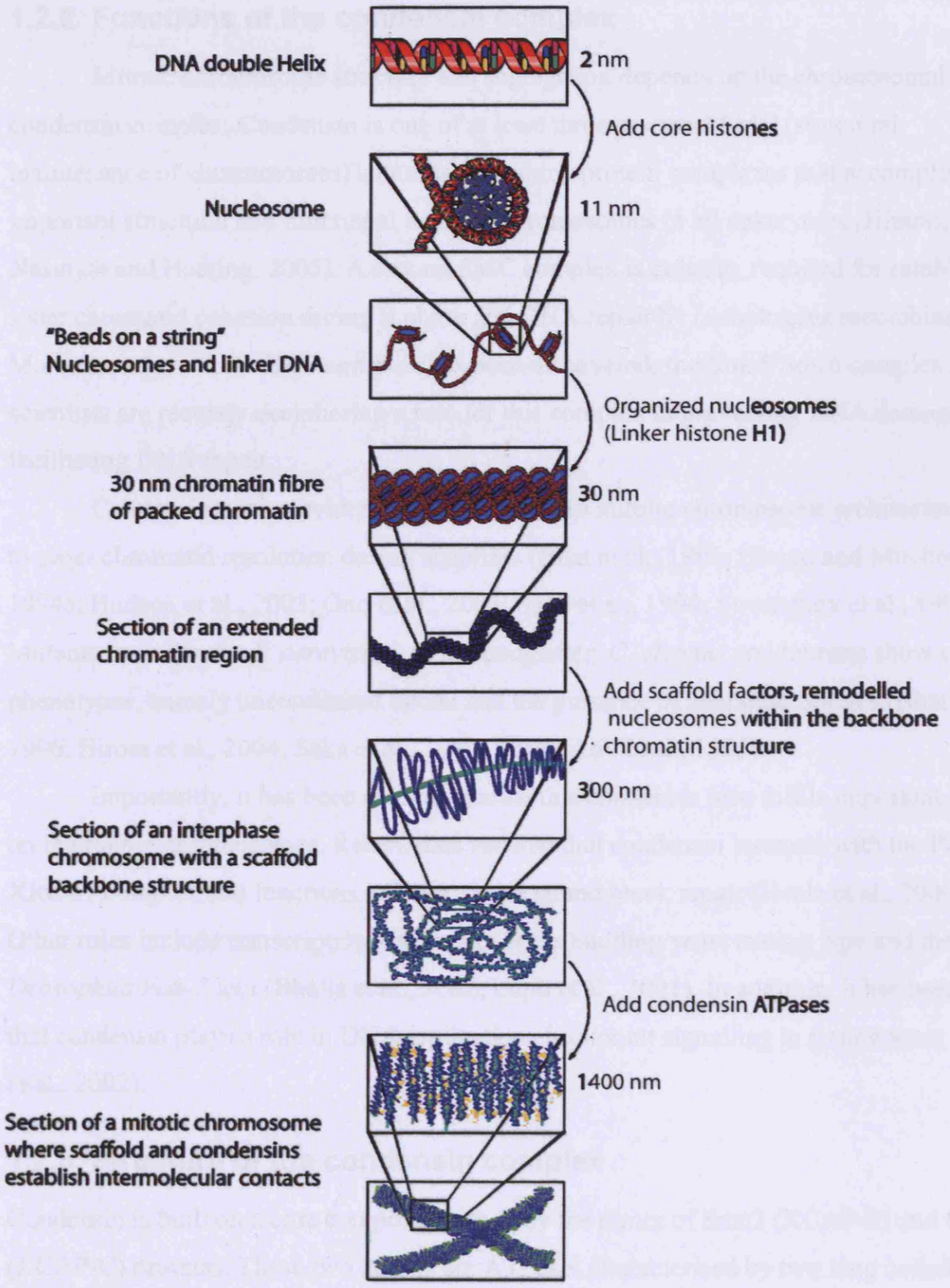

Figure 1.1. Current overview of the eukaryotic mode of DNA packaging within the nucleous

A hierarchical based mode of genome organization in eukaryotes is shown (as adapted from Wikipedia).

1.2.2 Functions of the condensin complex

Mitotic chromosome structure and segregation depends on the chromosomal condensin complex. Condensin is one of at least three essential SMC (structural maintenance of chromosomes) subunits containing protein complexes that accomplish important structural and functional tasks on chromosomes in all eukaryotes (Hirano, 2006; Nasmyth and Haering, 2005). A second SMC complex is cohesin, required for establishing sister chromatid cohesion during S phase and DNA repair by homologous recombination. More recently, a third SMC complex has been discovered: the Smc5/Smc6 complex; scientists are recently deciphering a role for this complex in preventing DNA damage and facilitating DNA repair.

Condensin's most evident function relates to mitotic chromosome architecture, and to sister chromatid resolution during anaphase (Bhat et al., 1996; Hirano and Mitchison, 1994a; Hudson et al., 2003; Ono et al., 2003; Saka et al., 1994; Strunnikov et al., 1995). Mutants in *S. Pombe, S. cerevisiae, D. melanogaster, C. elegans* and humans show similar phenotypes, namely uncondensed nuclei and the presence of anaphase bridges (Bhat et al., 1996; Hirota et al., 2004; Saka et al., 1994; Strunnikov et al., 1995).

Importantly, it has been recently shown that condensin also fulfils important roles on interphase chromosomes. Recent data showed that condensin interacts with the PARP-1-XRCC1 complex and functions in DNA single strand break repair (Heale et al., 2006). Other roles include transcriptional silencing at the budding yeast mating type and the *Drosophila Fab-7* loci (Bhalla et al., 2002; Lupo et al., 2001). In addition, it has been found that condensin plays a role in DNA replication checkpoint signalling in fission yeast (Aono et al., 2002).

1.2.3 Structure of the condensin complex

Condensin is built on a core component made by the dimer of Smc2 (XCAP-E) and Smc4 (XCAP-C) proteins. These two factors are ATPases characterised by two long coiled coil that interact with each other at both ends (Hirano and Mitchison, 1994b; Saitoh et al., 1994; Saka et al., 1994). Condensin in addition to the SMC core contains three additional subunits that are thought to have a regulatory role on the function of the holo-complex (Kimura and Hirano, 2000). In particular, the CAP-D2 and CAP-G subunits of the complex are HEAT

repeats containing proteins (Neuwald and Hirano, 2000) while the CAP-H (Brn1 in yeast, Barren in *Drosophila*) component of the complex is thought to be the bridging factor of the two SMC heads (often referred to as the 'kleisin subunit') (Schleiffer et al., 2003). This is supported by studies using recombinant human condensin subunits where it is shown that a non-Smc kleisin subunit directly binds the Smc head domains (Onn et al., 2007). The kleisin subunit itself in turn recruits the remaining two HEAT repeat containing non-Smc subunits (CAP-D2 and CAP-G in human, Ycs4 and Ycg1 in budding yeast) to the complex. Human cells contain at least two isoforms of condensin, condensin I and condensin II, that share the Smc2 and Smc4 subunits but contain distinct non-Smc subunits (Hirota et al., 2004; Ono et al., 2004; Ono et al., 2003) (see Figure 1.2 and table for a schematic representation of the known condensin complexes). Condensin I is approximately five times more abundant than condensin II but knock-out of condensin II specific subunits nonetheless results in decisive chromosome condensation and structural defects (Ono et al., 2003). The reciprocal affinity of sub-components of the whole complex has been also characterised. Importantly, human Smc2 and Smc4 form a heterodimer independently of the non-SMC subunits. The non-SMC subunits were also able to form subcomplex (Onn et al., 2007). These results go well with results in *Xenopus* where distinct condensin complexes exist of 13s (holo condensin), 11s (CAP-D2, CAP-G and CAP-H) and 8s (CAP-E AND CAP-C) (Kimura and Hirano, 1997; Kimura and Hirano, 2000). One striking structural feature shared by all the SMC complexes is their characteristic shape of a large molecular ring (Hirano, 2005b). In particular, condensin and cohesin complexes from both human cells and *Xenopus* extracts have been visualised by electron microscopy. Condensin in contrast to cohesin often displays a more closed conformation, with the arms emanating from the hinge at a smaller, perhaps more rigid and less variable angle (Anderson et al., 2002) (Figure 1.3). These structural differences have been speculated to at least contribute to the diverse *in vivo* functions of the two complexes (Hirano, 2005b).

A

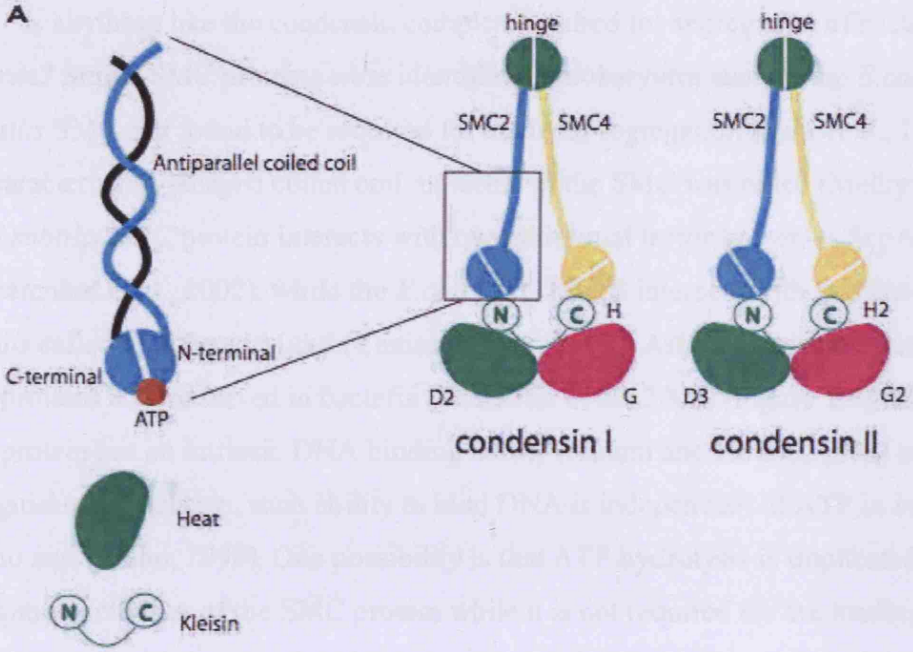

B

Condensin subunits	Human	*Drosophila*	*S. pombe*	*S. cerevisiae*
Core (I and II)				
SMC2	hCAP-E	DmSMC2	Cut14	Smc2
SMC4	hCAP-C	DmSMC4	Cut3	Smc4
I-specific				
HEAT	hCAP-D2	CG1911	Cnd1	Ycs4
HEAT	hCAP-G	CG17054	Cnd3	Ycg1
kleisin	hCAP-H	Barren	Cnd2	Brn1
II-specific				
HEAT	hCAP-D3	CG31989	-	-
HEAT	hCAP-G2	-	-	-
kleisin	hCAP-H2	CG14685	-	-

Figure 1.2 Schematic representation of the human condensin complexes (A) and subunit comparisons among different organisms (B)

1.2.4 A bacterial SMC complex like eukaryotic condensin

Is anything like the condensin complex required for segregation of bacteria genomes? Single SMC proteins were identified in prokaryotes such as the *E.coli* MukB and *B.subtilis* SMC and found to be required for nucleoid segregation (Niki et al., 1991). Again, the characteristic V shaped coiled coil molecule of the SMC was noted (Melby et al., 1998). The *B.subtilis* SMC protein interacts with two additional factor known as ScpA and ScpB (Mascarenhas et al., 2002), while the *E.coli* SMC MukB interacts with two accessory subunits called MukE and MukF (Yamazoe et al., 1999). Astoundingly, the 'Kleisin' non-SMC proteins are conserved in bacteria (Schleiffer et al., 2003) (Figure 1.4). The *B. subtilis* SMC protein has an intrinsic DNA binding ability (Hirano and Hirano, 1998) and, as distinguished by cohesin, such ability to bind DNA is independent of ATP in *in vitro* assays (Hirano and Hirano, 1998). One possibility is that ATP hydrolysis is implicated in DNA aggregation activities of the SMC protein while it is not required for the loading reaction onto DNA *per se*. Assays designed to measure protein aggregation revealed that the protein aggregation is dependent specifically on the presence of ATP and the aggregation occurs even in the presence of the non-hydrolyzable ATPγS analogue (Hirano and Hirano, 1998). Thus, binding, but not ATP hydrolysis, triggers aggregation of the SMC proteins. Since it is speculated that the condensin complex drives condensation through protein-protein interaction (Hirano, 2005a), this data would therefore suggests that the bacterial SMC complex shares an important feature with the eukaryotic condensin complex (see below). However, it is reasonable to assume that such an ancestral SMC factor represents functions shared by the specialised eukaryotic SMC complexes altogether.

1.2.5 *In vitro* and *in vivo* condensation activities

Holo condensin has the ability to bind DNA independently of ATP hydrolysis (Kimura and Hirano, 1997; Strick et al., 2004). This is in contrast to cohesin, where ATP binding is required for DNA binding (Onn et al., 2007). Interestingly, condensin ATPase activity is stimulated by the presence of DNA (Kimura and Hirano, 1997) and it is heavily dependent on the presence of the non-SMC subunits *in vitro* and *in vivo* (Kimura and Hirano, 2000; Stray and Lindsley, 2003). Condensin's use of ATP hydrolysis may be a prerequisite to condense DNA instead. Studies where purified condensin was incubated with DNA gave us important insights on how it might mechanistically organise DNA. In fact, purified

condensin holo-complex possesses the ability to introduce positive supercoils into plasmid DNA (Kimura and Hirano, 1997). Circular plasmid DNA incubated in the presence of condensin, ATP and type II topoisomerases is seen to undergo a positive knotting reaction and these specific DNA species are readily recognisable by electron microscopy (Kimura et al., 1999). Single molecule studies have also highlighted the possibility that condensin might work in a highly co-operative fashion. If the protein concentration in these single molecule reactions is halved it can completely knockout any condensation activity (Strick et al., 2004). This might suggest that condensin molecules work together in order to condense DNA, perhaps forming a co-operative chromosomal compacting machine made of several individual condensin holo-complexes. However, this scenario remains speculative at the moment since detailed characterisation of condensin binding sites and evidence for multimerisation *in vivo* remain elusive (Hirano and Hirano, 2006; Wang et al., 2005). Important insights into how condensin interacts with DNA has been obtained by visualization of the interaction by electron spectroscopic imaging (ESI). DNA seems to wrap around a globular domain of the condensin complex (presumably the ATPase head) and does so in an ATP hydrolysis dependent manner with approximately 190 bp of DNA being wound by a single condensin complex (Strick et al., 2004). Recently, the first models of condensin-driven chromatin compaction during mitosis have been proposed (Hirano, 2000; Hirano, 2006; Hirano et al., 1997). Figure 1.5 schematically represents some candidate models that explain the current view on how condensin might perform chromosome compaction. All models are compatible with both single (left panels) and multimeric mode (right panels) of condensin to act on chromatin. Condensin might wrap DNA around itself in a right-handed fashion therefore triggering the formation of complementary negative supercoils in adjacent portions of chromatin as a result of increased double helical twists (Figure 1.5 A). In this way, chromatin is shortened indirectly by the compensatory negative supercoils led by the association of condensin with DNA. Alternatively, condensin's role in compaction may merely (and directly) be mediated by local binding and wrapping of DNA by the complex (Figure 1.5 B).

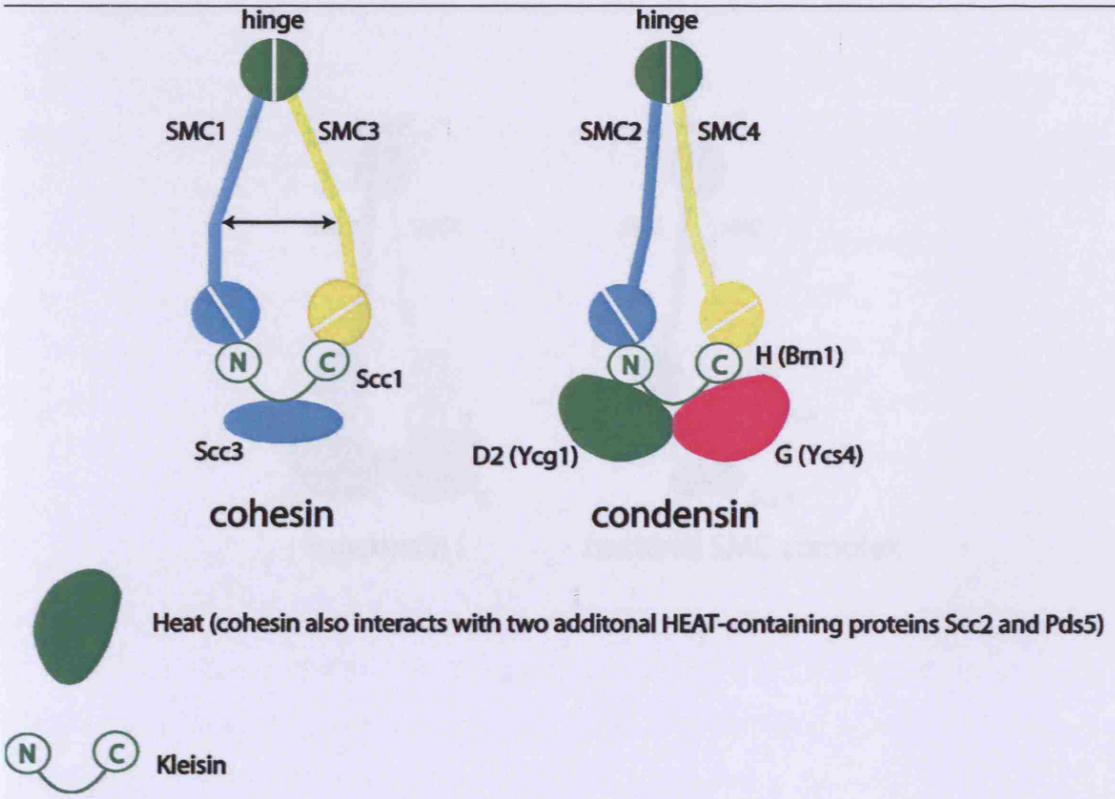

Figure 1.3 Schematic representation and comparison of cohesin and condensin

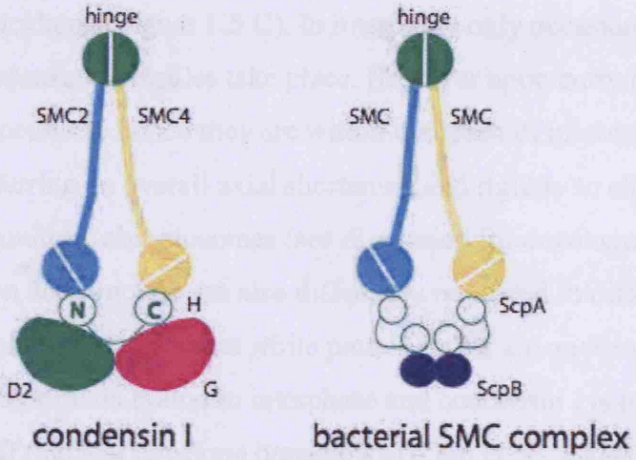

Figure 1.4 Schematic representation and comparison of the condensin and bacterial SMC complex

A third possibility is that condensin binds distinct sites largely spaced within the chromatin scaffold backbone (Figure 1.5 C). In interphase only occasional transient contacts between condensin molecules take place. However upon entry into mitosis such sites are more stably connected once they are within the reach of intermolecular interactions thus conferring an overall axial shortening and rigidity to chromatin, all features displayed by mitotic chromosomes (see discussion for development of this topic). Condensin localisation and function are also differently regulated in different organisms. In higher eukaryotes it has been shown that while protein levels are unchanged during the cell cycle condensin II is chromatin bound in interphase and condensin I is only recruited onto chromatin after NEBD (nuclear envelope breakdown) (Ono et al., 2004). Additional levels of regulation also underlie condensin function in *Xenopus*. Holo condensin complexes isolated from mitotic extracts have distinctive condensation abilities compared to complexes isolated from interphase extracts where those activities appear to be negligible. This was shown to be due to (possibly direct) stimulatory phosphorylation of CAP-D2 and CAP-H, by Cdc2 (Kimura et al., 1998). In fission yeast condensin is also subject to stimulatory phosphorylation by Cdc2 (on Cut3/Smc4), although this phosphorylation seems to be influential in nuclear targeting of condensin in mitosis (Sutani et al., 1999). In stark contrast, budding yeast condensin binds DNA throughout the cell cycle ((Freeman et al., 2000), this study) but its activity is once again somehow maximised upon entry into mitosis (Guacci et al., 1994).

1.2.6 A role for cohesins in chromosome condensation

In yeast, another striking feature of chromosome condensation is that it is dependent on sister chromatid cohesion (Guacci et al., 1997). Mutants in cohesion factors such as cohesin, CTF4 and CTF18 fail to establish and/or maintain chromosome condensation (Guacci et al., 1997; Hanna et al., 2001). However, a conserved role for cohesin in chromosome condensation has been disputed because studies made in organisms other than budding yeast failed to confirm such a requirement (Losada et al., 1998; Sonoda et al., 2001; Sumara et al., 2000; Waizenegger et al., 2000). To date, it seems condensin and cohesin do not interact, do not colocalise and do not affect the localisation of each other ((Lavoie et al., 2002; Losada et al., 1998; Tóth et al., 1999); this study). In addition, inactivation of cohesin does not lead to any obvious impairment in loading condensin onto

chromatin, excluding a straight forward explanation for the condensation defects (Lavoie et al., 2002). Thus, cohesin activates condensin at a stage subsequent of its loading onto chromosomes. How is cohesin involved into chromosome condensation? There are two possible answers: cohesin is directly implicated in chromosome condensation or, conversely, cohesin ensures proper chromosome folding by activating the condensin complex. One study suggested that the latter was the case. Koshland and colleagues showed by employing conditional mutant alleles of condensin that within a single budding yeast mitosis chromosome condensation was a readily reversible process (Lavoie et al., 2002). In contrast, unfolded chromosomes due to lack of cohesin are irreversibly unfolded. They went further showing that the inability of chromosomes to properly condense without cohesin was attributable to unregulated condensin activity. In fact uncondensed chromosomes of a temperature sensitive cohesin-condensin double mutant can re-condense again upon return to the permissive temperature (Lavoie et al., 2002). This suggests that inactivation of condensin alongside cohesin would prevent chromosomes to be irreversibly and improperly folded by a condensin complex that attempts to fold chromosomes without cohesin.

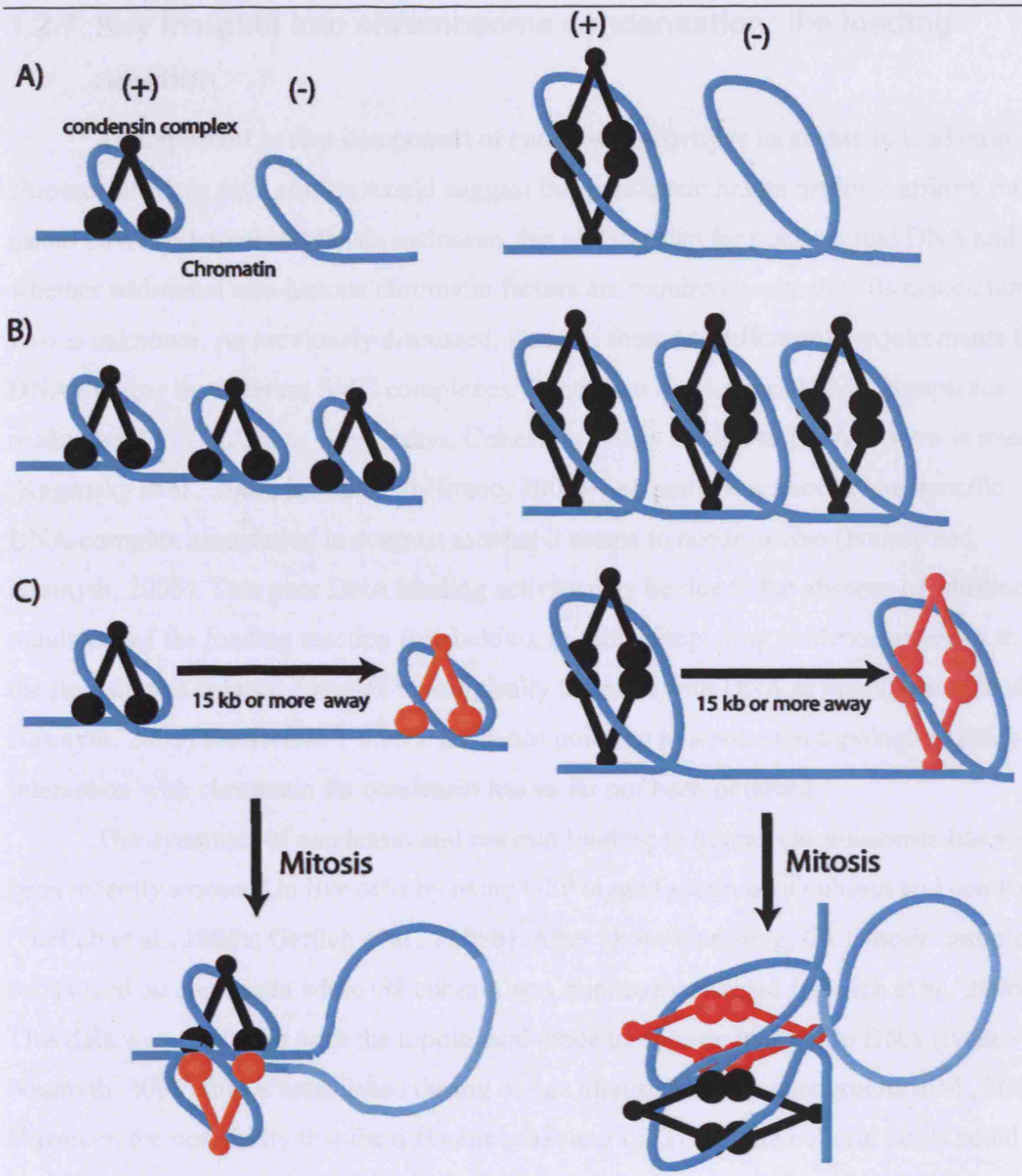

Figure 1.5 Three potential modes of condensin-mediated compaction

Left panels: condensin works as a monomer. Right panels: individual condensin complexes multimerise. Non-SMC subunits are excluded for simplicity.

A) Condensin binds and wraps DNA locally, an action that results in indirect supercoiling of neighbouring sites.

B) Condensin binds and shortens directly specific binding sites where it binds

C) Condensin binds distinct binding sites and the reciprocal affinity of individual complexes matures only upon entry into mitosis. This is in turn reflected in gluing *cis* sites spatially separated along the genome.

1.2.7 Key insights into chromosome condensation: the loading reaction

An important *in vivo* component of condensin activity is its ability to load onto chromosomes. *In vitro* studies would suggest that condensin has an intrinsic affinity for naked DNA. Whether condensin maintains this affinity also for nucleosomal DNA and/or whether additional non-histone chromatin factors are required to stabilize its association *in vivo* is unknown. As previously discussed, it seems there are differential requirements for DNA binding by different SMC complexes. Condensin and bacterial SMC complexes readily bind to DNA in *in vitro* assays. Cohesin's ability to bind to DNA *in vitro* is minor (Kagansky et al., 2003; Losada and Hirano, 2001), and perhaps reflects a non-specific DNA-complex association in contrast to what it seems to occur *in vivo* (Ivanov and Nasmyth, 2005). This poor DNA binding activity may be due to the absence of additional regulators of the loading reaction (see below). In fact, compelling evidence indicates that the ring-shaped cohesin complex topologically interacts with DNA *in vivo* ((Ivanov and Nasmyth, 2005) see section 1.2.7.1). Evidence pointing to a potential topological mode of interaction with chromatin for condensin has so far not been obtained.

The dynamics of condensin and cohesin binding to human chromosomes has also been recently assessed in live cells by using GFP tagged subunits of cohesin and condensin (Gerlich et al., 2006a; Gerlich et al., 2006b). After photo-bleaching, G1 cohesin completely exchanged on chromatin while G2 cohesin was minimally affected (Gerlich et al., 2006b). This data was consistent with the topological mode of cohesin binding to DNA (Ivanov and Nasmyth, 2005) that is established during or just after replication (Lengronne et al., 2006). However, the possibility that the different behaviour of G1 and G2 cohesin pools could be attributed to the presence of two daughter DNA molecules has not been formally ruled-out. As discussed before, human cells contain at least two condensin complexes. Condensin I gains access to chromosomes only after NEBD and it is proposed that its role is to stabilize chromatin sufficiently to resist spindle forces (Gerlich et al., 2006a). Remarkably, Condensin I supports the structural integrity of centromeric chromatin via highly transient interactions with chromosomes. Condensin II, in contrast, seems to be more stably associated with chromatin at the time when Condensin I enters the nuclei whereas its turnover is more dynamic during interphase (Gerlich et al., 2006a) (See discussion).

Whether additional cell cycle regulated factors modulate the dynamics of condensin I and II loading onto chromosomes is not known.

1.2.7.1 Lessons from the loading reaction of cohesin

Important insights into the manner in which SMC complexes bind DNA came from recent studies involving the cohesin complex (Ciosk et al., 2000; Lengronne et al., 2004). The cohesin complex consists of at least four subunits including Smc1 and Smc3 plus two non-SMC subunits called Scc1 (the kleisin subunit) and Scc3 (see Figure 1.3). Cohesin shows a remarkable structural similarity with condensin (Anderson et al., 2002). A large body of evidence summarised in the so called "embrace model" has proposed that the ring-shaped complex establishes cohesion by embracing both sister chromatids from DNA replication to anaphase onset (Ivanov and Nasmyth, 2005; Lengronne et al., 2006). The topological association of the ring shaped complex with DNA is unarguably a key feature that must now be incorporated in any model for cohesin association to chromatin (Ivanov and Nasmyth, 2005). Conceivably the dimension of the cohesin complexes is such that they are indeed capable of trapping within their inner circumference the replication products (Haering et al., 2002). However, this topological mode of interaction between cohesin and DNA posits a paradox: how can the replication machinery produce a copy of the DNA duplex while cohesin is entrapping the DNA? Cohesin binds DNA before DNA replication and cohesion can only be established during S phase (Lengronne et al., 2006; Uhlmann and Nasmyth, 1998). This infers that either cohesin transiently loses its association with DNA during fork progression or, alternatively, that the cohesin ring entraps the newly formed products as the DNA replication machinery moves through it. While the former scenario would be consistent with the behaviour of most chromatin associating factors, the second elegantly provides a mechanism for the cell to discriminate non-daughter DNA molecules. However, the size of the replication machinery plus the fact that the lagging strand is thought to form huge loops during replication, makes it unlikely that the 40 nm diameter of the ring would be large enough for the task. At the moment cohesion establishment is fuelling intense investigation by the chromosome segregation field (Nasmyth et al., 2000; Nasmyth and Schleifer, 2004). Important insights into the function of cohesin recently came from analyzing its pattern of chromosome binding in budding yeast. It had already been observed that cohesin binds to distinct sites along the arms and shows enrichment

around the centromere (Blat and Kleckner, 1999; Megee et al., 1999; Tanaka et al., 1999). Cohesin binding sites were also shown to correlate with an increased AT DNA content (Blat and Kleckner, 1999; Glynn et al., 2004). Several studies indicated that the mechanism of centromeric binding differs quantitatively and qualitatively from chromosome arms. In fact, creation of an ectopic centromere within a budding yeast chromosome is proficient in recruiting cohesin. This is dependent on the functionality of the kinetocore. In fact, the presence of mutant kinetochore proteins (Cse4, Mif2 or Ndc10) abolishes cohesin recruitment to such an ectopic centromere (Tanaka et al., 1999). Similarly, repression of centromere function by insertion of the strong (galactose inducible) *GAL1* promoter prevents Scc1 cohesin recruitment. Abolishment of cohesin binding upon repression of centromere function by strong transcription from the *GAL1* promoter was inconclusive as to whether disruption of the kinetochore or transcription itself is a major antagonist to cohesin binding to chromatin (Tanaka et al., 1999). A preliminary observation of cohesin binding within boundary regions of silenced chromatin instigated the view that transcription was incompatible with cohesin binding (Laloraya et al., 2000). More recent studies have clearly shown that transcription is indeed a major determinant of cohesin positioning onto budding yeast chromosomes. Induction of transcription is sufficient to quickly remove cohesin from a previously un-transcribed gene. Consistently, the vast majority of cohesin sites in budding yeast are found associated at intergenic converging transcription sites (Glynn et al., 2004; Lengronne et al., 2004). The relationship of cohesin with transcription is upheld in meiosis of budding yeast (Glynn et al., 2004) and in fission yeast mitosis (Lengronne et al., 2004) suggesting that this might be a universally conserved feature in eukaryotes.

1.2.7.2 The Scc2/4 complex and cohesin loading

As discussed in the previous section the requirement for ATP hydrolysis for DNA association is somehow distinguished between cohesin and condensin.

It has been recently established that a conserved protein complex called Scc2/4 was responsible for loading cohesin onto DNA. Fission yeast Scc2 was the first to be identified (Mis4) and shown to be required for the stable maintenance of a minichromosome and later for cohesion establishment (Furuya et al., 1998; Takahashi et al., 1994). Later Scc2 and Scc4 proteins were identified in *S. cerevisiae*, and shown to be responsible for cohesin loading in late G1 (Ciosk et al., 2000; Tóth et al., 1999). Scc2/4 loads cohesin in late G1 (Ciosk et al., 2000). However, upon cohesin loading onto DNA additional events need to

occur during S phase to generate sister chromatid cohesion (Uhlmann and Nasmyth, 1998). For example, inactivation of conditional alleles of Scc2 and Scc4 (*Scc2-4, Scc4-4*) retain robust cohesion in G2/M arrested cells (Ciosk et al., 2000) and, strikingly, Scc2 can be inactivated before release from an S phase arrest mediated by hydroxyurea (HU) without affecting the establishment of cohesion (Lengronne et al., 2006). Ectopically expressed cohesin can be loaded after S phase in a Scc2/4 depending manner, but this pool of cohesin is not able to maintain cohesion between sister chromatids (Uhlmann and Nasmyth, 1998). Intriguingly, during S phase, the ability of cohesin to establish linkages between sister chromatids, but not its loading onto chromosomes, depends on the putative acetyltransferase Eco1 (Tóth et al., 1999). The mechanism by which cohesin establishes sister chromatid linkages via Eco1 is currently unclear.

In support of a direct link between cohesin and Scc2/4 is the finding that they interact in co-immunoprecipitation experiments (Ciosk et al., 2000). Thus, these observations suggest that Scc2/4 is the 'loader' for cohesin complexes. The dependency on Scc2/4 for cohesin loading seems to be an evolutionary conserved mechanism since it is seen in human cells (Watrin et al., 2006) as well as *Xenopus* egg extracts (Gillespie and Hirano, 2004; Takahashi et al., 2004). Rather puzzling, however, was the finding that cohesin and Scc2/4 seam to occupy clearly distinct, if not alternating, binding sites on chromosomes (Ciosk et al., 2000). This paradox was resolved by the observation that cohesin complexes initially dock at these Scc2/4 binding sites from which they translocate to the more permanent places where opposing transcription machineries converge (Lengronne et al., 2004). How cohesin is loaded onto chromatin by Scc2/4 is not known. A speculative as well as elegant model states that Scc2/4 might stimulate the low intrinsic ATPase activity of Smc1 and Smc3 to facilitate complex loading (perhaps by triggering the opening of the ring-shaped complex) (Arumugam et al., 2003). After loading, cohesin complexes are quickly relocated (Lengronne et al., 2004) away from these docking sites by ongoing RNA pol II dependent transcription, thus spatially far beyond the reach of further interactions with Scc2/4. This could be instrumental in respect to avoiding dangerous second rounds of ATP hydrolysis therefore keeping cohesin complexes irreversibly shut onto chromatin. In keeping with this view, transcription is an essential prerequisite for cohesion establishment. It would be therefore interesting to ask whether cohesin is able to provide cohesion in a condition where it is prevented from relocating away from its Scc2/4 loading sites. A possible way to impede cohesin relocation could be achieved by allowing

cohesin loading onto chromatin in the absence of RNA pol II dependent transcription. Knowing that cohesin can establish sister chromatid cohesion while still in direct contact with Scc2/4 would have profound implications for the model discussed above of an Scc2/4 dependent stimulation of cohesin SMC ATPases. The answer to this question clearly requires a system where RNA pol II inactivation just after cohesin loading is unlinked to (at least) the synthesis of unstable Scc1/Mcd1, the key component required for holo-complex assembly. Nonetheless, it should be mentioned that recent work championed the notion that ATP hydrolysis by the SMC heads is the only key event required for the loading reaction. In fact opening of the cohesin hinge in the opposite portion of the large ring shaped complex might also be a prerequisite for the loading reaction (Gruber et al., 2006). This study shows that if the Smc1 and Smc3 hinge domains are forced to remain closed together, cohesin recruitment to chromosomes is prevented. Hence, any new models for cohesin binding need now to incorporate some mode of hinge opening as well as accommodate ATP hydrolysis by the heads and a reaction by Scc2/4.

The regulation of Scc2/4 binding to chromatin also seems not to be completely conserved between different species. In *S. cerevisiae* this complex is constitutively bound to chromatin (Ciosk et al., 2000). This is in contrast to the situation in human cells where Scc2/4 disappears from chromosomes during mitosis (Watrin et al., 2006). Similarly in *Xenopus* egg extracts, deposition of Scc2/4 on chromatin is dependent on origin licensing before S phase (Gillespie and Hirano, 2004; Takahashi et al., 2004). Hence, higher eukaryotes have an additional regulatory step that is not present in budding yeast. Interestingly a recent study has opened the possibility that Scc2/4 might function also in Smc5/6 chromatin recruitment beside its primary function in cohesion establishment (Betts Lindroos et al., 2006). However, regulation of Smc5/6 recruitment to chromosomes seems regulated by different pathways. In both *Xenopus* egg extracts and budding yeast its association to chromosomes in not observed before DNA replication (Betts Lindroos et al., 2006; Tsuyama et al., 2006). In budding yeast, like cohesin, Smc5/6 is recruited to sites of double stranded DNA breaks (DSB) (De Piccoli et al., 2006; Tsuyama et al., 2006) but in a way independent of Scc2/4. A functional link between cohesin and Smc5/6 recently emerged in view of the fact that it was shown that human Smc5/6 is required for recruiting cohesin to DSB to promote homologous recombination at these sites (Potts et al., 2006).

1.2.7.3 Scc2/4 and human diseases: Cornelia de Lange syndrome

Scc2/4 mutations are reported to cause Cornelia de Lange syndrome (reviewed in (Strachan, 2005). This developmental disorder is characterised by a large range of neuro-developmental abnormalities including mental handicap, growth retardation, distinctive facial deformities and limb malformations. From two initial studies, mutations in the human *SCC2* gene a homologue of the *Drosophila Nipped-B* and fungal *Scc2* were linked to the disease (Krantz et al., 2004; Tonkin et al., 2004) (see also 1.3.1). These mutations cluster in the C-terminal HEAT repeats of the gene products (Delangin-1 and -2). This disease is thought to be a consequence of cohesin mis-regulation. This correlates with the observation that low penetrating mutations in the Smc1 and Smc3 subunits of the cohesin complex have a similar causative effect in respect to the disease (Borck et al., 2007; Deardorff et al., 2007).

1.3 What is orchestrating nuclear structure in interphase?

1.3.1 Domain based organization of the eukaryotic genome

The eukaryotic genome is organized into domains. These are defined accordingly to different criteria including specific transcription status or by DNase I digestion sensitivity. Also patterns of histone modifications, presence of histone variants and non-histone proteins contribute to such definitions. In addition, chromatin is seen organized in a loop-based manner thus leading to the hypothesis that domains are topologically constrained regions (Laemmli et al., 1992). In this view, domains have also well defined borders distinguished by specific sequences and *trans*-factors that bind to them. Chromatin is organized into active expressed euchromatin and silenced repressed heterochromatin that can be clearly distinguished by staining. Heterochromatin is characterized by being hypoacetylated, rich in repetitive sequences, poor in genes and late replicating in the cell. Heterochromatin can be further divided into constitutive and facultative (Valenzuela and Kamakaka, 2006). The former is often interchangeably referred to as centromeric and telomeric chromatin. Heterochromatin is often repetitive and it is always condensed irrespective of the cell type. Facultative heterochromatin refers to regions that can be silenced upon establishment of specific developmental patterns. The most popular example is the polycomb-mediated heterochromatin that generates silencing in a way mechanistically similar to the one established over constitutive heterochromatin (Orlando,

2003). One model predicts that the establishment and stability of a certain domain is a function of the presence of proteins that bind the region. Competitive accessibility and binding of specific factors thus tip the balance in the formation and/or maintenance of a certain chromatin status. Consistently, mutations in such factors do impair the assembly of the domain (Locke et al., 1988). This also has implications in what is defining the boundaries of a domain; such elements might assume the form of culminating competing activities rather than a simple sequence, or may be both. Delineation of chromatin domains is also influenced by the so called insulators. Activation of a specific gene in high eukaryotes often involves a long-range contact between its promoter and an enhancer through establishment of a large chromatin loop (Valenzuela and Kamakaka, 2006). Studies with the human ß-globin locus for example, indicate that an enhancer in the locus control region is located some 40 to 60 kb from the globin genes and it is in close proximity to a globin gene promoter when that promoter is activated (Carter et al., 2002; Tolhuis et al., 2002). Insulators mark the boundaries of chromatin domains by regulating the range of action of enhancers and silencers. It is possible that such 'insulator activities' can be simply regulated by nearby regulatory elements (i.e. covalent DNA modifications and bound cofactors). In keeping with with this view, insulators should be ascribed as active participants of eukaryotic gene regulation. It is also likely that in the genome there are general facilitators that act widely to support enhancer-promoter communication in a large number of genes (Dorsett, 1999). The existence of general facilitators could explain how certain insulator sequences, such as the insulator in the *Drosophila* gypsy transposon, block enhancer-promoter interactions in different genes, and, amazingly in different organisms (Donze and Kamakaka, 2001; Dorsett, 1999). They might act by generally facilitating or stabilising certain folded or looped structures. A genetic screen aiming at identifying genes encoding factors that facilitate long-range activation of *Drosophila cut* and *Ultrabithorax* genes identified Nipped B (Scc2 homologue) (Rollins et al., 1999). In contrast, cohesin is thought to inhibit long-range activation of *cut* by acting as a boundary component between the enhancer and the promoters (Rollins et al., 1999). Cohesin working as a boundary factor has been actually observed in yeast (Donze and Kamakaka, 2001), (see next paragraph). Scc2/Nipped B might act by stimulating SMC ATPases therefore potentially triggering opening of the ring-shaped complex with consequent dissociation of cohesin from DNA (Rollins et al., 1999). Nipped B by locally unloading cohesin could facilitate *cut* activation by alleviating cohesin-mediated blocking of enhancer-promoter communication (Rollins et

al., 1999). Importantly, this model has been also strongly correlated with the impaired expression of genes involved in the Cornelia de Lange syndrome (see 1.2.6 and discussion). Different eukaryotes show a remarkable variation in the extent their genetic content is packed within nuclei. It is evident that the packaging of the 3 Gb human genome within 10-20 μm of space requires an impressive compaction ratio when compared with the budding yeast genome where only 14 Mb of chromatin have to be organized within 2 μm. However, this remarkable diverse compaction ratio may not necessarily be reflected in an increased organisational complexity. In fact, even the relatively small genome of *Saccharomyces cerevisiae* is domain-organised and seems to possess all the characteristics observed in the genomes of higher eukaryotes therefore constituting for many scientists an interesting model for studying chromatin organisation (Kimura and Horikoshi, 2004).

1.3.2 tRNAs functioning as boundary elements in *Saccharomyces cerevisiae*

In *cerevisiae* telomeres and the mating type loci HMR and HML are domains silenced through deacetylation of histone tails by the Sir pathway (Rusche et al., 2003). Close to the HMR locus there is a tRNA whose function is to act as a barrier for the spread of heterochromatic silencing (Donze and Kamakaka, 2001). These authors also showed that the overall RNA pol III machinery occupancy at the gene is important for barrier function (Donze and Kamakaka, 2001). Similarly, recent findings show that this mechanism is shared also at the centromeres in the yeast *Pombe* (Scott et al., 2006). Interestingly, among additional factors that reinforce tRNA mediated boundary activity there are the cohesin subunits Smc1 and Smc3 (Oki and Kamakaka, 2005). Chromatin remodelling factors also seem to act in a parallel pathway alongside tRNAs to sustain strong barrier activity (Oki and Kamakaka, 2005).

A screen aimed at identifying factors involved in the HML silencing retrieved components of the nuclear pores, Cse1 and Nup2 (Ishii et al., 2002). This striking finding led to the proposal that the nuclear pore is tethered by barrier acting DNA sequences thus creating a topologically independent chromatin loop domain. This may suggest also that relocation of a gene within the nucleus serves as a mean for gene expression regulation. However, recent studies question the view that nuclear pores are generally linked to gene repression. This is because specific sets of nuclear pores are seen associated with active genes while other nuclear pores make contact with inactive ones (Casolari et al., 2004). We

recently learnt about the existence of dynamic transcriptional foci and of early stages of gene activation correlating with gene relocation to a specific "activator" nuclear pole (Carter et al., 2002; Casolari et al., 2005; Schmid et al., 2006). From this it is clear that our view of a static nuclear organization during interphase is rapidly incorporating notions of high levels of dynamic regulation. It is still unclear how the cell accomplishes the maintenance of a specific overall nuclear architecture while the genome maintains high levels of chromosome metabolism. It is possible that specific factors in specific chromosomal regions delineate an overall nuclear geometry by cross-interacting with each other. Interestingly, yeast tRNA genes, despite being scattered through the entire genome linear sequence, are found clustered at the nucleolous (Thompson et al., 2003). These authors found most tRNAs genes spending most of the time at the nuclear periphery close to the 5S ribosomal DNA. They shows that such a tendency is dependent upon some aspects of transcription or complex formation since different RNA pol III mutants diminish the frequency of tRNA-nucleolous colocalisation (Thompson et al., 2003). Although this observation has profound implications for the three-dimensional organisation of the genome, it is not known whether the same occurs within metazoan nuclei. The previously mentioned boundary activity of tRNA genes and their apparent ability to define distinct domains might well be accomplished by a tethering mechanism to the nuclear periphery. Interestingly, in fission yeast, the transcription factor TFIIIC, which recognizes the intra-sequence promoter (B box) of tRNAs, is found clustered at the nuclear periphery. TFIIC, but not the other factors of the RNA pol III machinery, binds additional non-tRNA sequences. These additional TFIIIC association sites are also seen forming supplementary peripheral clusters fuelling the view that they might act as complementary genome anchoring sites (Noma et al., 2006). What the driving forces that sustain these structures are and whether this spatial geometry is cell cycle regulated remain interesting questions to address.

1.4 Condensin, topo II and resolution of chromosome linkages: old question yet modern enigma

1.4.1 Challenges faced by the separation of two identical daughter DNA molecules

Topological linkages are an inevitable consequence of the process of DNA replication. In this respect Watson and Crick early in 1953 stated that since the two strands in the helix are intertwined a large amount of uncoiling would be necessary to enable partitioning of the two newly formed double helixes during anaphase.

This task seems even more challenging for circular bacterial genomes like the one of *Escherichia coli*. They present a clear topological challenge during DNA replication (that linear chromosomes should not have) because unwinding of a parental DNA in such a closed system is not helpful since this would create an equivalent number of topological entanglements elsewhere. In the sixties Cairns stated that a nick in one of the strands would allow free DNA rotation and therefore it would suffice in eliminating the topological constraints of DNA replication (Cairns, 1963). A few years later Worcel and Burgi actually found that larger genomes behave exactly like circular DNA because of the existence of domains whose fixed ends act by preventing any free rotation (Worcel and Burgi, 1972). Thus, the initial prediction that DNA must be cut in several places (by endonucleases) in order to be segregated was proposed (Delbruck and Stent in 1957), but this idea received experimental confirmation only quite later on. A cell must preferably contain some factors to provide frequent single strand breaks (to have free DNA rotation) and additional double strand breaks when two double helixes are intertwined. The old suggestion that DNA is broken at a high rate during replication turned out to be true and these cleavages are performed by topoisomerases (not endonucleases). Topo I serves as a DNA replication swivel (Champoux and Dulbecco, 1972) whereas topo II freely passes double-stranded DNA through a second transiently broken double helix (Brown and Cozzarelli, 1979; Gellert et al., 1976). Following these discoveries topoisomerase inhibitors were widely used as anti-cancer agents (Nitiss, 2002). In eukaryotic chromosomes DNA catenation between sister chromatids most likely arises as the consequence of replication termination. Studies of simian virus 40 replication suggests that convergent replication forks are unable

to completely remove topological linkages between the unwound single strands, such that after completion of DNA synthesis the two replication products are left catenated (Sundin and Varshavsky, 1980). During S phase the opposing replication forks are able to get as close as 200 or 300 base pairs. Replication halts at this stage, possibly due to the steric exclusion of topo I that acted up to this point as a swivel for bilateral fork progression. Catenation between daughter DNA molecules arises as this residual region is unwound and replicated. Each helical turn replicated in this condition is converted into a topological duplex intertwining. How does the cell know by the time of anaphase onset that its huge genome has been totally disentangled? Furthermore, the reach of a thermodynamic equilibrium by the action of type I topoisomerases may not necessarily reflect a number of sister chromatid linkages of actually zero. This argument is probably solved by two different factors, as reviewed by Cozzarelli (Hardy et al., 2004). First, Topo II enzymes can "sense" the topology of DNA rather than binding randomly everywhere. This is suggested by their ability to interact with DNA crossovers (Dong and Berger, 2007; Zechiedrich and Osheroff, 1990). Additionally, topoisomerases are ATPases, thus capable of working uphill well past the thermodynamic equilibrium (Vologodskii et al., 2001). The second aspect is that in order to grow large the eukaryotic genomes had to organise themselves into domains. Thus, dividing chromatin into topologically constrained units meant that the number of entanglements created as a result of DNA replication did not increase with increasing DNA length.

Mutational analysis from different organisms concluded that topo II constitutes the major DNA decatenating activity in eukaryotic cells and is required for chromosome segregation during mitosis (Downes et al., 1991; Holm et al., 1985; Uemura et al., 1987). However despite several years of intense study, little is known about termination of cellular replication and whether, where, and for how long catenation persists after S-phase. Attempts to address such questions have been made (Spell and Holm, 1994). It is clear that chromosomes undergoing anaphase without topo II function dramatically fail to resolve, stretch and eventually breakdown. It is conceivable that, for example, in budding yeast between each pair of neighbouring active origins lies a broad region of late replication and eventual DNA catenation. Connie Holm and colleagues showed that in budding yeast the tendency of chromosomes to break upon topo II inactivation is a function of chromosome arm length (Spell and Holm, 1994). Interestingly, relocating a centromere on a chromosome would in turn relocate the breakage point approximately 200 kb from the

newly made centromere. Thus, perhaps termination of DNA replication does occur over broad regions in a non-sequence specific manner. It is also possible that intertwined duplex structures are mobile to a certain extent on chromosomes since small chromosomes seam able to decatenate passively through slip off of chromosome ends (Spell and Holm, 1994). This data does not prove that catenations are mobile but it does correlate with the observation that catenates accumulate at the end of replication obtained from studies on circular DNA of the simian virus 40 (Sundin and Varshavsky, 1980).

1.4.2 A partner to give directionality to topoisomerase function

Besides its function in chromatin structure, condensin is required for resolution of sister chromatids to allow their segregation during anaphase (Bhat et al., 1996; Hagstrom et al., 2002; Hudson et al., 2003; Ono et al., 2004; Saka et al., 1994; Strunnikov et al., 1995). The anaphase bridging phenotype in condensin mutant cells resembles that of cells lacking topo II activity. As amazing machines as topoisomerases are, they cannot disentangle chromosomes by themselves, because they do not know the directionality of their actions. It has therefore been suggested that condensin-mediated compaction of chromosome arms may provide directionality for resolution of catenation that persists between sister chromatids after DNA replication (DiNardo et al., 1984; Downes et al., 1991; Koshland and Strunnikov, 1996; Uemura et al., 1987) (a representation of this view can be found in Figure 1.6). However, promotion of DNA compaction *per se* cannot result in disentanglement of chromosomes even in presence of topoisomerases. Indeed, overall condensation triggered by polycations has a ruinous effect in terms of DNA organization and segregation. In these conditions, plasmid DNA in the presence of topoisomerase is transformed into a clumsy, highly unordered network of linkages (Kreuzer and Cozzarelli, 1980). Thus, condensation must occur in a different way *in vivo*. There is the possibility that condensin-mediated compaction is conjugated with directionality provided by pulling spindle forces and with condensation at the level of the single domain.

Studies in *Drosophila* illustrate that the mechanism of chromatin disentanglement is probably even more complicated. Specific mutant alleles of condensin allow chromosomes to be axially shortened comparably with wild type cells while still failing to resolve anaphase bridges (Coelho et al., 2003). Hence, condensin's roles in DNA resolution might be independent to its general ability to compact chromatin. Compaction-independent stimulation of sister chromatid resolution by condensin could involve interaction with, and

activation of, topo II. This has been observed for *Drosophila* condensin (Bhat et al., 1996; Coelho et al., 2003). An interaction of condensin and topo II was confirmed by a group studying Polycomb-mediated development in *Drosophila* (Lupo et al., 2001). However, in other model organisms such interaction has been difficult to be reproduced (Bhalla et al., 2002; Cuvier and Hirano, 2003; Lavoie et al., 2000). Nonetheless, a compaction-independent role of condensin in sister chromatid resolution is also seen in budding yeast ((D'Amours et al., 2004; Sullivan et al., 2004); see section 1.4.2).

One of the simplest explanations of the anaphase bridge phenotype could be mis-regulation of topo II recruitment onto chromatin without condensin. In a *Drosophila* condensin mutant, during anaphase, topo II is no longer confined to a central axial structure and becomes diffusely distributed all over the chromatin (Coelho et al., 2003). In yeast overproduction of topo II in a condensin mutant restores apparently normal binding of the former without rescuing the chromosome segregation defects ((Bhalla et al., 2002); this study). Thus, how condensin promotes sister chromatid resolution has remained controversial, and in particular it has so far not been possible to make sure that chromosome linkages in the absence of condensin are indeed due to persisting catenation. The possibility that condensin may have an alternative, or additional, function in sister chromatid resolution is still open.

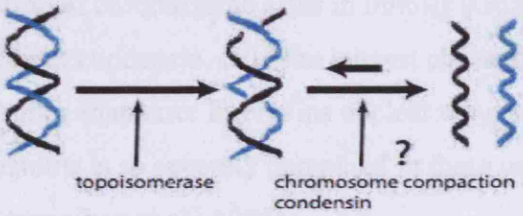

Figure 1.6 Chromosome condensation as a means to give directionality to topoisomerase

A historical view of how disentanglement of intertwined replicated daughter DNA molecules may be accomplished is shown. Topoisomerase II constitutes the major cellular decatenating activity. Shortening and separation of local domain between sister chromatids is facilitated by mitotic chromosome condensation. Whether sister chromatid linkages are resolved before the advent of chromosome condensation and whether condensin is the assistant of topoisomerase mediated DNA decatenation is not known.

1.4.3 The yeast ribosomal DNA

In budding yeast, inactivation of condensin results in approximately 1.5-fold undercompaction of chromosome arms in mitosis (Guacci et al., 1994) (this study). Therefore, without condensin, only the longest chromosome arms would be prevented from segregating during anaphase. It remains unclear why, as in other organisms, resolution of most of the genome is so severely hampered in these conditions (Bhalla et al., 2002; Lavoie et al., 2002; Strunnikov et al., 1995).

The budding yeast rDNA locus consists of 100-200 repeats of approximately 9.1 kb each and it is located on the longest arm of chromosome XII. This is the site of ribosome biogenesis as the nucleolous assembles on top of the array. Interestingly, the nucleolous is characterised by its peripheral location, and its previously noted late segregation during anaphase (Strunnikov et al., 1995). Two recent studies discovered that the sister chromatids at the rDNA array remain connected until mid-anaphase independently of the cohesin complex (D'Amours et al., 2004; Sullivan et al., 2004) (Figure 1.7). What drives resolution of the locus is a cell cycle regulated phosphatase, namely Cdc14, which is probably the most important player for down-regulation of mitotic cyclins during mitotic exit in *S. cerevisiae* (Visintin et al., 1998). A mechanistic explanation of how Cdc14 triggers late resolution of rDNA cohesion is not yet understood (Figure 1.7). Strikingly, to dissolve the rDNA linkage both condensin and topo II activities are needed (D'Amours et al., 2004; Sullivan et al., 2004). Whether the linkage is of a topological other than proteinaceous nature is not known. Despite requiring condensin, another amazing feature of rDNA segregation is that condensation of the locus is not strictly a prerequisite for its segregation (D'Amours et al., 2004; Sullivan et al., 2004). Compaction of the rDNA locus can be functionally separated from condensin-mediated resolution. In fact, compaction, but not resolution, depends on Aurora B kinase (D'Amours et al., 2004; Sullivan et al., 2004). Without the Aurora B kinase function (encoded by *IPL1* in yeast), uncondensed rDNA sister chromatids succeed in full rDNA disjunction. However, in these conditions, despite the two uncondensed sister rDNA arrays are fully resolved, fail to be efficiently segregated in the dividing cell (Sullivan et al., 2004). Thus, the most indispensable function condensin performs at the time of rDNA resolution is amazingly not chromatin compaction itself.

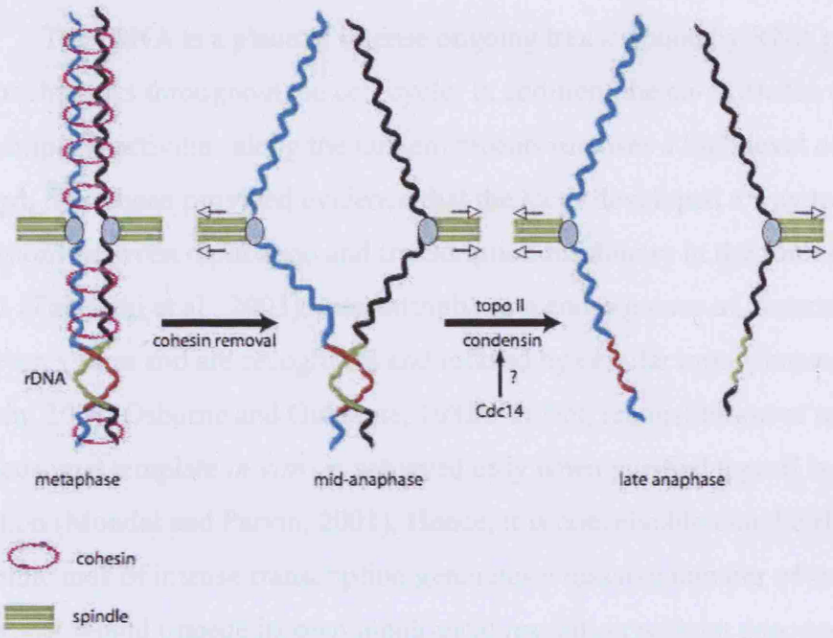

Figure 1.7 Resolution of rDNA cohesion does not require cohesin removal but condensin and topo II activities

A schematic representation shows the rDNA locus on the longest arm of chromosome XII (whose sister chromatids are shown in red and green) held connected until mid-anaphase after removal of cohesin from chromosomes. To dissolve the linkage Cdc14 activates condensin by a yet unknown mechanism. Topo II is also required for sister chromatid resolution at the rDNA.

1.4.4 rDNA linkages correlate with the late resolution of the locus

The rDNA is a place of intense ongoing transcription by RNA pol I and RNA pol III machineries throughout the cell cycle. In addition, the co-existence of replication and transcription activities along the tandem repeats imposes a high level of regulation. In this regard, it has been provided evidence that the locus developed a way to avoid deleterious collisions between replication and transcription machinery in the form of the protein barrier Fob1 (Takeuchi et al., 2003). Interestingly, as a consequence of transcription, specific DNA structures form and are recognized and relaxed by cellular topoisomerases (Mondal and Parvin, 2001; Osborne and Guarente, 1988). In fact, reconstitution of transcription on nucleosomal template *in vitro* is achieved only when purified topo II is added to the reaction (Mondal and Parvin, 2001). Hence, it is conceivable that the rDNA locus as a genomic area of intense transcription generates a massive number of structures within the array that would impede its own topological resolution without concerted action of topoisomerase and condensin. Condensin requirement for rDNA partitioning has been noticed since a while (Freeman et al., 2000). A recent study reports that cell cycle down-regulation of rDNA transcription inversely correlates with condensin's efficiency to bind the rDNA repeats (Wang et al., 2006). Consistently, it has been showed that growing yeast cells in the presence of a transcription inhibitor drug enhances rDNA segregation (Tomson et al., 2006). These data suggest that transcription is incompatible with its resolution perhaps by preventing stable condensin binding to DNA. On the other hand, since transcription continues during anaphase without any sign of abating ((Elliott and McLaughlin, 1979; Sullivan et al., 2004); this study), it is hard to explain how transcription could be fully responsible for sister chromatid linkages if these are dissolved during an unperturbed anaphase.

2 Chapter 2: Genome wide analysis of the condensation machinery in budding yeast

Our mechanistic understanding of the process of chromosome condensation is very poor. Whether or not new condensation activities are yet to be discovered, condensin is today viewed as the most important component for mitotic chromosome structure. This is based on considerable mutational analysis *in vivo* (Bhat et al., 1996; Hirano and Mitchison, 1994a; Hudson et al., 2003; Ono et al., 2003; Saka et al., 1994; Strunnikov et al., 1995). Biochemical *in vitro* experiments complement such data by showing that the mitosis purified condensin holo complex possesses a remarkable DNA supercoiling activity (Kimura and Hirano, 1997; Kimura et al., 1999). Whether, and how this observed *in vitro* activity of condensin is translated into its ability to structure large chromosomes is at present unclear. A possible answer to this will come when, and if, we will be able to reconstitute (and reproduce) the whole condensation process on nucleosomal DNA *in vitro* through purification of all the necessary components for condensin loading and function. Loading onto chromatin is an important component of condensin function. To date, we do not have detailed knowledge about *cis* and *trans* elements required for condensin association to chromatin *in vivo*.

At the resolution of light microscopy, condensin distributes in a reproducible pattern along vertebrate mitotic chromosomes (Hudson et al., 2003; Maeshima and Laemmli, 2003). The rDNA locus has been identified as the site where condensin binding is seen at its highest concentration in *S. cerevisiae* (Freeman et al., 2000). Condensin is also enriched in the nucleolar area in higher eukaryotes (Ouspenski et al., 2000) suggesting that its affinity for rDNA chromatin is conserved. In *S. cerevisiae*, condensin mutants display profound defects in nucleolar segregation, suggesting that an essential role for condensin in budding yeast is to promote resolution of rDNA cluster repeats (Freeman et al., 2000). However, in strains where the episomal rDNA replaces the tandem chromosomal repeats condensin remains essential (Freeman et al., 2000). These results strongly indicate that condensin has non-rDNA targets in *S. cerevisiae*, as it does in higher eukaryotes (Maeshima and Laemmli, 2003; Ono et al., 2004). A low resolution genome-wide localisation study has shown condensin to bind to discrete sites, on average every 10 kb,

along budding yeast chromosomes (Wang et al., 2005). The analysis did not reveal sufficient details to decipher a rule underlying the pattern or common features of the association sites. From this initial study it emerged that the condensin complex tends to bind preferably within putative termination zones of chromosomal DNA replication.

2.1 High resolution pattern of condensin binding along budding yeast chromosomes

To investigate condensin binding to budding yeast chromosomes, we performed chromatin immunoprecipitation followed by hybridisation to whole genome nucleotide micro-arrays using antibodies against both SMC and non-SMC subunits of the complex, namely Smc2 and Brn1. The micro-arrays have been designed in such a way to obtain up to 5 base pairs resolution. To achieve this, adjacent 25-mer oligonucleotides representing the whole genome are tiled at an average of 5 base pair resolution, as measured from the central position of the oligo, creating an overlap between adjacent probes of approximately 20 base pairs. The first question we aimed to address by this approach was determining whether the localisation of the complex changes during the cell cycle. This interest was partly fuelled by knowing that the localisation of the related cohesin complex was recently shown to be dynamic and responsive to local transcriptional activities (Glynn et al., 2004; Lengronne et al., 2004). We first analysed chromatin immunoprecipitates obtained from cells arrested in G1 phase of the cell cycle by treating the cells with the pheromone α-factor. Because it is thought that condensin performs chromatin compaction as a holo complex it was important to assess whether immunoprecipitation of two distinct subunits was generating coincident patterns. Indeed Figure 2.1A shows a similar pattern of association of the two subunits along chromosome V (a full map of condensin association on chromosome V and over the whole genome can be found in Map1 and Appendix respectively). Interestingly, as early as during G1, peaks of association were enriched around the centromere, consistent with an earlier report (Wang et al., 2005). Additional peaks were found at frequent intervals along the chromosome arms as well as close to telomeres. Budding yeast condensin is fully chromatin bound in G1; this is in contrast to other known eukaryotes where condensin appears to get full access to chromatin upon entry into mitosis (Freeman et al., 2000). However, chromosome condensation in this cell cycle phase is at its lowest. We therefore compared the G1 condensin pattern to that of cells

arrested in metaphase by treatment with the spindle poison nocodazole, when mitotic chromosome condensation is fully established (Guacci et al., 1994). The distribution of Smc2 peaks along chromosome V arms was qualitatively indistinguishable from cells in G1, but condensin enrichment at the centromere was more pronounced (Figure 2.1A). The unaltered pattern therefore suggests that mitotic chromosome condensation is not the simple consequence of condensin binding to specific sites, but rather a reaction performed by chromatin bound condensin. Mitosis-specific centromeric enrichment opens the possibility that condensin contributes to the structural integrity of budding yeast centromeres during attachment to the mitotic spindle, as has been observed in metazoan cells (Gerlich et al., 2006a; Oliveira et al., 2005; Ono et al., 2004).

In addition, we analysed the condensin pattern in cells arrested in early S-phase with the replication inhibitor hydroxyurea. Again, the pattern was similar to cells in G1 (Figure 2.1B). Condensin was enriched at the sites of early replication forks that have initiated replication but have stalled in the drug-induced arrest. This is clearly illustrated by the strong correlation of condensin with the regions that have incorporated the nucleotide analogue 5-bromo-2'-deoxyuridine (BrdU) as these were visualised in a parallel experiment. We do not know whether condensin also associates with replication forks during S-phase in physiological conditions or whether the checkpoint triggers its recruitment. The localisation to stalled forks is consistent with observations in fission yeast where condensin is required for cells to engage the replication checkpoint in response to hydroxyurea treatment (Aono et al., 2002).

2.2 *Intergenic enrichment of condensin, independent of a spacing rule*

As discussed in the previous section the condensin complex shows a striking structural similarity with cohesin despite the two distinguished roles *in vivo*. In our efforts to extrapolate a rule that underlies the condensin pattern, we first compared it to the binding pattern of the related cohesin complex. Previous cytological analysis has suggested that, despite their similarity, the two complexes do not overlap in their binding along chromosomes (Ciosk et al., 2000). The cohesin complex is thought to transiently dock at the loading sites in late G1 to then quickly relocate to places of convergent transcription where it can be found throughout the cell cycle up to anaphase onset (Glynn et al., 2004; Lengronne et al., 2004). Therefore we first compared condensin binding sites with the

places where cohesin spends most of its time. Although cohesin and condensin peaks partly overlapped at some sites, the patterns appeared largely distinct from each other (Figure 2.2A). This data was fully consistent with previously reported cytological analysis. Both cohesin and condensin are enriched at centromeres, but even there the peak distribution between cohesin and condensin was diverse. This suggests that the two related complexes differ in aspects of their binding to, or relocation from their loading sites on chromosomes.

As a next step, we addressed whether we could identify common features of condensin binding sites along chromosome arms. We used a peak picking algorithm to assign condensin binding sites over the entire budding yeast genome. We excluded a 40 kb region surrounding each centromere since the observed condensin enrichment at these places might result from a mechanism distinct to that along chromosome arms. (Map 1, Appendix and Table 1). This approach identified 419 peaks (Table 1E), about half of the previously reported number of sites (Wang et al., 2005). The difference stems from our conservative approach to assign only peaks with robust condensin binding. In addition, exclusion of centromeres from our analysis further restricted our collection of condensin binding sites. If on one hand we underestimated the number of actual association sites, on the other we certainly reduced the chance of false positive assignments.

Consistent with the earlier report the number of condensin peaks on each chromosome was proportional to its length (Table 1A; (Wang et al., 2005)). We observed that condensin was preferentially found between open reading frames (ORFs). Only 25% of peaks mapped within an annotated ORF. This turns out to be quite significant since approximately 60% of the chromosome sequence in *Saccharomyces cerevisiae* is covered by ORFs. This suggests that a mechanism exists that excludes condensin from ORFs ($p < 10^{-44}$). In addition, condensin peaks assigned to an ORF were often close to the beginning or end of the ORF. There was no bias with respect to ORF orientation. When all condensin peaks were assigned to their closest inter-ORF region, we found that they equally likely mapped between convergent, divergent and tandem ORFs (Table 1B). This is different from the association pattern of cohesin, which is preferentially found between convergent ORFs (Lengronne et al., 2004).

At this point we asked whether the condensin binding pattern was mediated by specific sequences or by a need for chromosomes to maintain a predetermined spatial geometry. Interestingly, along some, but not all, chromosome arms we observed an apparently regular spacing of peaks. The association sites lie approximately every 15 kb in

distance from each other. This preliminary observation was intriguing because models of mitotic chromosomes have been proposed in which chromatin is folded into equally sized loops that are stabilised by condensin. We therefore tested whether a geometric spacing rule determines condensin association that might be independent of the actual sequence of association. To address this we removed 8.5 kb between two condensin binding sites on the right arm of chromosome V. As this region included four non-essential genes, cells bearing the deletion showed no growth defects. Importantly, as this deletion accounts for half the distance between the two most proximal binding sites, this excluded the possibility that we were perturbing the geometry by removing exactly the unit of the pattern (ca 15 kb). If a spacing rule controlled condensin association, we would expect peaks surrounding the deletion to change their position with respect to the underlying DNA sequence in order to compensate for the disruption introduced in the geometric pattern. Conversely, if chromosomal features act autonomously to recruit condensin, we would expect to see a reduction of the distance between the two neighbouring condensin binding sites. The pattern was disrupted at this locus as shown in Figure 2.2B (bottom panel). The pattern of binding of condensin over the modified chromosome V arm shows that the latter is the case. In response to the deletion, condensin maintained its association relatively to the underlying sequence and the distance between the two peaks decreased. This does not exclude that condensin delineates units of chromatin folding, but suggests that such units are allowed to vary in size, depending on *cis*-acting sequences or chromatin features that define condensin's binding pattern.

2.3 Condensin colocalises with Scc2/4

As discussed in the previous section condensin does not colocalise with cohesin. When comparing the chromosomal binding pattern of condensin with that of the cohesin loader Scc2/4, we noticed nearly coincident colocalisation of the two. In cells arrested in early S-phase with HU, the colocalisation extended to both the constitutive chromosomal association sites as well as stalled replication forks (Figure 2.3A). To evaluate condensin and Scc2/4 binding sites with a more quantitative approach we performed real time quantitative PCR at four distinct loci over chromosome V where we usually see strong enrichment. In this way beside the close qualitative similarity of the patterns, we would be able to compare the intensity of binding at each site and also have a rate of false positives as determined by the ChIP on chip approach. These four sites (Figure 2.3B) were in turn

compared with two other intergenic sites where condensin and Scc2/4 are not associated, thus serving as an internal negative control. Figure 2.3B shows that condensin indeed associates with the four sites as previously displayed by our maps (compare with Figure 2.1A and Map 1). In addition, these DNA sequences were comparably recognised by Scc2. Importantly, the relative intensities of each site remarkably reflected what was previously observed from the whole genome microarray, hence bolstering our whole genome approach as a powerful and accurate tool to analyse association of our marker proteins to chromatin. We also corroborated the apparent visual colocalisation by statistical means. Condensin and Scc2/4 sites were seen on average 3.5 kb from each other. If condensin and Scc2/4 were randomly located over three chromosomes (such as III, IV and V), colocalisation of binding sites (within 3.5 kb) from the two patterns would occur in approximately 5% of the cases ($p<0.0535$) (Table 2.1D).

The localisation of the Scc2/4 complex has never been compared with that of the condensin complex before. We aimed to validate whether condensin colocalises with Scc2/4 by employing an approach that does not rely on PCR amplification of immunoprecipitated DNA fragments. Cytological staining of Scc2 and the condensin subunit Brn1 on spread metaphase chromosomes confirmed close colocalisation of the two proteins (Figure 2.3C). The same was observed on chromosome spreads from other stages of the cell cycle (data not shown).

A recent analysis of the Smc5/Smc6 complex suggested that its chromosomal recruitment in the absence of DNA damage depends on Scc2/4 (Betts Lindroos et al., 2006). This opened the possibility that condensin's association with chromosomes is regulated by Scc2/4, and that Scc2/4 acts as a generic Smc complex loader.

2.4 Scc2/4 stabilises condensin binding to chromatin

To test whether Scc2/4 was required for condensin association with chromosomes, we compared wild type and *scc2-4* mutant cells arrested in early S-phase by HU treatment. Both cultures were shifted to 35.5°C in the arrest, a restrictive temperature for the *scc2-4* allele, for one hour before chromatin immunoprecipitation against Brn1 was performed. Condensin association with its binding sites was still detectable in the *scc2-4* mutant, but the signals were weaker compared to the wild type control (Figure 2.4A). Strikingly, some binding sites remained minimally affected while others showed remarkable loss of binding. This first approach suggested that binding to chromosomes was somewhat compromised.

However, while this technique allows relative quantitative differences to be inferred between loci, it does not speak for the absolute amount of protein bound to chromosomes. To obtain a quantitative estimate of condensin binding, we performed real time quantitative PCR at the six previously characterised sites on chromosome V. In this experiment, cells were first arrested in mitosis by nocodazole treatment and subsequently kept for two hours at 37°C to inactivate *scc2-4*. Under these conditions binding of condensin at all the four tested sites was either abolished or reduced up to two fold (Figure 2.4B). Another standard way to quantify total level of binding of a factor to chromatin in certain conditions (wich does not involve PCR amplification) has been established (Ciosk et al., 2000). We separated whole cell extracts into soluble and chromatin bound fractions and detected condensin in these fractions by Western blotting. Before temperature shift, similar amounts of the condensin subunit Brn1 were present on chromatin from wild type, *scc2-4*, and also *scc4-4* mutant cells. After the temperature shift, the amount of chromatin-bound Brn1 remained constant in wild type cells, but decreased in both *scc2-4* and *scc4-4* mutants (Figure 2.4C). As a control, the level of chromatin-bound histone H3 remained unchanged in all strains at both temperatures. This suggests that the Scc2/4 complex is required to maintain condensin association with chromosomes. However, loss of chromatin binding was not accompanied by enrichment in the soluble fraction. One possibility is that the condensin subunit is unstable under these conditions when not chromosome bound. Indeed, the amount of condensin observed in the soluble fraction is already barely detectable in wild type cells throughout the cell cycle. As a further means of confirmation we immunostained condensin on spread chromosomes from cells of an experiment conducted in the same way to the one described above. While the condensin subunit Brn1 was readily detectable on chromosomes from wild type cells, the signal was significantly weaker in response to inactivation of the *scc2-4* allele (Figure 2.4D). Residual staining often coincided with poorly DAPI-stained regions that likely correspond to the rDNA where condensin is particularly enriched. A direct protein interaction between Scc2/4 and cohesin might be involved in the recruitment of cohesin to chromosomes (Arumugam et al., 2003). We therefore tested whether we could observe a physical interaction also between Scc2/4 and condensin. Using coimmunoprecipitation we could confirm the interaction of Scc2/4 with cohesin, but not condensin (Figure 2.4E). The requirement of Scc2/4 for stable condensin association with chromosomes suggests that the two complexes functionally

interact, even though a physical interaction may be unstable or because Scc2/4 does not support DNA-condensin association via a physical protein-protein interaction.

2.5 Impaired condensin binding in Scc2/4 mutants correiates with impaired chromosome condensation

If Scc2/4 is required for condensin binding to chromatin, we would predict that Scc2/4 should be required for chromosome condensation. To date, chromosome condensation in budding yeast has been monitored by employing FISH (fluorescent *in situ* hybridization) on spread chromosomes (Guacci et al., 1994). To analyse chromosome condensation in live cells, we established a condensation assay based on two lac operator arrays spaced 137 kb from each other on the left arm of chromosome XII and visualised by expression of a lacI-GFP fusion protein. In G1 cells, the average distance between the two GFP-marked loci, measured in three dimensions, was 0.60±0.24 μm. This distance decreased in metaphase arrested cells to 0.43±0.20 μm, consistent with a 1.5-fold mitotic chromosome condensation (Figure 2.5A). These values concord with those obtained by fluorescent *in situ* hybridisation of similarly spaced loci on spread chromosomes (Guacci et al., 1994). We next arrested wild type, *scc2-4* and condensin mutant *brn1-9* cells in metaphase by nocodazole treatment and then inactivated the mutant alleles by temperature shift to 37°C for one hour. While condensation of wild type chromosomes remained intact, the distance of the GFP marked loci in both *brn1-9* and *scc2-4* mutant cells increased. Such distribution resembled that of uncondensed chromosome arms in G1 cells (Figure 2.5B). This suggests that Scc2/4 is required to maintain mitotic chromosome condensation.

We also analysed chromosome condensation of the rDNA locus by visualising the rDNA binding protein Net1 fused to GFP. The rDNA serves as a distinctive cellular marker for chromosome condensation (Guacci et al., 1994; Lavoie et al., 2002) The ribosomal DNA is seen to assume an uncondensed structure in G1 cells (rDNA puff) and to undergo after S phase a series of condensin-dependent intermediates of chromatin organisation ending in a linear rigid structure usually referred to as an rDNA loop. In this experiment, we released wild type, condensin *ycg1-10*, *scc2-4* and *scc4-4* mutant cells from a HU-induced block in S-phase into nocodazole-imposed metaphase arrest at the restrictive temperature. This strategy was a prerequisite to exclude any involvement of sister chromatid cohesion in our condensation assay. Cohesin loading in the HU block at

permissive conditions leads to intact sister chromatid cohesion which in budding yeast is also required for mitotic chromosome condensation. In metaphase, wild type cells displayed characteristic condensed rDNA loops (Guacci et al., 1994). As expected, the rDNA in *ycg1-10* mutant cells showed an uncondensed, puff-like appearance (Figure 2.5C). Both, *scc2-4* and *scc4-4* cells also failed to form rDNA loops. Uncondensed rDNA puffs were also seen in the *scc4-4* mutant, while *scc2-4* cells contained more often a compact rDNA structure, similar to rDNA clusters that have been described as an intermediate of rDNA condensation (Lavoie et al., 2002). These results indicate that inactivation of Scc2/4 results in defective condensation, most likely due to impaired chromosomal association of the condensin complex.

2.6 Condensin binding sites coincide with TFIIIC sites at tRNAs and ribosomal protein genes

The above results suggest that a link between condensin and Scc2/4 exists but leaves open the question of how condensin, and perhaps Scc2/4, recognise the underlying binding sites. During our analysis, we noticed a strong correlation of condensin peaks with tRNA genes along chromosome arms (Figures 2.6A, Table 1C and Map1). Of the 419 condensin peaks identified, 142 (34%) were assigned to within 1 kb of a tRNA gene, with an average distance from the start of the tRNA gene of 66 bp. This represents over half of the approximately 274 tRNA genes in *S. cerevisiae*. On visual inspection, all of the remaining tRNA genes were also found to be bound by condensin, even though they were not recognised by our peak picking algorithm due to the lower intensity of the peaks (Map 1 and Appendix). In addition, we found strong condensin association with several additional RNA polymerase III transcribed genes, including *SNR6*, *SCR1*, *RPR1* and *SNR52*. This correlation suggests that polymerase III transcribed genes contain features that recruit Scc2/4 and condensin to chromosomes.

2.6.1 Condensin association sites coincides with those of TFIIIC

tRNAs and other RNA polymerase III genes are strongly transcribed. Therefore one possibility is that transcription of these elements may determine condensin binding to DNA. However, inhibition of transcription by addition of the RNA polymerase III inhibitor ML-60218 (Wu et al., 2003) to the growth medium did not alter condensin binding to these genes despite remarkably impeding the cells to progress any further through the cell cycle

(data not shown). Instead, an alternative to the above hypothesis was that sequence elements present at RNA polymerase III transcribed genes, and the transcription factors that recognise them, might confer Scc2/4 and condensin binding. Indeed the first step in the assembly of RNA polymerase III machinery is the recognition of a core promoter element (B box) by the transcription factor TFIIIC. TFIIIC interacts *in vivo* and *in vitro* with TFIIIB which establishes contacts with a second promoter element called the A box which in turn provides the first signal for transcription initiation (Schramm and Hernandez, 2002). TFIIIB in turn recruits several additional polypeptides required to sustain transcription including the RNA pol III catalytic core component (Schramm and Hernandez, 2002). Recent studies have found TFIIIC not only at known RNA polymerase III genes, but also numerous additional loci throughout the budding and fission yeast genomes (Harismendy et al., 2003; Noma et al., 2006). It is conceivable that TFIIIC is also able to recognise sequences similar, but not identical to that of the tRNA promoter. Consistently, in budding yeast a variant B box element appears to recruit TFIIIC, but not other components of the RNA polymerase III machinery, to these sites (Moqtaderi and Struhl, 2004; Noma et al., 2006). We therefore tested whether a relationship existed between TFIIIC and condensin binding sites. We performed chromatin immunoprecipitation against epitope-tagged Tfc3, the τ138 subunit of the budding yeast TFIIIC complex that makes direct contact with the B box (Huang and Maraia, 2001). This revealed that TFIIIC colocalised with condensin not only at RNA polymerase III genes, but also at nearly all the remaining binding sites along chromosome arms (Figure 2.6A and Map 2). Only centromeres were an exception, where the strong enrichment of condensin was not reflected by increased Tfc3 binding. Nonetheless, an attentive inspection of centromeres shows that Tfc3 binding profiles were qualitatively over-imposable to the ones of condensin (see 2.6A and Map1 and 2). The nature of centromeric condensin enrichment remains to be further investigated. We confirmed that such colocalisation was statistically significant by performing a peak-picking analysis between condensin and Tfc3 sites (Table 1D).

Thus our results pointed at the B box binding factor Tfc3 as an interesting candidate for condensin loading onto chromatin.

2.6.2 Condensin localises close to ribosomal protein genes and small nucleolar RNAs

The Tfc3 association pattern clearly indicated that this factor interacts with tRNA genes (as expected) as well as several other sites. After careful examination, we comprehended that many condensin and TFIIIC non-tRNA binding sites were actually close to ribosomal protein genes (RPL and RPS) including small nucleolar components (snoRNAs). We therefore evaluated non-tRNA condensin binding sites for their proximity with RPL, RPS and snoRNAs. Of the 416 sites 95 (23%) were assigned within 5 kb of distance from one of these elements (Table 1C). A bias for condensin to lie closer to the terminator rather than to the promoter of these genes was also evident (62 %; Table 1C). This observation is quite interesting with respect to the fact that these genes are strongly transcribed, and that the cohesin complex is often found associated with converging terminators of RNA pol II transcribed genes. Taken together this evidence along with the fact that condensin is excluded from ORFs, it is conceivable that also condensin relocates in response to strong transcriptional activities although intermediate stages of localisation might be too transient to be experimentally captured.

2.6.3 Search for a potential sequence bias mode of condensin binding to chromatin

The condensin pattern of association correlates with TFIIIC. Since the latter is widely regarded as a DNA motif recognising factor we asked whether such a pattern of binding would indeed correlate with B box-like sequences scattered through the whole genome. In particular, it was of our special interest to correlate condensin binding to B box sequences at non-tRNA binding sites. It is possible that the genome is rich in B box-like motifs whose different ranking exactness would in turn reflect into the efficiency of TFIIIC binding (and maybe the chance of each of those elements to develop into functional condensin binding sites). Interestingly, Tfc3 signals at tRNAs are usually more intense than those at non-tRNA sites (Map 2).

A B box motif has been agreed as the sequence of nucleotides that with good approximation is found embedded within tRNA coding sequences (G/AGTTCGANC/TCC/T) (Huang and Maraia, 2001). We used an unbiased approach (MEME algorithm) to search for common sequence motifs within 2 kb regions surrounding

the assigned condensin peaks (Roth et al., 1998). The algorithm for each of the condensin peaks did actually list sequences highly resembling the B box consensus. This may suggest that a B box-like element recognised by TFIIIC, delineates every condensin binding site, and by inference those of the Scc2/4 complex. However, B box sequences are short and within tRNA genes several variants of the consensus can be seen, suggesting that the B box-like sequences are indeed degenerate consensuses. In fact, B box-like sequences could be scattered very frequently along the sequence of DNA. This also implies that there are far more B box motifs than condensin binding sites. Thus determinants in addition to the primary nucleotide sequence are important in defining true binding sites.

This preliminary observation left open two possibilities. First, the correlation we find between condensin and B boxes may be just coincidental, due to the fact that B box-like sequences occur very often along the DNA sequence. Alternatively, B boxes do define condensin binding sites but this cannot be verified by employing a mathematical search tool as it would necessarily spot degenerate motifs at each screened site.

2.6.4 Tfc3 is required for stable association of condensin with chromatin

The previous genome-wide data indicates that a link exists between condensin and TFIIIC irrespective of whether or not a DNA sequence is involved.
We therefore asked whether TFIIIC serves as a component of the condensin loading machinery. To this end we made use of the *tfc3-tsv115* conditional mutant allele (Lefebvre et al., 1994) to assess whether inactivation of Tfc3 would result in a loss of condensin binding at both tRNA and non-tRNA binding sites. At the same time the fact that Scc2/4 also closely occupies the same sites as condensin prompted us to include this complex in our analysis. We shifted exponentially growing cultures of wild type and *tfc3-tsv115* mutant cells to the restrictive temperature of 37°C, and analysed chromosome association of Scc2/4 and condensin on spread chromosomes. We followed the dynamics of Scc2/4 and condensin binding to chromatin by immunostaining of the epitope tagged Scc4 and Brn1 proteins respectively. For 4 hours after the temperature shift, both mutant and wild type cells continued to grow without noticeable difference as suggested by optical density measurements taken during the course of the experiment. However, association of both Scc4 and Brn1 was reduced by about 50 % in the *tfc3-tsv115* mutant compared to wild type chromosomes (Figure 2.6B). The chromosome binding defects after 4 hours were therefore

due to a role of TFIIIC in recruiting or stabilising Scc2/4 and condensin on chromosomes. To gain a more confident quantitative assessment we then performed real time quantitative PCR at the previously characterized condensin binding sites. Indeed Figure 2.6C shows that in the mutant cells condensin association is reduced about two fold at its canonical binding sites (especially at the ribosomal protein genes). This result suggests that TFIIIC stabilises condensin-DNA interactions. One may explain that the partial effects on condensin binding to chromatin caused by the inactivation of Tfc3 could be attributed to an indirect effect rather than a direct one. Although this remains a possible scenario it is plausible that the *tfc3-tsv115* mutation behaves hypomorphically in respect of condensin recruitment onto chromatin.

2.7 A B box defines a minimal condensin binding site

We then focused on the identification and characterisation of the *cis*-acting elements for condensin loading.

Two key aspects of our findings reinforced the hypothesis of a direct link between the Tfc3 promoter and condensin binding. First, condensin correlates with tRNA genes where TFIIIC is known to be associated. Second, condensin associates with TFIIIC also in non-tRNA genes (mostly at RP genes and snoRNAs). The B box could therefore serve as a *cis*-acting element for recruiting condensin through TFIIIC. From this hypothesis two key predictions would follow.

First, creating an artificial B box in a region where condensin binding is poor would now target condensin to this region.

Second, removal or mutation of a tRNA or even just the B box within the tRNA should result in the loss of condensin binding at that locus.

2.7.1 A B box is the minimal *cis*-acting element for condenisn binding to DNA *in vivo*

We tested the first prediction by initially integrating a tandem of two tRNA sequences (including upstream TATA and T-rich terminator sequences) in a chromosomal region not bound by condensin (Figure 2.7A upper left panel). These do contain B boxes and they should be transcribed. The tRNA sequence employed was generated by PCR from the natural tRNA (*tH(GUG)E1*) (located around coordinates 207000 of chromosome V), cloned into a plasmid and integrated upstream *LSM4* at coordinate 386500. Strikingly, this

newly made locus was now targeted by condensin (2.7A upper panel). The above result indicates that within the tRNA sequence something contains the property of recruiting condensin. Because our previous experiments correlated condensin with TFIIIC within and also outside tRNA genes, we were tempted to test whether just a single B box integrated in the same genomic location would be sufficient to recruit condensin. A canonical B box as found in several tRNA genes was integrated upstream of *LSM4*. This, amazingly, also resulted into a small yet distinct association of condensin at the locus (Figure 2.7B). Interestingly integration of both tRNA or B box sequence led condensin to associate with the terminator of the *LSM4* gene perhaps suggesting that its transcription triggers relocation of some molecules. This observation is interesting in respect of the known transcription-dependent relocation of the related cohesin complex. Now it was important to assess whether the newly made condensin binding site would correlate with binding of Tfc3 at the locus. In fact a sharp signal for Tfc3 binding at this locus was now visible, indicating that Tfc3 is indeed capable of recognizing a B box inserted in this genomic region *in vivo* (Figure 2.7B). Notably, the binding of Tfc3 (and condensin) to such isolated B boxes generates a signal several fold less intense than what is observed at B boxes embedded within the tRNA sequences. The reason for this observation is unclear but it could suggest that within tRNAs Tfc3 binds DNA more stably due to additional inputs that reinforce the interaction with other factors and/or DNA (see next paragraph). These results demonstrate that the B box serves as a minimal *cis*-acting element *in vivo* to prime condensin binding to DNA.

2.7.2 B boxes and tRNA sequences along with other chromatin features contribute to the formation of functional condensin binding sites

A second important prediction is that removal of a tRNA or even just a B box sequence should result in the loss of condensin binding at that locus. To test this possibility we first tested whether eliminating the sequence encoding a B box within a natural tRNA would lead to loss of condensin binding. To address this question we chose a strong condensin association site coincident with tRNA *tE(UUC)E2* on chromosome V. The B box within this tRNA could be easily identified (GGTTCGACTCC) and the six core base pairs were replaced by an equally long random sequence. When we immunoprecipitated DNA cross-linked by Brn1 from this region we could detect an almost unaffected signal at

the locus as compared to the unmodified tRNA (Figure 2.7C). This result suggests that at natural tRNA genes the establishment of a condensin association site is mediated by a B box consensus as well as additional chromatin features developed around the tRNA sequence. To test whether this was the case we now carried out a deletion of a tRNA coding sequence and we replaced it with a URA3 marker. We removed just the coding sequence of a different tRNA *tE(UUC)J* (on chromosome X) and replaced it with the URA3 marker gene. Upon deletion the binding of condensin at the locus was still visible although reduced (Figure 2.7D). Notably, a comparable binding site formed a few kilobases upstream of the deleted region that was absent in the control. Because the effects on condensin association were not as dramatic as expected we were now tempted to assess whether Tfc3 could still be detected at this tRNA-deleted locus. When we immunoprecipitated Tfc3 we could indeed note that it was still binding at the locus (Figure 2.7D). However, a robust decline in intensity association was also evident. This result can be accounted for by acknowledging the presence of more than one Tfc3 molecule bound at natural tRNAs *in vivo*. Conversely, *in vivo* association of a single Tfc3 molecule with DNA might be supported by other chromatin related features. These results together suggest that condensin association sites are primed in a sequence-specific way, through Tfc3. It is possible that once an association site is established, additional features (e.g. epigenetic regulation) contribute to the development of a productive condensin binding site. The finding that even Tfc3 cannot be fully displaced by removal of a tRNA sequence may be consistent with this view and with a TFIIIC dependent mode of condensin association to chromatin.

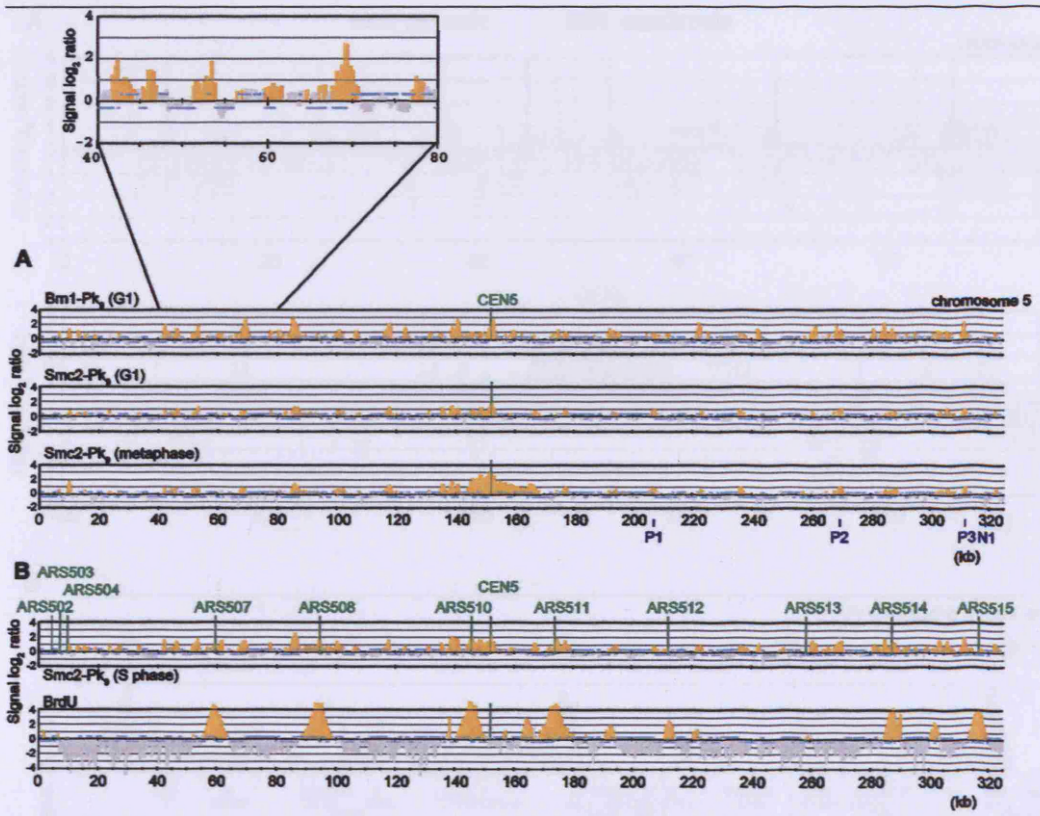

Figure 2.1 Condensin pattern of binding during the cell cycle

(**A**) Comparison of the condensin subunits Smc2-Pk9 and Brn1-Pk9 between G1 and metaphase.

Cultures of strain Y2315 (*MATa SMC2-Pk9*) and Y2200 (*MATa BRN1-Pk9*) were arrested in G1 (by α-factor), or in metaphase (by nocodazole). In the insert (above) is shown an enlarged portion of a 40 kb region. Each bar represents the average of 16 oligonucleotide probes within adjacent 300 bp windows. The y-axis scale is log2. Orange signals represent significant binding as described (Katou et al., 2003). Blue bars above and below the midline represent ORFs transcribed from left to right and opposite, respectively. The centromere and origins of replication are depicted in green. P1 – P3 indicate three of the four positive, and N1 one of the two negative, association sites that were confirmed by quantitative PCR (compare Figure 2.3)

(**B**) Accumulation of Smc2 at stalled replication forks.

Cells of strain Y2315 were synchronised in G1, and released into medium containing (HU) for 2 hours. Cells of strain K5601 (*MATa GPD-TK*) were treated in the same way, but were released from α -factor arrest in the presence of 400 μg/ml bromodeoxyuridine (BrdU). Chromatin immunoprecipitation against Smc2-Pk9 or BrdU was performed.

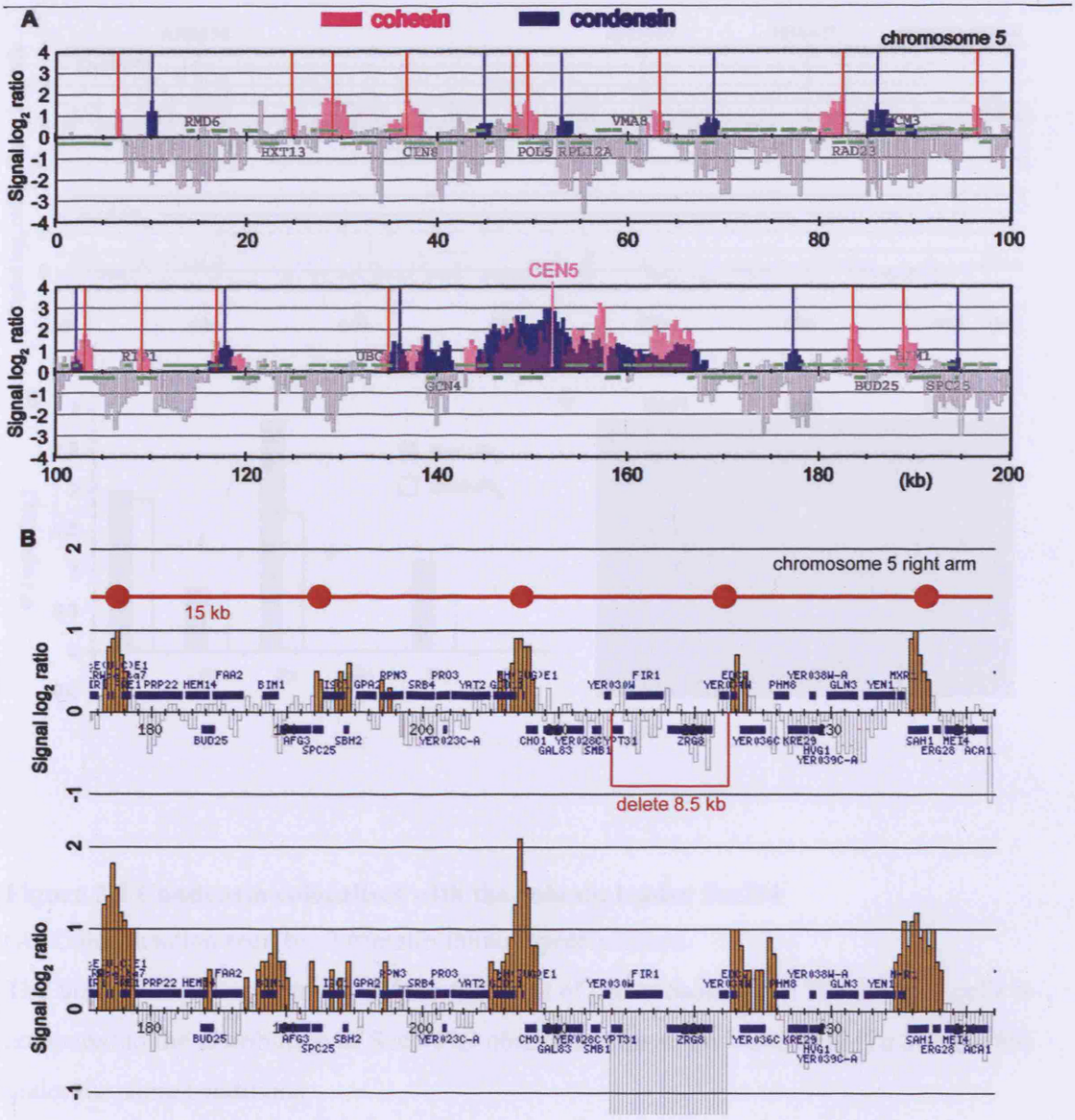

Figure 2.2 Characterization of condensin binding sites along chromosome V

(**A**) Condensin binding sites are distinct from those of the related cohesin complex. The distribution of Smc2-Pk9 in nocodazole arrested cells from the experiment in Figure 2.1 (significant peaks in blue) was overlaid with that of Scc1-HA6 (red; (Lengronne et al., 2004). 200 kb of chromosome V are shown. ORFs are depicted in green.

(**B**) Condensin binding does not follow a geometric spacing rule but adheres to sequence or chromatin determinants. The pattern of Brn1-Pk9 within 67 kb of chromosome V right arm is shown in strains Y2200 and Y2565 (*MATa BRN1-Pk9 ChrVΔ213,898-222,402*) (above). In the bottom panel the same chromosome arms harbours an 8.5 kb deletion between two neighbouring condensin binding sites.

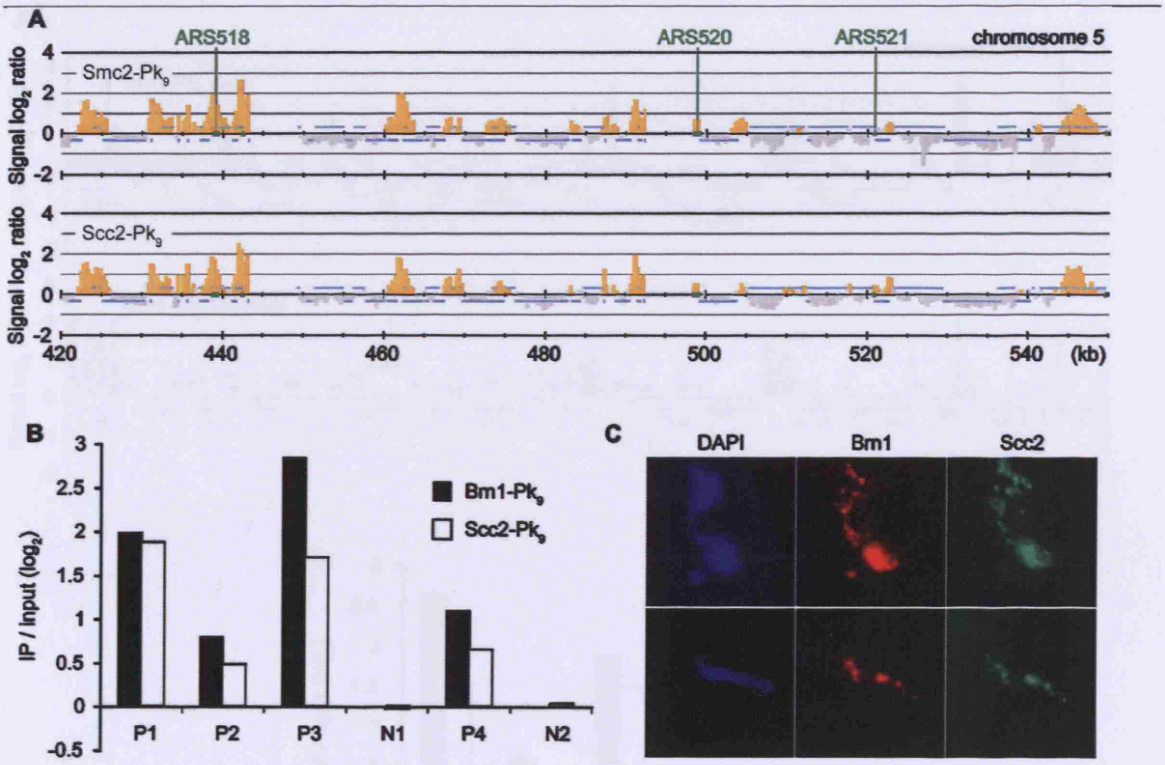

Figure 2.3 Condensin colocalises with the cohesin loader Scc2/4

(**A**) Colocalisation seen by chromatin immunoprecipitation.

The Smc2-Pk9 pattern along a 130 kb fragment of chromosome V in HU arrested cells is compared to the distribution of Scc2-Pk9 obtained from strain Y2422 (*MATa SCC2-Pk9*) under the same conditions.

(**B**) Confirmation of colocalisation by chromatin immunoprecipitation followed by quantitative PCR analysis. Four positive (P1 – P4) and two negative (N1, N2) association sites identified by microarray analysis (compare Figure 2.1, Map1) were examined. Enrichment over a whole genome DNA sample is depicted, with the average of the two negative association sites normalised to 0 = log2 1.

(**C**) Colocalisation on chromosome spreads.

Strain Y2717 (*MATa BRN1-myc9 SCC2-HA6*) was arrested in metaphase by nocodazole treatment. Chromosome spreads were stained to detect the epitope tagged condensin subunit Brn1-myc9 and Scc2-HA6.

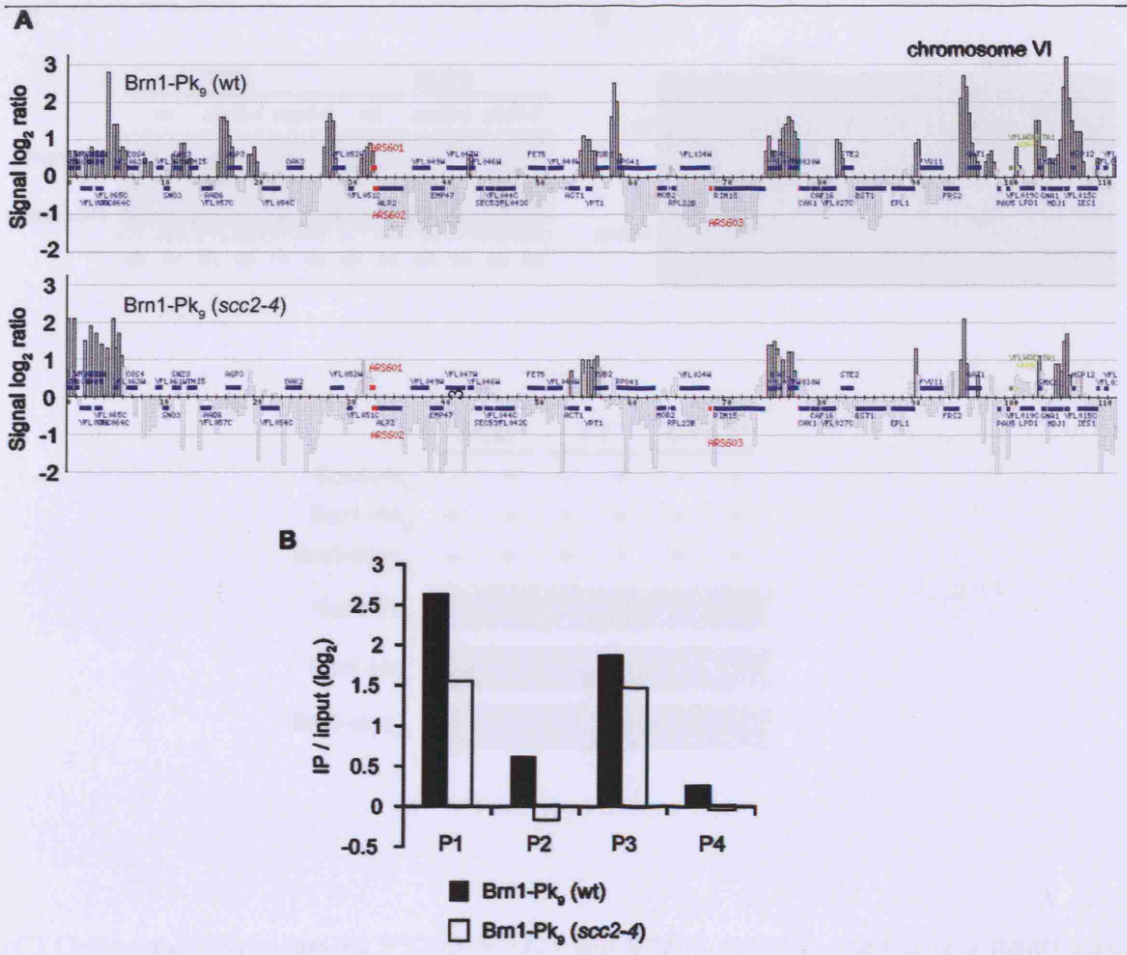

Figure 2.4 Scc2/4 is required to maintain condensin association with chromosomes

(**A**) Chromatin IPs were obtained from cells of strains Y2200, Y2421 (*MATa scc2-4 BRN1-Pk9*) arrested in S phase by treatment with HU at 23°C and shifted to 35.5°C for 2 hours. Maps are showing the left 110 kb end of chromosome 6.

(**B**) Quantification of condensin association under the same conditions by chromatin immunoprecipitation followed by real time PCR analysis of the four binding sites (P1 – P4) characterised in Figure 2.3B. Again, the two negative sites were included in the analysis and used for normalisation (not shown).

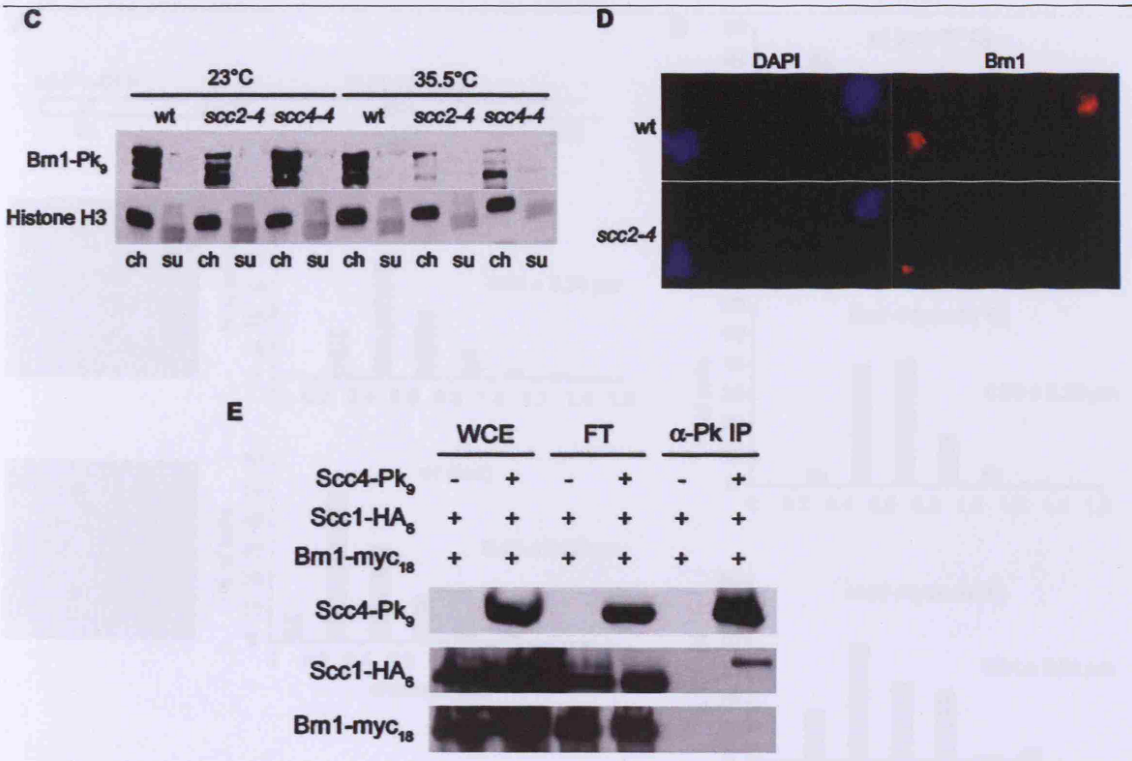

(**C**) Cell extracts from strains Y2200, Y2421 and Y2611 (*MATa scc4Δ scc4-4 BRN1-Pk9*), arrested in metaphase by nocodazole treatment at 23°C and shifted to 35.5°C for 1 hour, were separated into soluble and chromatin bound fractions and analysed by Western blotting against the condensin subunit Brn1-Pk9 and histone H3 as a chromosomal loading control.

(**D**) Chromosome spreads of nocodazole arrested cells of strains Y2521 (*MATa BRN1-HA6 SCC1-Pk9*) and Y2423 (*MATa scc2-4 BRN1-HA6 SCC1-Pk9*) shifted to 35.5°C for 1 hour were stained for the condensin subunit Brn1-HA6.

(**E**) An interaction between Scc2/4 and cohesin, but not condensin, detected by coimmunoprecipitation. Cell extracts from exponentially proliferating cultures of strains Y2821 (*MATa SCC1-HA6 BRN1-myc18*) and Y2822 (as Y2821, but *SCC4-Pk9*) were prepared, and coimmunoprecipitation of Scc1-HA6 and Brn1-myc18with Scc4-Pk9 was analysed. Aliquots of the whole cell extract (WCE), flow through after immunoprecipitation (FT), and of the immunoprecipitate (IP) were analysed by SDS-PAGE followed by Western blotting.

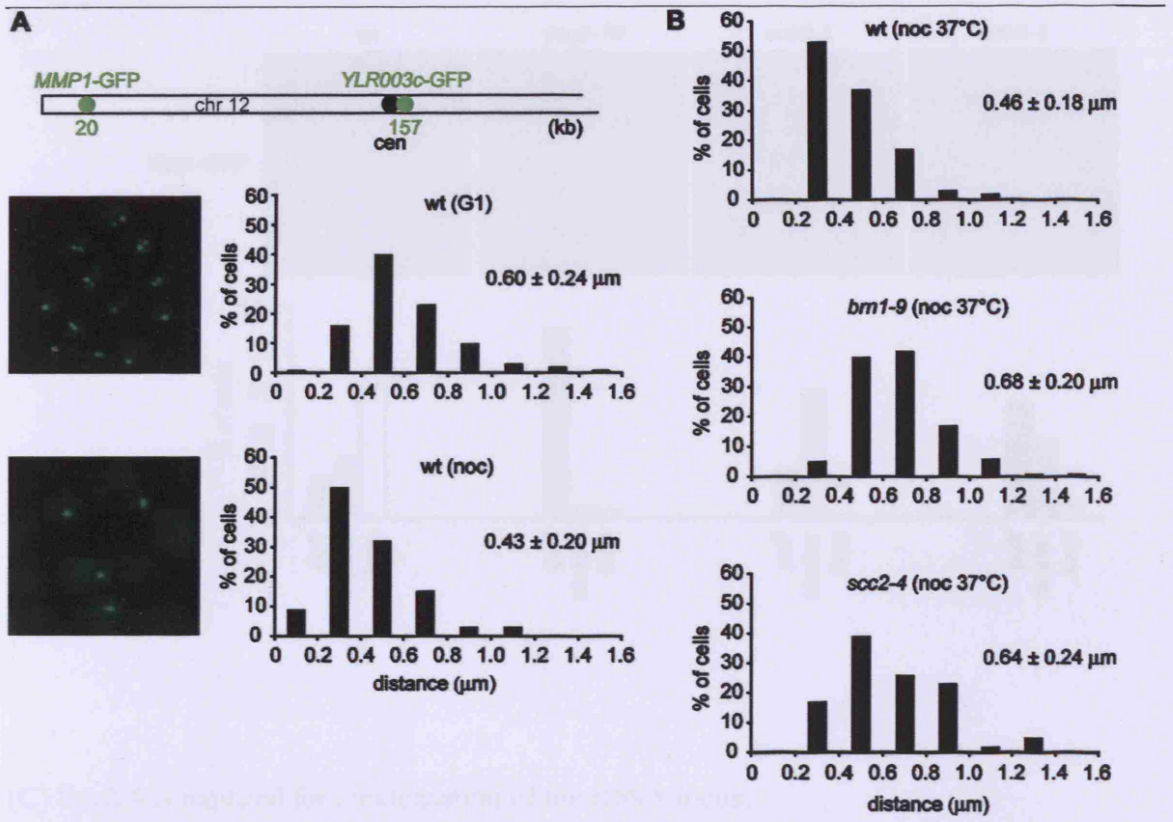

Figure 2.5 Scc2/4 requirement for chromosome condensation

(**A**) A condensation assay for the chromosome XII left arm. Strain Y2869 (*MATa lacOs::YLR003c-1 lacOs::MMP1 LacI-GFP*) was arrested in G1 by α -factor, and in metaphase by nocodazole treatment. Chromosome condensation was assessed by measuring the distance between the two fluorescent loci located 137 kb from each other on chromosome 12 in three dimensions. Examples of wild type cells in G1 and metaphase are shown, as well as the distribution of the distances measured. The mean distances, with their standard deviations, are given.

(**B**) Scc2/4 is required to maintain chromosome arm condensation.

Metaphase arrested cells of strains Y2869, Y3104 (as Y2869 but *brn1-9*) and Y2887 (as Y2869 but *scc2-4*) were shifted to 35.5°C for 1 hour, and the condensation status of the chromosome XII left arm analysed as in (A).

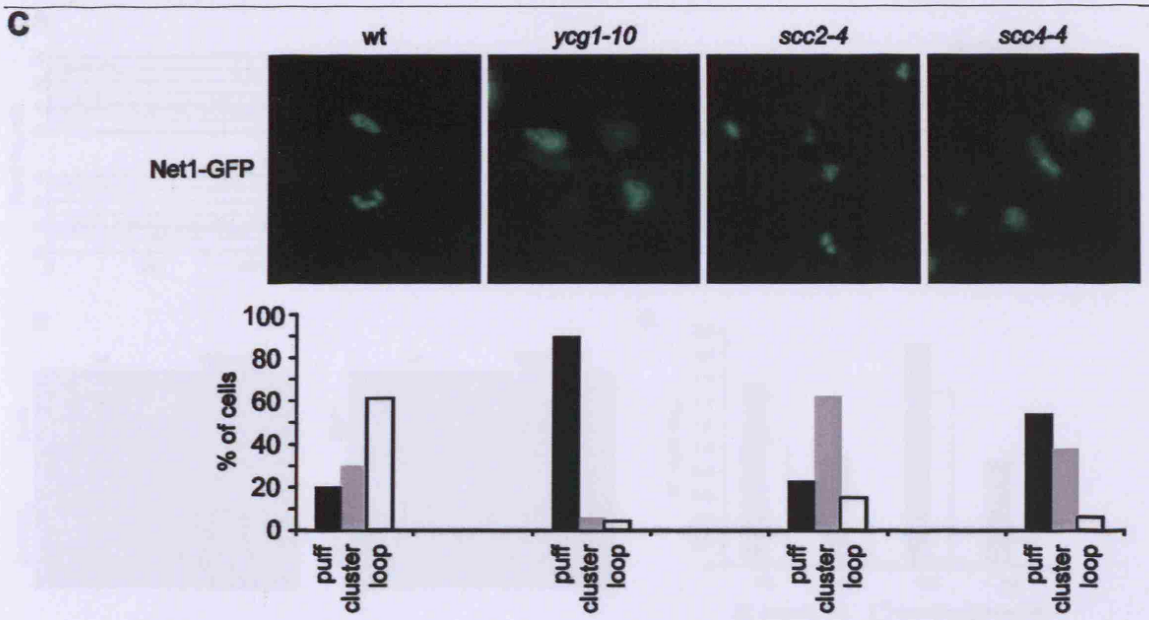

(**C**) Scc2/4 is required for condensation of the rDNA locus.

Strains Y2727 (*MATa NET1-GFP*), Y2729 (*MATa ycg1-10 NET1-GFP*), Y2750 (*MATa scc2-4 NET1-GFP*) and Y2728 (*MATa scc4Δ scc4-4 NET1-GFP*) were arrested in S-phase by HU treatment at 23°C, and released into nocodazole containing medium at 35.5°C. rDNA condensation in these strains was analysed by visualising the rDNA binding protein Net1 fused to GFP. Examples of the cells are shown, and the number of nuclei displaying puff-, cluster-, or loop-shaped rDNA loci (Lavoie et al., 2004) were counted in > 100 cells in each sample.

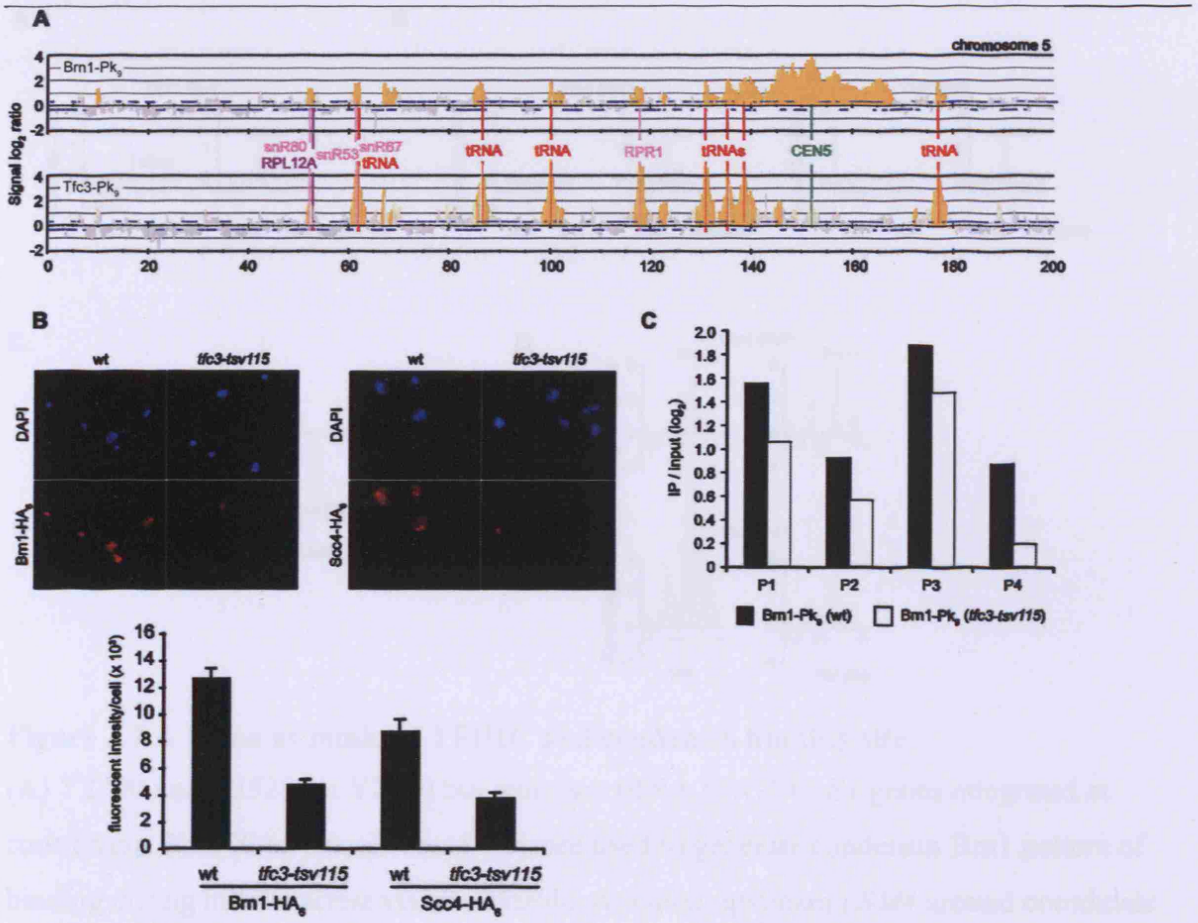

Figure 2.6 Condensin localisation characterized by the RNA polymerase III transcription factor TFIIIC

(A) Colocalisation of condensin with TFIIIC at tRNA genes, and genes encoding ribosomal protein components and small non-coding RNAs. Strains Y2200 and Y3096 (*MATa TFC3-Pk9 BRN1-HA6*) were arrested in metaphase by nocodazole treatment and chromatin immunoprecipitation against Brn1-Pk9 and Tfc3-Pk9 performed. A 200 kb region including the centromere of chromosome V is shown.

(B) Reduced chromosome association of Scc2/4 and condensin in the temperature sensitive Tfc3 mutant tfc3-tsv115. Cultures of strains Y3343 (*MATa SCC4-HA6*), Y3344 (as Y3343 but *tfc3-tsv115*), Y3345 (*MATa BRN1-HA6 SCC1-Pk9*) and Y3346 (as Y3345 but *tfc3-tsv115*) were shifted to 37°C for 4 hours, and chromosome binding of Scc4-HA6 and Brn1-HA6 was analysed by staining on spread chromosomes.

(C) Quantitative PCR analysis of Brn1-Pk9 chromatin immunoprecipitates from strains Y2200 and Y3406 (as Y2200 but *tfc3-tsv115 SCC4-HA6*) after 4 hours at 37°C. Four binding sites (P1 – P4) were analysed, and normalised against the two negative sites (compare Figure 2.3B).

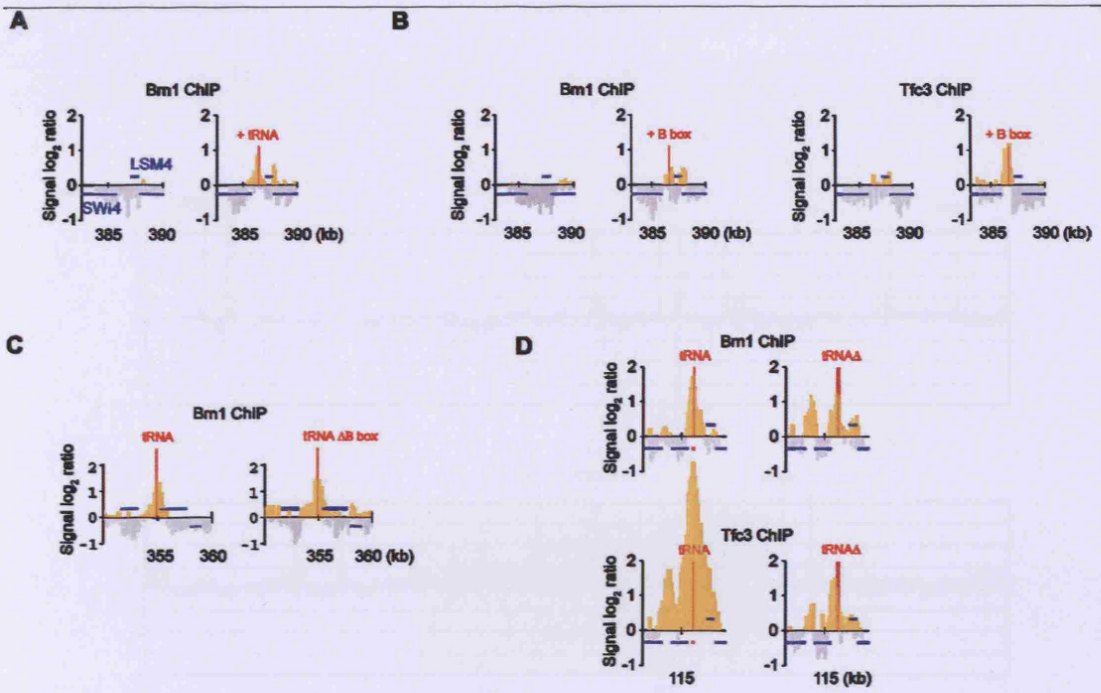

Figure 2.7 A B box as minimal TFIIIC and condensin binding site

(**A**) Y2200 and Y3528 (as Y2200 but with two tRNA *tH(GUG)E1* genes integrated at coordinates 386500 on chromosome V) were used to generate condensin Brn1 pattern of binding during mitotic arrest via nocodazole. A region upstream *LSM4* around coordinate 385000 on chromosome V is showed.

(**B**) Condensin Brn1 pattern of binding (above panels) is shown around LSM4 gene on an untouched chromosome V (Y2200) and when an ectopic B box has been integrated upstream of *LSM4* coding sequence (Y3485; as Y2200 with a B box). Tfc3 pattern of binding (panels below) in the same conditions is also shown (Y3096 and Y3475 which is as Y3096 with an ectopic B box promoter inserted as in Y3485). Signal log ratio above the zero line is arbitrarily coloured in dark yellow for simplicity.

(**C**) Removal of a B box does not preclude condensin binding at natural tRNAs. Y2200 and Y3528 (as Y2200 but with a B box motif replaced with random sequence at tRNA *tE(UUC)E2* on chromosome V). A region around 355000 is shown.

(**D**) Deletion of a tRNA sequence affects but not abolishes condensin association to DNA. Condensin binding at tRNA gene *tE(UUC)J* before (Y2200) and after exact deletion of the tRNA coding sequence replaced by the *URA3* gene (Y3521; as Y2200 but with tRNA sequence of *tE(UUC)J* on chromosome X replaced by *URA3*) is shown (above). Tfc3 pattern of binding under the same conditions (Y3096 and Y3522 which is as Y3521 but *TFC3-myc18*) in the same region is shown in the panels below.

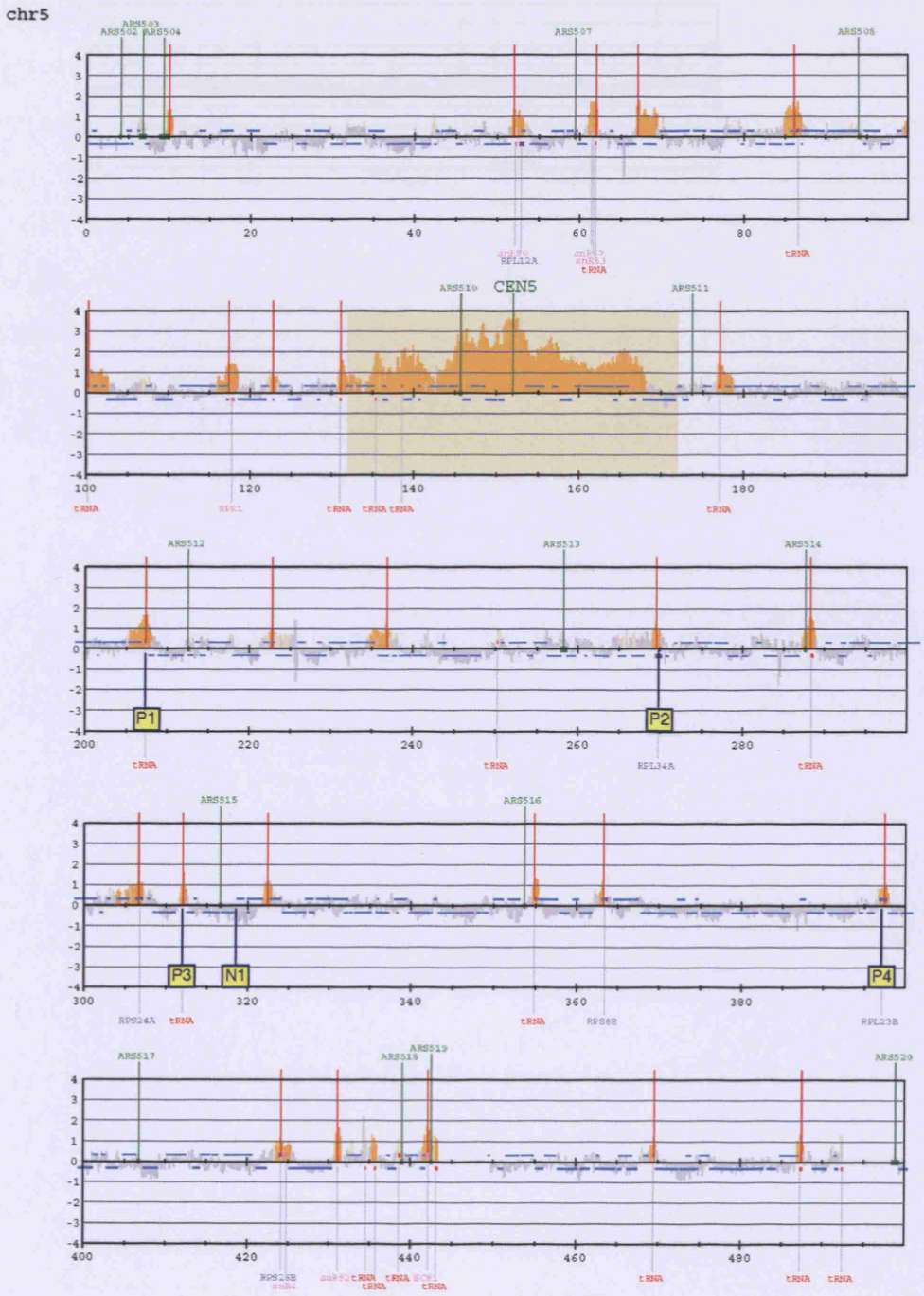
chr5
ARS503
ARS502
ARS504
ARS507
ARS508
CEN5
ARS510
ARS511
ARS512
ARS513
ARS514
P1
P2
ARS515
ARS516
P3
N1
P4
ARS517
ARS518
ARS519
ARS520

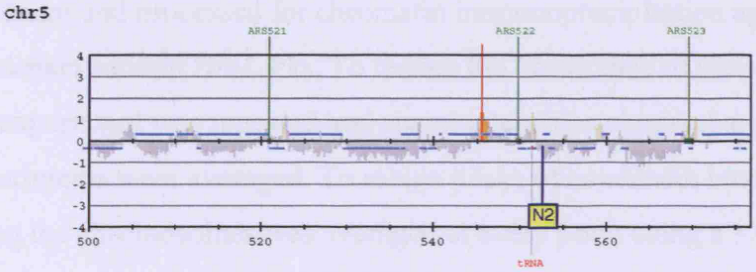

Map1. Legend in next page

Map 1. Condensin association along the budding yeast chromosome V

Cells of strain Y2200 (*MAT*a *BRN1-Pk$_9$*) were arrested in metaphase by nocodazole treatment and processed for chromatin immunoprecipitation against the epitope-tagged condensin subunit Brn1-Pk$_9$. To reduce the occurrence of unspecific background signals, the experiment was repeated and signal intensities obtained at every locus in the two experiments were averaged. To assign peaks of condensin binding, Brn1-Pk$_9$ association along the chromosomes was averaged at every point using a +/- 1,000 bp sliding window. Peaks of condensin association were then automatically picked depending on a signal p value relative to a whole genome DNA sample of <0.001 (orange colouring in the bar representation), and a signal $\log_2$ ratio of at least 0.6. A 40 kb region surrounding the centromeres, shaded in yellow, was excluded from this analysis. The locations of four positive (P1 – P4) and two negative (N1, N2) condensin bindings sites on chromosome V, that were analysed by chromatin immunoprecipitation followed quantitative real time PCR, are indicated.

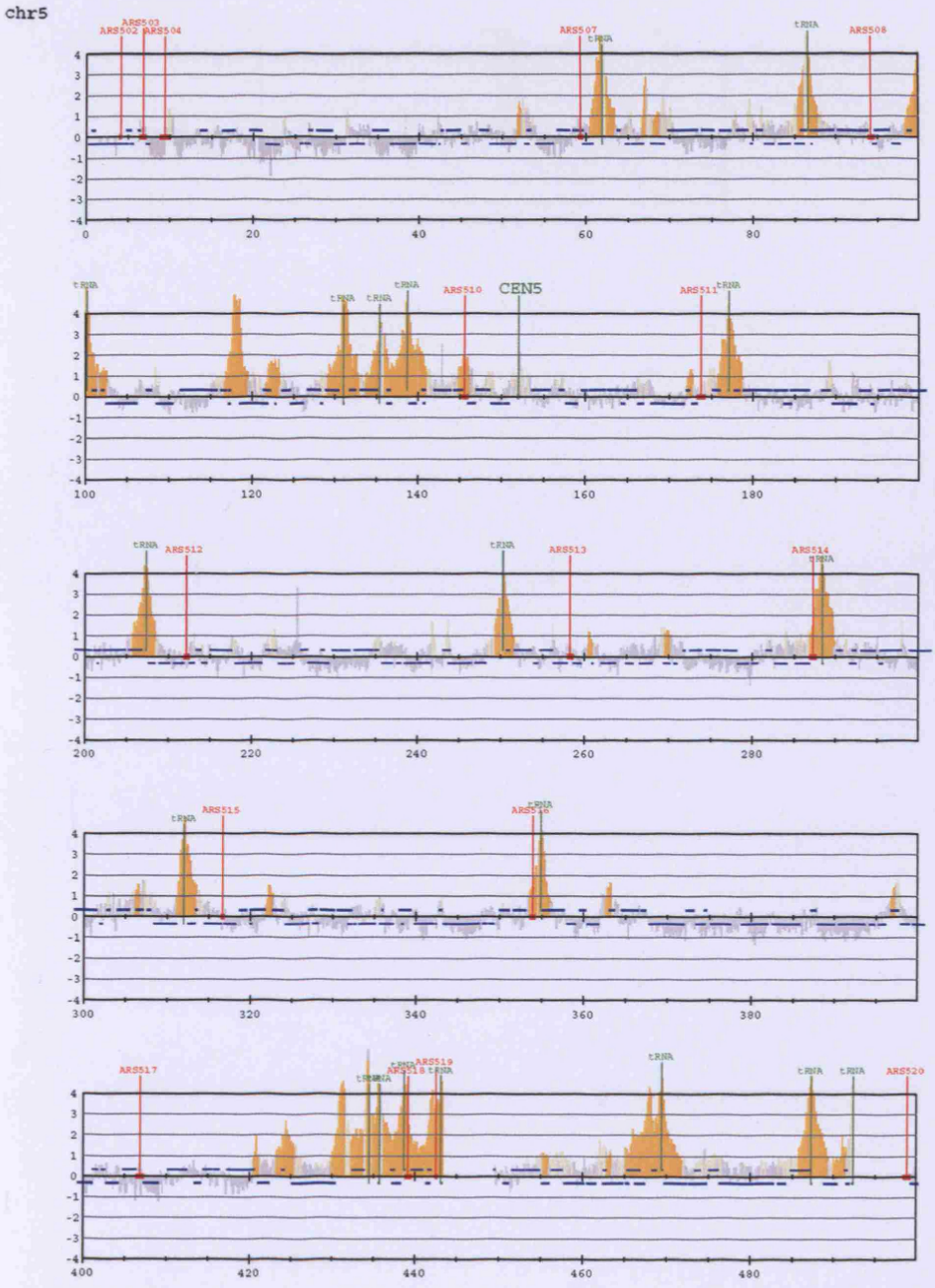
chr5
ARS503
ARS502
ARS504
ARS507
tRNA
tRNA
ARS508
ARS510
CEN5
ARS511
ARS512
ARS513
ARS514
ARS515
ARS516
ARS517
ARS519
ARS520

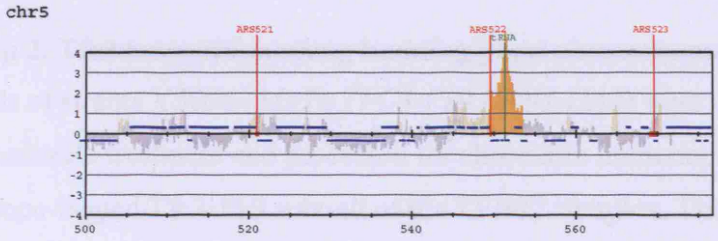

Map2. Legend in the next page

Map 2. Tfc3 association along budding yeast chromosome V

Cells of strains Y3096 (*MATa TFC3-Pk9 BRN1-HA6*) were arrested in metaphase by nocodazole treatment and processed for chromatin immunoprecipitation against the epitope-tagged Tfc3-Pk9 subunit of the TFIIIC complex. The binding pattern of Tfc3-Pk9 along budding yeast chromosome V is shown. Significant peaks in dark yellow were identified as for Map 1.

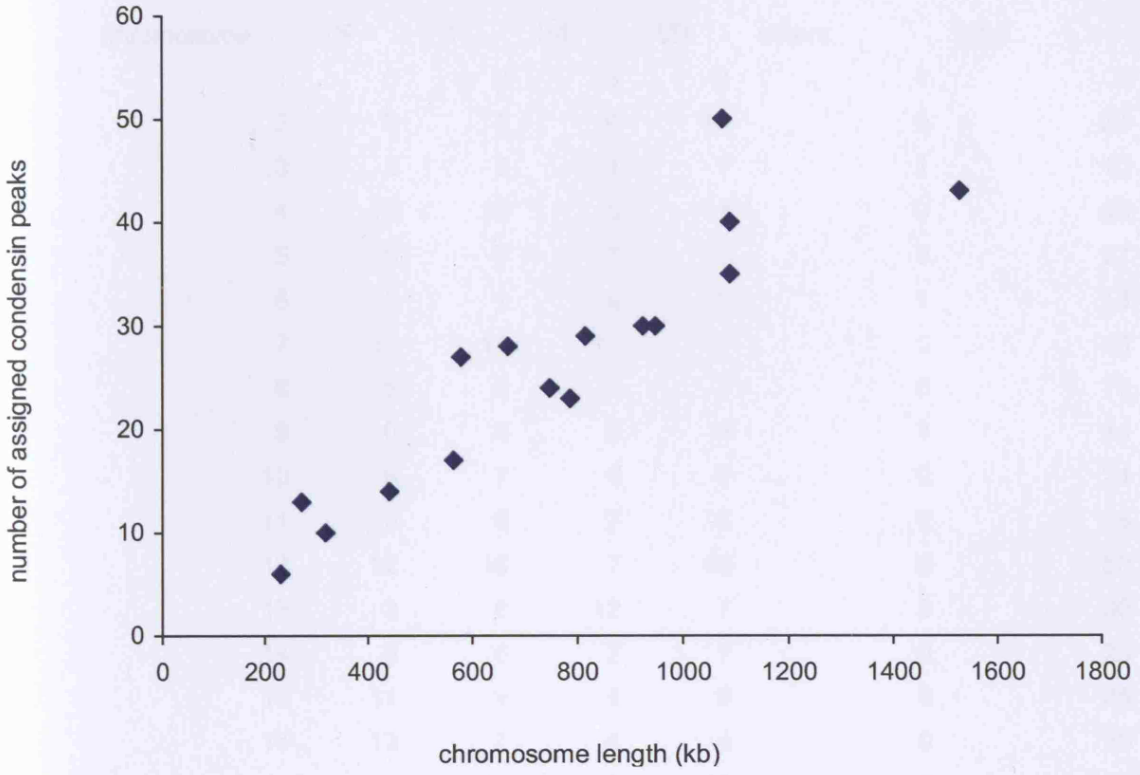

Tab 1. Statistical analysis of the condensin peaks identified

(**A**) Condensin distribution along the 16 chromosomes as a function of chromosome length. The linear relationship between the number of assigned condensin peaks with chromosome length suggests that the density of condensin is similar on all chromosomes

chromosome	F/F	F/R	R/F	R/R	others	total
1	0	2	3	0	1	6
2	5	8	6	10	0	29
3	2	5	1	1	1	10
4	15	12	5	11	0	43
5	8	7	7	5	0	27
6	1	1	4	6	1	13
7	11	11	11	7	0	40
8	5	6	3	3	0	17
9	0	4	5	4	1	14
10	6	7	4	7	0	24
11	9	6	7	4	2	28
12	12	16	7	15	0	50
13	3	8	12	7	0	30
14	8	6	2	7	0	23
15	11	9	9	6	0	35
16	13	7	4	6	0	30
	109	115	90	99	6	419
%	26.39	27.85	21.79	23.97		
expected %	24.35	25.92	26.06	23.67		
enrichment	1.084	1.074	0.836	1.013		

(**B**) Condensin peak distribution relative to open reading frame (ORF) orientation. Of the 419 assigned condensin peaks, 312 lie between ORFs (inter-ORF regions). The 107 peaks that lie within ORFs were assigned to their closest inter-ORF region, then the orientation of the two flanking ORFs was analysed. The four possible orientations of neighbouring ORFs are forward/forward (F/F, i.e. tandem ORF orientation), forward/reverse (F/R, i. e. convergent ORF orientation), reverse/forward (R/F, i. e. divergent ORF orientation) and reverse/reverse (R/R i. e. again tandem ORF orientation). The table below summarises the observed condensin peak distribution, compared to the expected distribution if condensin peaks were randomly distributed between the inter-ORF regions present along the 16 chromosomes. The actual distribution is not significantly different from random.

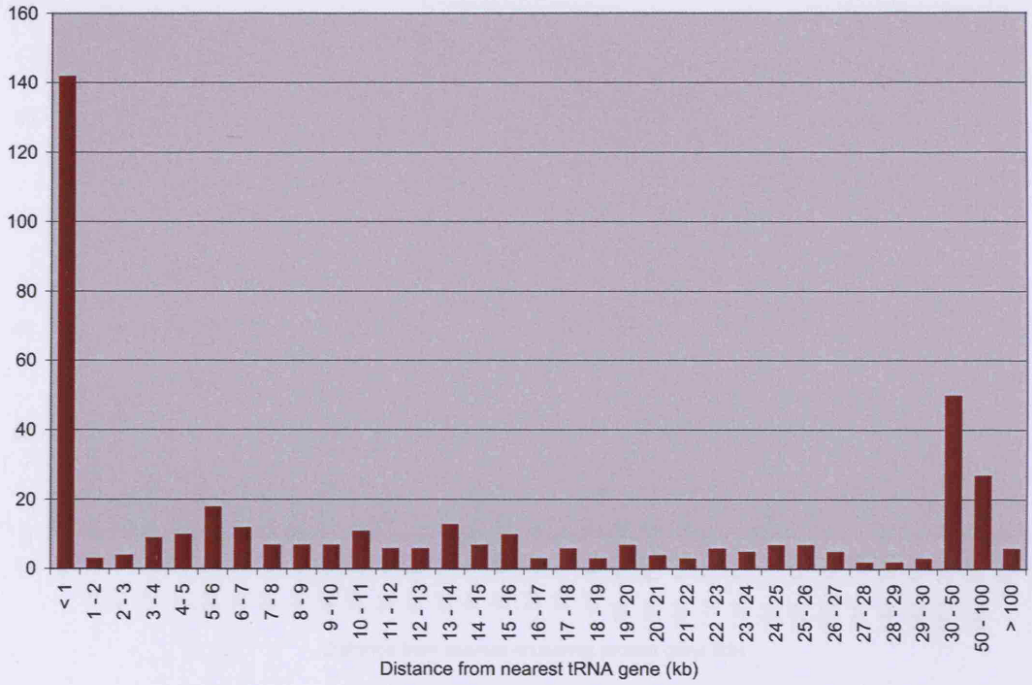

(**C**) Condensin peaks are enriched at tRNA genes and genes encoding ribosomal protein components. (**i**) The distance of all assigned condensin binding sites from the nearest tRNA gene is depicted. 142 of 419 (34%) condensin peaks are found within 1 kb from a tRNA. The average distance of these to the start of the tRNA gene is 66 bp, implying a close link of these condensin peaks with tRNA genes.

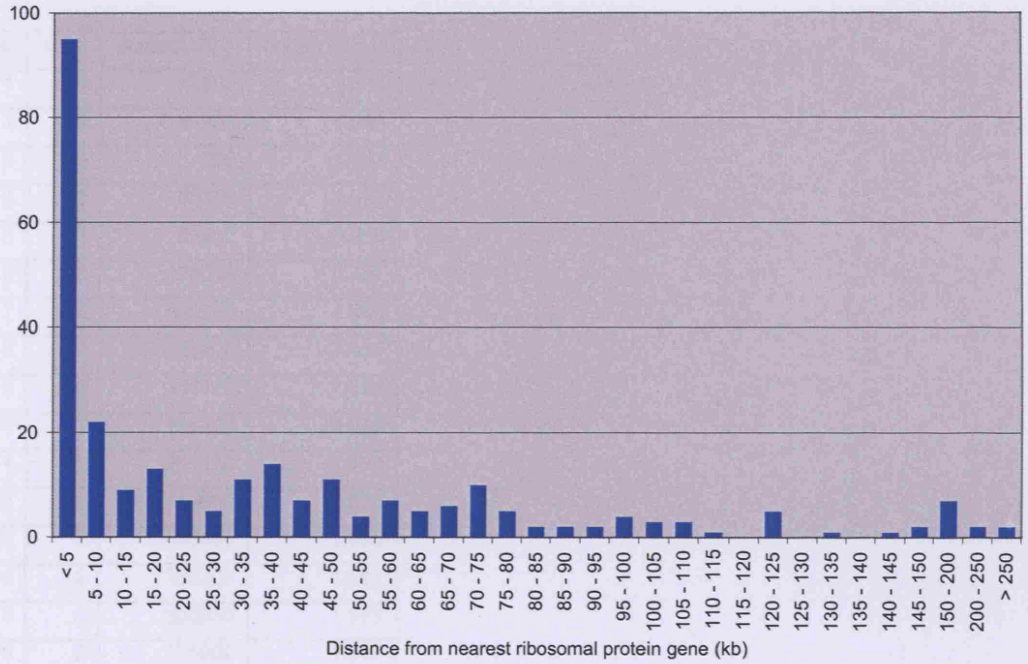

(**ii**) The distance of condensin peaks that are further than 2 kb from a tRNA gene is depicted relative to the nearest ribosomal protein gene (gene names RPL... or RPS...). 95 peaks (23% of all 419 condensin peaks) lie within 5 kb from a ribosomal protein gene. Of these, 36 lie towards the start of the ORF (average distance from the 5' end: 336 bp), while 59 are closer to the 3' end (average distance 351 bp).

(**D**) Colocalisation of condensin with Scc2/4 and Tfc3.

The observed average distance from a condensin peak to the nearest Scc2/4 peak was 3765 bp, with an expected distance of a random distribution of 4732 bp. Bootstrap analysis of 1000 random peak distribution patterns suggests that condensin and Scc2/4 colocalise ($p<0.0535$).

The observed average distance from a condensin peak to the nearest Tfc3 peak was 2726 bp, with an expected distance of a random distribution of 3804 bp. Bootstrap analysis of 1000 random peak distribution patterns suggests that condensin and Tfc3 colocalise ($p<0.0119$)

peak	chr.	position (bp)	height (log_2)
1	1	71600	1.638
2	1	181100	1.562
3	1	800	1.261
4	1	65100	1.002
5	1	92800	0.956
6	1	126000	0.797
7	2	680700	1.893
8	2	88200	1.815
9	2	406150	1.751
10	2	197400	1.698
11	2	281150	1.682
12	2	266600	1.655
13	2	605650	1.635
14	2	169300	1.555
15	2	300950	1.523
16	2	375900	1.517
17	2	326700	1.507
18	2	415000	1.441
19	2	347600	1.424
20	2	36450	1.400
21	2	643050	1.332
22	2	174850	1.300
23	2	6550	1.286
24	2	45700	1.233
25	2	258550	1.220
26	2	212450	1.166
27	2	591600	1.106
28	2	614100	1.062
29	2	333750	0.987
30	2	308900	0.969
31	2	290750	0.950
32	2	141600	0.898
33	2	60650	0.862
34	2	393700	0.815
35	2	271950	0.618
36	3	30850	2.726
37	3	139050	2.577
38	3	292950	1.985
39	3	177650	1.911
40	3	92650	1.774
41	3	14800	1.507
42	3	1400	1.446
43	3	228050	1.345
44	3	78500	0.997

45	3	144700	0.853
46	4	1403050	2.247
47	4	1201850	2.022
48	4	472900	1.802
49	4	230550	1.761
50	4	491400	1.707
51	4	359750	1.701
52	4	541850	1.654
53	4	410950	1.648
54	4	1462050	1.629
55	4	667900	1.592
56	4	1095350	1.574
57	4	118600	1.567
58	4	1237800	1.536
59	4	568900	1.530
60	4	332800	1.478
61	4	309700	1.443
62	4	130250	1.436
63	4	1150700	1.413
64	4	946250	1.405
65	4	1305550	1.400
66	4	1175850	1.399
67	4	579900	1.398
68	4	45700	1.398
69	4	1450100	1.370
70	4	428650	1.365
71	4	509400	1.361
72	4	478000	1.349
73	4	1075450	1.349
74	4	555300	1.348
75	4	392450	1.345
76	4	1524400	1.341
77	4	1359900	1.326
78	4	372250	1.317
79	4	1245800	1.278
80	4	386950	1.160
81	4	379000	1.056
82	4	340600	1.055
83	4	417200	1.010
84	4	527400	0.970
85	4	216500	0.929
86	4	930100	0.904
87	4	1492450	0.865
88	4	1013050	0.826
89	5	100300	1.934
90	5	131150	1.893

91	5	177150	1.889
92	5	86200	1.875
93	5	62000	1.834
94	5	67050	1.776
95	5	431200	1.718
96	5	442150	1.711
97	5	207450	1.691
98	5	354950	1.633
99	5	288300	1.574
100	5	312100	1.566
101	5	117450	1.510
102	5	52050	1.373
103	5	10100	1.345
104	5	487400	1.344
105	5	545500	1.301
106	5	269500	1.295
107	5	322450	1.228
108	5	236900	1.207
109	5	397450	1.198
110	5	469500	1.193
111	5	363250	1.163
112	5	306700	1.157
113	5	424150	1.110
114	5	222800	1.091
115	5	122750	0.895
116	6	269900	2.198
117	6	101200	1.682
118	6	74800	1.557
119	6	181100	1.549
120	6	226650	1.545
121	6	64350	1.423
122	6	54550	1.299
123	6	191600	1.283
124	6	5300	1.176
125	6	204850	1.106
126	6	172100	1.013
127	6	90450	0.781
128	6	221600	0.774
129	7	541850	2.464
130	7	857500	2.350
131	7	845650	2.064
132	7	440750	1.959
133	7	287450	1.937
134	7	561650	1.911
135	7	311850	1.880
136	7	531800	1.826

137	7	115600	1.803
138	7	882500	1.771
139	7	73950	1.752
140	7	472450	1.695
141	7	738950	1.678
142	7	828800	1.671
143	7	278400	1.590
144	7	779600	1.565
145	7	365350	1.550
146	7	328850	1.547
147	7	700900	1.506
148	7	555300	1.473
149	7	609950	1.454
150	7	122250	1.395
151	7	205550	1.387
152	7	147950	1.365
153	7	346200	1.361
154	7	727900	1.321
155	7	961000	1.311
156	7	939750	1.289
157	7	412300	1.213
158	7	405450	1.205
159	7	648900	1.159
160	7	254300	1.142
161	7	788350	1.132
162	7	521150	1.066
163	7	228100	1.059
164	7	320150	0.981
165	7	102150	0.954
166	7	971000	0.909
167	7	1083450	0.834
168	7	526250	0.791
169	8	76200	2.406
170	8	35250	2.077
171	8	382000	2.014
172	8	85200	1.951
173	8	134350	1.889
174	8	237850	1.829
175	8	388850	1.609
176	8	375450	1.501
177	8	62750	1.464
178	8	146150	1.454
179	8	452750	1.382
180	8	411300	1.364
181	8	160550	1.306
182	8	126900	1.278

183	8	556850	1.276
184	8	358450	1.253
185	8	505000	1.050
186	9	384350	2.196
187	9	325700	1.879
188	9	394900	1.799
189	9	248750	1.765
190	9	317550	1.662
191	9	175000	1.440
192	9	335550	1.365
193	9	377200	1.318
194	9	389550	1.188
195	9	439750	1.188
196	9	421100	1.131
197	9	138250	1.111
198	9	257650	1.090
199	9	214950	0.934
200	10	74400	2.068
201	10	416050	1.995
202	10	228050	1.989
203	10	139600	1.891
204	10	374350	1.844
205	10	116000	1.608
206	10	59150	1.599
207	10	396500	1.589
208	10	464400	1.586
209	10	204700	1.582
210	10	663550	1.566
211	10	531750	1.510
212	10	197300	1.470
213	10	355550	1.444
214	10	391050	1.435
215	10	524000	1.411
216	10	349100	1.397
217	10	172650	1.306
218	10	542750	1.281
219	10	233850	1.247
220	10	608700	1.149
221	10	652500	1.128
222	10	409500	1.067
223	10	90450	0.756
224	11	517650	2.051
225	11	302600	1.882
226	11	578850	1.824
227	11	162500	1.771
228	11	379500	1.649

228	11	313000	1.640
230	11	490600	1.575
231	11	141050	1.475
232	11	74650	1.461
233	11	284200	1.453
234	11	327050	1.446
235	11	307850	1.381
236	11	558450	1.369
237	11	216600	1.358
238	11	202650	1.353
239	11	666200	1.325
240	11	364150	1.322
241	11	334100	1.308
242	11	462700	1.218
243	11	419800	1.197
244	11	84200	1.163
245	11	410700	1.047
246	11	109750	1.033
247	11	650	1.033
248	11	618200	1.023
249	11	393050	0.997
250	11	471600	0.983
251	11	38700	0.917
252	12	369550	5.699
253	12	451150	2.592
254	12	794300	2.447
255	12	232350	2.381
256	12	838300	2.056
257	12	442750	1.941
258	12	199600	1.927
259	12	780900	1.789
260	12	640000	1.689
261	12	818800	1.658
262	12	427050	1.627
263	12	931950	1.605
264	12	348500	1.596
265	12	282950	1.586
266	12	856250	1.566
267	12	875350	1.559
268	12	129350	1.553
269	12	215000	1.548
270	12	499500	1.536
271	12	673950	1.535
272	12	97800	1.452
273	12	108550	1.417
274	12	121800	1.412

275	12	179750	1.410
276	12	329550	1.387
277	12	92550	1.375
278	12	242600	1.349
279	12	1052100	1.328
280	12	962950	1.325
281	12	402650	1.264
282	12	374700	1.229
283	12	949600	1.186
284	12	899100	1.186
285	12	48900	1.179
286	12	421600	1.172
287	12	263350	1.153
288	12	1064250	1.139
289	12	523400	1.064
290	12	810850	1.040
291	12	605300	1.002
292	12	491550	0.989
293	12	289600	0.969
294	12	382050	0.943
295	12	1029300	0.868
296	12	1018200	0.846
297	12	415450	0.840
298	12	395200	0.819
299	12	342700	0.810
300	12	209950	0.790
301	12	171550	0.741
302	13	298000	2.874
303	13	290800	2.155
304	13	363150	2.069
305	13	652750	1.968
306	13	372450	1.754
307	13	352250	1.721
308	13	158750	1.685
309	13	762550	1.536
310	13	222700	1.515
311	13	499250	1.463
312	13	379400	1.451
313	13	463550	1.404
314	13	861100	1.339
315	13	195950	1.275
316	13	184000	1.260
317	13	168900	1.250
318	13	420750	1.250
319	13	808400	1.245
320	13	131850	1.223

321	13	557450	1.182
322	13	550000	1.165
323	13	485850	1.127
324	13	768550	1.087
325	13	236100	1.020
326	13	753300	0.986
327	13	672450	0.938
328	13	887300	0.935
329	13	306700	0.927
330	13	147000	0.827
331	13	163850	0.780
332	14	500250	2.133
333	14	568200	1.846
334	14	586350	1.821
335	14	715900	1.807
336	14	89600	1.761
337	14	560600	1.749
338	14	96300	1.579
339	14	302900	1.544
340	14	63700	1.543
341	14	443000	1.504
342	14	102800	1.461
343	14	230150	1.442
344	14	331850	1.415
345	14	663700	1.408
346	14	653900	1.391
347	14	253600	1.339
348	14	602350	1.289
349	14	648850	1.225
350	14	495050	1.084
351	14	608500	0.990
352	14	108400	0.932
353	14	721950	0.882
354	14	425150	0.877
355	15	780500	2.501
356	15	301200	2.154
357	15	446000	2.002
358	15	226600	1.996
359	15	353950	1.932
360	15	438750	1.922
361	15	288150	1.797
362	15	94000	1.760
363	15	976550	1.660
364	15	464600	1.615
365	15	274750	1.574
366	15	1028350	1.565

367	15	282150	1.550
368	15	832600	1.457
369	15	407950	1.339
370	15	506750	1.277
371	15	594250	1.270
372	15	380800	1.237
373	15	842100	1.217
374	15	1000	1.214
375	15	759150	1.199
376	15	722050	1.184
377	15	867800	1.175
378	15	487400	1.163
379	15	160500	1.161
380	15	678100	1.145
381	15	900800	1.118
382	15	571800	1.088
383	15	259350	1.058
384	15	218350	1.057
385	15	80950	1.018
386	15	366950	1.009
387	15	253850	0.971
388	15	413750	0.810
389	15	347950	0.727
390	16	819500	2.389
391	16	582000	2.253
392	16	576950	2.142
393	16	281200	1.867
394	16	338850	1.835
395	16	405950	1.797
396	16	533600	1.736
397	16	700600	1.685
398	16	622900	1.639
399	16	718900	1.623
400	16	744350	1.593
401	16	303900	1.463
402	16	795900	1.462
403	16	689600	1.461
404	16	436050	1.432
405	16	695400	1.413
406	16	592150	1.360
407	16	645100	1.323
408	16	860400	1.248
409	16	73400	1.186
410	16	880400	1.150
411	16	769000	1.076
412	16	654250	1.074

413	16	587050	1.048
414	16	499950	0.997
415	16	174100	0.992
416	16	90350	0.954
417	16	472850	0.931
418	16	528550	0.922
419	16	730950	0.861

(E) Condensin peaks assigned along the 16 metaphase budding yeast chromosomes. The positions and heights of the Brn1-Pk_9 association sites, as identified in the chromosome V extracted in Map 1, are listed. Regions spanning 40 kb surrounding the centromeres were excluded from the analysis. Condensin is enriched in these regions, making individual peak assignments difficult.

3 Chapter 3: Condensin dependent decatenation promotes late resolution of the budding yeast rDNA

A striking phenotype shared by all organisms that undergo mitosis without condensin is the presence of anaphase bridges. This observation has been historically linked to persistency of topological entanglements between sister chromatids that fail to unravel by the time of anaphase onset (Bhat et al., 1996; Hagstrom et al., 2002; Hudson et al., 2003; Ono et al., 2004; Saka et al., 1994; Strunnikov et al., 1995). Why topoisomerases fail to recognise (or resolve) these DNA cross-overs in the absence of condensin while succeeding in doing so in presence of condensin is not known. So far, the anaphase bridge phenotype in the condensin mutant has been only correlated with topoisomerase mis-regulation (Bhat et al., 1996; Coelho et al., 2003). Are the bridges observed of a topological nature? If so, what is the activity related with condensin that potentiates topo II function: is the ability to organise and compact chromatin or a more direct regulation of topo II catalytic activity?

3.1 rDNA bridge phenotype in Saccharomyces cerevisiae

The ribosomal DNA in budding yeast consists of a 100-200 tandem repeat array located on one chromosome arm only, namely the longest arm of chromosome XII. Previous work showed that sister chromatid rDNAs remain connected well after cohesin removal at anaphase onset. Only later in anaphase are the two daughter molecules fully unzipped in a reaction involving Cdc14, condensin and topo II (D'Amours et al., 2004; Sullivan et al., 2004; Wang et al., 2004). We reasoned that this system could serve as an excellent tool to investigate the relationship between condensin and topo II in chromosome resolution. Given the repetitiveness and high rate of compaction of the budding yeast rDNA locus, it is tempting to imagine that it could serve as a nice model to understand the mechanisms of segregation of larger scale chromosomes such as in higher vertebrates.

3.1.1 Increased dosage of endogenous topo II does not rescue rDNA segregation defects of a condensin mutant

The chromosome segregation defects of a condensin mutant could be in principle explained by the absence, or limited presence of disentangling activities loaded onto

chromatin. Based on this assumption we therefore first asked whether increased dosage of topo II could allow the protein to bind DNA even without condensin. If so, could it also overcome the segregation defects? Although the observation that increased topo II levels cannot suppress the temperature sensitive growth defect of a condensin mutant (Bhalla et al., 2002) would argue against this idea we were nonetheless tempted to test it within a single cell cycle experiment. Cells with the temperature sensitive condensin mutation *ycg1-10* were arrested in metaphase at permissive conditions to allow condensation and resolution of most of the genome, except the rDNA. Then yeast topo II was overexpressed under control of the galactose inducible *GAL1* promoter. Now condensin was inactivated by temperature shift, and cells released from the metaphase block into anaphase. To monitor rDNA segregation we followed the Net1 protein, which neatly binds the whole ribosomal DNA array throughout the cell cycle (Machin et al., 2005). Topo II binding to yeast chromosomes was only mildly reduced in the absence of condensin, but its overexpression restored chromosome binding to even greater levels than in wild type ((Bhalla et al., 2002) and Figure 3.1B). Inactivation of condensin in anaphase impeded rDNA segregation (Sullivan et al., 2004), and this was, if any, only minimally overcome by increased topo II dosage (Figure 3.1A). This suggests that reduced topo II recruitment to chromosomes in absence of condensin is not limiting rDNA segregation.

3.2 Topo II from Chlorella virus overcomes late segregation of rDNA

The inability of increased levels of topo II to restore rDNA segregation left unclear whether or not linkages other than catenation prevent rDNA segregation in the condensin mutant. An alternative possibility is that endogenous topo II is less efficient at resolving the topological linkages at the rDNA without condensin. If the latter case was true, supplying a condensin-independent decatenation activity might be able to resolve the rDNA. We decided to employ an exogenous type II topoisomerase that would unlikely require yeast condensin function. Human topo IIα for example appears to be regulated by yeast condensin since it can suppress the temperature-sensitivity of yeast *top2-4* (Nitiss and Wang, 1988) thus disqualifying it as an appropriate candidate for addressing our question. We therefore ectopically expressed the small topo II enzyme (cv-topo II) encoded in the *Paramecium bursaria chlorella* virus PBCV-1 genome (Lavrukhin et al., 2000). This

enzyme has been shown to have all the characteristics of eukaryotic type II topoisomerases with an extraordinary DNA cleavage activity (Lavrukhin et al., 2000). Because of its evolutionary distinct origin it might escape possible condensin-dependent regulation in the yeast host. cv-topo II shows 43% sequence identity to budding yeast topo II over the catalytic domain but lacks the C-terminal extension. Although controversial data has been provided in this regard (Caron et al., 1994) this domain has been implicated in regulation of eukaryotic topo II. When we expressed cv-topo II in metaphase arrested yeast cells, upon releasing them into anaphase, rDNA segregation in the condensin mutant was vividly enhanced (Figure 3.2A). The observed rescue suggests that indeed decatenation failure was responsible for the rDNA segregation defect.

3.2.1 Chromosomes remain intact upon cv-topo II expression

Cv-topo II possesses strong DNA cleavage activity (Fortune et al., 2001), so it could be that rDNA segregation was a consequence of DNA breakage rather than decatenation. To control for this aspect we analysed chromosome size by pulsed field gel electrophoresis followed by Southern blotting. We employed a DNA probe that hybridises within the 5S genes within the rDNA repeats. Figure 3.2B showed that chromosomes remained intact during anaphase carried out in these conditions.
Therefore, cv-topo II most likely acted to resolve catenation of the rDNA locus, a function that yeast topo II performs inefficiently without condensin.

3.2.2 rDNA transcription continues unabted during anaphase with and without the exogenous topoisomerase

Recent works linked rDNA transcription with late segregation of the locus. Moreover a model has been put forward suggesting that Cdc14 regulates condensin in anaphase to lessen rDNA transcription, which is a prerequisite for rDNA resolution (Machin et al., 2006; Tomson et al., 2006; Wang et al., 2006). A key prediction can be extrapolated from this view: during anaphase, at the time where rDNA sister chromatids disjoin, transcription must decrease. Our results suggest that catenation but not transcription are regulated during anaphase to allow partition of the locus. However, if the latter was true, we should observe rDNA transcription decreasing in cells expressing the exogenous topoisomerase in a way similar to wild type cells.

We took the occasion to test this hypothesis by Northern analysis of the amount of 35S nascent transcript produced at the time of rDNA resolution in wild type and in condensin mutant cells expressing or not cv-topo II. We probed the regions between the 18S and 5.5S that is spliced from the nascent transcript (Internal Transcribed Spacer 1 or ITS1). We compared as shown in Figure 3.3 samples obtained before release into anaphase and at 20 minutes when resolution of rDNA peaks highest. Convincingly, similar amount of RNA was generated by wild type cells in anaphase as compared to metaphase. In addition, expression of the exogenous topoisomerase did not affect transcription of the 35S gene. Thus this result is less consistent with the view that a decline in rDNA transcription contributes to rDNA resolution but it is coherent with previous results showing unaltered transcription throughout the cell cycle in budding yeast (Elliott and McLaughlin, 1979).

3.2.3 cv-topo II advances the normally late segregation of rDNA

During wild type mitosis the rDNA segregates late, trailing behind most other chromosomes during anaphase. When we monitored rDNA segregation in condensin mutant cells expressing cv-topo II in the experiment described in Figure 3.3 we noticed that, strikingly, rDNAs were splitting in several instances quite early in anaphase. It was possible that persistent catenation provides one of the antagonising forces to sister chromatid segregation able to explain late resolution of the rDNA. We therefore asked whether late segregation was the consequence of late decatenation of the locus. As an internal standard for segregation timing we measured the anaphase spindle length at which the Net1 signal separated. In wild type cells, rDNA segregation occurred when the spindle reached 6-7 μm in length (Fig. 3.4A), consistent with previous reports (Machin et al., 2005; Sullivan et al., 2004) while not even 50% of condensin mutant cells showed resolved rDNAs. However, after condensin inactivation, when the spindle length was over 10 μm a high fraction of cells showed segregated rDNA (see below). Expression of cv-topo II advanced segregation of uncondensed rDNAs in condensin mutant cells to a spindle length of about 6-7 μm, close to what is observed in wild type cells. Notably, expression of cv-topo II in wild type cells led to a further, although small advance of rDNA segregation. This only partial contribution was probably undermined by the fact that chromosome XII is by far the longest chromosome and its sister kinetochores must be pulled widely apart before chromosome arms can fully unzip. However, if cv-topo II increases the chances of rDNAs to fully decatenate there should be some evidence of this at early points of

anaphase. In fact this effect was mostly apparent at early anaphase stages when rDNA segregation relatively to bulk chromosome segregation was analysed. In wild type early anaphase cells, displaying a dumbbell-shaped nucleus, the rDNA was unavoidably found unsegregated, stalling in the middle of the dividing nucleus in a stage referred to as rDNA bridging ((Machin et al., 2005) and Fig. 3.4B). Later in anaphase, the rDNA trailed behind the rest of the genome on its way towards the cell poles. After cv-topo II expression, the rDNA split in many early anaphase nuclei, rDNA bridges were never seen, and in many cells the rDNA migrated close to the leading edge of the chromosome mass. This suggests that the physiological anaphase bridging and consequent late segregation of the rDNA is due to persistent catenation.

3.3 Condensin and topo II co-localises within and outside the rDNA repeats

The above results are consistent with a functional interaction between condensin and topo II. In *Drosophila* condensin (Barren subunit) is seen to physically interact with topoisomerase and to positively enhance its activity *in vitro*, in a plasmid decatenation assay (Bhat et al., 1996). Such a physical interaction has been confirmed in *Drosophila* (Lupo et al., 2001) but not other organisms (Bhalla et al., 2002; Cuvier and Hirano, 2003) suggesting that the interaction might be very elusive depending on the conditions. Thus, confirmation of cooperation between condensin and topoisomerase II would be an important contribution towards our understanding of chromosome segregation.

We analysed in detail whether condensin colocalises with topo II in yeast by employing high resolution microarrays (Katou et al., 2003). Our results that rDNA resolution depends on condensin-mediated DNA decatenation prompted us to include the rDNA repeats in our analysis. We were excited to notice that the patterns of the two proteins although not identical, showed a high degree of match. Within the 9.1 kb long rDNA repeats both factors show a clear preference for the 35S promoter and the Fob1 mediated barrier while they both weakly associate with the replication origins (Autonomous Replication Sequences). The similarity of the patterns also extended to loci along the remainder of chromosome XII (Fig. 3.5A). The colocalisation was specific since topo II and cohesin do not show any clear resemblance in the binding patterns (Figure 3.5B). Colocalisation of condensin and topo II was further confirmed by immunostaining on spread chromosomes (Fig. 3.5C). While the mechanism underlying the stimulation of

topo II activity by condensin remains to be elucidated, the colocalisation of the two proteins is consistent with their functional relationship. Colocalisation of topo II and condensin not only at the rDNA locus opens the possibility that condensin might act in a similar fashion to promote decatenation at other places in the genome.

3.4 Condensin promotes but is not essential for DNA decatenation

As discussed in Chapter 1, along with condensin additional factors could contribute to provide directionality to the double stranded passing activity of topoisomerases. Among these, the spindle is of particular interest.

We noticed that even in the condensin mutant, the rDNA was able to segregate in cells when anaphase spindles were very elongated. This could be because the *ycg1-10* mutation did not completely inactivate condensin, or because the rDNA can segregate in the absence of condensin albeit with a delay. In this regard, one possibility for condensin-independent rDNA segregation could be that the pulling force of the elongating spindle pushes sites of catenation along the chromosome until sister chromatids are released as catenation slips off chromosomes ends. To test this possibility we analysed rDNA segregation where decatenation was fully prevented by inactivating topo II at anaphase onset using the temperature sensitive *top2-4* mutation. We monitored two loci, on both sides of the rDNA locus, by integration of *lacO* repeats recognised by a lacI-GFP fusion protein (Sullivan et al., 2004). We also stained the nucleolous, as this, alongside the spindle confers spatial clues on the position of the centromeric versus telomeric pairs of GFP dots. In metaphase, all cells showed two GFP dots representing the two loci. After release from metaphase, wild type cells transiently displayed one strong and two weaker signals, indicating that one of the loci had split while the other was still joined (Fig. 3.6A). The split locus was almost always found closer to the spindle than the unsplit locus, suggesting it was the centromere proximal locus that separated first. This also points to the spindle as one important means for providing directionality to the resolution of sister chromatids in physiological conditions. After this, all cells accumulated four GFP dots, two in each cell half, indicative of complete rDNA segregation. When condensin was inactivated, cells accumulated with one split and one unresolved locus for a longer time, before eventually cells appeared with fully separated rDNA. This also suggests that the spindle attempts to segregate the rDNA even without condensin but the process is slower as it encounters some sort of resistance in

the resolution of the locus. After inactivation of topo II, both pairs of loci failed to split in most cells throughout the course of the experiment. This suggests that persistent catenation cannot be pushed along the rDNA at least when the locus is fully catenated.

There are two possibilities to explain the intermediate result obtained with the condensin mutant. First, condensin is not indispensable for rDNA resolution because of a basal level of condensin-independent decatenation activity. However, in these conditions a functional spindle (slowly) replaces condensin's role in rDNA partitioning. Conversely, the spindle achieves (slow) rDNA segregation only due to the hypomorphic nature of the *ycg1-10* mutation. In support of the first hypothesis there is the fact that condensin may not be indispensable for slow decatenation also of other chromosome arms. This is indicated by the observation that the *top2-4* mutation impedes resolution of the chromosome IV arm during anaphase more decisively than inactivation of condensin (as judged by employment of the different mutant allele *ycs4-1*) (Bhalla et al., 2002).

However to really distinguish whether condensin was incompletely inactivated, or whether pulling by the elongating spindle can promote decatenation even in the absence of condensin we needed to repeat the above experiment in the absence of the spindle. We therefore analysed the effect on rDNA segregation of abolishing mitotic spindle function by the microtubule poison nocodazole. Cells were synchronised in G1 by mating pheromone α-factor treatment, and released into the cell cycle in the presence or absence of nocodazole. The spindle checkpoint was inactivated in these cells by deletion of *MAD2* so that cell cycle could progress into anaphase despite the absence of a mitotic spindle. In wild type cells, the presence of nocodazole only caused a slight delay to rDNA resolution, visualised by splitting of the GFP-markers at both ends of the locus (Fig. 3.6B). In the condensin mutant, rDNA separation was almost completely abolished in the presence of nocodazole. This suggests that the *ycg1-10* allele largely eliminates condensin function in rDNA resolution when spindle forces are absent. In the presence of a spindle, as expected, slow segregation of the rDNA was observed over time. This suggests that the pulling force of the spindle promotes rDNA decatenation by a basal level of condensin-independent topo II activity. Delayed resolution of anaphase bridges has also been observed in human cells depleted of condensin (Gerlich et al., 2006a). We suggest that these bridges might also be due to persisting catenation that is only slowly resolved by topo II in the absence of condensin.

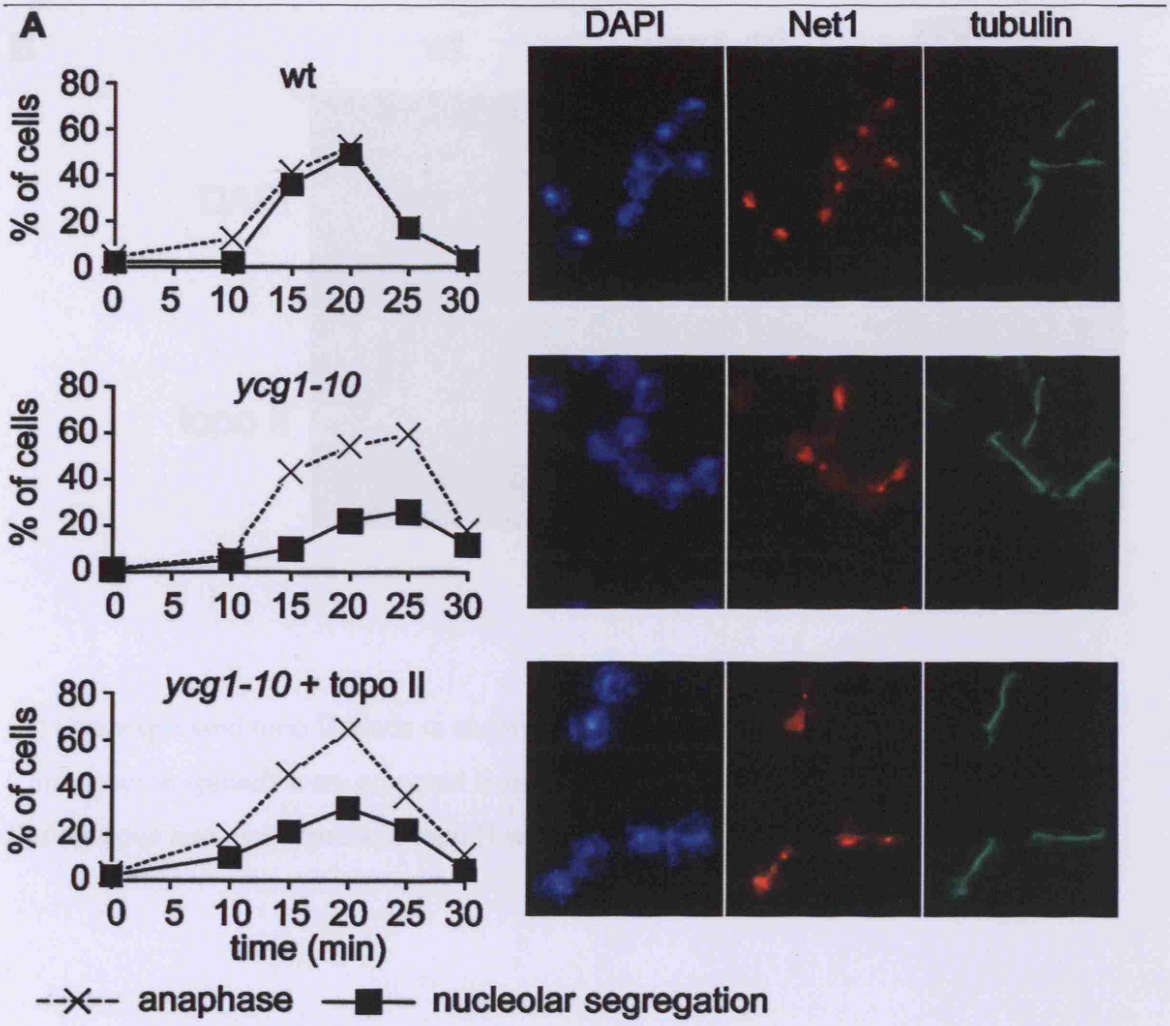

Figure 3.1 Overexpressed yeast topo II restores its own localisation to chromatin but not rDNA segregation defects in a condensin mutant.

(**A**) Yeast topo II overexpression does not rescue rDNA segregation.

Cells of strains Y3405 (*MATa MET3-CDC20 TOP2-Pk3 NET1-GFP*), Y3310 (*MATa ycg1-10 MET3-CDC20 TOP2-Pk3 NET1-GFP*) and Y3363 (*MATa ycg1-10 MET3-CDC20 TOP2-Pk3 GAL1-TOP2-Pk3 NET1-GFP*), were arrested in metaphase, condensin inactivated by shift to 37°C, and expression of topo II induced before cells were released into synchronous anaphase. rDNA segregation was monitored by staining the rDNA binding protein Net1 fused to GFP using an anti-GFP antibody.

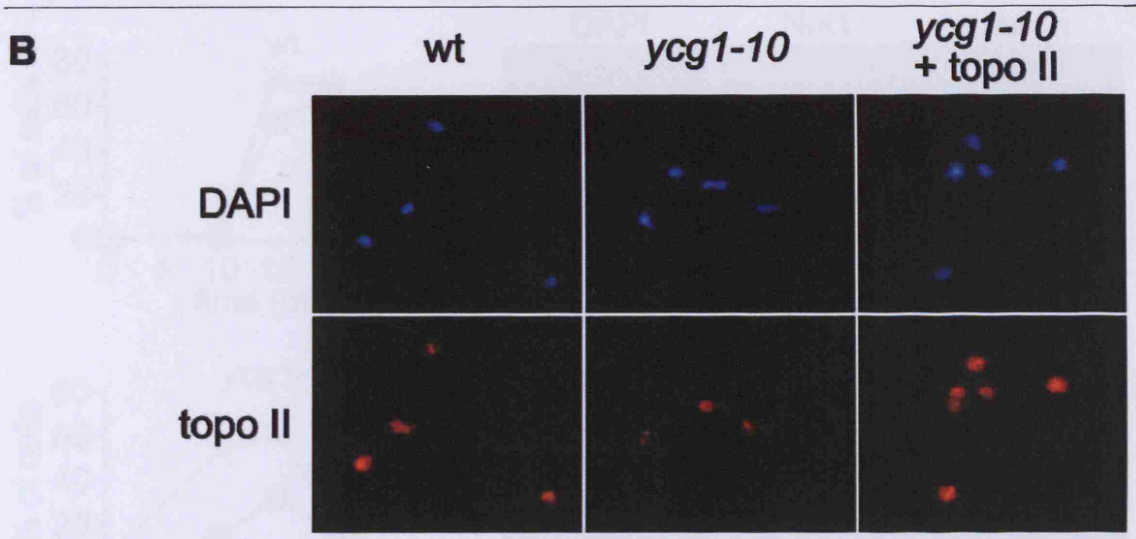

(**B**) Overexpressed topo II binds to chromatin in the condensin mutant.
Chromosome spreads were prepared from the cells in A during anaphase (20 min).
Endogenous and overexpressed topo II were both visualised via their Pk epitope tags.

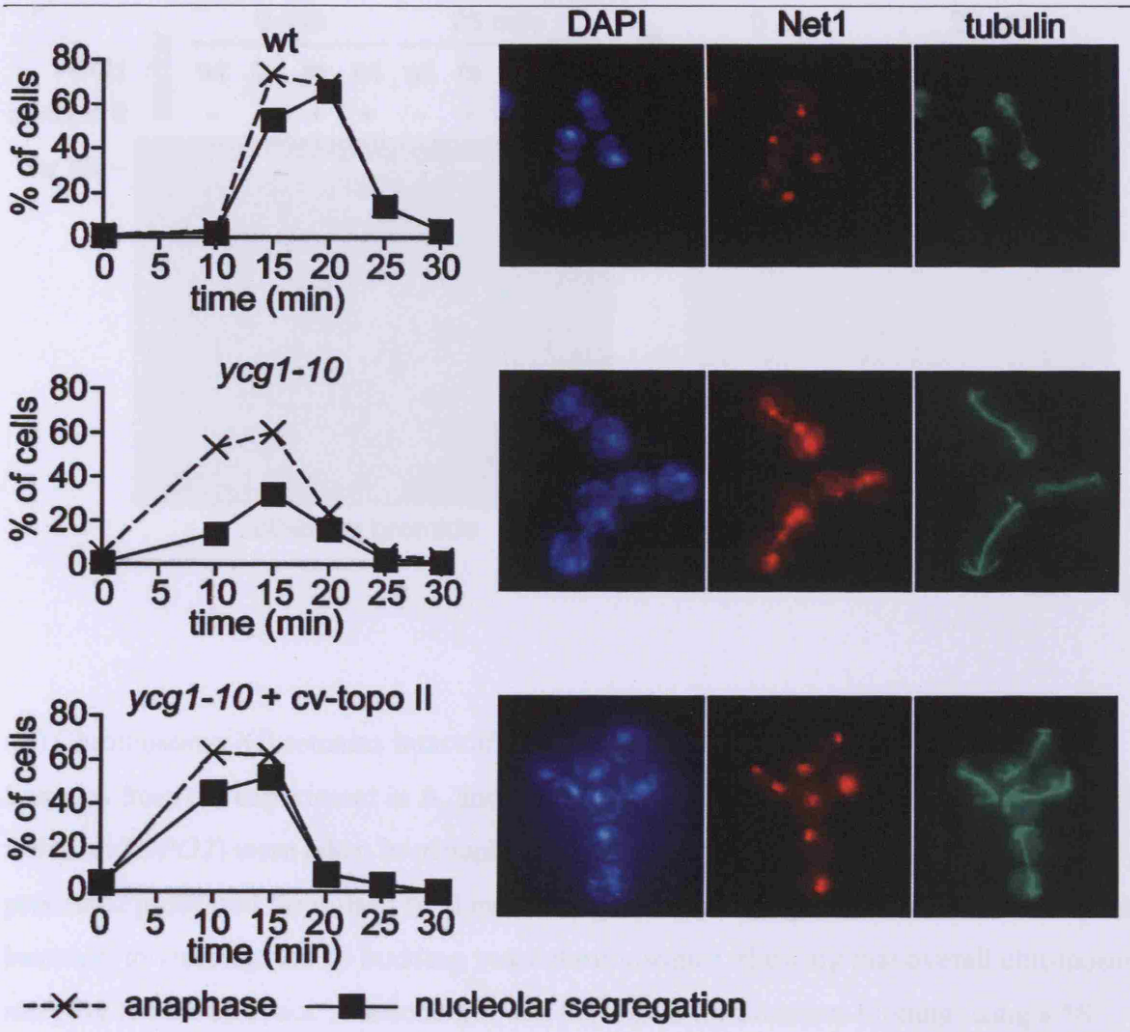

Figure 3.2 Chlorella virus topo II (cv-topo II) rescues rDNA segregation in a condensin mutant

(**A**) Cells of strains Y2748 (*MATa MET3-CDC20 NET1-GFP*), Y2749 (*MATα ycg1-10 MET3-CDC20*). Chromosome spreads were prepared from the cells in A during anaphase (20 min). Endogenous metaphase and released into anaphase after condensin inactivation and cv-topo II expression as in Figure 3.1.

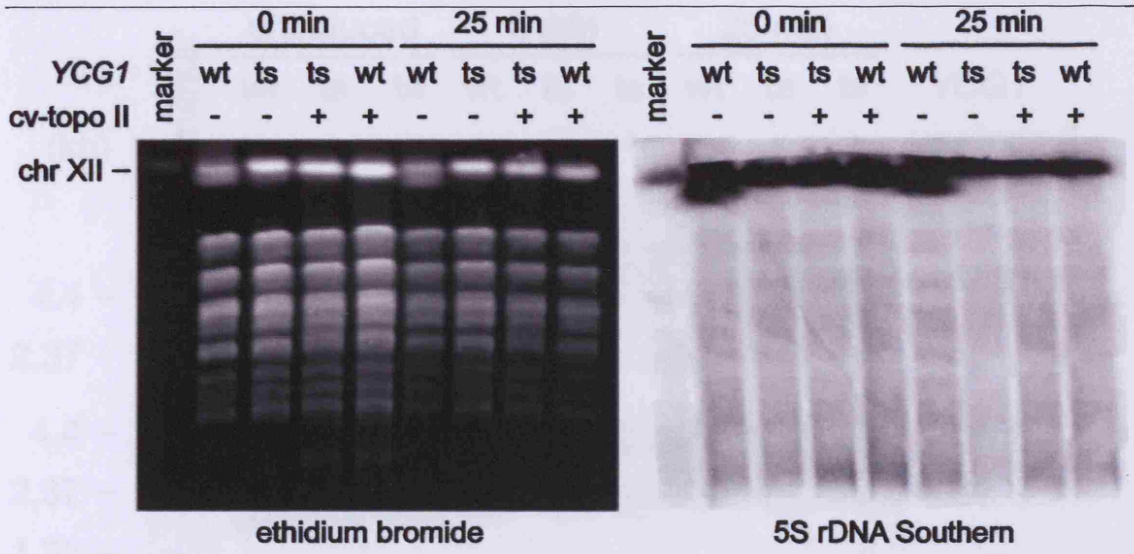

(**B**) Chromosome XII remains intact after cv-topo II expression.

Samples from the experiment in A, and of strain Y2883 (*MATa MET3-CDC20 NET1-GFP GAL1-cvTOPO2*) were taken in metaphase (0 min) and late anaphase (25 min) and processed processed for pulsed field gel electrophoresis. One gel was stained with ethidium bromide, to visualise the 16 budding yeast chromosomes, showing that overall chromosome integrity remained intact. A second gel was processed for Southern blotting using a 5S rDNA probe. Chromosome XII fragments were not detected after cv-topo II expression, suggesting that rDNA resolution is not the consequence of DNA breakage.

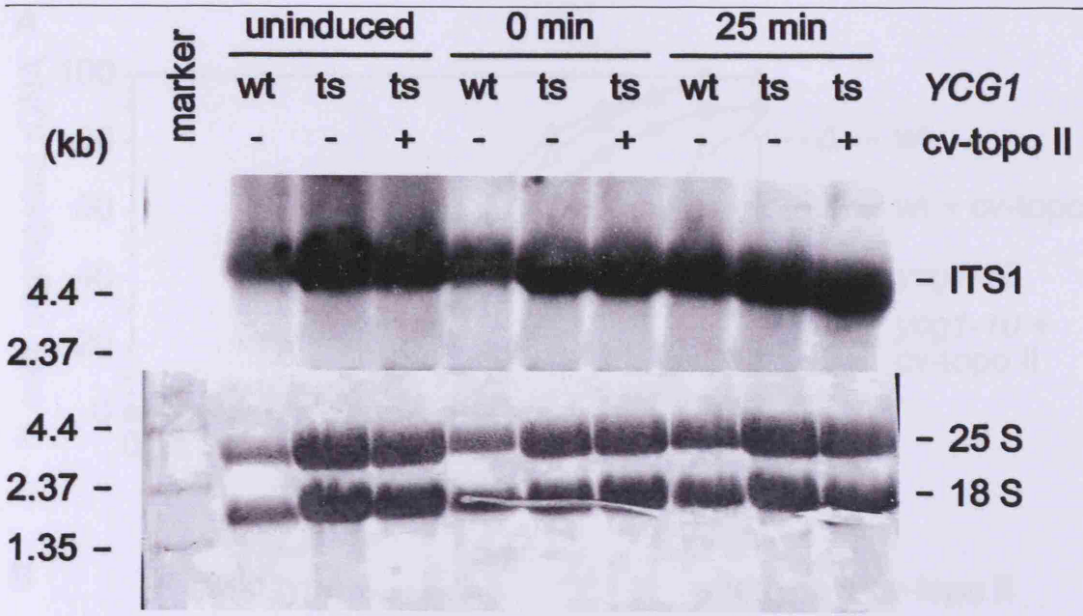

Figure 3.3 rDNA transcription is not affected by expression of the exogenous topoisomerase in anaphase

rDNA transcription is unaffected by cv-topo II expression. Whole RNA preparations from strains in Figure 3.2 were prepared in metaphase arrest before cv-topo II induction (uninduced), after induction (0 min), and 25 minutes after release into anaphase (25 min). RNA was separated on an agarose/formaldehyde gel and blotted for Northern detection of the internal transcribed spacer 1 (ITS1) region of the nascent 35S rRNA transcript. The membrane was stained with methylene blue to visualise the 25S and 18S ribosomal RNAs as a loading control (below).

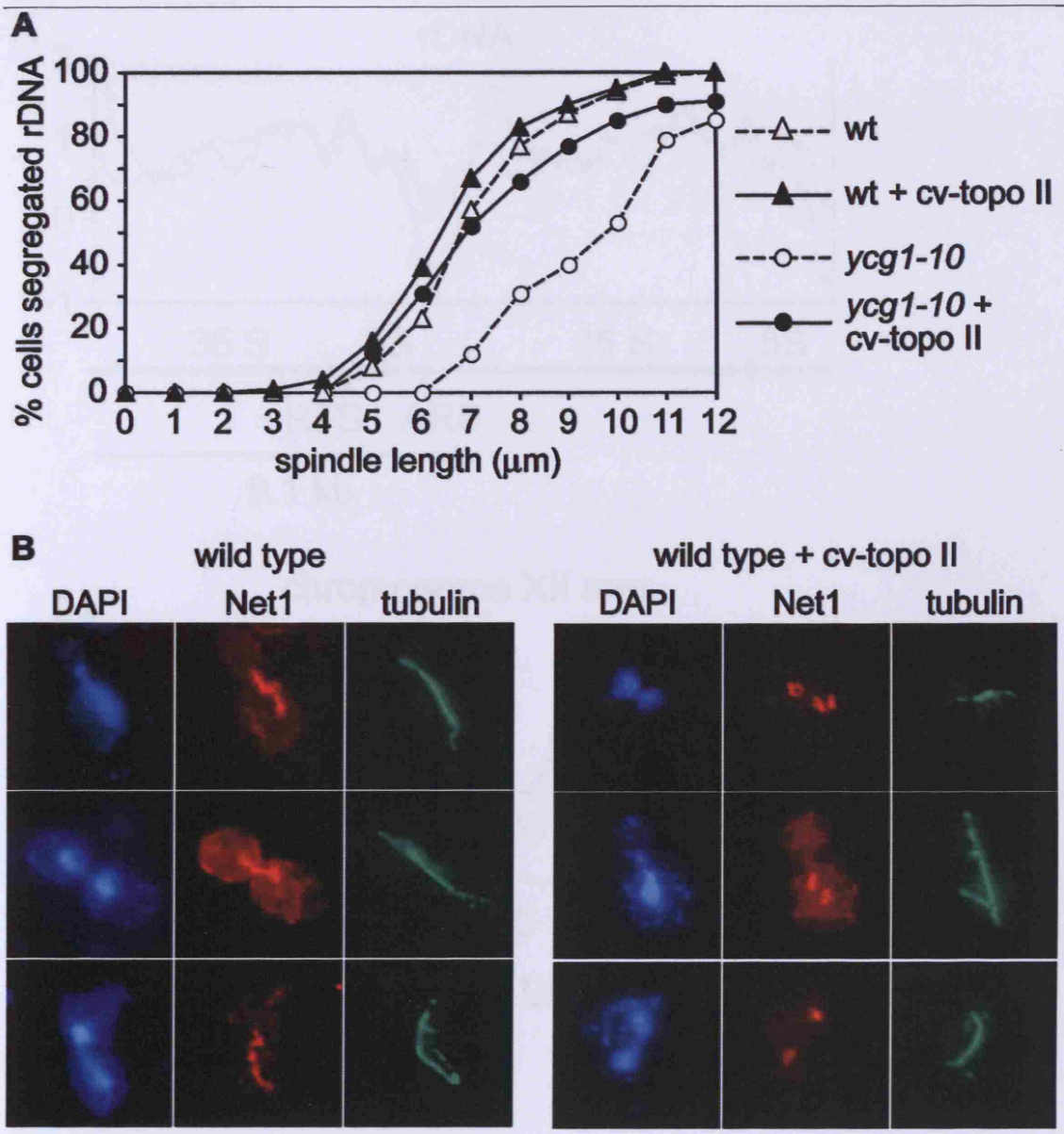

Figure 3.4 cv-topo II expression advances rDNA segregation

(**A**) rDNA segregation as a function of spindle length is depicted during the experiment shown in Figure 3.2. At least 30 cells at each length were scored for rDNA segregation (100 cells each for spindle lengths of 2, 3 and 4 µm).

(**B**) Examples of wild type cells displaying typical late rDNA segregation and of cells expressing cv-topo II that show complete rDNA segregation already at early stages of anaphase.

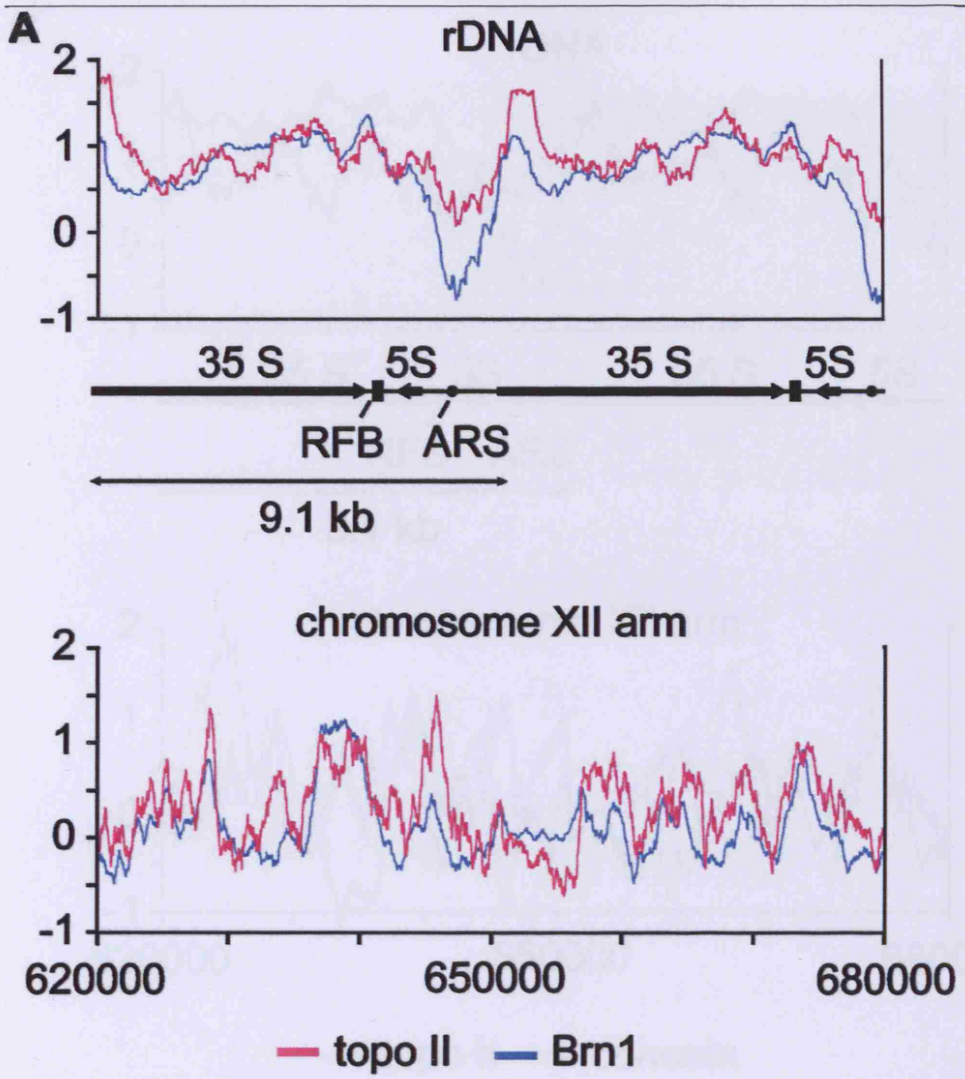

Figure 3.5 Colocalisation of condensin and yeast topo II within and off the rDNA repeats

(**A**) Cells of strains Y2200 (*MATa BRN1-Pk9*) and Y2280 (*MATa TOPO2-Pk9*) were arrested in metaphase by nocodazole treatment. Cells were processed for ChIP against the epitope tagged condensin subunit barren (Brn1) and topo II. Binding along the rDNA and chromosome XII between nucleotide coordinates 620,000 and 680,000 is shown.

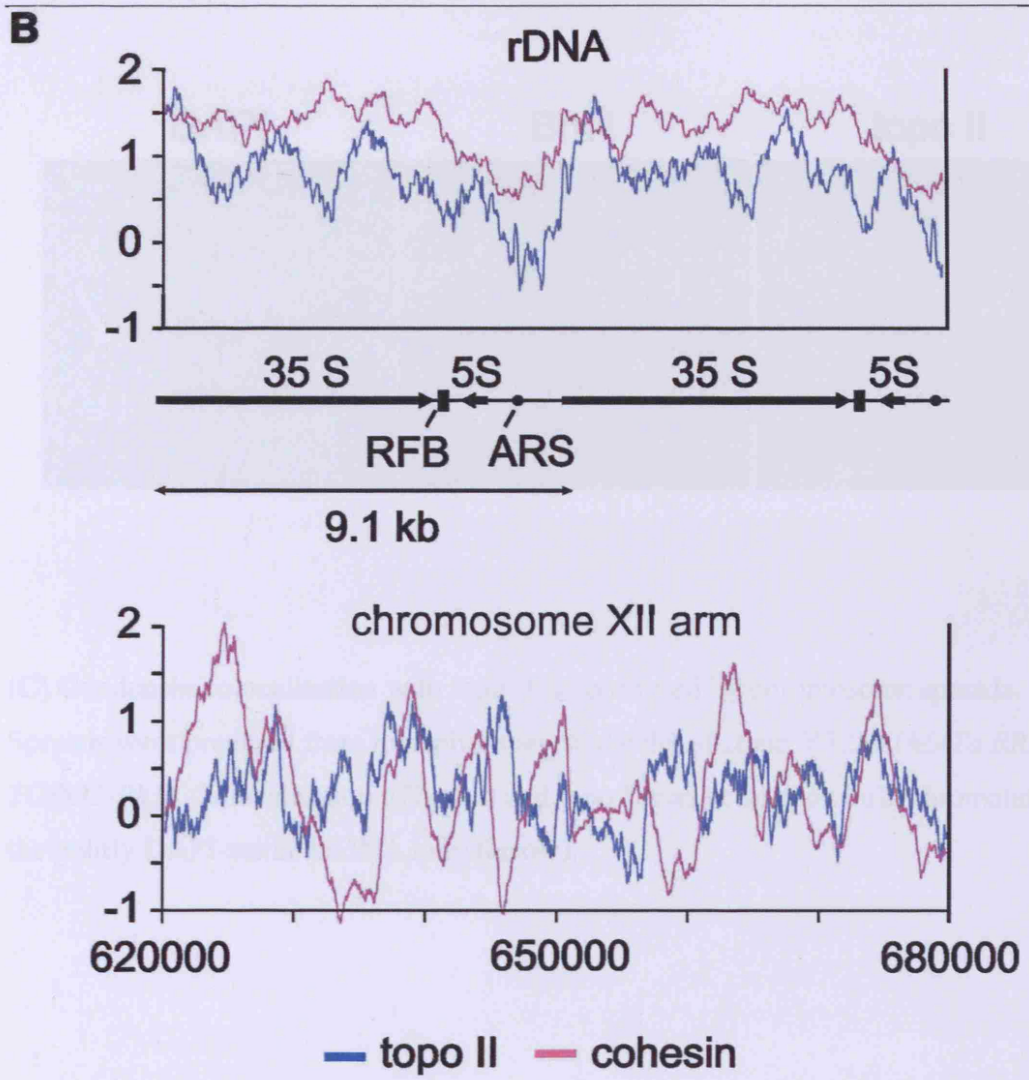

(**B**) Localisation of topo II is distinct from that of cohesin.

The association pattern of topo II along the rDNA repeats, and a region along the chromosome XII arm (see A), is compared to that of cohesin in strain Y2269 (*MATa SCC1-Pk9*) obtained as in A.

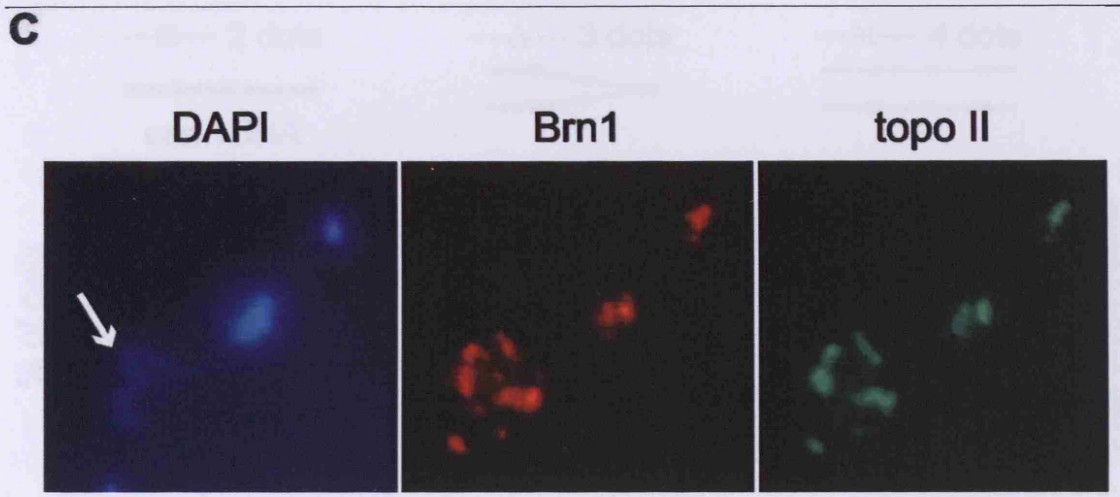

(**C**) Condensin colocalisation with topo II is confirmed by chromosome spreads. Spreads were prepared from metaphase arrested cells of strain Y3278 (*MATa BRN1-HA6 TOPO2-Pk3*). Colocalisation of barren and topo II can be seen on bulk chromatin as well as the poorly DAPI-stained rDNA loop (arrow).

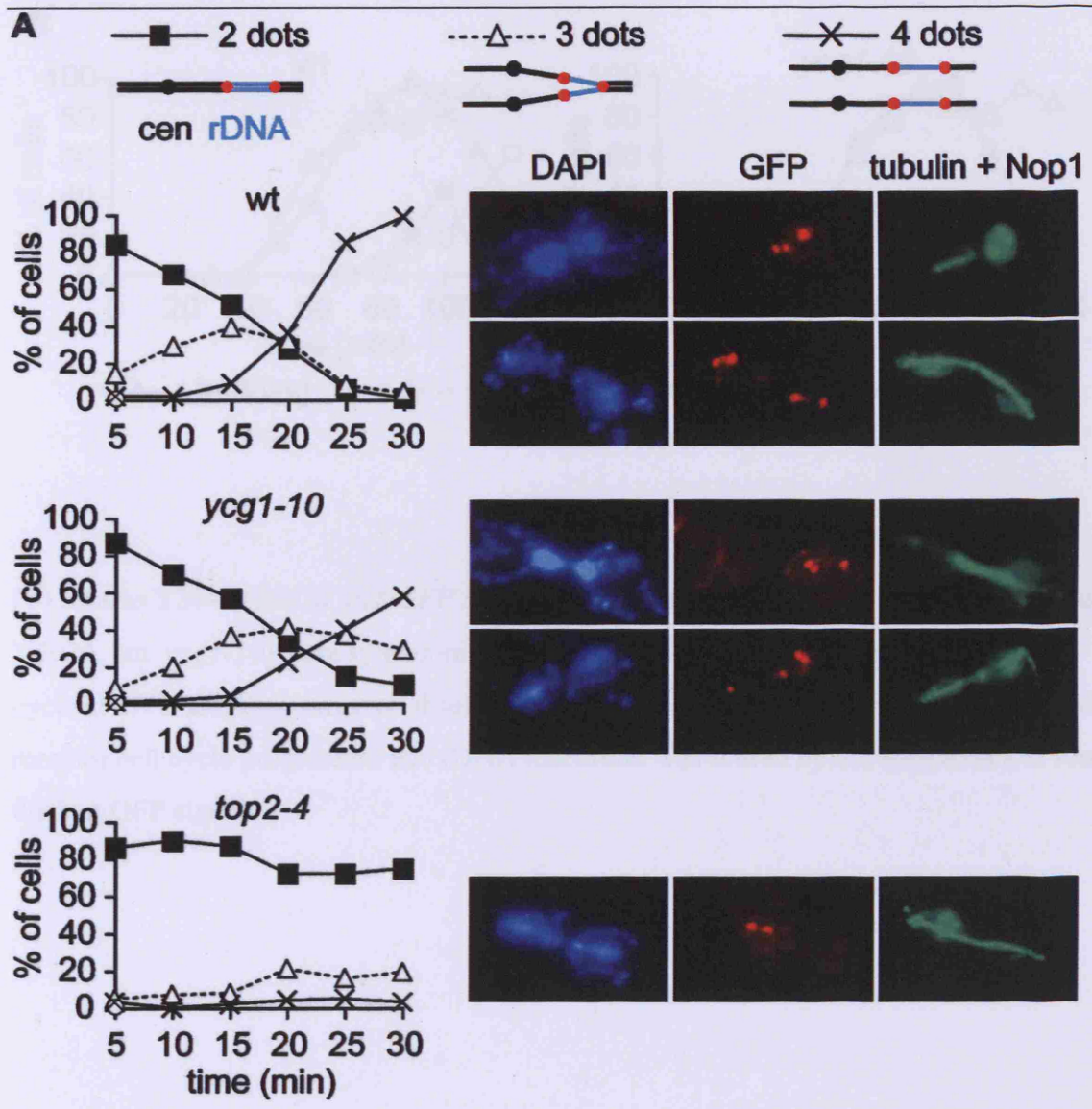

Figure 3.6 Residual, spindle-mediated rDNA decatenation in the absence of condensin
(**A**) Delayed rDNA resolution after condensin but not after topoisomerase II inactivation. Cells of strains Y2945 (*MATa MET3-CDC20 lacI-GFP LacOs::MAS1 LacOs::ACS2*), Y2944 (as Y2945, but *ycg1-10*) and Y3152 (as Y2945, but *top2-4*) were arrested in metaphase and released into synchronous anaphase after temperature shift. Resolution of the rDNA proximal (*MAS1*) and rDNA distal (*ACS2*) locus were analysed by splitting of the GFP dots at these loci. Staining of the mitotic spindle and the nucleolar marker Nop1 provided spatial clues as to the orientation of the rDNA array.

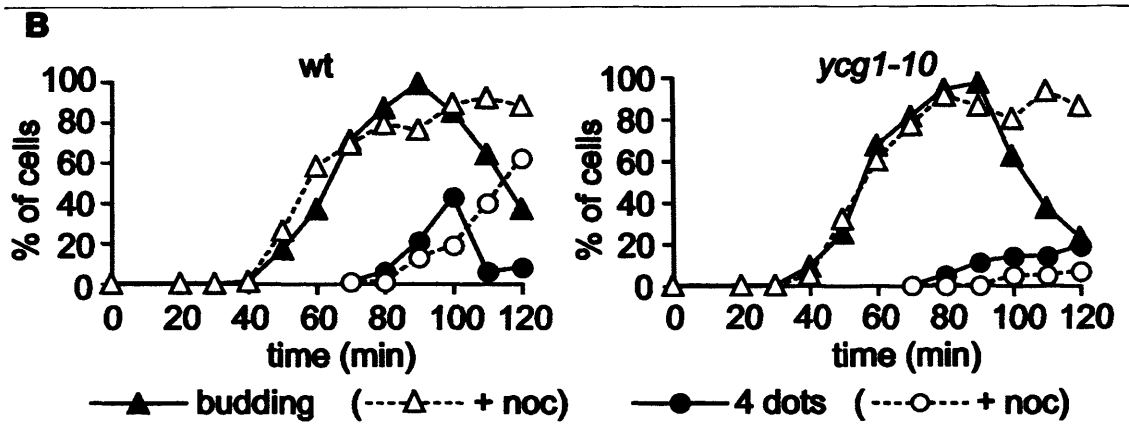

(**B**) Strains Y3042 (*MATa lacI-GFP LacOs::MAS1 LacOs::ACS2 mad2Δ*) and Y3245 (as Y3024, but *ycg1-10*) were synchronised in G1 with α-factor and released into the cell cycle at 37°C in the presence or absence of nocodazole. The budding index was analysed to monitor cell cycle progression and rDNA resolution was scored by the appearance of four distinct GFP signals

.

4 Chapter 4: Discussion

4.1 Condensin localisation along budding yeast chromosomes

In this thesis we have examined the localisation of the condensin complex on budding yeast chromosomes. Previous work approached this question through employment of a low-resolution genome-wide analysis of budding yeast chromosomes (Wang et al., 2005). The high density of tiled oligonucleotides in the microarrays used in this study significantly enhanced our ability to spot detailed features of condensin binding sites. Our finding that the condensin pattern of chromatin association is qualitatively unchanged through the cell cycle is consistent with previous results (Wang et al., 2005). A similar amount of condensin is chromatin bound throughout the cell cycle. However, as in other organisms, condensin performs chromosome condensation upon entry into mitosis, thus championing the idea that chromatin compaction and CDK-driven condensin association to DNA are un-separable reactions (Sutani and Yanagida, 1997). Budding yeast condensin therefore constitutes an interesting model where the ability to bind to DNA is possibly genetically uncoupled from its compacting activity. On the other hand the notion that a modification of condensin by CDK drives mitotic condensation remains fully consistent with our data (Kimura et al., 1999). In one possible scenario, the activity *per se* of condensin molecules is unchanged during the cell cycle, but lower turnover of condensin binding upon mitosis entry (as a result of a CDK-dependent modification) accomplishes chromatin compaction. In fact, preliminary evidence for this phenomenon came from the analysis of the behaviour of the condensin II complex in humans (see Introduction and (Gerlich et al., 2006a)). During G1, in contrast, similarly active condensin, acts transiently and unproductively due to its fast turnover on chromatin (see Figure 4.1). Since FRAP (fluorescence recovery after photobleaching) experiments have recently proved to be an efficient tool to determine protein-DNA association dynamics *in vivo* (Gerlich et al., 2006a), these hypotheses can be easily tested by comparing G1 versus mitotic condensin turnover onto budding yeast chromosomes.

Recent results expanded even more the already vast range of important functions of condensin in structuring eukaryotic chromosomes (Gerlich et al., 2006a). Our chromatin immunoprecipitation experiments indicate condensin affinity for sequences around

centromeres increases as cells enter mitosis. This observation is fully consistent with the ability of condensin to confer stability to centromere structures in metazoans (Gerlich et al., 2006a). Taking all the evidence together, including microscopy and functional assays (Gerlich et al., 2006a; Yong-Gonzalez et al., 2007), local enrichment is unlikely the consequence of multiplicative cross-linking reactions that occur around the centromere due to its over-folded structure but it rather reflects a real enhancement of the number of molecules that bind to these sequences upon entry into mitosis. The fact that centromeres may require further stabilisation during the establishment of tension between kinetochores and spindle appears to be a convincing explanation to the observed phenomenon. However, less clear at the moment is the mechanism that signals the requirement for additional recruitment.

From this study we gathered important insights on how and where condensin prefers to establish and maintain contacts with chromosome arms. Condensin association sites clearly developed along with other important aspects of chromatin metabolism including transcription and sister chromatid cohesion. While our experiments favour the idea that a spatial geometric pattern is not strictly determining where these sites evolved, they clearly suggest that the binding sites must be distinct from sequences highly processed by RNA polymerase II for transcription purposes. As opposed to cohesin, the observed "coding region exclusion mechanism" on chromatin seems more an inherent static feature of condensin association to DNA rather than a dynamic one. However, it is also possible that condensin relocates from different loading sites in response to transcriptional activities fast enough to give an illusory snapshot of binding pattern. It would be interesting to evaluate condensin localisation in the absence of transcription (RNA pol II in particular).
The condensin and cohesin complexes do not colocalise on chromosome arms. This was previously noted (Ciosk et al., 2000) and it is confirmed by our ChIP on chip data and relative statistical comparison. The reason for this is now clear: while cohesin very transiently interacts with Scc2/4 to then quickly, for the most part relocates elsewhere, condensin sticks at these sites where its own DNA association rate remains dependent upon Scc2/4. An additional contribution to the observed non-colocalisation of the two complexes may find explanation within their individual relationship with ongoing transcription. While cohesin (whatever the mechanism) can be forced by transcription to relocate elsewhere (Lengronne et al., 2004), condensin may be intrinsically more resistant to these inputs. Therefore chromatin developed regions where condensin could associate where there is less

competition with ongoing transcription for underlying sequences. In this regard, the fact that Scc2/4 and condensin sites map at redundant (RNA pol III transcribed) tRNAs and downstream short highly transcribed ribosomal genes fit well with such a view. The relationship of transcription with SMC complexes and now even more, with Scc2/4 is of great interest for the chromosome segregation field.

4.2 *Scc2/4 organises eukaryotic chromosomes through orchestration of SMC complexes*

Our study points towards an important functional link between condensin and Scc2/4. Firstly, we revealed the two complexes closely occupy the same sequences on DNA suggesting that either the rule underlying the two patterns is the same or, conversely, that the establishment of one complex (condensin's) depends on the other (Scc2/4). In between these two extreme case scenarios other intermediate explanations are attainable. Secondly, we correlated impaired condensin binding to chromatin in the absence of Scc2/4 with compromised chromosome condensation in these conditions.

The Scc2/4 complex was first characterised as a chromosomal loading factor for the cohesin complex. It is not yet known how Scc2/4 loads cohesin onto DNA but it possible that Scc2/4 upon interacting with cohesin may stimulate its low intrinsic ATPase activity, an essential prerequisite for cohesin loading onto DNA (Arumugam et al., 2003; Weitzer et al., 2003). Our results suggest that Scc2/4 is also required for chromosome condensation by facilitating the association of condensin with chromosomes. The observation that binding of the Smc5/6 complex to chromosomes also depends on Scc2/4 (Betts Lindroos et al., 2006) invites us to consider that besides Scc2/4's primary function in cohesin loading, it may also act in the recruitment of Smc complexes with broad specificity. While a direct protein interaction between Scc2/4 and cohesin has been documented, we failed to observe a similar interaction between Scc2/4 and condensin. It is possible that the affinity, dynamics or directness of the interactions might differ between Scc2/4 with cohesin and condensin. Also plausible is that the Scc2/4 complex facilitates condensin association with chromosomes by an indirect, totally distinct mechanism from that involved in cohesin loading. Irrespective of the details of how Scc2/4 accomplishes functional chromatin binding of eukaryotic SMC complexes, it is interesting to ask how ancient such a complex may be. However, the difficulty of spotting similarities in the sequences of the different Scc2 and Scc4 homologues in eukaryotes (Strachan, 2005; Tonkin et al., 2004; Watrin et

al., 2006) make the identification of an Scc2/4-like player in prokaryotes a hard challenge to enbark on.

Despite several models continuing to challenge the literature, compelling evidence shows that cohesin association with chromosomes involves topological binding to DNA (Ivanov and Nasmyth, 2005). It appears likely that the Scc2/4-dependent loading step is important to achieve cohesin's topological DNA embrace. The requirement of Scc2/4 for productive binding of condensin and the Smc5/6 complex opens the possibility that these Smc complexes are also topologically loaded onto DNA. The fact that condensin, unlike cohesin, does not (or only with reduced processivity) translocate away from the loading sites does not preclude a topological mode of condensin loading onto chromosomes. The dissociation rate after loading is faster than that of cohesin, as illustrated by the finding that very little turnover of cohesin on chromosomes can be detected after S phase (Gerlich et al., 2006b; Lengronne et al., 2006). Condensin, in contrast, may exist in a dynamic binding equilibrium at its TFIIIC sites, and, consistently, in our experiments Scc2/4 is necessary to maintain condensin association with chromosomes even in mitosis. This result is consistent with the observation that mitotic chromosome condensation is a readily reversible process in budding yeast (Lavoie et al., 2002). In addition, a faster turnover of condensin on human chromosomes, as compared to cohesin has been observed (Gerlich et al., 2006a; Gerlich et al., 2006b).

Do Scc2 and Scc4 proteins in other organisms promote chromosome condensation? Here several studies have yielded ambiguous results as to a contribution of the Scc2/4 complex to the process. *mis4-242* cells (mutant of the fission yeast Scc2 orthologue) do not manifest signs of chromosome condensation defects beside the evident failure in the establishment of sister chromatid cohesion (Furuya et al., 1998). The Scc2 orthologue in the fungus *Coprinus cinereus*, encoded by its *RAD9* gene, is required for meiotic chromosome condensation, but whether or not this correlates with an abnormal condensin recruitment to chromatin has not been analysed (Seitz et al., 1996). When Scc2/4 was depleted from *Xenopus* egg extracts (Gillespie and Hirano, 2004), no defects in chromosome structure were seen. Reduced levels of condensin itself by RNA interference in human cells (Gerlich et al., 2006a), did not trigger apparent chromosome condensation defects. In these cells Scc2/4 seems to disappear from chromosomes during mitosis (Watrin et al., 2006). It is worth mentioning that vertebrate cells undergo an apparently normal process of mitotic chromosome condensation even with largely reduced levels of condensin (Gerlich et al.,

2006a; Hudson et al., 2003; Ono et al., 2004). However, the fact that these chromosomes lack structural stability makes the analysis of condensin levels on chromatin in the absence of Scc2/4 still an interesting point to assess. In *Drosophila*, mutants of *Nipped-B* (Scc2 orthologue) make mitotic chromosomes appear structurally compromised (Rollins et al., 1999). Our finding that Scc2/4 stabilises condensin binding to chromatin is of clinical interest since mutation of a single copy of human Scc2 causes Cornelia de Lange syndrome (see Chapter 1). So far the disease has been correlated mainly with cohesin misregulation that might reflect on impaired expression of developmental genes (Rollins et al., 1999). In addition, a recent work showed that G2, but not G1, CdL human cells also have reduced capacity to tolerate DNA damage (Vrouwe et al., 2007). The authors linked impairment of sister chromatid pairing with reduced homologous recombination as a potential explanation for this phenotype. However, the data presented here may warrant further investigation for an eventual involvement of the condensin complex in the establishment and/or stabilization of chromatin-looped structures in these cells. In fact, the stabilisation of specific chromatin arrangements may constitute a prerequisite for productive action of recombination factors during repair (see section 4.3).

4.3 Condensin and nuclear structure

In this study we report the striking discovery that condensin binding sites coincide with those of the RNA pol III factor TFIIIC. These sites include tRNAs, several RNA pol III transcribed genes and a large set of ribosomal protein genes. Thus, the finding that TFIIIC binds chromatin also outside tRNA genes gives to this factor a completely novel function: shaping nuclear structure through the condensin machinery during both interphase and mitosis.

We provide clear evidence that B box promoters and tRNAs constitute *cis*-acting sites for condensin loading onto DNA through TFIIIC. Are non-tRNA TFIIIC binding sites determined by degenerate B box motifs recognised by TFIIIC that developed into important chromatin structural assets? Our finding that the generation of an isolated B box triggers TFIIIC binding as well as condensin would suggest so. It is tempting to speculate that a hierarchical mode of chromatin packaging must have had evolved *in primis* from specific DNA sequences codes. However, in the case of condensin binding to DNA, considering the high frequency of B box like motifs scattered through the genome, additional determinants must also come into play (including epigenetic and histone modification codes) to establish

a fully functional condensin association site. In this regard (and this links to the first part of the discussion) it is worth remembering that RP genes and tRNAs are highly transcribed genes (although by different polymerases). Therefore, as mentioned above, transcription might play a role in the establishment of condensin binding sites. Within our list, there is a large set of binding sites (approximately 60) that seems linked to neither tRNAs nor RP genes. To ultimately and widely correlate establishment of the most important condensin binding (or Scc2/4) sites with transcription, it will be of interest to assess whether also these genes are intensively transcribed.

What happens to TFIIIC-Scc2/4 sites during mitosis-specific chromosome condensation? *In vitro*, the ATP-hydrolysis dependent DNA supercoiling activity of *Xenopus* condensin is stimulated by Cdk phosphorylation of its XCAP-D2 subunit (Kimura et al., 1998). How such maximization of condensin activity is reflected in terms of nuclear structure is currently unclear.

In one possible model condensin bound to one association site might be permitted to contact a second TFIIIC-Scc2/4 binding site while maintaining (topological) contact with the first (see Introduction). Condensin in this way could form dynamic linkages between neighbouring TFIIIC binding sites. Interestingly, the position of loci within nuclei is highly mobile, a process that so far has been attributed to the ongoing activities of RNA polymerases and remodelling complexes on chromatin (Gasser, 2002). The ability of condensin to link TFIIIC-Scc2/4 sites would increase during, but may not be exclusive to, mitosis. A basal level of interactions could contribute to the structural identity of interphase chromosomes. It has been noted that tRNA genes, and the TFIIIC complex, form clusters of association within interphase nuclei (Noma et al., 2006; Thompson et al., 2003). Whether formation of this cluster has implications for the establishment of large loop domains and for transcription is not yet known. Strikingly, these sites correlate with Scc2/4 whose function in higher eukaryotes might include the stabilisation of long distance promoter-enhancer contacts (Rollins et al., 1999). Now, the fact that we also find the condensation machinery at these sites and the finding that tRNA gene clustering depends on the condensin complex (personal communication from R. Haussler and D. Engelke) provides the first example of condensin-mediated linkages between more than one locus. It will be interesting to ask whether, condensin discriminates between the many TFIIIC sites within the nucleus during interphase and during mitotic chromosome condensation. Of particular interest would be to assess whether the range of action of condensin binding sites within the

nuclear space is delineating (rather than be a consequence of) the observed borders of chromosome territories (Cremer and Cremer, 2001). In any case, an implicit corollary following this model would be the existence of condensin-dependent clusters of sequences scattered through the genome. This task, interestingly, might be accomplished through multimerisation of individual condensin holo complexes (for a summary of the topics here discussed see model in Figure 4.1).

Condensin's described roles in interphase gene regulation, and the known boundary function of tRNA genes within loop-like chromatin domains, may also relate to the ability of condensin to establish contacts between neighbouring binding sites (Valenzuela and Kamakaka, 2006). In this regard it has been long noted that vertebrate Alu containing sequences are rich in tRNA-like promoters although function of Alu as boundaries and/or in condensin recruitment has not been yet investigated (Paolella et al., 1983). Interestingly, it is worth mentioning that a link between Alu with the related cohesin complex has been made (Hakimi et al., 2002). tRNA genes are known to be slow zones of chromosomal DNA replication, and it is now possible to address whether this is a consequence of condensin binding. Analogously, strong non-tRNA condensin binding sites could act in a similar way. Irrespective of the answer, can these binding sites be ascribed to chromosomal regions of late replication (Wang et al., 2005)? It is possible that the reduced speed of DNA replication at tRNA genes maximises the chances that a fork from the opposite direction will merge, and possibly disassemble at these sites. Replication termination reactions may benefit from anchoring of the locus by condensin, as well as from the presence of topoisomerase II in close vicinity (see Chapter 3) (Lupo et al., 2001). In response to fork stalling outside of condensin binding sites, Scc2/4 and condensin are recruited to the replication fork. The establishment by Scc2/4 of a condensin anchoring site may contribute to the stability of stalled forks within the nuclear environment while repair and restart processes are underway (see section 4.2).

Like budding yeast condensin, the human condensin II complex is nuclear throughout the cell cycle (Hirota et al., 2004; Ono et al., 2004). These condensin molecules may act similarly in human cells to provide structural integrity of interphase chromosomes, and, because of the results here reported, this is now an even more inviting question to be address. Once activated in mitosis, relatively few condensin molecules could be sufficient to establish extended interactions between Scc2/4-TFIIIC binding sites along chromosomes. While this would suffice to define the mitotic chromosome shape, addition

of the condensin I complex may reinforce interactions at these or additional sites (like centromeres) to stabilise large chromosomes (Hirota et al., 2004; Ono et al., 2004). A clear function of condensin I seems to support centromere structure in preparation for establishment of tension between kinetochore and spindle (Gerlich et al., 2006a). This is in line with the chromosomal pattern of condensin I being distinct from that of condensin II (Ono et al., 2003). It is conceivable that condensin I, which gains access to chromosomes as transcription is largely downregulated in mitosis, requires less targeting specificity and might be able to associate with chromosomes in an Scc2/4-independent manner, thereby adding stabilisation to the chromosome. In this regard it is tempting to speculate that recruitment of the unique budding yeast condensin complex is at least differently regulated between centromere and chromosome arms. This is suggested by our observation that centromere enrichment is not reflected by a similar increase in TFIIIC binding. Thus while one yeast complex fulfils distinct tasks, higher eukaryotes developed two complexes with specialised competences.

In summary, our identification of specific loading and anchoring sites for chromosomal Smc subunit-containing protein complexes opens a full range of new possibilities to explore eukaryotic chromosome function and architecture.

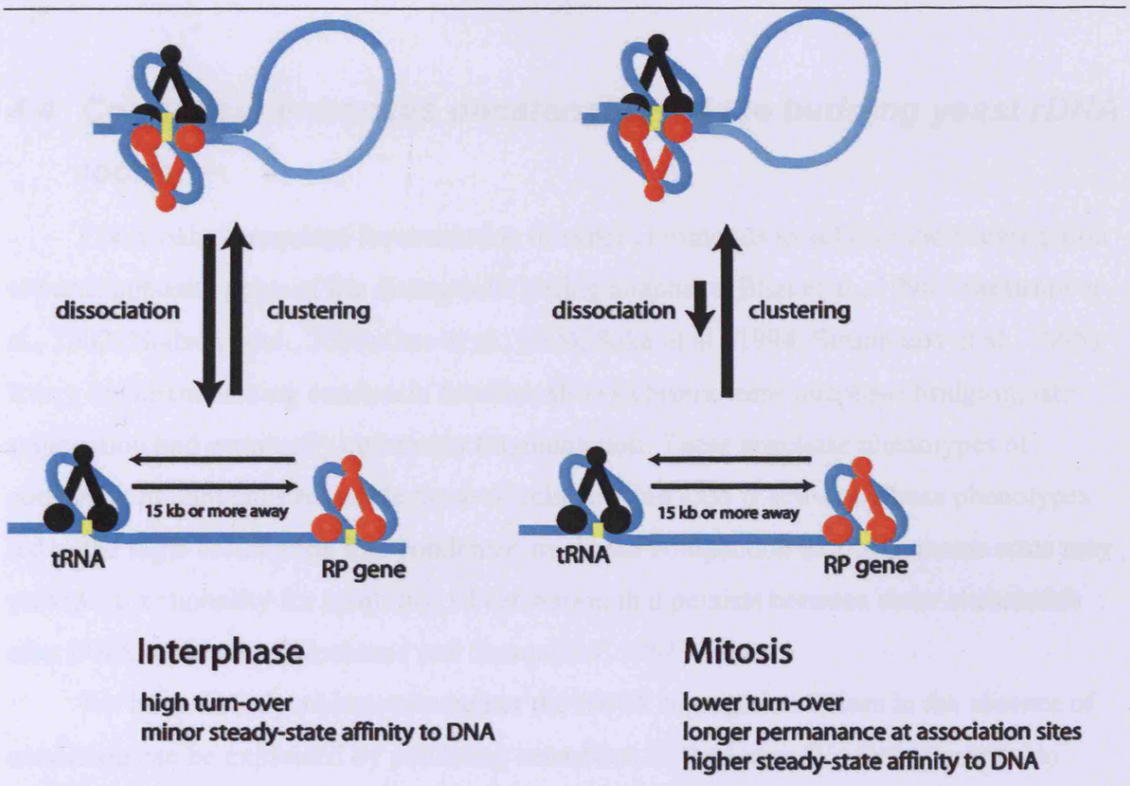

Figure 4.1 Condensin mediated chromatin organization during interphase and mitosis
Condensin mediates transient contacts of distant DNA sequences in *cis* by its highly dynamic interactions with chromatin. This is supported by the observation that the TFIIIC and tRNA clustering are observed during interphase as well as the existence of chromosome territories. During mitosis, a CDK-dependent modification on condensin makes it more stably chromatin bound (lower turn-over) thus firmly stabilizing chromatin shape.

4.4 Condensin enhances decatenation of the budding yeast rDNA locus

Condensin is required for resolution of sister chromatids to achieve their segregation towards opposite poles of the diving cells during anaphase (Bhat et al., 1996; Hagstrom et al., 2002; Hudson et al., 2003; Ono et al., 2004; Saka et al., 1994; Strunnikov et al., 1995). Every organism lacking condensin function shows chromosome anaphase bridging, late segregation and eventually chromatin fragmentation. These anaphase phenotypes of condensin mutant cells resemble those of cells lacking topo II activity. These phenotypes led to the logic assumption that condensin-mediated compaction of chromosome arms may provide directionality for resolution of catenation that persists between sister chromatids after DNA replication (Koshland and Strunnikov, 1996).

We have directly addressed whether the rDNA segregation failure in the absence of condensin can be explained by persisting catenation of the locus. We first attempted to overcome the segregation defects by increasing the dosage of topo II during an anaphase carried out in the absence of condensin. This led to negligible effects in enhancing timely segregation of rDNA, despite topo II's increased affinity for chromosomes in these conditions. In fact our results suggest that the already abundant enzyme can be forced to bind DNA even more when synthesised under the control of a strong promoter, hence giving a probable explanation for its observed toxicity in these conditions (Adachi et al., 1997). Here we find that the highly active type II topoisomerase from *Chlorella virus* relieves impaired, late segregation or the rDNA in a condensin mutant. This provides the first direct evidence that in the absence of condensin, chromatin bridges are actually of topological nature. This finding cannot fully exclude that topological linkages arises merely a consequence of condensin malfunction. However, our observation that in wild type cells rDNAs can resolve earlier when supplied with exogenous topoisomerase make this argument less forceful and rather suggests that condensin enhances decatenation of naturally intertwined sister chromatids.

What distinguishes *Chlorella virus* topo II from its yeast counterpart that makes it a more efficient condensin-independent instrument for rDNA resolution?
Cv-topo II is a much more active type II topoisomerase than yeast or mammalian topo II (Fortune et al., 2001), hence, it is possible that regions of catenation are more efficiently

disentangled by the exogenous topoisomerases simply because of its higher potency. Alternatively, if it is not solely a matter of cleavage activity it is possible that yeast topo II function, but not cv-topo II, normally reaches optimal activity due to a condensin-dependent stimulatory role, possibly through its C terminal extension that is missing in cv-topo II. However, in a preliminary attempt to create a condensin-independent yeast topo II (by truncation of the largest portion of the C terminal), we found that it did not improve rDNA segregation in the same conditions.

When rDNA repeats are moved to episomal form, condensin remains essential for chromosome segregation (Freeman et al., 2000). This can be accounted for by the possibility that condensin dependent decatenation helps the resolution of several loci along the genome. When we attempted to rescue overall chromosome segregation in a condensin mutant by expressing the exogenous topoisomerase earlier in anaphase we could not rescue the massive chromosome segregation defects (our unpublished observation). Condensin is a fundamental chromatin factor with several functions in chromatin metabolism. Therefore it is technically very challenging to find experimental windows where its diverse roles can be unravelled and analysed individually. It seems plausible that in these conditions a larger number of topological linkages and the lack of robust anchoring of kinethocores by the spindle (Gerlich et al., 2006a; Yong-Gonzalez et al., 2007) constitute challenges that cannot be tackled by the the exogenous topoisomerase.

How does condensin maximise topo II function at a mechanistic level?

As discussed in the introduction, chromatin condensation is seen as a way to direct the disentangling activity of topo II. While we cannot exclude it, this scenario would not explain how cv-topo II efficiently decatenates rDNA without condensin. Our data suggest that condensin must enhance DNA decatenation, at least of the rDNA repeats, independently of the overall compaction of the locus. Indeed, as previously noted, condensation of the locus is not a prerequisite for its segregation ((D'Amours et al., 2004; Sullivan et al., 2004); this study) whereas condensin and/or decatenating activities are. We currently favour alternative explanations that include a direct boost of topo II decatenation activity as has been proposed in *Drosophila* (Bhat et al., 1996). Interestingly, this can be accomplished by condensin through exerting a local directional pull closely beside the range of action of topoisomerase rather than through a physical protein-protein interaction. The fact that topo II and condensin colocalise is consistent with this view. So far, the yeast condensin mutants isolated (including *ycg1-10*), beside the chromosome condensation

defects all show negligible ability of chromosome association. It is not known what the consequences are for chromatin structure immediately close to where condensin associate. Perhaps, the sole association of condensin with chromatin constitutes most of the required substrate for optimal decatenation activity. The eventual isolation of a condensin mutant allele that does not function in overall chromosome compaction while retaining its DNA binding activity might give us clearer insights as to whether or not the above hypothesis is founded. Clearly, to fully elucidate how condensin regulates topo II function we must wait for the establishment of an experimental system where decatenation of chromosomes *in vivo* can be followed, evaluated and quantified in different conditions.

5 Chapter 5: Material and Methods

5.1 Yeast techniques

5.1.1 Yeast growth conditions

Haploid yeast cells were employed in this study for all applications. Cells were grown in YP (1.1% w/v yeast extract, 2.2% w/v bacto-peptone and 0.0055 % w/v adenine-HCL) supplemented with 2% w/v glucose (YP-Glu) or 2% (or 3%) w/v raffinose/galactose (YP-Raff/Gal). For growth of strains containing Cdc20 under the control of the methionine repressible *MET3* promoter, cells were grown in synthetic YNB media (Yeast Nitrogen Base: 0.8% w/v yeast nitrogen base, and 60μg/ml of each of the following amino acids: tyrosine, uracil, tryptophan, leucine, adenine, histidine, isoleucine and phenylanine, 3 μg/ml arginine, 4 μg/ml lysine and 5 μg/ml threonine) supplemented with either 2% w/v glucose or 2% w/v raffinose/galactose. For the selection of transformants, YNB agar plates (as per YNB except 2.2% w/v agar) were used lacking the auxotrophic amino acid used for selection. Alternatively for selection based on Kanamycin resistance YP-Glucose plates were supplemented of the kanamycin derivative Geneticin G418 (50 μg/ml).

5.1.2 Cell synchronisation

Mating type a yeast cells were arrested in G1 with the mating pheromone α-factor. To arrest cells, an early log phase culture (OD_{600} = 0.1) was treated with α -factor (provided by peptide services, Cancer Research UK) at a concentration of 2.5μg/ml. One and two hours later another 1.8μg/ml and 1.25μg/ml of α -factor were added. Arrests were generally complete within two generations time. Cell cycle arrest were determined both cytologically by the appearance of a pear-shaped 'Schmoo' and by FACS analysis of DNA content. G1 arrested cells were released by filtration within media devoid of α-factor. For filtration, cells were collected on a membrane filter (Schlechter & Schuell, ME28, 1.2μm) using a filtration apparatus from Millipore. Cells were extensively washed with (at least 4 volumes) YP before release into YP media supplemented with the appropriate source of sugar. For the collection of equal amount of cells post G1 release for chromatin

fractionation, the culture was subjected to mild sonication conditions to eliminate clumping of schmooing G1 cells.

For arrest in metaphase, nocodazole (Sigma) was added at 5μg/ml. Cell cycle arrests were assessed cytologically by the presence of large budded cells. For arrest using Gal1-Cdc20, cells were cultured in media containing 2% raffinose and 2% galactose before being filtered, washed and transfered to media containing only raffinose. For arrest using the repression of *MET3-CDC20*, cells were grown in YNB lacking methionine and supplemented with 2% glucose. To arrest cells, cells were transferred to rich media (YP) and 2% methionine was added. Cell cycle arrests were again checked cytologically and by DNA content.

Early S phase arrest was performed by the addition of Hydroxyurea (HU, Sigma, a ribonucleotide reductase inhibitor) (at 200mM) to previously G1 arrested cells. The presence of small buds indicates S phase arrest. Arrest in S phase was also achieved by adding HU to cycling cells.

5.1.3 Protein overexpression from the *GAL1* promoter

For overexpression of proteins from the *GAL1* promoter, cells were grown in YP supplemented with 2% raffinose (Sigma) until mid log phase and protein expression was induced by the addition of 2% galactose (Sigma) for 2- 3 hours.

For protein repression (e.g. Cdc20) cultures were grown in YP containing both 2% galactose and 2% raffinose. To repress expression, the culture was filtered, extensively washed with YP, and transferred to YP media containing raffinose as the sole sugar source. Protein expression was checked by western blotting.

5.1.4 Protein expression and repression from the *MET3* promoter

To repress Cdc20 expression from the *MET3* promoter, the endogenous Cdc20 promoter was first replaced by the *MET3* promoter by one step promoter swap PCR reaction. Positive transformants were grown in complete YNB lacking methionine media containing 2% glucose, or when expression from the *GAL1* promoter is required 2% of raffinose. To repress Cdc20, cells were transferred in complete media (YP) and methionine was added to a final concentration of 2mM.

5.1.5 Yeast transformation

Transformation of yeast was performed using PCR products as described below. 50ml of a mid log phase culture was pelleted at 3,000rpm for 5 minutes. The cell pellet was washed with 1 ml de-ionized water before washing with 1ml TEL (10 mM Tris/HCL pH 7.5, 100 mM EDTA and 100 mM Lithium acetate) before resuspension in a final volume of 100µl TEL. To this cell suspension was now added approximately 1 µg of either linearised vector DNA or PCR product and 2 µl of a 10 mg/ml single stranded carrier DNA from salmon sperm and 600ml TELP (TEL plus 40% PEG 3350 or 4000), followed by a short vortex. After incubation at 25°C for 2-3 hours, cells were heat shocked at 42°C for 15 minutes. After this point cells were allowed to recover for several hours in liquid media prior to plating. The cells were then pelleted at 6,000 rpm for 2 minutes, washed in 1ml sorbitol and plated on selective media. Transformants were checked for the correct integration of the PCR cassette by western blot analysis or death on methionine (in the case of *MET3-CDC20*) or glucose (*GAL1-CDC20*) containing media.

5.1.6 Cell cycle analysis using flow cytometry

To determine cell cycle progression by DNA content, 1ml of a mid log phase culture (OD_{600} = 0.4) was pelleted and fixed in 70% ethanol on ice for 2 hours. Cells were then RNAse treated in 1ml 200 mM Tris-HCL pH 7.5 containing 0.1 mg/ml RNAse A overnight at 37°C. After pelleting, DNA was now stained using 400µl of a propidium iodide containing solution (200 mM Tris-HCL pH 7.5, 211 mM NaCL, 78 mM $MgCL_2$ 50µg/ml propidium iodide). Cells were sonicated (Sanyo, Soniprep 150) before being analysed on a FACScan (Becton Dickinson). Subsequent image preparation was performed using CellQuest software.

5.2 Biochemistry and related techniques

5.2.1 Immunoprecipitation

Immunoprecipitation reactions were performed on soluble yeast extracts as described previously (Liang and Stillman, 1997). Usually between 100 and 250ml of mid log phase culture (OD_{600} = 0.5) were pelleted at 3000rpm for 10 minutes. Cell pellets were then resuspended in 5ml PIPES/KOH buffer (100mM PIPES/KOH pH 9.4, 10mM DTT)

for 10 minutes at room temperature. Cells were then pelleted at 2000rpm for 2 minutes and resuspended in 5ml Kpi/Sorbitol buffer (50mM K_2HPO_4/KH_2PO_4, 0.6M Sorbitol, 10mM DTT). The cells were then spheroplasted by the addition of Zymolase T-100 (MP Biomedicals) in the above buffer to reach a final concentration of 40µg/ml for 10 minutes at 37°C. The cells were then collected by centrifugation (800 rpm for 5 minutes), washed with ice cold Spheroplast wash buffer (50mM HEPES pH 7.5, 100mM KCL, 2.5mM $MgCl_2$, 0.4M sorbitol), and subsequently resuspended in 20 ml ice-cold EB buffer (50mM HEPES/KOH pH 7.5, 100mM KCL, 2.5mM $MgCl_2$ 1mM DTT) supplemented with protease inhibitors (1mM PMSF, 2µg/ml leupeptin, 2µg/ml aprotinin, 2µg/ml pepstatin, 200µg/ml bacitracin, 2mM benzamidine, plus complete mini-EDTA free protease inhibitor tablets from Roche. This cell suspension was then lysed by the addition of Triton-X-100 at 0.25% (or up to 1 % in cases where high detergent is required) for 3 minutes while vortexing intermittingly. The cell lysate was now carefully layered onto a sucrose cushion of EBXS (EB, plus 30% sucrose) and centrifuged at 4°C for 10 minutes at 12,000rpm to separate soluble and insoluble fractions. After centrifugation, the soluble extract consists of an upper yellow layer above the sucrose. This soluble extract was removed for subsequent immunoprecipitation reactions. The extract was first pre-cleared to prevent non-specific protein binding by the addition of 1/10 volume of Protein-A-sepharose (Sigma) to the extract for 30 minutes on a rotating wheel at 4°C. After centrifugation (800rpm for 1 minute) the lysate was removed and incubated with either anti-PK (Serotec), anti-myc (ICRF, 9E10) or HA (ICRF, 12CA5) at concentrations of 1:450, 1:180 and 1:450 respectively. After incubation on ice for 1 hour, Protein-A-Sepharose was added to a final concentration of 1/40 the extract for 30 minutes on a rotating wheel at 4°C. The antibody-coupled beads were then washed 8 times with EBX containing protease inhibitors and 1mg/ml BSA. The immunoprecipitated proteins were then eluted with 2xSDS loading buffer and analysed by western blotting.

5.2.2 Chromatin fractionation

To analyse protein binding to chromatin, lysates were prepared in the same way as for immunoprecipitation reactions described in the previous section with the following changes. After the separation of the soluble from insoluble material on the sucrose cushion, the soluble extract on the top layer was now separated and eventually mixed with an equal

volume 2x SDS loading buffer for western blotting. The remaining chromatin pellet was resuspended in 200µl EBX. An aliquot of this material was then added to an equal volume of 2x SDS loading buffer as before. As controls for chromatin bound and soluble proteins we used antibodies against Histone H3 and PSTAIRE (both Santa Cruz) respectively.

5.2.3 Chromatin immunoprecipitation followed by hybridisation to a high density oligonucleotide array (ChiP on chip)

200 ml of late log phase culture ($OD_{600} > 0.6$) cells grown in YPD medium were fixed by the addition of formaldehyde (final concentration of 1% v/v) overnight on a rotating wheel at 4°C. The cell pellets were then washed in ice-cold TBS (200 mM Tris-HCL pH 7.5, 1.5M NaCl) before transfer to 1.6ml lysis buffer (50mM HEPES-KOH, pH 7.5, 140mM NaCl, 1mM EDTA, 1% triton-X-100, 0.1% Na-deoxycholate, 1mM PMSF). The cells were then broken on a multi-bead shocker (MB400U, Yasui Kikai, Osaka, Japan), which is able to work at very cold environment (below 4°C) therefore limiting protein degradation. This soluble extract was then sonicated (Sanyo, Soniprep 150) to obtain DNA fragments of between 400bp-800bp. The extract was then incubated with anti-PK (clone SV5-Pk1, Serotec) or anti-myc antibodies (ICRF, 9E10) coupled Protein-A Dyna beads (Dynal) on a rotating wheel at 4°C for 3 hours. The presence of immunoprecipitated protein was confirmed by western blotting. After washing the beads with lysis buffer, the immunoprecipitates were eluted using elution buffer (50mM Tris-HCL pH8.0, 10mM EDTA, 1% SDS) at 65°C for 10 minutes. To one volume of the eluate was now added three volumes of TES (10mM Tris-HCL, pH 8.0, 1mM EDTA, 1% SDS) and this mixture was incubated overnight at 65°C to reverse the crosslinks. The immunoprecipitate was incubated with Proteinase K to remove protein as follows: to 160µl of the reaction was added 140µl TE pH8.0, 3µl Glycogen (10mg/ml) and 7.5µl Proteinase K (20mg/ml). This mixture was then incubated at 37°C for at least two hours. The DNA was then extracted two times using phenol/chloroform/isoamylalcohol, and subsequently ethanol precipitated, dried in a speed-vac (Savant) and diluted in a final volume of 30µl TE. This sample was then treated with RNAse A (0.3µg/µl) at 37°C for 1 hour to remove any contaminating RNA before amplification. The DNA was now further purified over QIAprep spin columns (Qiagen). The volume was reduced by a further round of ethanol precipitation, dried, and resuspended in a final volume of 7µl. This DNA was amplified by PCR after random

priming (Iyer et al., 2001). Approximately 10μg of amplified DNA was digested with DNAseI to an average size of 100bp. After DNAseI inactivation at 95°C these DNA fragments were subsequently end-labelled with biotin-N6-ddATP as previously described (Winzeler et al., 1998). Each sample was prepared in a 150μl reaction containing 6xSSPE, 0.005% triton-X-100, 15μg denatured salmon sperm DNA (Gibco-BRL), and 1 nmole control oligo B2 that hybridises to specific border regions of the chip to facilitate alignment. The samples were boiled at 100°C for 10 minutes before cooling on ice and hybridisation to the microarray in a hybridisation oven (GeneChip hybri oven 320, Affymetrix, CA) at 42°C for 16 hours. Washing and scanning procedures were performed automatically on the affymetric fluidics station (GeneChip fluidics station 400, Affymetrix). Scanning of the microarray was carried out on a HP GeneAray Scanner (Affymetrix).

The chromosome VI CHIP was produced by the Affymetrix custom express service (rikDAF,P/N 510636, Affymetrix) as well as whole genome tiling array (P/N 520286) and chromosomes 3, 4, 5 and 6 left arm arrays (SC3456a520015F; P/N 520015). Briefly the oligonucleotide array has been designed in a manner to contain sixteen 25mer probes per every 300bp partially tiled over each other to fully cover both coding and non-coding sequences. To distinguish between positive and negative signals we compared the ChIP fraction to a 'SUP' sample representing whole genome DNA, using the criteria as set out in (Katou et al., 2003).

5.2.4 Preparation of yeast extracts

Yeast extracts were prepared according to the previously described method based on NaOH (Kushnirov, 2000). 10ml mid log phase culture (OD_{600} = 0.25) was pelleted at 3,000rpm for 5 minutes. The cell pellets were then washed in 1ml of distilled water before resuspension in 100μl water. 100μl 0.2M NaOH was then added to the cell suspension and incubated at room temperature for 2 minutes. The cells were then pelleted at 13,000rpm for 1 minute and resuspended in 50μl 2x SDS buffer (100mM Tris-HCL pH 6.8, 200mM DTT, 4% SDS, 0.2% Bromophenol blue, 20% glycerol) and then boiled at 95°C for 5 minutes. 5-10 μl were then loaded on an SDS-polyacrylamide gel for western blot analysis.

5.2.5 SDS-PAGE electrophoresis and western blotting

Protein samples were resolved on acrylamide/bis-acrylamide (37.5:1, Amresco) 375mM Tris-HCL pH 8.8 and 0.1% SDS. Small proteins of less than 30 kDa were typically resolved on 10% -15% and larger proteins over 100 kDa on 6% -8% gels. A stacking gel was used on top of the separating gel and was composed of 125mM Tris-HCL pH 6.8, 5% bis-acrylamide and 0.1% SDS.

Proteins were allowed to migrate through the stacking gel at 80 volts and through the separating gel at 120 volts using SDS-PAGE running buffer (25mM Tris, 250mM glycine and 0.1% SDS) in electrophoresis tanks from CBS scientific, CA. To monitor the position of the proteins in the gel and subsequently on the membrane, a broad range pre-stained protein marker (New England Biolabs) was used. Separated protein bands were transferred onto pre-equilibrated nitrocellulose membranes (Schleicher & Schuell) using either a semi-dry transfer apparatus (Hoefer) or a wet-transfer tank (Biorad). Semi dry transfer buffer contained 14.4g/l glycine, 3g/l Tris base, 0.02% SDS and 10% v/v methanol. Wet transfer buffer contained 3.03g/L Tris base, 14.1g/l glycine, 0.05% SDS and 20% v/v methanol. Semi-dry transfer was performed at 1.2mA/cm^2 for 3 hours. Transfer was carried out at 5.3mA/cm^2 for 40 minutes for the wet transfer protocol. The efficiency of transfer was then checked with Ponceau S solution (Sigma). The membrane was then blocked with a 1% skimmed milk solution (Marvel) in PBST (170mM NaCl, 3mM KCL, 10mM Na_2HPO_4, 2mM KH_2PO_4, 0.01% tween 20) for 1 hour at room temperature. Membranes were then incubated with primary antibodies diluted in PBST containing 1% milk for one hour at room temperature. The concentration of antisera used were as following: anti-HA (12CA5, ICRF 1:5000), anti-myc (9E10, ICRF, 1:2000), anti-PK (Serotec, 1;5000), anti-Hmo1 (From S. Brill, 1:2000), anti-PSTAIRE (Santa Cruz, 1:1000), anti-FLAG (Sigma, M2, 1:1000) and anti-tubulin (Sigma, YOL1/34, 1:1000). Membranes were then washed in an excess of PBST three times for ten minutes. Horseradish peroxidase (HRP) coupled secondary antibodies (anti-mouse or anti-rabbit, Amersham, 1:5000) were then incubated with the membrane in PBST containing 1% milk for a further hour. Membranes were washed a further three times as before developing with ECL (Amersham) according to the manufacturer's instructions.

5.3 Molecular Biology

5.3.1 Polymerase chain reaction

5.3.1.1 C-terminal tagging

Epitope tagging of endogenous genes was performed by gene targeting using polymerase chain reaction (PCR) products (Knop et al., 1999). Forward primers contained approximately 50 bp of homology to the 3' end of the gene of interest before the STOP codon. This is followed by 18mer homologous sequence to the vector used for tagging. The reverse primer again contains sequence homologous to the 3'UTR region of the gene, followed by sequence to facilitate priming to the vector. The subsequent PCR product contains flanking regions homologous to the gene of interest, thus targeting the epitope-containing cassette for in-frame fusion with the desired gene. Integration and/or replacement of tRNA or B box sequences were performed with the same principle. Transformants were subsequently selected on plates either using Geneticin G418 resistance (in the case of KanMX4), or by using auxotrophic markers. In the case of auxotrophic markers, these are derived from either *K. lactis* or *S.pombe* to minimise the chance of integration at the endogenous marker locus. When tRNA (or B box) sequences were transferred, the URA3 marker was subsequently lost after counterselection with 5-Fluoroorotic Acid (5-FOA) leaving integrated the ectopic sequences plus one of the inverted repeats flanking the URA3 marker. Vectors used for one step tagging are listed in the table below. The PCR reaction was set up as follows:

Template DNA	5-10 ng
Forward primer	0.5μM
Reverse primer	0.5μM
dNTP (each of four)	100 μM
10x Expand high fidelity buffer (Roche)	5μl
Expand high fidelity Taq	3.5 Units
dH_20 up to 50μl	

The PCR reaction was then performed on a Peltier Thermal Cycler (MJ Research) using the following programme:

1 x Cycle	2 min at 95°C
20 x Cycle	30 sec at 95°C
	2 min at 50-60°C (depending on the T_M of the primer)
	2 min at 72°C
1 x Cycle	7 min at 72°C

After completion of the cycle, the PCR products were first ethanol precipitated and then checked by agarose gel electrophoresis. To precipitate the DNA, 1/10 volume of 3M sodium acetate was added, vortexed briefly, followed by the addition of 2 volumes of 100% ethanol. This mix was then incubated at -20°C for 20 minutes. The DNA was then pelleted at 13,000 rpm for 15 mins before washing with 70% ethanol and drying in a speed vac. The resulting pellet was then resuspended in 7 -15µl dH_20 for transformation to yeast.

5.3.1.2 Real time quantitative PCR

Chromatin immunoprecipitations were performed identically as described before for ChIP on chip except that after purification of the DNA fragments via QIAprep spin columns (Qiagen) samples (including input) were diluted up to 300 µl in elution buffer (from same Sigma purification kit) including the input sample. Quantitative real-time PCRs (qPCRs) were performed using an MJ Research Chromo 4 real-time PCR system (MJ). PCR mixtures (25 µl) contained 10.5 µl of template DNA (ChIP or 2.5 µl of input), 12.5 µl of 2x SYBR Green Master Mix (Stratagene), and 2µl of 3 nM primers. PCR cycle parameters were 1 min at 95°C, 30 s at 55°C, and 1 min at 72°C. Primer efficiency was first analysed in a preliminary experiment with dilution of primers to define the exponential ("linear") range of the PCR for quantitative analysis. All primer sequences are shown below. Forty-cycle (endpoint) PCR amplification was carried out in duplicated samples and quantitative values reported are from the qPCR analyses. DNA was quantified in the input and immunoprecipitated samples and the ratio was calculated (%IP).

5.3.2 Restriction digestion and phosphatase treatment of plasmid DNA for cioning

Restriction digests were performed using New England Biolabs enzymes and buffers according to the manufacturer's instructions. Typically approximately 1 – 2 μg of plasmid DNA was digested in a 20 μl reaction for 1 hour at 37°C or the appropriate temperature for digestion.

To prevent the re-ligation of plasmid DNA, 5' phosphates were removed from plasmid DNA by treatment with Calf Intestinal Phosphatase (CIP, New England Biolabs) according to the manufacturers instructions. This was carried out immediately after the restriction reaction.

5.3.3 Agarose gel electrophoresis

Agarose gels were prepared by the addition of 1-2% w/v agar (depending on the size of the DNA) in 1 x TAE buffer (40 mM Tris base pH 7.5, 2 mM EDTA and 0.115% v/v acetic acid). After boiling and cooling to below 60°C, ethidium bromide was added to a final concentration of 0.5 μg/ml. 6 x DNA loading buffer (0.25% w/v bromophenol blue, 0.25% xylene cyanol FF and 30% v/v glycerol) was added to DNA samples before loading. DNA gels were ran at between 1 -5 volts/cm (distance between electrodes) in electrophoresis tanks from Anachem Biosciences. The position of the DNA within the gel was monitored by running a DNA marker (Novagene) sample in parallel. DNA fragments were visualised under a UV transilluminator (BioDoc-It).

5.3.4 Mapping by Pulsed-Field Gel Electrophoresis

50 ml of log phase culture was harvested. Spheroplastization was carried out as for chromosome spreads (see below). Meanwhile melted (low melting point agar 1%) in TSE; 10 mM Tris-HCL pH 7.5, 0.9M Sorbitol, 45mM EDTA) was kept at 50°C. Spheroplasts were resuspended by gently mixing in 0.25 ml of melted agar to give an approximate final concentration of 1 X 10^8 cells in 100 μl (which makes 2-3 plugs). 100 μl of suspension was dispensed in triplicates in plug moulds and were allowed to solidify at 4°C for 10 minutes. Plugs were transferred into 12 ml tubes containing 3 ml of 0.25 M EDTA, 50 mM Tris-HCL (pH 7.5), 1% SDS and incubated at 55°C for 90 minutes.

Subsequently the solution was removed and replaced by 0.5 M EDTA (pH 9.5), 1% lauryl sarcosine, with 1 mg/ml Proteinase K for 48 hours. Washes were conducted in TE alone at 25°C, and TE plus 0.04 mg/ml of PMSF at 55°C.

PFGE agar (1%) in TBE 0.5 X was used for running yeast chromosomes.

A Biorad pump and CHEF-DRIII system was used. Briefly, intact yeast chromosome migration was carried out for 24 hours at 6.0 volts/cm and with two opposite inclination angles of 120° that were set to switch intermittently after 60 and 120 seconds.

5.3.5 Southern and Northern analyses

Southern transfer was carried out as described (Southern 1975). Briefly, agar gel was treated with NaOH 0.5M (1.5 M NaCl) for 40 minutes to denature the DNA and then neutralised for 30 minutes (TRIS 1M, 1.5 M NaCl).

For transfer N+ membrane (GE healthcare Amersham Hybond +) was used. 3M paper was put below the gel and dipped into 10X SCC buffer. The membrane and 2 equally sized pieces of 3M paper were put on top of the gel and additional paper and a weight was used to firm the whole blot.

After blotting overnight the membrane was left to dry and cross-linked briefly and ready for hybridisation.

Northern blotting was done essentially as for Southern. Total yeast RNA was obtained by harvesting 50 ml log phase growing culture. Cells were pelletted within microfuge tubes and resuspended in 0.6 ml extraction buffer (50 mM sodium acetate pH 5.0, 10 mM EDTA and 1% SDS). To the samples on ice were added 0.6 ml of pre-warmed phenol (pH 4.3 P4682 Sigma), vortex and incubated at 65°C for 5 minutes. Tubes were vortexed every minute during the incubation. After spin the upper layer was collected and extracted again with warm phenol/chloroform (pH 8.0 P3803 Sigma). The samples were transferred to fresh tubes and RNA was precipitated by ethanol-sodium acetate on ice for 30 minutes. After spin, liquid was removed, the pellet washed with ethanol 70%. The final pellet was resuspended in water and kept in the cold at -20°C.

Total RNA was visualised by electrophoresis through gel containing formaldehyde as a denaturing agent. 200 ml of agarose was melted in water, cooled to 60°C. Formaldehyde buffer 5X (0.1 M MOPS pH 7.0, 40 mM sodium acetate, 5 mM EDTA pH 8.0) was added to the solution in order to achieve a gel containing 3.5 parts of agarose in water, 1.1 parts of 5X buffer and 1 part of formaldehyde 12.3 M (37% solution v/v). The samples were

prepared by mixing in sterile tubes 25μg of RNA (in 4.5 μl of water), 2.0 μl of 5X buffer, 3.5 μl of formaldehyde (37%) and 10.0 μl formamide. These samples were incubated at 65°C for 15 minutes and then chilled in ice. 2 μl of loading buffer was added to each sample (50% glycerol, 1 mM EDTA pH 8.0, 0.25% brophenol blue, 0.25% xylene cyanol FF). Gel was run for two hours at 4 Volts/cm submerged in 1X formaldehyde buffer. Detection of the specific size of the migrating fragments was facilitated by visualisation of an RNA ladder (0.24-09.5 kb Ladder, GIBCO BRL). After run the gel was soaked in 0.05 N NaOH in order to partially hydrolise the RNA thus facilitating its transfer. The gel was rinsed in 20 X SSC for 45 minutes before transfer.

Northern blotting was carried out essentially as described before (Southern). The bands blotted on the membrane were first visualised by treating the membrane with 5% acetic acid for 15 minutes at room temperature. The membrane was then transferred to a solution containing 0.5 M sodium acetate (pH 5.2) and 0.04% methylene blue for 5 minutes and bands were becoming visible upon de-staining the membrane through rinsing in water.

5.3.5.1 Radioactive probe hybridisation of acid nucleic blotted onto membrane

DNA or RNA blotted on Hybond N+ membrane were visualised by sequence specific radioactive (DNA) probes. 50 ng of the DNA template was diluted in 23 μl of water. 10 μl of 9mer primer (Stratagene random primer kit) was added to the template and the sample was left at 95°C for 5 minutes to denature the DNA. Straight after 10 μl of 5X dATP buffer, 5 μl of ^{32}P dATP and 1 μl of Klenow polymerase were added to the mix and the reaction was left at 37°C for at least 10 minutes. The excess of un-reacted radioactive nucleotides in the mix was removed by passing the sample through a resin containing tube (Amersham 50 G50 ProbeQuant columns). The 50 μl reaction was added to a pre-warmed (65°C) hybridisation solution.

For analysis of DNA, the filter was immersed in pre-hybridisation solution (SSC 2X at 65°C) and blocked for 40 minutes with previously boiled salmon sperm DNA (100 μl/ml). After hybridization washes were carried out with SSC 2X, 1% SDS for four times for ten minutes each. For RNA identification on the membrane the hybridization with the probe was carried out in the presence of the Denhardt's reagent (50X contains 5g Fycoll, 5g polyvinylpyrrolidone, 5g bovine serum albumin and water up to 500 ml). The reagent was

diluted into the hybridisation buffer (6X SSC, 2X Denhardt's reagent, 0.1-0.5 SDS). The denatured radiolabelled probe was added as before and the washes were done with 1X SSC, 0.1% SDS, followed by three washes in 0.2 X SSC, 0.1% SDS at 65°C. The filters (with DNA or RNA blotted) were exposed for 2-24 hours to X-ray film (Kodak BioMax MR Film, MR-1) in the presence of an intensifying screen.

5.3.6 Retrieval of DNA fragments from agarose gels

After resolving the DNA molecules by electrophoresis, bands of interest were excised from the gel using a scalpel. DNA was recovered from these bands using a Qiagen gel extraction kit according to the manufacturerer's instructions.

5.3.7 DNA ligation

After quantification of the recovered DNA by a Nano-drop system, ligation reactions were performed. The following formula was used to determine the relative amounts of vector and insert to include in the ligation reaction:

$$Mass_{\text{insert}} = \frac{Base_{\text{insert}}}{Base_{\text{vector}}} \times 3 \times Mass_{\text{vector}}$$

The ligation reaction was set up as follows:

Approximately 50 ng of vector DNA
3x molar excess of insert
800 U T4 DNA ligase (New England Biolabs)
5µl 10 x T4 DNA ligase buffer (New England Biolabs)
dH_20 up to 50µl

Ligation reactions were performed at 16°C overnight or at room temperature for 2-3 hours. After ligation, 25 µl of this reaction was transformed into 100 µl chemically competent *E. coli* (DH5α) cells.

5.3.8 Transformation of E.coli with plasmid DNA

Chemically competent DH5α *E. coli* cells were employed for plasmid DNA amplification. *E. coli* cells were transformed by the addition of 25 µl of the ligation reaction to 100 µl of bacteria on ice. After incubation on ice for 30 minutes, the cells were heat shocked for 2 minutes at 42°C, followed by an additional 2 minutes on ice. The cells were allowed to grow in liquid media by the addition of 1 ml LB (10 % w/v Bacto-Tryptone, 5 % w/v Yeast extract and 170 mM NaCl), before plating for selection on LB agar plates (LB plus 1.5% w/v agar) supplemented with ampicillin (100 µg/ml). Plates were incubated at 37°C overnight. The resulting colonies were inoculated into 5 ml LB-AMP overnight at 37°C and DNA was extracted from the pellets using Qiagen miniprep kits as described below.

5.3.9 Isolation of plasmid DNA from E. coli

Plamsid DNA was recovered from bacterial pellets using Qiagen miniprep kits according to the manufacturers instructions. The principle of the technique is the alkaline lysis of the bacteria followed by DNA adsorption onto a silica matrix in the presence of high salt. After washing the column with ethanol, the DNA was eluted in TE (10 mM Tris, 1mM EDTA pH 8).

5.4 Cell Biology and microscopy

5.4.1 Chromosome condensation assays

Lac operator repeats were inserted at the *MMP1* and *YLR003c-1* loci on chromosome XII, at a distance of approximately 137 kb from each other, and visualised by expression of a lacI-GFP fusion protein as described (Sullivan et al., 2004). Cells were fixed in 100% ethanol, mounted on a 2% agarose patch, and images were acquired as z-stacks of 10 frames at 0.15 µm distance with an Axioplan 2 imaging microscope (Zeiss) equipped with a 100x (NA = 1.45) Plan-Neofluar objective. Distance measurements were then performed in 3 dimensions using Volocity (Improvision) software in at least 100 cells, and the distance distribution analysed using JMP 5.1 software (SAS Institute). rDNA condensation was analysed in ethanol fixed cells expressing a Net1-GFP fusion protein.

5.4.2 In situ immunofluorescence (IF)

2 ml of log phase culture (1 X 10^5 cells) were resuspended in 1 ml ice cold 1% formaldehyde buffer (100 nM KH_2PO_4/K_2HPO_4, $MgCl_2$ 0.5 mM pH6.4) and either fixed over night at 4°C. Cells were first washed in the same buffer lacking formaldehyde once and then resuspended in a new sorbitol based buffer (Solution 1; as before but with Sorbitol 1.2 M, pH 7.4). Cells were resuspended in 200 µl of spheroplasting solution (as above plus 2 µl of ß-mercaptoethanol and 2 µl of 20 mg/ml zymolyase T-100 for each millilitre of solution) and incubated at 30°C for 20 to 40 minutes. After this point spheroplast were delicately washed once and resuspended in the fore mentioned buffer. 5 µl of cells were loaded on previously polylysine coated wells on 15 multi-well slides (MP Biomedical). Slides were blocked with a blocking buffer (0.5% Bovine Serum Albumin) after washing the slides in methanol for 3 minutes and fixing for 10 seconds the cells in acetone. Incubation with primary and secondary antibodies was carried out in the dark in a humid chamber for 1 hour each. Wells were washed with blocking buffer 3 times between antibody staining and 4 times before addition of mounting media with 0.1 µg/ml of DAPI in antifade medium. Slides were then covered with a cover slip and sealed. Antibodies used were, α-Nop1 clone 28F2 (EnCor Biotechnology), α-tubulin clone YOL1/34 (Serotec), α-Pk clone SV5-Pk1 (Serotec), α-GFP clone TP401 (Torrey Pines Biolabs, Houston, TX), α–HA 3F10 (Roche).

5.4.3 Chromosome spreads

1 X 10^5 cells were resuspended in 1 ml of Solution 1, incubated for 12-15 minutes at 37°C in the presence of DTT and zymolyase T-100 (20 µl 1M DTT and 15 µl 10 mg/ml T-100 zymolyase per each millilitre of solution). The reaction was stopped by adding 1 ml of ice cold Solution 2 (0.1 M MES (2-(N-morpholino) ethane sulfonic acid), 1 mM EDTA, 0.5 nM $MgCl_2$, 1M Sorbitol, pH 6.4). Cells were resuspended in 200 µl of Sol 2 and 20 µl were loaded in the middle of a slide (Menzel Superfrost) followed by 40 µl of fixative, 80 µl of 1% lipsol and another 80 µl of fixative. This amount of liquid was spread along the slide by gently using a rod shaped glass in contact with the drop. Slides were left dry over night. The morning after the slides were dipped into PBS for 10 minutes, blocked with blocking buffer (as in IF but with 0.5 % gelatin from porcine skin) and incubated for 2 hours with primary antibodies. Washes were carried out between incubations with primary and

secondary antibodies and before adding 0.1 μg/ml of DAPI in antifade medium and blocking buffer in equal ratio. Slides were covered and sealed as for IF. When quantification of the signal was required, signals from >50 chromosomes spread samples generated from identical exposure conditions were measured using the Image J software.

5.4.4 Sister chromatid separation assay around rDNA locus

Sister chromatid separation was performed using the tetracycline Operator/Repressor GFP system as described in (Michaelis et al., 1997). Under conditions when sister chromatids are tightly cohered, the GFP coated tetracycline arrays appear as one dot. Upon separation of sister chromatids, two GFP dots can be seen. 2 ml culture was pelleted (13,000 rpm for 1 min) and resuspended in 1ml ice cold absolute ethanol or in formaldehyde buffer for IF. Resolution of the rDNA centromeric proximal (*MAS1*) and rDNA centromeric distal (*ACS2*) locus were analysed by splitting of the GFP marks at these loci. Staining of the mitotic spindle and the nucleolar marker Nop1 provided spatial clues as to the orientation of the rDNA array. GFP dots were imaged on an Axioplan 2 microscope (Zeiss). Cells were kept at -80°C for long term storage.

5.5 Statistics

5.5.1 Peack picking of condensing association sites

Briefly, the condensin binding sites were assigned, and a list created accordingly to the following constraints. To reduce the occurrence of unspecific background signals, the experiment was repeated and signal intensities obtained at every locus in the two experiments were averaged. To assign peaks of condensin binding, Brn1-Pk_9 association along the chromosomes was averaged at every point using a +/- 1,000 bp sliding window. Peaks of condensin association were then automatically picked depending on a signal p value relative to a whole genome DNA sample of <0.001 (orange colouring in the bar representation), and a signal $\log_2$ ratio of at least 0.6. A 40 kb region surrounding the centromeres, shaded in yellow, was excluded from this analysis. This revealed 419 sites of condensin association, indicated by red lines rising above the graphs (the list of the peak coordinates relative to Appendix can be found in Tab 1D).

5.5.2 Analysis of significancy of two sets of binding sites

Significance testing of the alignment of peaks between two sets of chromosomal coordinates was carried out using a bootstrap analysis of size N=1000. Peak locations were fixed for one sample, but chosen uniformly across the chromosome for the comparison sample, and the bootstrap statistic was the average distance between peaks in the template sample and the corresponding nearest peak in the other sample. Peak detection was carried out in R (R Development Core Team, 2007) using Kendall's information theoretic approach, as implemented in R's 'pastecs' package (Ibanez, 2007). The fifty most likely peaks from the smoothed signal (running average of 100 contiguous oligonucleotides) from each of chromosomes 3, 4 and 5 were used as representatives.

5.6 Table of strains

Strain nomenclature is followed as per the guidelines set out on the *Saccharomyces* Genome Database (http://genome-www.stanford.edu/Saccharomyces/). Briefly, gene names are represented by three italicised upper case letters followed by a number e.g. *SMC2*. Mutant alleles are represented as lower case italicised letters e.g. *smc3-42*. Alleles created by recombinant DNA technology are named by the use of the symbol for the gene that is altered, followed by a symbol to indicate the nature of the alteration: disruption (::), deletion (-Δ) or replacement (Δ::). Additionally, the symbol used after the '::' symbol indicates the marker used for selection whether for one step PCR tagging (*BRN1-HA6::URA3*), vector integration (*GAL-HA1-SMC2::TRP1*) or promoter swapping (*GAL-CDC20-TRP1*). All the strains used were haploid. The presence of an epitope after the gene name denotes C-terminal tagging (*SMC2-GFP*).

Unless otherwise stated, all strains are isogenic in the W303 background (*MAT*a, *ade2-1 trp1-1 can1-100 leu2-3, Leu112, his3-11, his15, ura3-52*).

Strain	Genotype
Y2200	*MATa* *BRN1-Pk9::HIS3MX6*
Y2269	*MATa* *SCC1-Pk9::TRP1*

Y2280	*MATa* *TOPOII-Pk9::HIS3MX6*
Y2315	*MATa* *SMC2-Pk9::HIS3MX6*
Y2341	*MATa* *ycg1-10/spu4-1 MET-HA3-Cdc20::TRP1* *leu2::LEU2::GAL1-TOP2-Pk3*
Y2423	*MATa* *scc2-4 Scc1-Pk9::TRP1 BRN1-HA6::SpHIS5*
Y2565	*MATa BRN1-Pk9::HIS3MX6* *KLURA3::sequence from YER030W stop to YER034W stop* *(ChrVΔ213,898-222,402) KLURA3 loop out*
Y2611	*MATa scc4::HIS3, scc4-4::LEU2, SCC2HA6::HIS3MX6* *BRN1-Pk9::TRP1*
Y2727	*MATa NET1-GFP::TRP1*
Y2728	*MATa scc4::HIS3MX6, scc4-4::LEU2, SCC2-HA6::HIS3MX6* *NET1-GFP::TRP1*
Y2729	*MATα ycg1-10/spu4-1, NET1-GFP::TRP1*
Y2750	*MATa scc2-4, NET1-GFP::TRP1*
Y2793	*MATa ycg1-10/spu4-1, NET1-GFP::TRP1, MET-HA3-CDC20::LEU* *GAL1-TOPOIIChlorella virus::URA3*
Y2748	*MATa NET1-GFP::TRP1, MET-HA3-CDC20::LEU*
Y2749	*MATα ycg1-10/spu4-1, NET1-GFP::TRP1, MET-HA3-CDC20::LEU*
Y2882	*MATa ycg1-10/spu4-1, MET-HA3-Cdc20::TRP1* *leu2::LEU2::GAL1-TOP2-Pk3, TOP2-Pk3::HIS3MX6*
Y2883	*MATa NET1-GFP::TRP1, MET-HA3-CDC20::LEU2* *GAL1-TOPOIIcv::URA3*
Y2884	*MATa ycg1-10/spu4-1, MET-HA3-Cdc20::TRP1* *TOPOII-Pk3 (LEU2)*
Y2903	*MATa MET-HA3-CDC20::LEU2, Cdc14-myc18-TRP1* *TOPOII-Pk3::HIS3MX6*
Y2421	*MATa scc2-4, SMC2-Pk9-HIS3MX6*

Y2422	*MATa Scc2-Pk9-TRP1*
Y2544	*MATa BRN1-PK9::HIS3MX6, KLURA3::SUF9 (tRNA gene) KLURA3 looped out*
Y2611	*MATa scc4::HIS3MX6, scc4-4::LEU2, SCC2-HA6::HIS3MX6 BRN1-Pk9::TRPP*
Y2512	*MATa Scc1-9PK-TRP1, BRN1-HA6-SpHIS5*
Y2821	*MATa SCC1-HA6::HIS3MX6, BRN1 myc18::URA3*
Y2822	*MATa SCC1-HA6::HIS3MX6, BRN1-myc18::URA3 SCC4-Pk9::TRP1*
Y2869	*MATa lacOs::YLR003c-1 locus, GFP-lacI::HIS3MX6, lacOs::MMP1 locus*
Y2887	*MATa scc2-4, GFP-lacI::HIS3MX6, lacOs::YLR003c-1 locus lacOs::MMP1 locus*
Y2945	*MATa MET-HA3-CDC20::TRP1, LacR-GFP::HIS3MX6, LacOs::ACS2::URA3 locus, LacOs::MAS1::URA3 locus*
Y2944	*MATa ycg1-10/spu4-1, MET-HA3-Cdc20::TRP1, LacR-GFP::HIS3MX6, LacOs::ACS2::URA3 locus LacOs::MAS1::URA3 locus*
Y3042	*MATa mad2::TRP1, LacR-GFP::HIS3MX6, LacOs::ACS2::URA3 locus, LacOs::MAS1::URA3 locus*
Y2717	*SCC2-HA6::HIS3MX6, BRN1-myc9::TRP1*
Y3104	*MATa brn1-9::TRP1, lacOs::YLR003c-1 locus, GFP-lacI::HIS3MX6 lacOs::MMP1 locus*
Y3152	*MATa top2-4, LacR-GFP::HIS3, LacOs::ACS2::URA3 locus LacOs::MAS1::URA3 locus, MET-HA3-CDC20::TRP1*
Y3245	*MATa mad2::KLTRP1, ycg1-10, LacR-GFP::HIS3MX6, LacOs::ACS2::URA3 locus, LacOs::MAS1::URA3 locus*
Y3343	*MATa SCC4-HA6::HIS3MX6*
Y3344	*MATa tsv115, SCC4-HA6::HIS3MX6*
Y3345	*MATa Scc1-Pk9-TRP1, BRN1-HA6::SpHIS5*
Y3346	*MATa tsv115, Scc1-PK9-TRP1, BRN1-HA6-SpHIS5*
Y3406	*MATa tsv115, SCC4-HA6-HIS3MX6*

	BRN1-Pk9::TRP1
Y3475	*MATa BRN1-HA6::HIS3MX6, TFC3-pK9::TRP1* *B box* ggttcgaaccc *integrated in Lsm1-Swi1 region, KLURA3 looped out*
Y3485	*MATa BRN1-PK9::HIS3MX6* *B box* ggttcgaaccc *integrated in LSM4-SWI4 region 386600 (KLURA3 looped out)*
Y3504	*MATa BRN1-PK9::HIS3MX6, B box of tRNA tE(UUC)E2 gene 355000 on Chr V replaced with random sequence (KLURA3 looped out)*
Y3503	*MATa ycg1-10/spu4-1, NET1-GFP::TRP1, MET-HA3-CDC20::LEU2 GAL1-TOP2Chlorella virus::URA3, rad52::HIS3*
Y3520	*MATa ku70::HIS3MX6, ycg1-10/spu4-1, NET1-GFP::TRP1, MET-HA3-CDC20::LEU2, GAL1-TOPOIIChlorella virus::ura3*
Y3521	*MATa BRN1-Pk9::HIS3MX6, tRNA tE(UUC)J deleted (chr X 116000) replaced with URA3*
Y3522	*MATa BRN1-Pk9::HIS3MX6, TFC3-myc18::TRP1* *tRNA tE(UUC)J deleted (chr X 116000) replaced with URA3*
Y3528	*MATa BRN1-Pk9::HIS3MX6, 2 tRNAs tH(GUG)E1 cloned from ChrV at 207400 integrated on chr V at 386500. KLURA3 looped out*
Y3096	*MATa BRN1-HA6::HIS3MX6, TFC3-Pk9::TRP1*

5.7 Table of DNA vectors

Basic vectors for integration in yeast

Number	Name	Description	Origin
1	YIplac 128	*LEU2* based integrative vector	Gietz and Sugino
2	YIplac 204	*TRP1* based integrative vector	Gietz and Sugino
13	YIplac 128	*GAL1* cloned between EcoRI and BamHI in YIplac 128	Frank Uhlmann
9	pRS303	*HIS3* based integrative vector	Sikorski and Hieter

698	pRS303-*GAL1*	*HIS3* based integrative vector with *GAL1* cloned BamHI/EcoRI into pRS303	This study
210	pBSII	pBluescript was digested with Xho1/Hind3 and 1.45kb *URA3* gene (K.lactis) inserted	Matt Sullivan
211	pBSII	pBluescript was digested with EcoR1/HindIII and 2kb *LEU2* gene (*K. lactis*) inserted	Matt Sullivan
212	pBSII	Bluescript was digested with EcoR1/Hind3 and 1.4kb *HIS3* gene (*S. pombe*) inserted	Matt Sullivan
32	pBSII	*K. lactis TRP1* complementing *S. cerevisiae TRP1* in pBluescript	Matt Sullivan
626	pWJ1077	pWJ1077 Reid (yeast, 2002) Plasmid for PCR-based gene disruption *K. lactis URA3* flanked by 2 repeats (*URA3* can be pop-out on 5FOA)	Armelle Lengronne
837	pWJ1077	pWJ1077 Plasmid for PCR-based gene disruption *K. lactis URA3* flanked by 2 repeats (*URA3* can be pop-out on 5FOA) 2 Tandem tRNAs tH(GUG)E1 chrV (207400) with 100 bp up and downstream and SacI designed	This study

		ends cloned into SacI site (626) just before one repeat	
367	pAFS163	pASF163 was digested with BamH1/BglII and a PCR product (*ACS2* locus) cloned in as a BamH1 fragment. Digest with Sma1 to integrate at the *ACS2* locus	Matt Sullivan
368	pAFS163	pASF163 was digested with BamH1/BglII and a PCR product (*MMP1* locus) cloned in as a BamH1 fragment. Digest with Kpn1 to integrate at the *MMP1* locus	Matt Sullivan
355	pASF163	pASF163 was digested BglII/BamH1 and a 1kb PCR product (*MAS1* locus) inserted (BamHI).For integration of GFP dots at the *MAS1* locus (Digest Mfe1).	Matt Sullivan
599	pASF163	pASF163 was digested with BamH1/BglII and a PCR product (*REC102* locus) cloned in as a BamH1 fragment. Digest with BsrGI to integrate at the *REC102* locus	Matt Sullivan
344	YIplac211	YIplac211-*GAL1-TOPOII-Pk3*. YIplac211 was digested BamH1/Sph1 and ligated to the	Matt Sullivan

		TOPOII ORF BamHI/SphI (4.5kb)	
644	YIplac211	YIplac211*GAL1-NLS-NLS-chlorella TOPOII-Pk3* Annealed primers (FuI23 and FuI24) encoding for an NLS are introduced in BamHI site upstream the topoisomerase coding sequence. Linearise with StuI for integration at *URA3*	This study

Vectors for epitope tagging in yeast

Number	Name	Description	Origin
694	pUC19-Pk9	One step C-terminal Pk tagging vector (Kan marker)	Wolfgang Zachariae
690	pUC19-Pk9	One step C-terminal Pk tagging vector (*K.lactis His3* marker)	Wolfgang Zachariae
684	pUC19-Pk9	One step C-terminal Pk tagging vector (*K.lactis Trp1* marker)	Wolfgang Zachariae
556	pUC19-Pk3	One step C-terminal Pk tagging vector (Kan marker)	Wolfgang Zachariae
36	pUC19-HA6	One step C-terminal HA tagging vector (*S,pombe His5* marker)	Gustav Ammerer
776	pUC19-myc18	One step C-terminal Myc tagging vector (*K.lactis Leu2* marker)	Toru Higuchi
35	pUC19-HA3	One step C-terminal HA tagging vector (*K.lactis Trp1* marker)	Wolfgang Zachariae
555	pUC19-pk3	One step C-terminal Pk tagging vector (*K.lactis His3* marker)	Wolfgang Zachariae
40	pUC19-	One step C-terminal HA tagging	Frank Uhlmann

	HA3	vector (*K.lactis Ura3* marker)	

Integrative vectors for one step promoter swapping in yeast

Number	Name	Description	Origin
453	YCplac111 *GAL1-CDC20*	Construct to replace the endogenous *CDC20* promoter with the *GAL1* inducible promoter (*LEU2* marker)	Armelle Lengronne
49	pBS-*GAL1*	Construct for promoter swapping with the *GAL1* inducible promoter (*K,lactis TRP1* marker)	Frank Uhlmann
109	YIp22	YIp22 *MET3-CDC20* promoter exchange construct. (*TRP1* marker) From 108, 3' end of *CDC20* and CEN (MluNI-NheI) replaced by a piece of *CDC20* 5' upstream sequence. Cut with MluNI to integrate for promoter exchange at *CDC20.*	Frank Uhlmann
640	YIp22	YIp22 *MET3-CDC20 (LEU2)* promoter exchange construct. AhdI/NheI *LEU2* fragment is cloned into AhdI/NheI fragment of YIp22. Linearise with MscI for promoter exchange at *CDC20.*	Chris Lehane

Numbers listed in these tables refer to DNA or strain number entries in the Uhlmann Lab database.

6 Chapter 6: References

Adachi, N., Miyaike, M., Kato, S., Kanamaru, R., Koyama, H. and Kikuchi, A. (1997) Cellular distribution of mammalian DNA topoisomerase II is determined by its catalytically dispensable C-terminal domain. *Nucleic Acids Res*, **25**, 3135-3142.

Anderson, D.E., Losada, A., Erickson, H.P. and Hirano, T. (2002) Condensin and cohesin display different arm conformations with characteristic hinge angles. *J. Cell Biol.*, **156**, 419-424.

Aono, N., Sutani, T., Tomonaga, T., Mochida, S. and Yanagida, M. (2002) Cnd2 has dual roles in mitotic condensation and interphase. *Nature*, **417**, 197-202.

Arumugam, P., Gruber, S., Tanaka, K., Haering, C.H., Mechtler, K. and Nasmyth, K. (2003) ATP hydrolysis is required for cohesin's association with chromosomes. *Curr. Biol.*, **13**, 1941-1953.

Betts Lindroos, H., Ström, L., Itoh, T., Katou, Y., Shirahige, K. and Sjögren, C. (2006) Chromosomal association of the Smc5/6 complex reveals that it functions in differently regulated pathways. *Mol. Cell*, **22**, 755-767.

Bhalla, N., Biggins, S. and Murray, A.W. (2002) Mutation of *YCS4*, a budding yeast condensin subunit, affects mitotic and nonmitotic chromosome behavior. *Mol. Biol. Cell*, **13**, 632-645.

Bhat, M.A., Philp, A.V., Glover, D.M. and Bellen, H.J. (1996) Chromatid segregation at anaphase requires the *barren* product, a novel chromosome-associated protein that interacts with topoisomerase II. *Cell*, **87**, 1103-1114.

Blat, Y. and Kleckner, N. (1999) Cohesins bind to preferential sites along yeast chromosome III, with differential regulation along arms versus the centric region. *Cell*, **98**, 249-259.

Borck, G., Zarhrate, M., Bonnefont, J.P., Munnich, A., Cormier-Daire, V. and Colleaux, L. (2007) Incidence and clinical features of X-linked Cornelia de Lange syndrome due to SMC1L1 mutations. *Hum Mutat*, **28**, 205-206.

Brown, P.O. and Cozzarelli, N.R. (1979) A sign inversion mechanism for enzymatic supercoiling of DNA. *Science*, **206**, 1081-1083.

Cairns, J. (1963) The bacterial chromosome and its manner of replication as seen by autoradiography. *J Mol Biol*, **6**, 208-213.

Caron, P.R., Watt, P. and Wang, J.C. (1994) The C-terminal domain of Saccharomyces cerevisiae DNA topoisomerase II. *Mol Cell Biol*, **14**, 3197-3207.

Carter, D., Chakalova, L., Osborne, C.S., Dai, Y.F. and Fraser, P. (2002) Long-range chromatin regulatory interactions in vivo. *Nat Genet*, **32**, 623-626.

Casolari, J.M., Brown, C.R., Drubin, D.A., Rando, O.J. and Silver, P.A. (2005) Developmentally induced changes in transcriptional program alter spatial organization across chromosomes. *Genes Dev*, **19**, 1188-1198.

Casolari, J.M., Brown, C.R., Komili, S., West, J., Hieronymus, H. and Silver, P.A. (2004) Genome-wide localization of the nuclear transport machinery couples transcriptional status and nuclear organization. *Cell*, **117**, 427-439.

Champoux, J.J. and Dulbecco, R. (1972) An activity from mammalian cells that untwists superhelical DNA--a possible swivel for DNA replication (polyoma-ethidium bromide-mouse-embryo cells-dye binding assay). *Proc Natl Acad Sci U S A*, **69**, 143-146.

Ciosk, R., Shirayama, M., Shevchenko, A., Tanaka, T., Toth, A., Shevchenko, A. and Nasmyth, K. (2000) Cohesin's binding to chromosomes depends on a separate complex consisting of Scc2 and Scc4 proteins. *Mol. Cell*, **5**, 1-20.

Coelho, P.A., Queiroz-Machado, J. and Sunkel, C.E. (2003) Condensin-dependent localisation of topoisomerase II to an axial chromosomal structure is required for sister chromatid resolution during mitosis. *J. Cell Sci.*, **116**, 4763-4776.

Cremer, T. and Cremer, C. (2001) Chromosome territories, nuclear architecture and gene regulation in mammalian cells. *Nat Rev Genet*, **2**, 292-301.

Cuvier, O. and Hirano, T. (2003) A role of topoisomerase II in linking DNA replication to chromosome condensation. *J. Cell. Biol.*, **160**, 645-655.

D'Amours, D., Stegmeier, F. and Amon, A. (2004) Cdc14 and condensin control the dissolution of cohesin-independent linkages at repeated DNA. *Cell*, **117**, 455-469.

De Piccoli, G., Cortes-Ledesma, F., Ira, G., Torres-Rosell, J., Uhle, S., Farmer, S., Hwang, J.Y., Machin, F., Ceschia, A., McAleenan, A., Cordon-Preciado, V., Clemente-Blanco, A., Vilella-Mitjana, F., Ullal, P., Jarmuz, A., Leitao, B., Bressan, D., Dotiwala, F., Papusha, A., Zhao, X., Myung, K., Haber, J.E., Aguilera, A. and Aragon, L. (2006) Smc5-Smc6 mediate DNA double-strand-break repair by promoting sister-chromatid recombination. *Nat Cell Biol*, **8**, 1032-1034.

Deardorff, M.A., Kaur, M., Yaeger, D., Rampuria, A., Korolev, S., Pie, J., Gil-Rodriguez, C., Arnedo, M., Loeys, B., Kline, A.D., Wilson, M., Lillquist, K., Siu, V., Ramos, F.J., Musio, A., Jackson, L.S., Dorsett, D. and Krantz, I.D. (2007) Mutations in cohesin complex members SMC3 and SMC1A cause a mild variant of cornelia de Lange syndrome with predominant mental retardation. *Am J Hum Genet*, **80**, 485-494.

DiNardo, S., Voelkel, K. and Sternglanz, R. (1984) DNA topoisomerase II mutant of *Saccharomyces cerevisiae*: topoisomerase II is required for segregation of daughter

molecules at the termination of DNA replication. *Proc. Natl. Acad. Sci. USA*, **81**, 2616-2620.

Dong, K.C. and Berger, J.M. (2007) Structural basis for gate-DNA recognition and bending by type IIA topoisomerases. *Nature*, **450**, 1201-1205.

Donze, D. and Kamakaka, R.T. (2001) RNA polymerase III and RNA polymerase II promoter complexes are heterochromatin barriers in Saccharomyces cerevisiae. *Embo J*, **20**, 520-531.

Dorsett, D. (1999) Distant liaisons: long-range enhancer-promoter interactions in Drosophila. *Curr Opin Genet Dev*, **9**, 505-514.

Downes, C.S., Mullinger, A.M. and Johnson, R.T. (1991) Inhibitors of DNA topoisomerase II prevent chromatid separation in mammalian cells but do not prevent exit from mitosis. *Proc. Natl. Acad. Sci. USA*, **88**, 8895-8899.

Elliott, S.G. and McLaughlin, C.S. (1979) Regulation of RNA synthesis in yeast III. *Mol. Gen. Genet.*, **169**, 237-243.

Fortune, J.M., Lavrukhin, O.V., Gurnon, J.R., Van Etten, J.L., Lloyd, R.S. and Osheroff, N. (2001) Topoisomerase II from *Chlorella* virus PBCV-1 has an exceptionally high DNA cleavage activity. *J. Biol. Chem.*, **276**, 24401-24408.

Freeman, L., Aragon-Alcaide, L. and Strunnikov, A. (2000) The condensin complex governs chromosome condensation and mitotic transmission of rDNA. *J. Cell Biol.*, **149**, 811-824.

Furuya, K., Takahashi, K. and Yanagida, M. (1998) Faithful anaphase is ensured by Mis4, a sister chromatid cohesion molecule required in S phase and not destroyed in G_1 phase. *Genes Dev.*, **12**, 3408-3418.

Gasser, S.M. (2002) Visualizing chromatin dynamics in interphase nuclei. *Science*, **296**, 1412-1416.

Gellert, M., Mizuuchi, K., O'Dea, M.H. and Nash, H.A. (1976) DNA gyrase: an enzyme that introduces superhelical turns into DNA. *Proc Natl Acad Sci U S A*, **73**, 3872-3876.

Gerlich, D., Hirota, T., Koch, B., Peters, J.-M. and Ellenberg, J. (2006a) Condensin I stabilizes chromosomes mechanically through a dynamic interaction in live cells. *Curr. Biol.*, **16**, 333-344.

Gerlich, D., Koch, B., Dupeux, F., Peters, J.-M. and Ellenberg, J. (2006b) Live-cell imaging reveals a stable cohesin-chromatin interaction after but not before DNA replication. *Curr. Biol.*, **16**, 1571-1578.

Gillespie, P.J. and Hirano, T. (2004) Scc2 couples replication licensing to sister chromatid cohesion in *Xenopus* egg extracts. *Curr. Biol.*, **14**, 1598-1603.

Glynn, E.F., Megee, P.C., Yu, H.G., Mistrot, C., Unal, E., Koshland, D.E., DeRisi, J.L. and Gerton, J.L. (2004) Genome-wide mapping of the cohesin complex in the yeast *Saccharomyces cerevisiae*. *PLoS Biol.*, **2**, 1325-1339.

Gruber, S., Arumugam, P., Katou, Y., Kuglitsch, D., Helmhart, W., Shirahige, K. and Nasmyth, K. (2006) Evidence that loading of cohesin onto chromosomes involves opening of its SMC hinge. *Cell*, **127**, 523-537.

Guacci, V., Hogan, E. and Koshland, D. (1994) Chromosome condensation and sister chromatid pairing in budding yeast. *J. Cell Biol.*, **125**, 517-530.

Guacci, V., Koshland, D. and Strunnikov, A. (1997) A direct link between sister chromatid cohesion and chromosome condensation revealed through analysis of *MCD1* in S. cerevisiae. *Cell*, **91**, 47-57.

Haering, C.H., Löwe, J., Hochwagen, A. and Nasmyth, K. (2002) Molecular architecture of SMC proteins and the yeast cohesin complex. *Mol. Cell*, **9**, 773-788.

Hagstrom, K.A., Holmes, V.F., Cozzarelli, N.R. and Meyer, B.J. (2002) *C. elegans* condensin promotes mitotic chromosome architecture, centromere organization, and sister chromatid segregation during mitosis and meiosis. *Genes Dev.*, **16**, 729-742.

Hakimi, M.-A., Bochar, D.A., Schmiesing, J.A., Dong, Y., Barak, O.G., Speicher, D.W., Yokomori, K. and Shiekhattar, R. (2002) A chromatin remodelling complex that loads cohesin onto human chromosomes. *Nature*, **418**, 994-997.

Hanna, J.S., Kroll, E.S., Lundblad, V. and Spencer, F.A. (2001) *Saccharomyces cerevisiae* CTF18 and CTF4 are required for sister chromatid cohesion. *Mol. Cell. Biol.*, **21**, 3144-3158.

Hansen, J.C. (2002) Conformational dynamics of the chromatin fiber in solution: determinants, mechanisms, and functions. *Annu Rev Biophys Biomol Struct*, **31**, 361-392.

Hardy, C.D., Crisona, N.J., Stone, M.D. and Cozzarelli, N.R. (2004) Disentangling DNA during replication: a tale of two strands. *Philos Trans R Soc Lond B Biol Sci*, **359**, 39-47.

Harismendy, O., Gendrel, C.G., Soularue, P., Gidrol, X., Sentenac, A., Werner, M. and Lefebvre, O. (2003) Genome-wide location of yeast RNA polymerase III transcription machinery. *Embo J*, **22**, 4738-4747.

Heale, J.T., Ball, A.R., Jr., Schmiesing, J.A., Kim, J.S., Kong, X., Zhou, S., Hudson, D.F., Earnshaw, W.C. and Yokomori, K. (2006) Condensin I interacts with the PARP-1-XRCC1 complex and functions in DNA single-strand break repair. *Mol Cell*, **21**, 837-848.

Hirano, M. and Hirano, T. (1998) ATP-dependent aggregtion of single-stranded DNA by a bacterial SMC homodimer. *EMBO J.*, **17**, 7139-7148.

Hirano, M. and Hirano, T. (2006) Opening closed arms: Long-distance activation of SMC ATPase by hinge-DNA interactions. *Mol. Cell*, **21**, 175-186.

Hirano, T. (2000) Chromosome Cohesion, Condensation, and Separation. *Annu. Rev. Biochem.*, **69**, 115-144.

Hirano, T. (2005a) Condensins: organizing and segregating the genome. *Curr Biol*, **15**, R265-275.

Hirano, T. (2005b) SMC proteins and chromosome mechanics: from bacteria to humans. *Philos Trans R Soc Lond B Biol Sci*, **360**, 507-514.

Hirano, T. (2006) At the heart of the chromosome: SMC proteins in action. *Nat. Rev. Mol. Cell. Biol.*, **7**, 311-322.

Hirano, T., Kobayashi, R. and Hirano, M. (1997) Condensins, chromosome condensation protein complexes containing XCAP-C, XCAP-E and a Xenopus homolog of the Drosophila barren protein. *Cell*, **89**, 511-521.

Hirano, T. and Mitchison, T.J. (1994a) A heterodimeric coiled-coil protein required for mitotic chromosome condensation in vitro. *Cell*, **79**, 449-458.

Hirano, T. and Mitchison, T.J. (1994b) A heterodimeric coiled-coil protein required for mitotic chromosome condensation in vitro. *Cell*, **79**, 449-458.

Hirota, T., Gerlich, D., Koch, B., Ellenberg, J. and Peters, J.-M. (2004) Distinct functions of condensin I and II in mitotic chromosome assembly. *J. Cell Sci.*, **117**, 6435-6445.

Holm, C., Goto, T., Wang, J.C. and Botstein, D. (1985) DNA topoisomerase II is required at the time of mitosis in yeast. *Cell*, **41**, 553-563.

Huang, Y. and Maraia, R.J. (2001) Comparison of the RNA polymerase III transcription machinery in *Schizosaccharomyces pombe*, *Saccharomyces cerevisiae* and human. *Nucl. Acids Res.*, **29**, 2675-2690.

Hudson, D.F., Vagnarelli, P., Gassmann, R. and Earnshaw, W.C. (2003) Condensin is required for nonhistone protein assembly and structural integrity of vertebrate mitotic chromosomes. *Dev. Cell*, **5**, 323-336.

Ibanez, A. (2007) Complexity and cognition: a meta-theoretical analysis of the mind and brain as a topological dynamical system. *Nonlinear Dynamics Psychol Life Sci*, **11**, 51-90.

Ishii, K., Arib, G., Lin, C., Van Houwe, G. and Laemmli, U.K. (2002) Chromatin boundaries in budding yeast: the nuclear pore connection. *Cell*, **109**, 551-562.

Ivanov, D. and Nasmyth, K. (2005) A topological interaction between cohesin rings and a circular minichromosome. *Cell*, **122**, 849-860.

Iyer, V.R., Horak, C.E., Scafe, C.S., Botstein, D., Snyder, M. and Brown, P.O. (2001) Genomic binding sites of the yeast cell-cycle transcription factors SBF and MBF. *Nature*, **409**, 533-538.

Jallepalli, P.V. and Lengauer, C. (2001) Chromosome segregation and cancer: cutting through the mystery. *Nat. Rev. Cancer*, **1**, 109-117.

Kagansky, A., Freeman, L., Lukyanov, D. and Strunnikov, A. (2003) Histone-tail independent chromatin-binding activity of recombinant cohesin holocomplex. *J. Biol. Chem.*, **Epub ahead of print**.

Katou, Y., Kanoh, Y., Bandoh, M., Noguchi, H., Tanaka, H., Ashikari, T., Sugimoto, K. and Shirahige, K. (2003) S-phase checkpoint proteins Tof1 and Mrc1 form a stable replication-pausing complex. *Nature*, **424**, 1078-1083.

Kimura, A. and Horikoshi, M. (2004) Partition of distinct chromosomal regions: negotiable border and fixed border. *Genes Cells*, **9**, 499-508.

Kimura, K., Hirano, M., Kobayashi, R. and Hirano, T. (1998) Phosphorylation and activation of 13S condensin by Cdc2 in vitro. *Science*, **282**, 487-490.

Kimura, K. and Hirano, T. (1997) ATP-Dependent positive supercoiling of DNA by 13S condensin: a biochemical implication for chromosome condensation. *Cell*, **90**, 625-634.

Kimura, K. and Hirano, T. (2000) Dual roles of the 11S regulatory subcomplex in condensin functions. *Proc. Natl. Acad. Sci. USA*, **97**, 11972-11977.

Kimura, K., Rybenkov, V.V., Crisona, N.J., Hirano, T. and Cozzarelli, N.R. (1999) 13S condensin actively reconfigures DNA by introducing global positive writhe: implications for chromosome condensation. *Cell*, **98**, 239-248.

Knop, M., Siegers, K., Pereira, G., Zachariae, W., Winsor, B., Nasmyth, K. and Schiebel, E. (1999) Epitope tagging of yeast genes using a PCR-based strategy: more tags and improved practical routines. *Yeast*, **15**, 963-972.

Konig, P., Braunfeld, M.B., Sedat, J.W. and Agard, D.A. (2007) The three-dimensional structure of in vitro reconstituted Xenopus laevis chromosomes by EM tomography. *Chromosoma*, **116**, 349-372.

Koshland, D. and Strunnikov, A. (1996) Mitotic chromosome condensation. *Annu. Rev. Cell Dev. Biol.*, **12**, 305-333.

Krantz, I.D., McCallum, J., DeScipio, C., Kaur, M., Gillis, L.A., Yaeger, D., Jukofsky, L., Wasserman, N., Bottani, A., Morris, C.A., Nowaczyk, M.J.M., Toriello, H., Bamshad, M.J., Carey, J.C., Rappaport, E., Kawauchi, S., Lander, A.D., Calof,

A.L., Li, H., Devoto, M. and Jackson, L.G. (2004) Cornelia de Lange syndrome is caused by mutations in *NIPBL*, the human homolog of *Drosophila melanogaster Nipped-B*. *Nat. Genet.*, **36**, 631-635.

Kreuzer, K.N. and Cozzarelli, N.R. (1980) Formation and resolution of DNA catenanes by DNA gyrase. *Cell*, **20**, 245-254.

Kushnirov, V.V. (2000) Rapid and reliable protein extraction from yeast. *Yeast*, **16**, 857-860.

Laemmli, U.K., Kas, E., Poljak, L. and Adachi, Y. (1992) Scaffold-associated regions: cis-acting determinants of chromatin structural loops and functional domains. *Curr Opin Genet Dev*, **2**, 275-285.

Laloraya, S., Guacci, V. and Koshland, D. (2000) Chromosomal addresses of the cohesin component Mcd1p. *J. Cell Biol.*, **151**, 1047-1056.

Lavoie, B.D., Hogan, E. and Koshland, D. (2002) In vivo dissection of the chromosome condensation machinery: reversibility of condensation distinguishes contributions of condensin and cohesin. *J. Cell Biol.*, **156**, 805-815.

Lavoie, B.D., Hogan, E. and Koshland, D. (2004) In vivo requirements for rDNA chromosome condensation reveal two cell-cycle-regulated pathways for mitotic chromosome folding. *Genes Dev.*, **18**, 76-87.

Lavoie, B.D., Tuffo, K.M., Oh, S., Koshland, D. and Holm, C. (2000) Mitotic chromosome condensation requires Brn1p, the yeast homologue of barren. *Mol. Biol. Cell*, **11**, 1293-1304.

Lavrukhin, O.V., Fortune, J.M., Wood, T.G., Burbank, D.E., Van Etten, J.L., Osheroff, N. and Lloyd, R.S. (2000) Topoisomerase II from *Chlorella* Virus PBCV-1: Characterization of the smallest known type II topoisomerase. *J. Biol. Chem.*, **275**, 6915-6921.

Lefebvre, O., Ruth, J. and Sentenac, A. (1994) A mutation in the largest subunit of yeast TFIIIC affects tRNA and 5 S RNA synthesis. Identification of two classes of suppressors. *J Biol Chem*, **269**, 23374-23381.

Lengronne, A., Katou, Y., Mori, S., Yokobayashi, S., Kelly, G.P., Itoh, T., Watanabe, Y., Shirahige, K. and Uhlmann, F. (2004) Cohesin relocation from sites of chromosomal loading to places of convergent transcription. *Nature*, **430**, 573-578.

Lengronne, A., McIntyre, J., Katou, Y., Kanoh, Y., Hopfner, K.-P., Shirahige, K. and Uhlmann, F. (2006) Establishment of sister chromatid cohesion at the *S. cerevisiae* replication fork. *Mol. Cell*, **23**, 787-799.

Lewis, C.D. and Laemmli, U.K. (1982) Higher order metaphase chromosome structure: evidence for metalloprotein interactions. *Cell*, **29**, 171-181.

Liang, C. and Stillman, B. (1997) Persistent initiation of DNA replication and chromatin-bound MCM proteins during the cell cycle in cdc6 mutants. *Genes Dev*, **11**, 3375-3386.

Locke, J., Kotarski, M.A. and Tartof, K.D. (1988) Dosage-dependent modifiers of position effect variegation in Drosophila and a mass action model that explains their effect. *Genetics*, **120**, 181-198.

Lohka, M.J. and Masui, Y. (1983) Formation in vitro of sperm pronuclei and mitotic chromosomes induced by amphibian ooplasmic components. *Science*, **220**, 719-721.

Losada, A., Hirano, M. and Hirano, T. (1998) Identification of *Xenopus* SMC protein complexes required for sister chromatid cohesion. *Genes Dev.*, **12**, 1986-1997.

Losada, A. and Hirano, T. (2001) Intermolecular DNA interactions stimulated by the cohesin complex in vitro: Implications for sister chromatid cohesion. *Curr. Biol.*, **11**, 268-272.

Lupo, R., Breiling, A., Bianchi, M.E. and Orlando, V. (2001) *Drosophila* chromosome condensation proteins topoisomerase II and barren colocalize with polycomb and maintain *Fab-7* PRE silencing. *Mol. Cell*, **7**, 127-136.

Machin, F., Torres-Rosell, J., De Piccoli, G., Carballo, J.A., Cha, R.S., Jarmuz, A. and Aragon, L. (2006) Transcription of ribosomal genes can cause nondisjunction. *J. Cell. Biol.*, **173**, 893-903.

Machin, F., Torres-Rosell, J., Jarmuz, A. and Aragon, L. (2005) Spindle-independent condensation-mediated segregation of yeast ribosomal DNA in late anaphase. *J. Cell. Biol.*, **168**, 209-219.

Maeshima, K. and Laemmli, U.K. (2003) A two-step scaffolding model for mitotic chromosome assembly. *Dev Cell*, **4**, 467-480.

Mascarenhas, J., Soppa, J., Strunnikov, A. and Graumann, P.L. (2002) Cell cycle-dependent localization of two novel prokaryotic chromosome segregation and condensation proteins in *Bacillus subtilis* that interact with SMC protein. *EMBO J.*, **21**, 3108-3118.

Megee, P.C., Mistrot, C., Guacci, V. and Koshland, D. (1999) The centromeric sister chromatid cohesion site directs Mcd1p binding to adjacent sequences. *Mol. Cell*, **4**, 445-450.

Melby, T.E., Ciampaglio, C.N., Briscoe, G. and Erickson, H.P. (1998) The symmetrical structure of structural maintenance of chromosomes (SMC) and MukB proteins: long, antiparallel coiled coils, folded at a flexible hinge. *J. Cell Biol.*, **142**, 1595-1604.

Michaelis, C., Ciosk, R. and Nasmyth, K. (1997) Cohesins: Chromosomal proteins that prevent premature separation of sister chromatids. *Cell*, **91**, 35-45.

Mondal, N. and Parvin, J.D. (2001) DNA topoisomerase IIalpha is required for RNA polymerase II transcription on chromatin templates. *Nature*, **413**, 435-438.

Moqtaderi, Z. and Struhl, K. (2004) Genome-wide occupancy profile of the RNA polymerase III machinery in *Saccharomyces cerevisiae* reveals loci with incomplete transcription complexes. *Mol. Cell. Biol.*, **24**, 4118-4127.

Nasmyth, K. and Haering, C.H. (2005) The structure and function of SMC and kleisin complexes. *Annu. Rev. Biochem.*, **74**, 595-648.

Nasmyth, K., Peters, J.-M. and Uhlmann, F. (2000) Splitting the chromosome: cutting the ties that bind sister chromatids. *Science*, **288**, 1379-1384.

Nasmyth, K. and Schleifer, A. (2004) From a single double helix to paired double helices and back. *Phil Trans R Soc B*, **359**, 99-108.

Neuwald, A.F. and Hirano, T. (2000) HEAT repeats associated with condensins, cohesins, and other complexes involved in chromosome-related functions. *Genome Res.*, **10**, 1445-1452.

Niki, H., Jaffe, A., Imamura, R., Ogura, T. and Hiraga, S. (1991) The new gene mukB codes for a 177 kd protein with coiled-coil domains involved in chromosome partitioning of E. coli. *Embo J*, **10**, 183-193.

Nitiss, J. and Wang, J.C. (1988) DNA topoisomerase-targeting antitumor drugs can be studied in yeast. *Proc Natl Acad Sci U S A*, **85**, 7501-7505.

Nitiss, J.L. (2002) DNA topoisomerases in cancer chemotherapy: using enzymes to generate selective DNA damage. *Curr Opin Investig Drugs*, **3**, 1512-1516.

Noma, K., Cam, H.P., Maraia, R.J. and Grewal, S.I.S. (2006) A role for TFIIIC transcription factor complex in genome organization. *Cell*, **125**, 859-872.

Oki, M. and Kamakaka, R.T. (2005) Barrier function at HMR. *Mol Cell*, **19**, 707-716.

Oliveira, R.A., Coelho, P.A. and Sunkel, C.E. (2005) The condensin I subunit barren/CAP-H is essential for the structural integrity of centromeric heterochromatin during mitosis. *Mol. Cell. Biol.*, **25**, 8971-8984.

Onn, I., Aono, N., Hirano, M. and Hirano, T. (2007) Reconstitution and subunit geometry of human condensin complexes. *EMBO J.*, **26**, 1024-1034.

Ono, T., Fang, Y., Spector, D.L. and Hirano, T. (2004) Spatial and temporal regulation of condensin I and II in mitotic chromosome assembly in human cells. *Mol. Biol. Cell*, **15**, 3296-3308.

Ono, T., Losada, A., Hirano, M., Myers, M.P., Neuwald, A.F. and Hirano, T. (2003) Differential contributions of condensin I and condensin II to mitotic chromosome architecture in vertebrate cells. *Cell*, **115**, 109-121.

Orlando, V. (2003) Polycomb, epigenomes, and control of cell identity. *Cell*, **112**, 599-606.

Osborne, B.I. and Guarente, L. (1988) Transcription by RNA polymerase II induces changes of DNA topology in yeast. *Genes Dev*, **2**, 766-772.

Ouspenski, I.I., Cabello, O.A. and Brinkley, B.R. (2000) Chromosome condensation factor Brn1p is required for chromatid separation in mitosis. *Mol. Biol. Cell*, **11**, 1305-1313.

Paolella, G., Lucero, M.A., Murphy, M.H. and Baralle, F.E. (1983) The Alu family repeat promoter has a tRNA-like bipartite structure. *Embo J*, **2**, 691-696.

Potts, P.R., Porteus, M.H. and Yu, H. (2006) Human SMC5/6 complex promotes sister chromatid homologous recombination by recruiting the SMC1/3 cohesin complex to double-strand breaks. *Embo J*, **25**, 3377-3388.

Rollins, R.A., Morcillo, P. and Dorsett, D. (1999) Nipped-B, a Drosophila homologue of chromosomal adherins, participates in activation by remote enhancers in the *cut* and *Ultrabithorax* genes. *Genetics*, **152**, 577-593.

Roth, F.P., Hughes, J.D., Estep, P.W. and Church, G.M. (1998) Finding DNA regulatory motifs within unaligned noncoding sequences clustered by whole-genome mRNA quantitation. *Nat. Biotech.*, **16**, 939-945.

Rusche, L.N., Kirchmaier, A.L. and Rine, J. (2003) The establishment, inheritance, and function of silenced chromatin in Saccharomyces cerevisiae. *Annu Rev Biochem*, **72**, 481-516.

Saitoh, N., Goldberg, I.G., Wood, E.R. and Earnshaw, W.C. (1994) ScII: an abundant chromosome scaffold protein is a member of a family of putative ATPases with an unusual predicted tertiary structure. *J. Cell Biol.*, **127**, 303-318.

Saka, Y., Sutani, T., Yamashita, Y., Saitoh, S., Takeuchi, M., Nakaseko, Y. and Yanagida, M. (1994) Fission yeast cut3 and cut14, members of a ubiquitous protein family, are required for chromosome condensation and segregation in mitosis. *EMBO J.*, **13**, 4938-4952.

Schleiffer, A., Kaitna, S., Maurer-Stroh, S., Glotzer, M., Nasmyth, K. and Eisenhaber, F. (2003) Kleisins: A superfamily of bacterial and eukaryotic SMC protein partners. *Mol. Cell*, **11**, 571-575.

Schmid, M., Arib, G., Laemmli, C., Nishikawa, J., Durussel, T. and Laemmli, U.K. (2006) Nup-PI: the nucleopore-promoter interaction of genes in yeast. *Mol Cell*, **21**, 379-391.

Schramm, L. and Hernandez, N. (2002) Recruitment of RNA polymerase III to its target promoters. *Genes Dev*, **16**, 2593-2620.

Scott, K.C., Merrett, S.L. and Willard, H.F. (2006) A heterochromatin barrier partitions the fission yeast centromere into discrete chromatin domains. *Curr Biol*, **16**, 119-129.

Seitz, L.C., Tang, K., Cummings, W.J. and Zolan, M.E. (1996) The *rad9* gene of *Coprinus cinereus* encodes a proline-rich protein required for meiotic chromosome condensation and synapsis. *Genetics*, **142**, 1105-1117.

Sonoda, E., Matsusaka, T., Morrison, C., Vagnarelli, P., Hoshi, O., Ushiki, T., Nojima, K., Fukagawa, T., Waizenegger, I.C., Peters, J.-M., Earnshaw, W.C. and Takeda, S. (2001) Scc1/Rad21/Mcd1 is required for sister chromatid cohesion and kinetochore function in vertebrate cells. *Dev. Cell*, **1**, 759-770.

Spell, R.M. and Holm, C. (1994) Nature and distribution of chromosomal intertwinings in Saccharomyces cerevisiae. *Mol Cell Biol*, **14**, 1465-1476.

Strachan, T. (2005) Cornelia de Lange Syndrome and the link between chromosomal function, DNA repair and developmental gene regulation. *Curr Opin Genet Dev*, **15**, 258-264.

Stray, J.E. and Lindsley, J.E. (2003) Biochemical analysis of the yeast condensin Smc2/4 complex. An ATPase that promotes knotting of circular DNA. *J. Biol. Chem.*, **278**, 26238-26248.

Strick, T.R., Kawaguchi, T. and Hirano, T. (2004) Real-time detection of single-molecule DNA compaction by condensin I. *Curr Biol*, **14**, 874-880.

Strunnikov, A., Hogan, E. and Koshland, D. (1995) *SMC2*, a *Saccharomyces cerevisiae* gene essential for chromosome segregation and condensation, defines a subgroup within the SMC family. *Genes Dev.*, **9**, 587-599.

Sullivan, M., Higuchi, T., Katis, V.L. and Uhlmann, F. (2004) Cdc14 phosphatase induces rDNA condensation and resolves cohesin-independent cohesion during budding yeast anaphase. *Cell*, **117**, 471-482.

Sumara, I., Vorlaufer, E., Gieffers, C., Peters, B.H. and Peters, J.-M. (2000) Characterization of vertebrate cohesin complexes and their regulation in prophase. *J. Cell Biol.*, **151**, 749-761.

Sundin, O. and Varshavsky, A. (1980) Terminal stages of SV40 DNA replication proceed via multiply intertwined catenated dimers. *Cell*, **21**, 103-114.

Sutani, T. and Yanagida, M. (1997) DNA renaturation activity of the SMC complex implicated in chromosome condensation. *Nature*, **388**, 798-801.

Sutani, T., Yuasa, T., Tomonaga, T., Dohmae, N., Takio, K. and Yanagida, M. (1999) Fission yeast condensin complex: essential roles of non-SMC subunits for

condensation and Cdc2 phosphorylation of Cut3/SMC4. *Genes Dev.*, **13**, 2271-2283.

Takahashi, K., Yamada, H. and Yanagida, M. (1994) Fission yeast minichromosome loss mutants mis cause lethal aneuploidy and replication abnormality. *Mol Biol Cell*, **5**, 1145-1158.

Takahashi, T.S., Yiu, P., Chou, M.F., Gygi, S. and Walter, J.C. (2004) Recruitment of Xenopus Scc2 and cohesin to chromatin requires the pre-replication complex. *Nat Cell Biol*, **6**, 991-996.

Takeuchi, Y., Horiuchi, T. and Kobayashi, T. (2003) Transcription-dependent recombination and the role of fork collision in yeast rDNA. *Genes Dev*, **17**, 1497-1506.

Tanaka, T., Cosma, M.P., Wirth, K. and Nasmyth, K. (1999) Identification of cohesin association sites at centromeres and along chromosome arms. *Cell*, **98**, 847-858.

Thompson, M., Haeusler, R.A., Good, P.D. and Engelke, D.R. (2003) Nucleolar clustering of dispersed tRNA genes. *Science*, **302**, 1399-1401.

Tolhuis, B., Palstra, R.J., Splinter, E., Grosveld, F. and de Laat, W. (2002) Looping and interaction between hypersensitive sites in the active beta-globin locus. *Mol Cell*, **10**, 1453-1465.

Tomson, B.N., D'Amours, D., Adamson, B.S., Aragon, L. and Amon, A. (2006) Ribosomal DNA transcription-dependent processes interfere with chromosome segregation. *Mol. Cell. Biol.*, **26**, 6239-6247.

Tonkin, E.T., Wang, T.-J., Lisgo, S., Bamshad, M.J. and Strachan, T. (2004) NIPBL, encoding a homolog of fungal Scc2-type sister chromatid cohesion proteins and fly Nipped-B, is mutated in Cornelia de Lange syndrome. *Nat. Genet.*, **36**, 636-641.

Tóth, A., Ciosk, R., Uhlmann, F., Galova, M., Schleiffer, A. and Nasmyth, K. (1999) Yeast Cohesin complex requires a conserved protein, Eco1p (Ctf7), to establish cohesion between sister chromatids during DNA replication. *Genes Dev.*, **13**, 320-333.

Trimborn, M., Bell, S.M., Felix, C., Rashid, Y., Jafri, H., Griffiths, P.D., Neumann, L.M., Krebs, A., Reis, A., Sperling, K., Neitzel, H. and Jackson, A.P. (2004) Mutations in microcephalin cause aberrant regulation of chromosome condensation. *Am J Hum Genet*, **75**, 261-266.

Trimborn, M., Schindler, D., Neitzel, H. and Hirano, T. (2006) Misregulated chromosome condensation in MCPH1 primary microcephaly is mediated by condensin II. *Cell Cycle*, **5**, 322-326.

Tsuyama, T., Inou, K., Seki, M., Seki, T., Kumata, Y., Kobayashi, T., Kimura, K., Hanaoka, F., Enomoto, T. and Tada, S. (2006) Chromatin loading of Smc5/6 is

induced by DNA replication but not by DNA double-strand breaks. *Biochem Biophys Res Commun*, **351**, 935-939.

Uemura, T., Ohkura, H., Adachi, Y., Morino, K., Shiozaki, K. and Yanagida, M. (1987) DNA topoisomerase II is required for condensation and separation of mitotic chromosomes in S. pombe. *Cell*, **50**, 917-925.

Uhlmann, F. and Nasmyth, K. (1998) Cohesion between sister chromatids must be established during DNA replication. *Curr. Biol.*, **8**, 1095-1101.

Valenzuela, L. and Kamakaka, R.T. (2006) Chromatin Insulators. *Annu. Rev. Genet.*, **40**, 107-138.

Visintin, R., Craig, K., Hwang, E.S., Prinz, S., Tyers, M. and Amon, A. (1998) The phosphatase Cdc14 triggers mitotic exit by reversal of Cdk-dependent phosphorylation. *Mol. Cell*, **2**, 709-718.

Vologodskii, A.V., Zhang, W., Rybenkov, V.V., Podtelezhnikov, A.A., Subramanian, D., Griffith, J.D. and Cozzarelli, N.R. (2001) Mechanism of topology simplification by type II DNA topoisomerases. *Proc. Natl. Acad. Sci. USA*, **98**, 3045-3049.

Vrouwe, M.G., Elghalbzouri-Maghrani, E., Meijers, M., Schouten, P., Godthelp, B.C., Bhuiyan, Z.A., Redeker, E.J., Mannens, M.M., Mullenders, L.H., Pastink, A. and Darroudi, F. (2007) Increased DNA damage sensitivity of Cornelia de Lange syndrome cells: evidence for impaired recombinational repair. *Hum Mol Genet*, **16**, 1478-1487.

Waizenegger, I.C., Hauf, S., Meinke, A. and Peters, J.-M. (2000) Two distinct pathways remove mammalian cohesin complexes from chromosome arms in prophase and from centromeres in anaphase. *Cell*, **103**, 399-410.

Wang, B.-D., Butylin, P. and Strunnikov, A. (2006) Condensin function in mitotic nucleolar segregation is regulated by rDNA transcription. *Cell Cycle*, **5**, 2260-2267.

Wang, B.-D., Eyre, D., Basrai, M., Lichten, M. and Strunnikov, A. (2005) Condensin binding at distinct and specific chromosomal sites in the *Saccharomyces cerevisiae* genome. *Mol. Cell. Biol.*, **25**, 7216-7225.

Wang, B.-D., Yong-Gonzalez, V. and Strunnikov, A.V. (2004) Cdc14p/FEAR pathway controls segregation of nucleolus in *S. cerevisiae* by facilitating condensin targeting to rDNA chromatin in anaphase. *Cell Cycle*, **3**, 960-967.

Watrin, E., Schleiffer, A., Tanaka, K., Eisenhaber, F., Nasmyth, K. and Peters, J.-M. (2006) Human Scc4 is required for cohesin binding to chromatin, sister-chromatid cohesion, and mitotic progression. *Curr. Biol.*, **16**, 863-874.

Weitzer, S., Lehane, C. and Uhlmann, F. (2003) A model for ATP hydrolysis-dependent binding of cohesin to DNA. *Curr. Biol.*, **13**, 1930-1940.

Winzeler, E.A., Richards, D.R., Conway, A.R., Goldstein, A.L., Kalman, S., McCullough, M.J., McCusker, J.H., Stevens, D.A., Wodicka, L., Lockhart, D.J. and Davis, R.W. (1998) Direct allelic variation scanning of the yeast genome. *Science*, **281**, 1194-1197.

Worcel, A. and Burgi, E. (1972) On the structure of the folded chromosome of Escherichia coli. *J Mol Biol*, **71**, 127-147.

Wu, L., Pan, J., Thoroddsen, V., Wysong, D.R., Blackman, R.K., Bulawa, C.E., Gould, A.E., Ocain, T.D., Dick, L.R., Errada, P., Dorr, P.K., Parkinson, T., Wood, T., Kornitzer, D., Weissman, Z., Willis, I.M. and McGovern, K. (2003) Novel small-molecule inhibitors of RNA polymerase III. *Eukaryotic Cell*, **2**, 256-264.

Yamazoe, M., Onogi, T., Sunako, Y., Niki, H., Yamanaka, K., Ichimura, T. and Hiraga, S. (1999) Complex formation of MukB, MukE and MukF proteins involved in chromosome partitioning in Escherichia coli. *Embo J*, **18**, 5873-5884.

Yong-Gonzalez, V., Wang, B.D., Butylin, P., Ouspenski, I. and Strunnikov, A. (2007) Condensin function at centromere chromatin facilitates proper kinetochore tension and ensures correct mitotic segregation of sister chromatids. *Genes Cells*, **12**, 1075-1090.

Zechiedrich, E.L. and Osheroff, N. (1990) Eukaryotic topoisomerases recognize nucleic acid topology by preferentially interacting with DNA crossovers. *Embo J*, **9**, 4555-4562.

7 Appendix: condensin pattern of binding

419 condensin association sites are indicated by red lines rising above the graphs (a list of the peak coordinates can be found in Tab 1, panel D).

The graphic representation of the 16 budding yeast chromosomes shows the location of centromeres (dark green), origins of DNA replication (light green), tRNA genes (red), genes encoding small nuclear and nucleolar and cytoplasmic RNAs (pink), and genes encoding ribosomal protein subunits (purple). RNA polymerase II-transcribed open reading frames are depicted in blue above and below the midline, transcribed from left to right, and opposite, respectively.

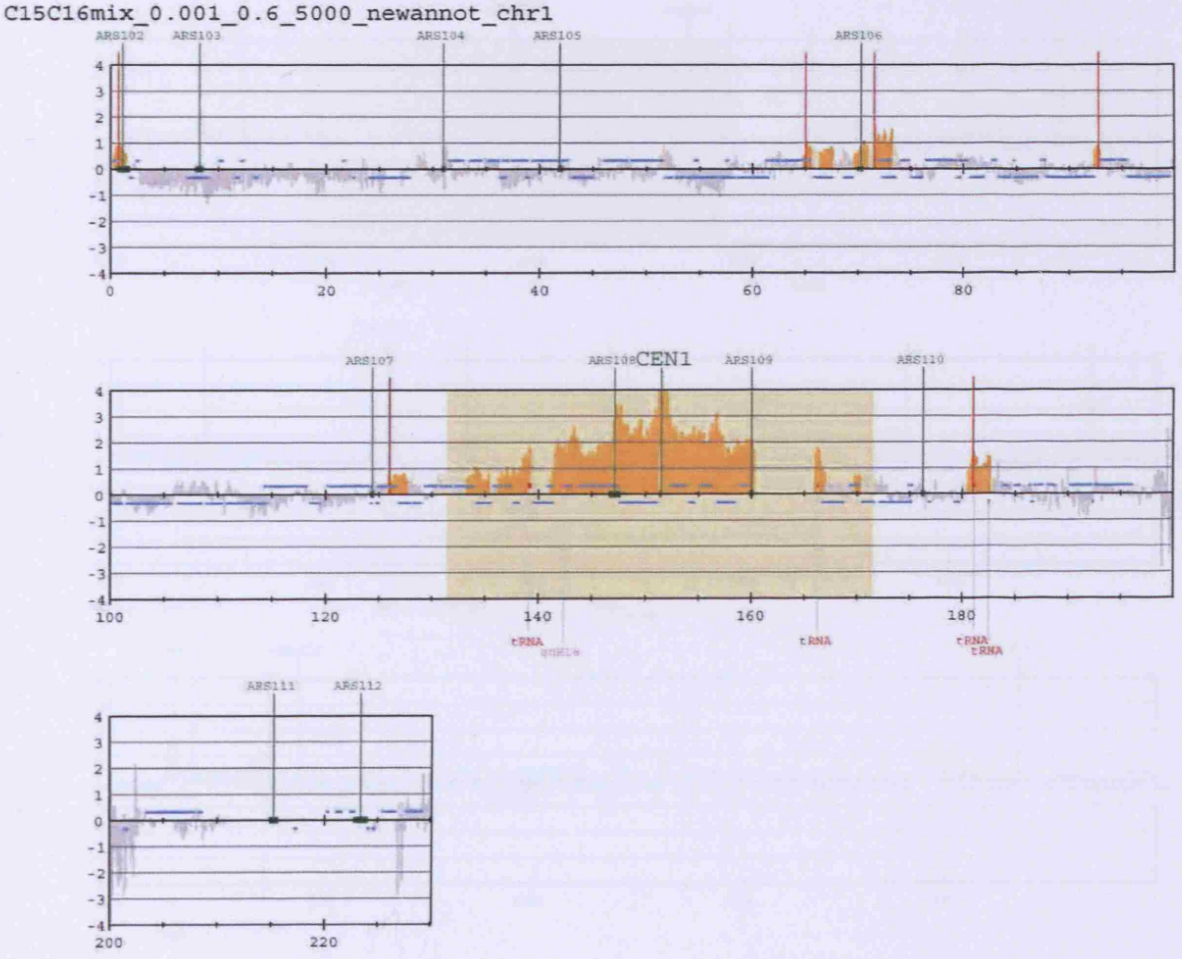

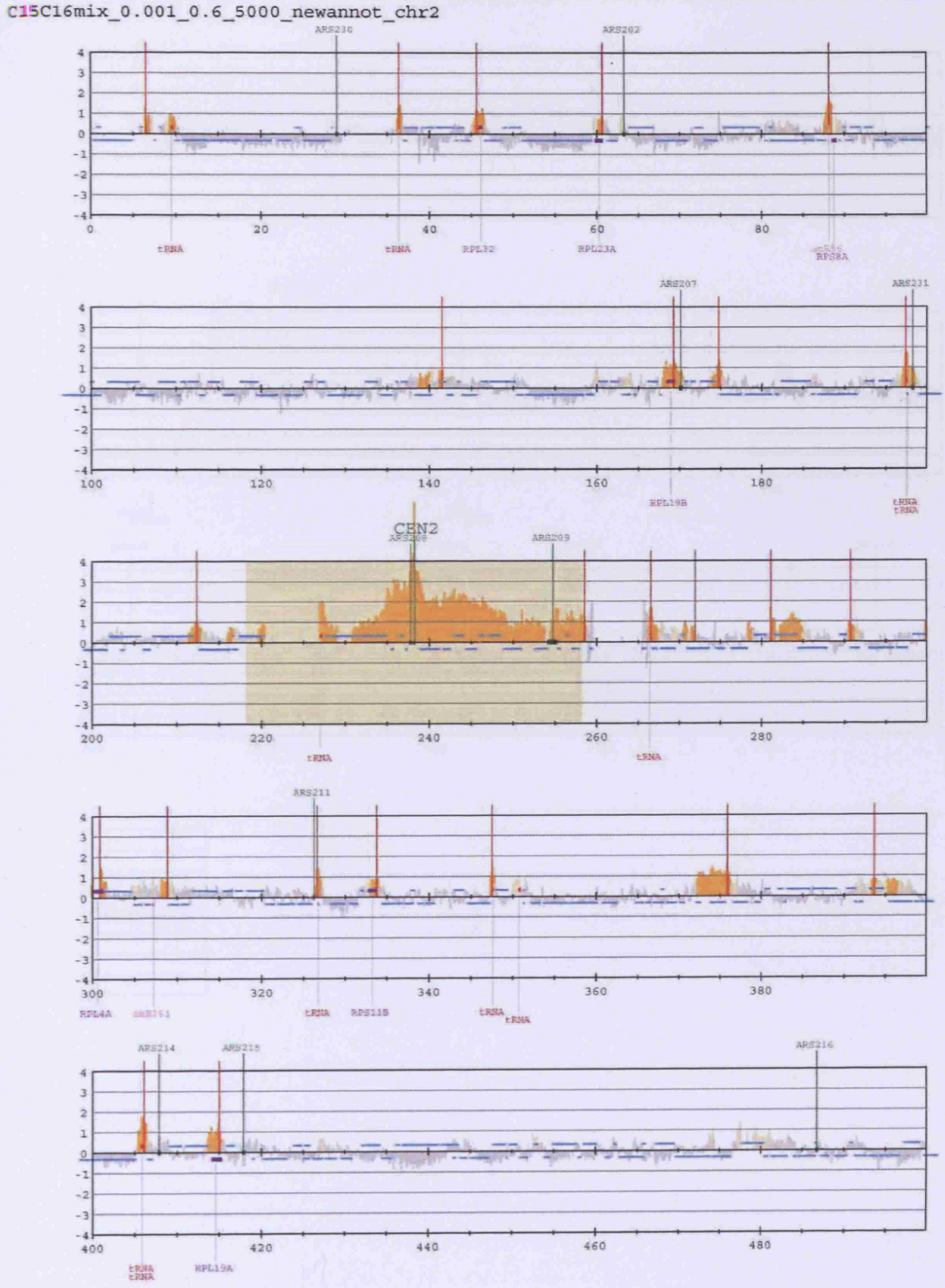
C15C16mix_0.001_0.6_5000_newannot_chr2
ARS230
ARS202
tRNA
tRNA
RPL32
RPL23A
RPS8A
ARS207
ARS231
RPL19B
tRNA
tRNA
CEN2
ARS208
ARS209
tRNA
tRNA
ARS211
RPL4A
tRNA
RPS11B
tRNA
tRNA
ARS214
ARS215
ARS216
tRNA
tRNA
RPL19A

C15C16mix_0.001_0.6_5000_newannot_chr2

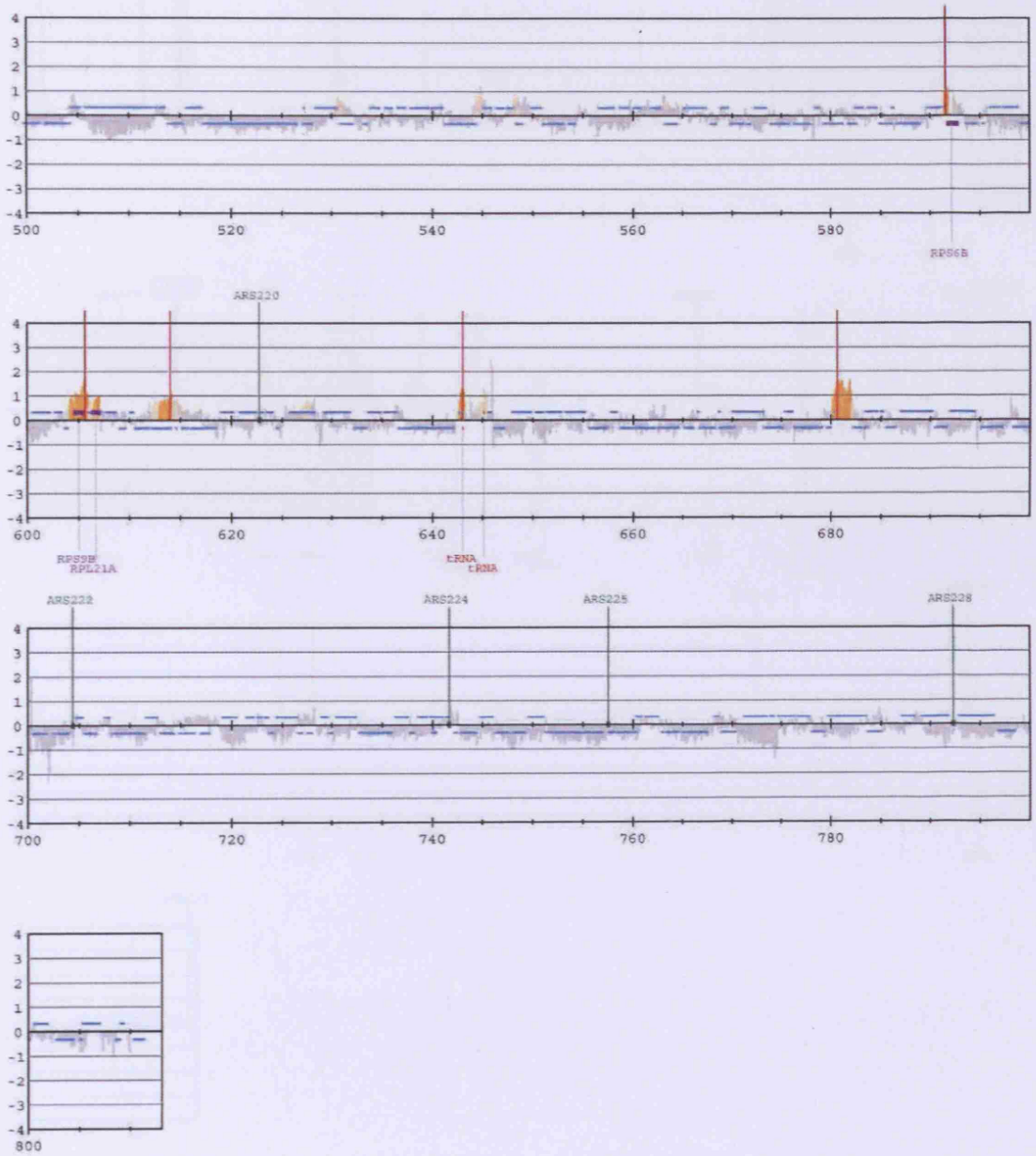

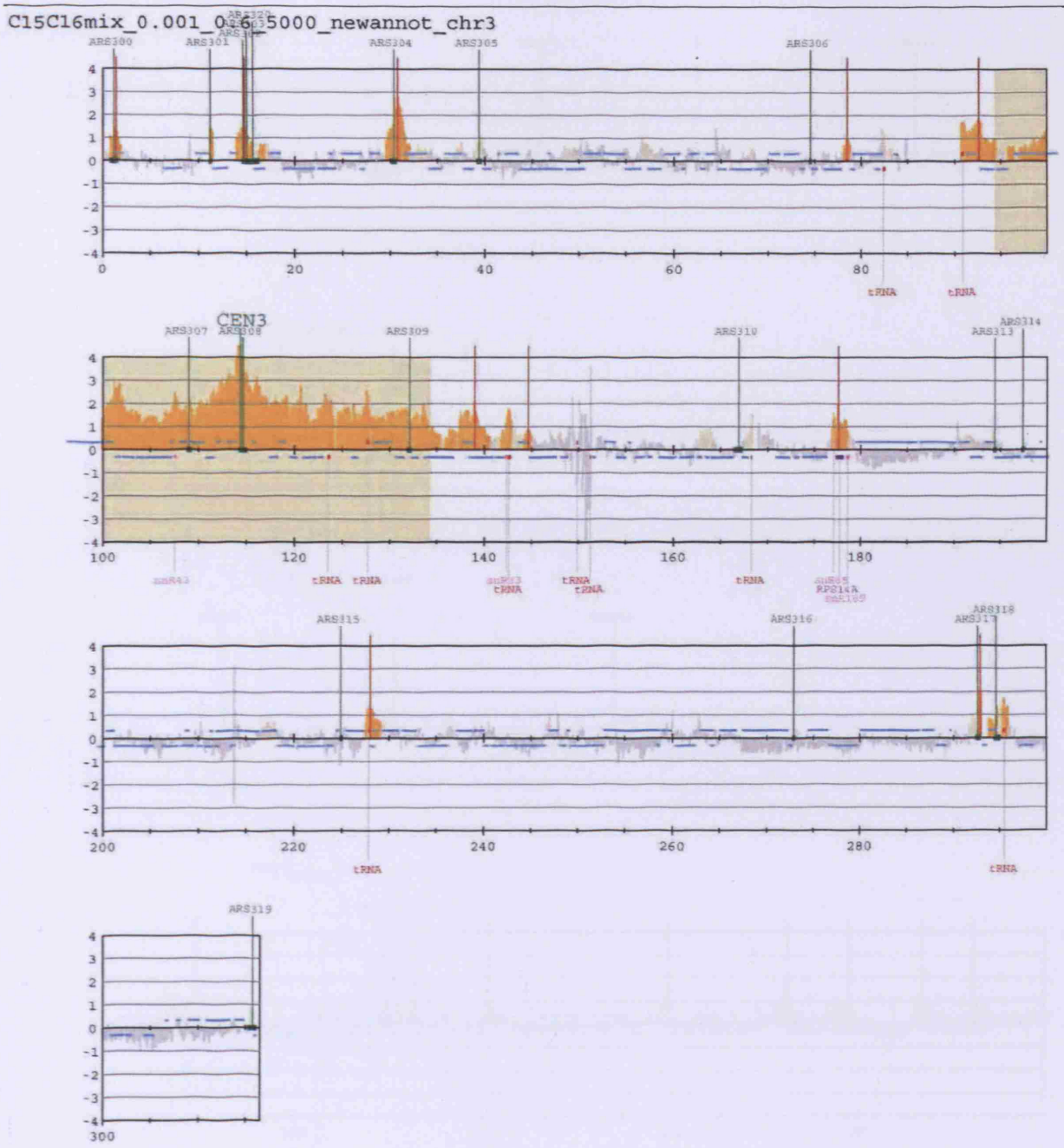
C15C16mix_0.001_0.6_5000_newannot_chr3
ARS300
ARS301
ARS304
ARS305
ARS306
tRNA
tRNA
CEN3
ARS307
ARS308
ARS309
ARS310
ARS313
ARS314
tRNA
tRNA
tRNA
tRNA
tRNA
RPS14A
ARS315
ARS316
ARS317
ARS318
tRNA
tRNA
ARS319

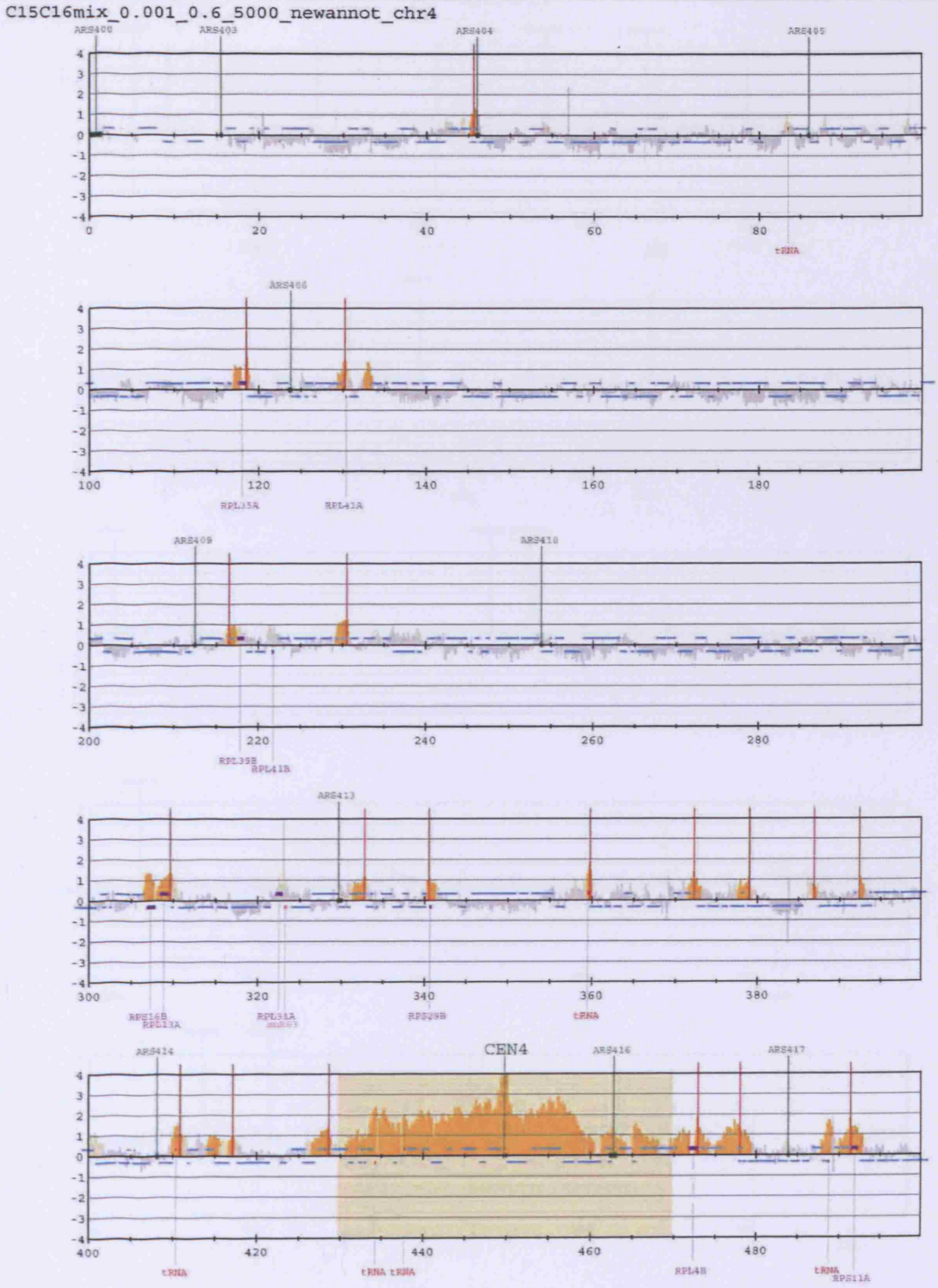
C15C16mix_0.001_0.6_5000_newannot_chr4
ARS400
ARS403
ARS404
ARS405
tRNA
ARS406
RPL35A
RPL41A
ARS409
ARS410
RPL35B
RPL41B
ARS413
RPS29B
tRNA
CEN4
ARS414
ARS416
ARS417
tRNA
tRNA tRNA
RPL4B
RPS11A

C15C16mix_0.001_0.6_5000_newannot_chr4

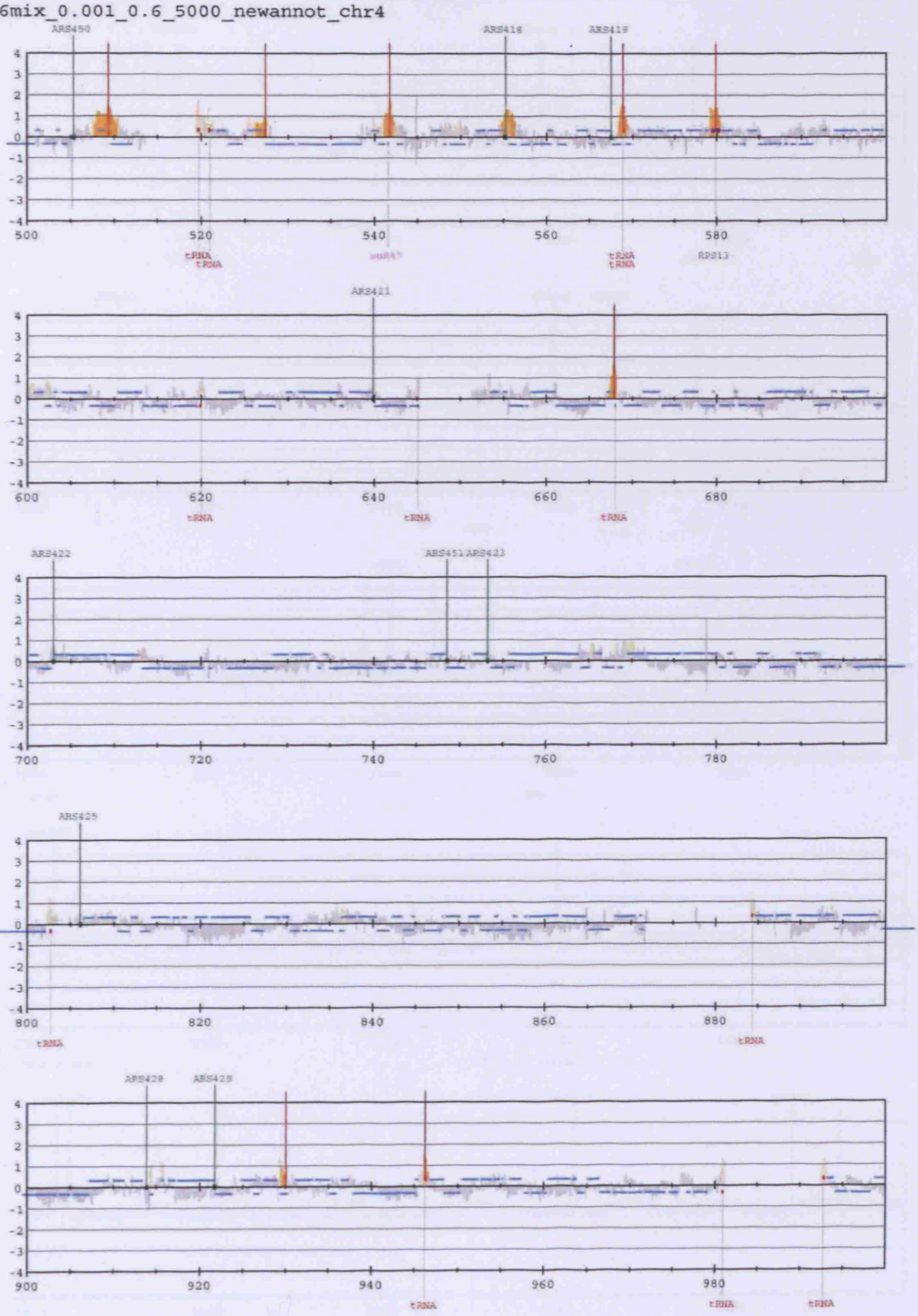

C15C16mix_0.001_0.6_5000_newannot_chr4

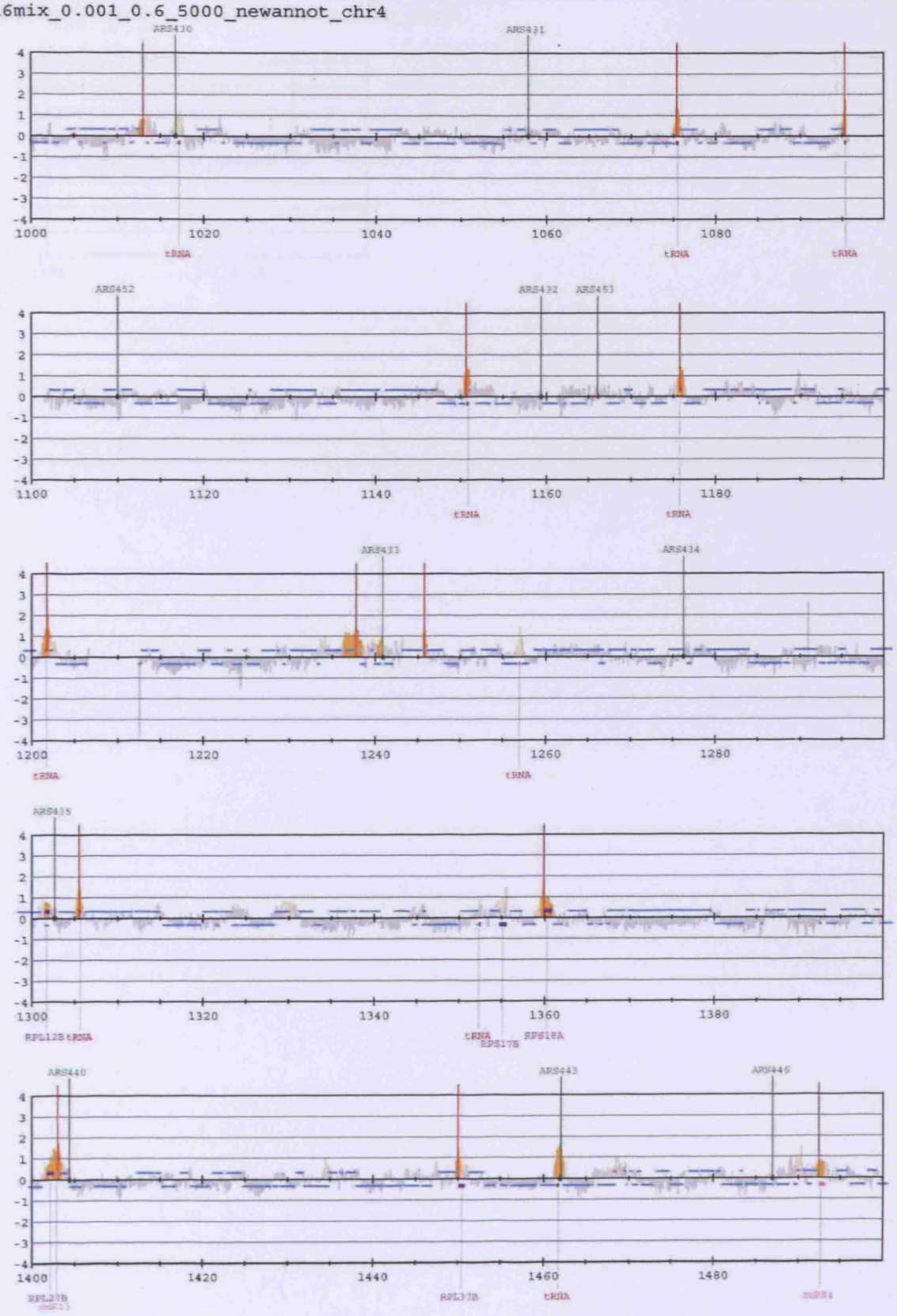

C15C16mix_0.001_0.6_5000_newannot_chr4

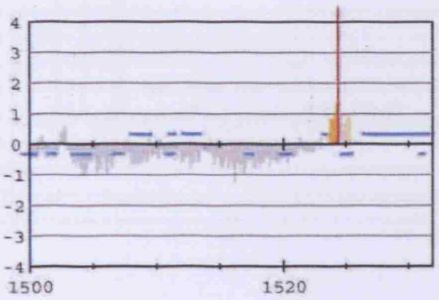

C15C16mix_0.001_0.6_5000_newannot_chr5

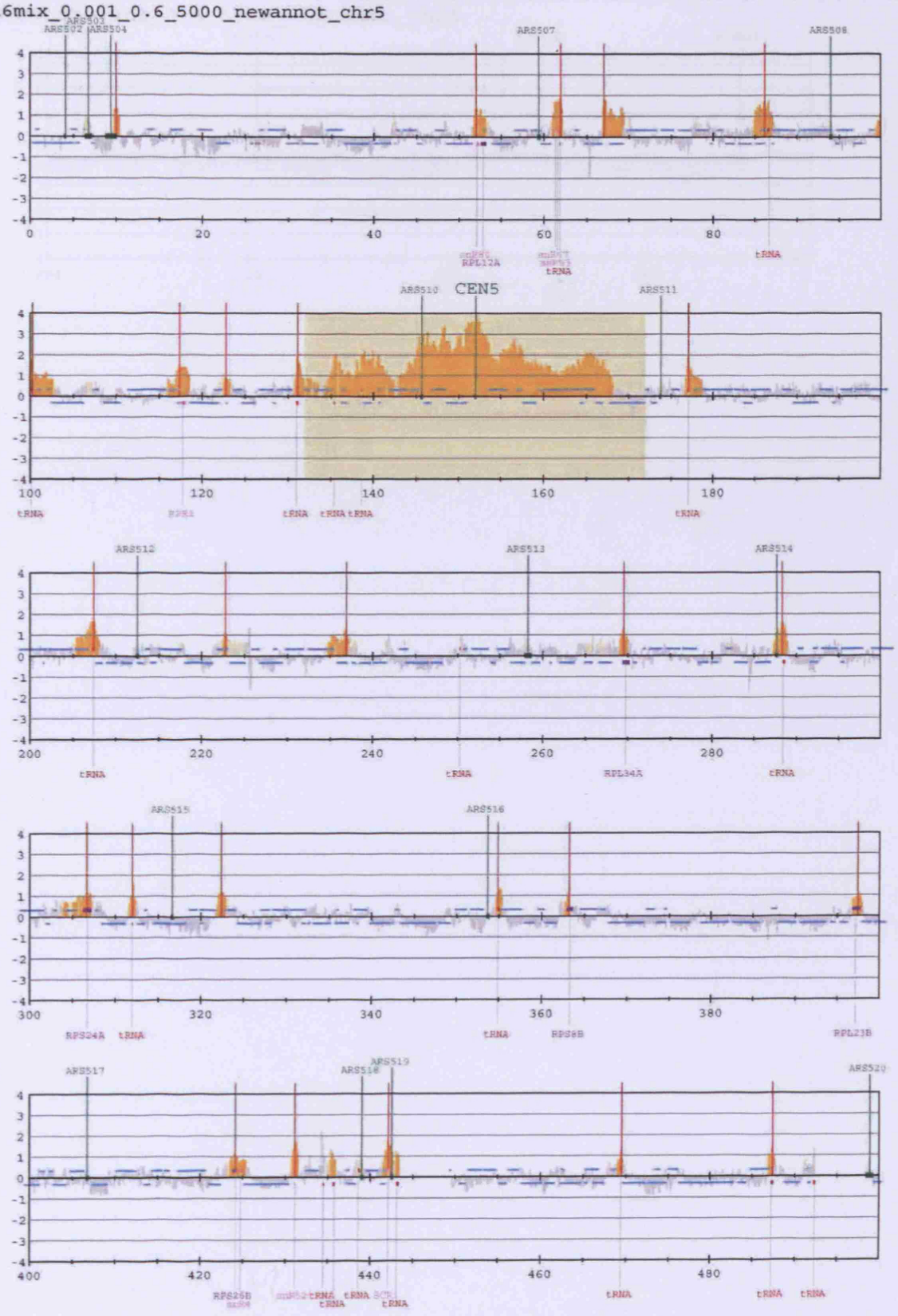

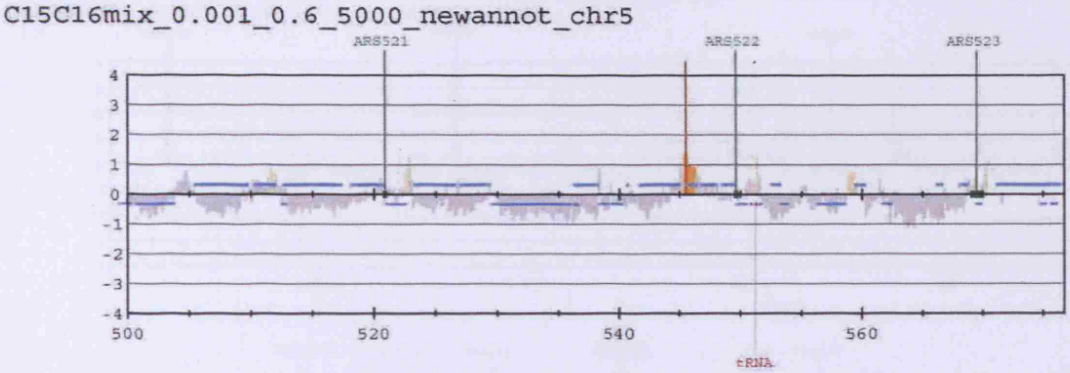
C15C16mix_0.001_0.6_5000_newannot_chr5
ARS521
ARS522
ARS523
4
3
2
1
0
-1
-2
-3
-4
500
520
540
560
tRNA

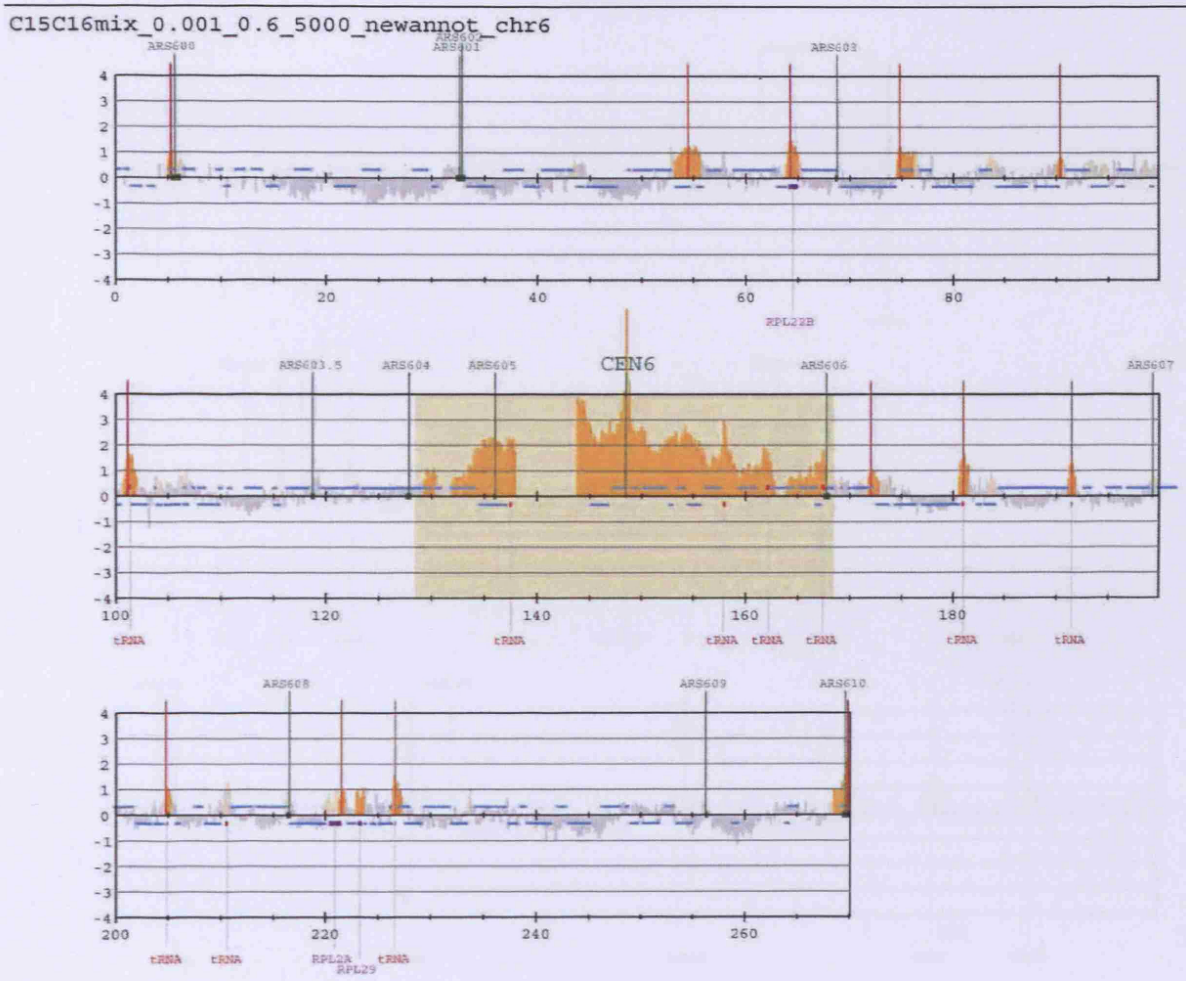
C15C16mix_0.001_0.6_5000_newannot_chr6
ARS600
ARS601
ARS603
RPL22B
ARS603.5
ARS604
ARS605
CEN6
ARS606
ARS607
tRNA
ARS608
ARS609
ARS610
RPL2A
RPL29

C15C16mix_0.001_0.6_5000_newannot_chr7

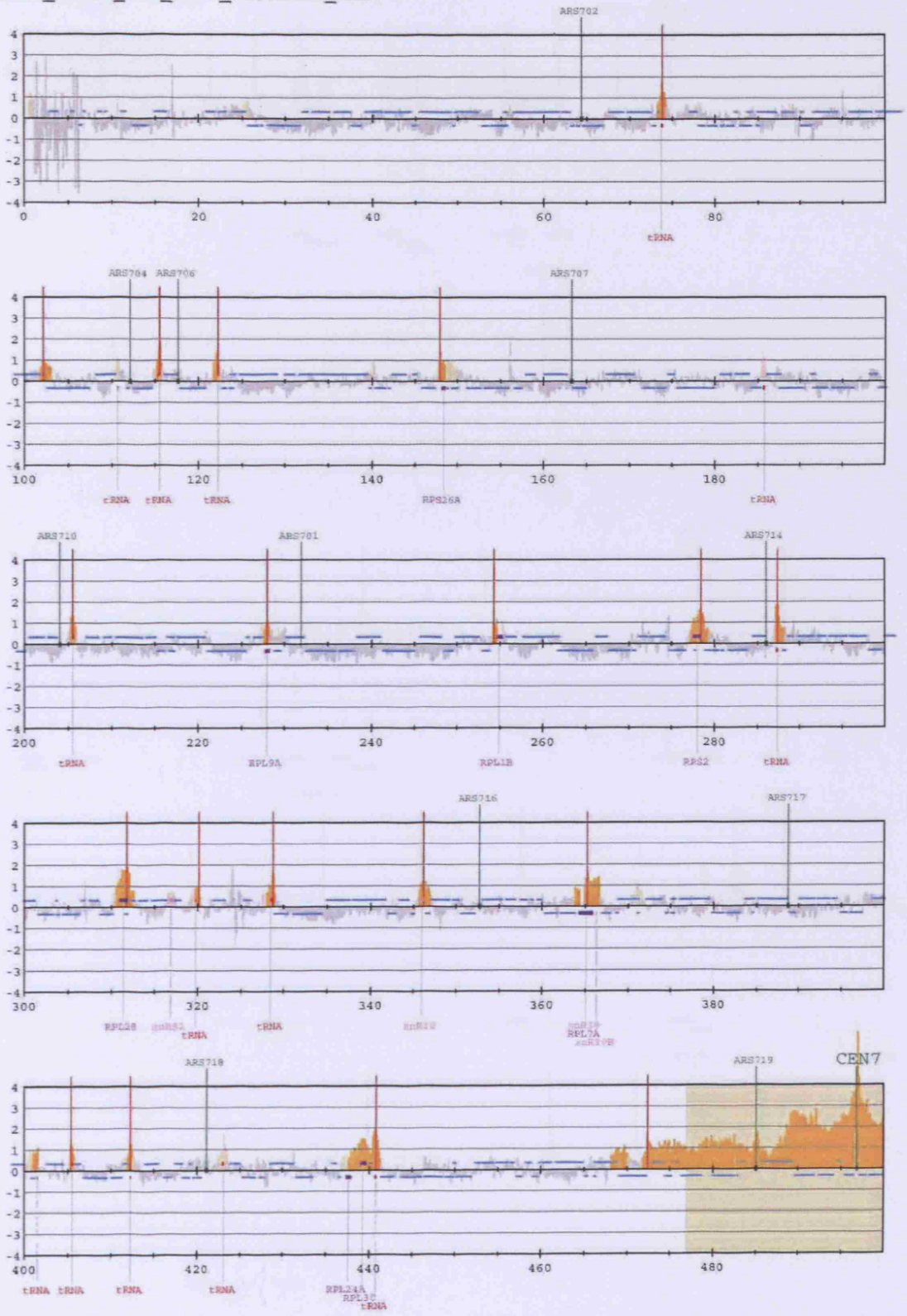

C15C16mix_0.001_0.6_5000_newannot_chr7

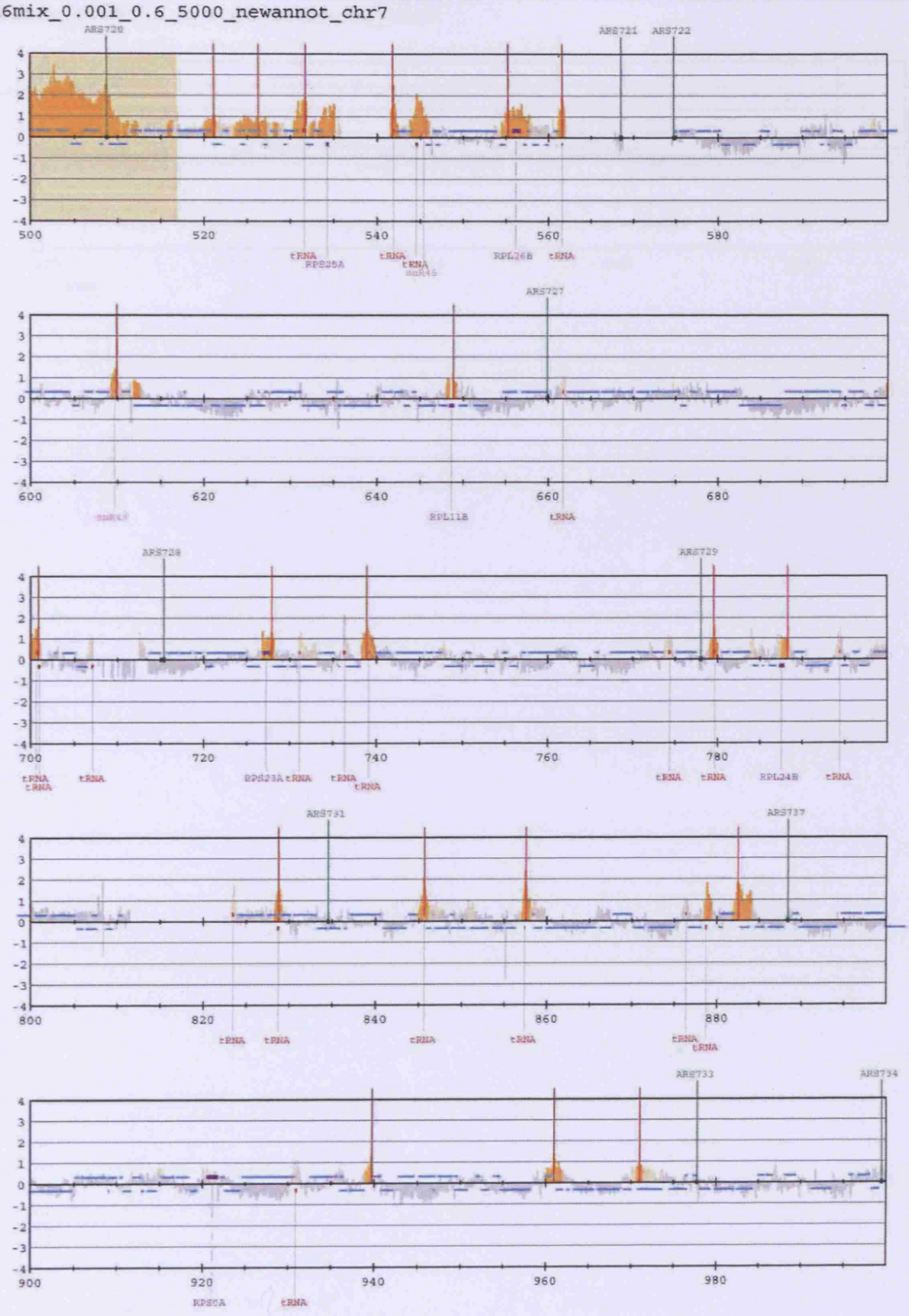

C15C16mix_0.001_0.6_5000_newannot_chr7

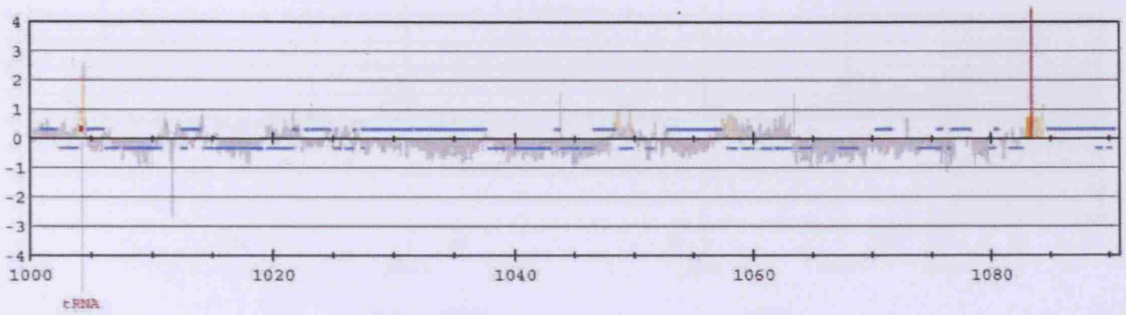

C15C16mix_0.001_0.6_5000_newannot_chr8

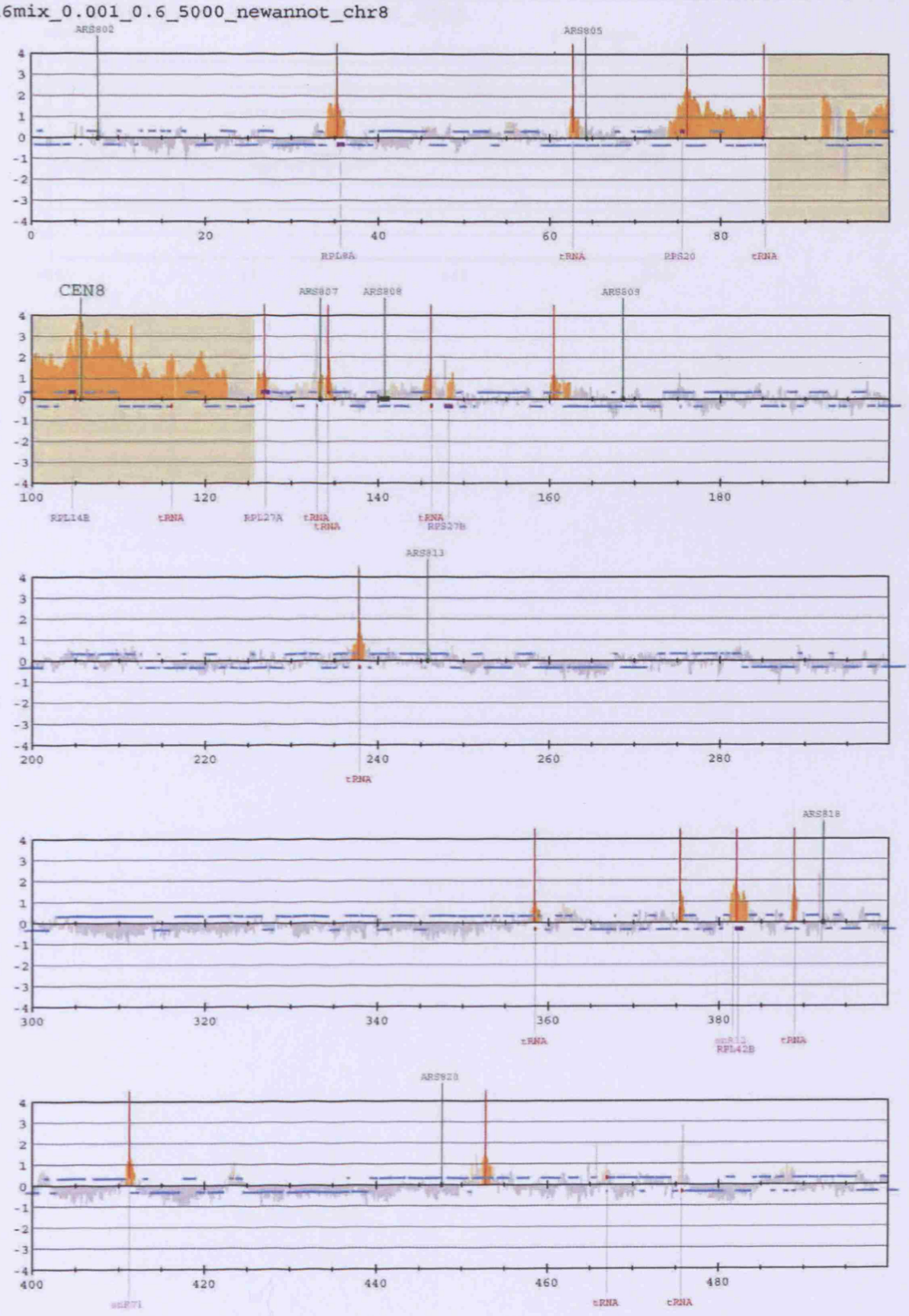

C15C16mix_0.001_0.6_5000_newannot_chr8

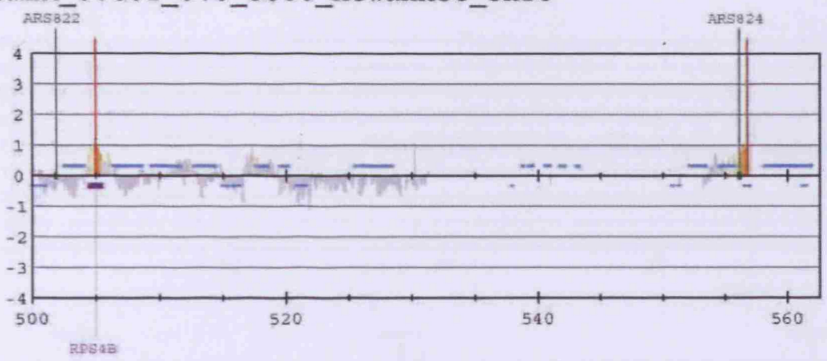

C15C16mix_0.001_0.6_5000_newannot_chr9

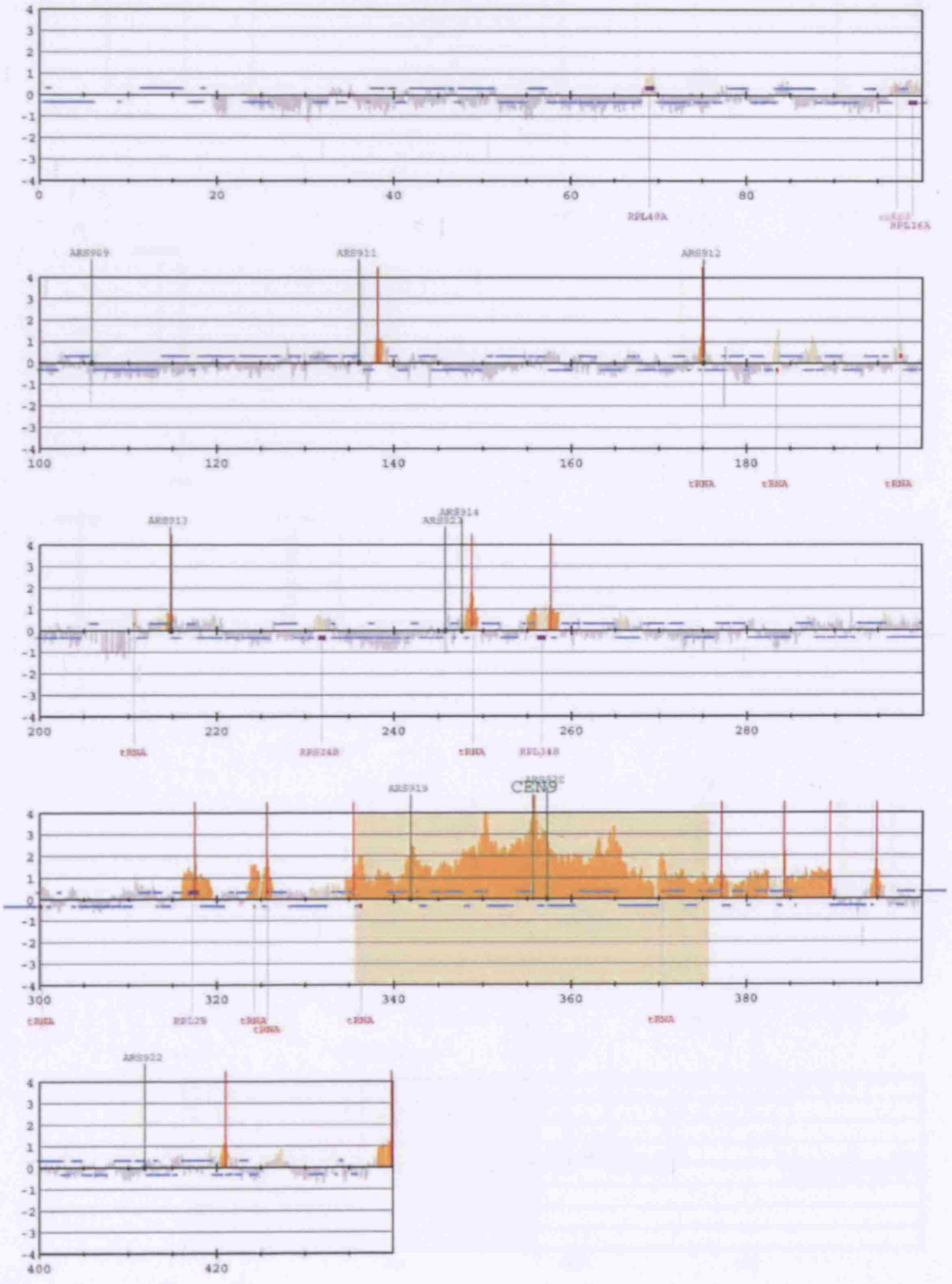

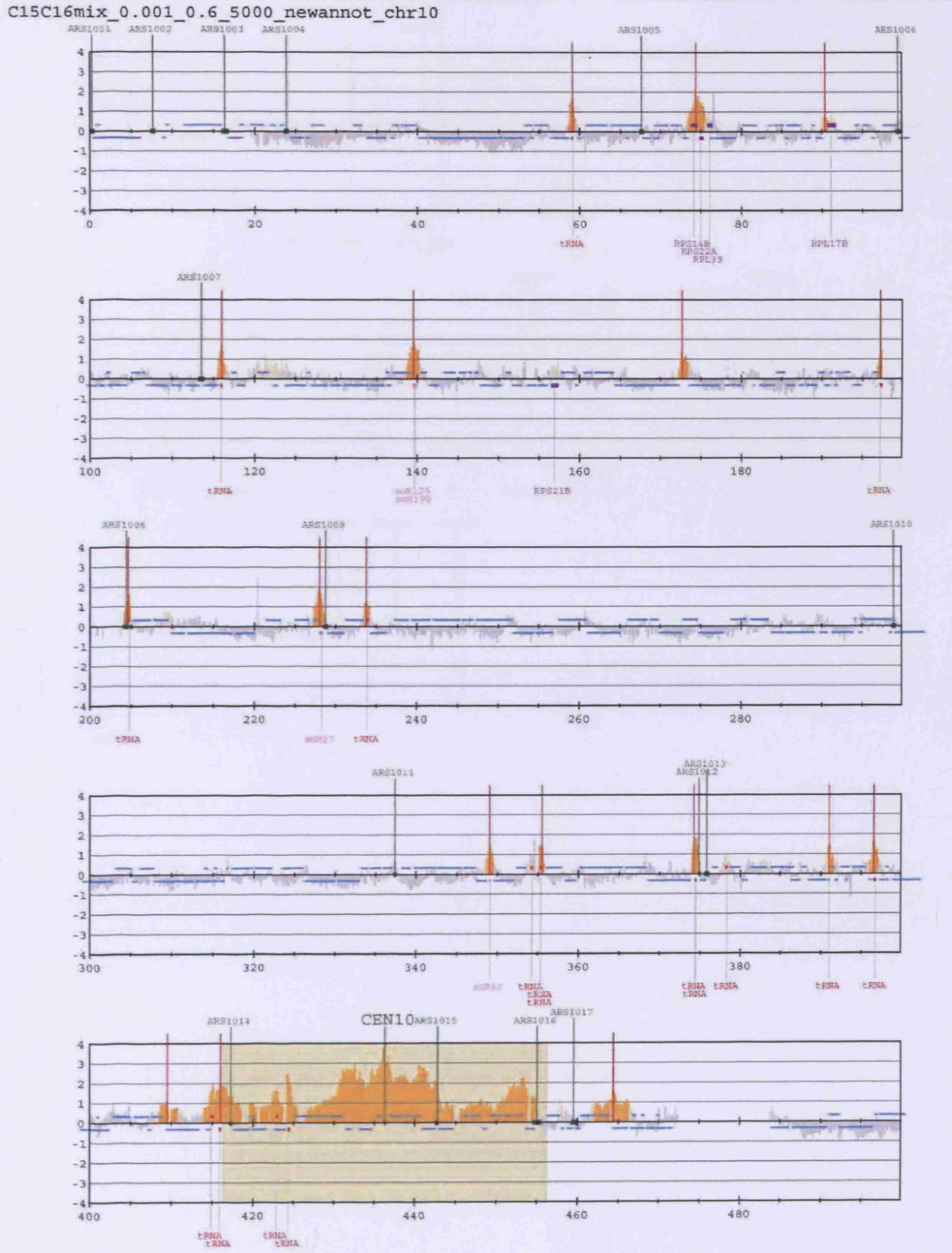
C15C16mix_0.001_0.6_5000_newannot_chr10
ARS1001
ARS1002
ARS1003
ARS1004
ARS1005
ARS1006
ARS1007
ARS1008
ARS1009
ARS1010
ARS1011
ARS1012
ARS1013
ARS1014
CEN10
ARS1015
ARS1016
ARS1017
tRNA
RPS14B
RPS22A
RPL39
RPL17B
RPS21B

C15C16mix_0.001_0.6_5000_newannot_chr10

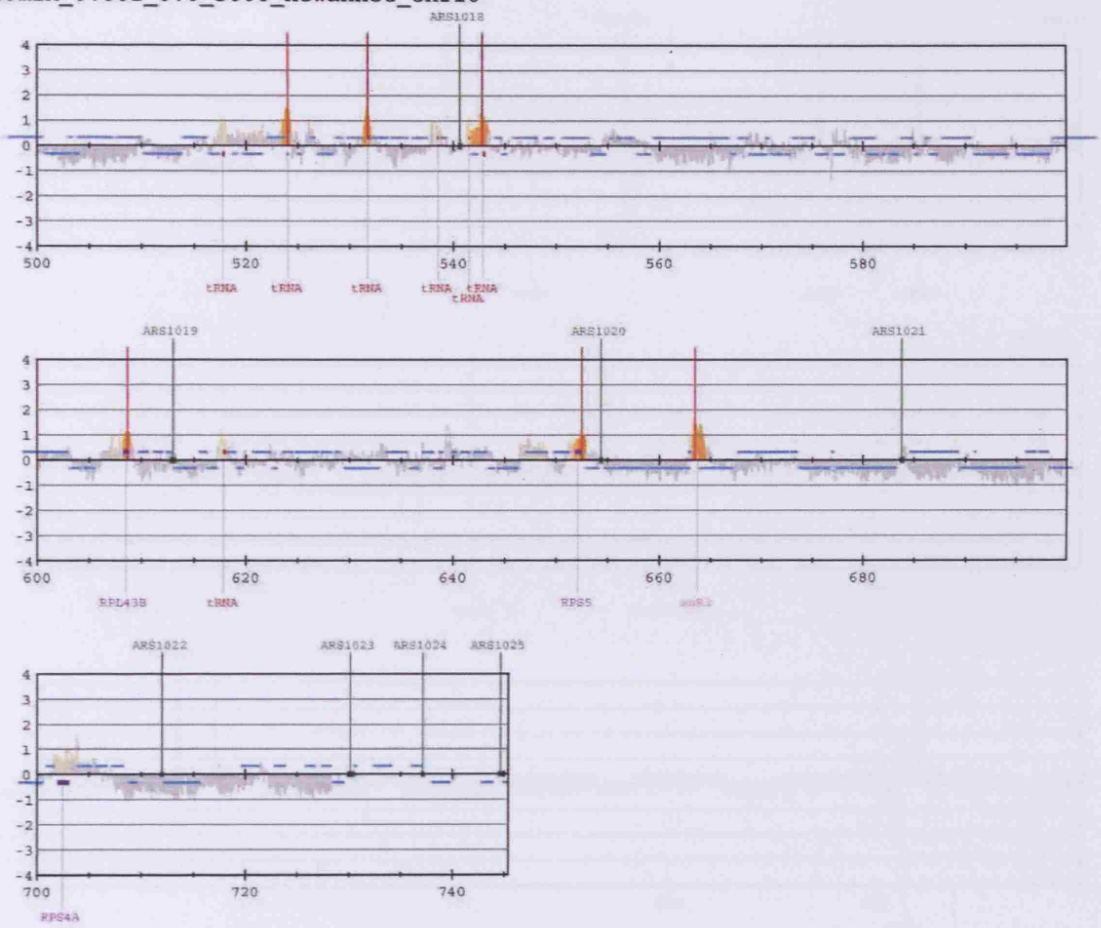

C15C16mix_0.001_0.6_5000_newannot_chr11

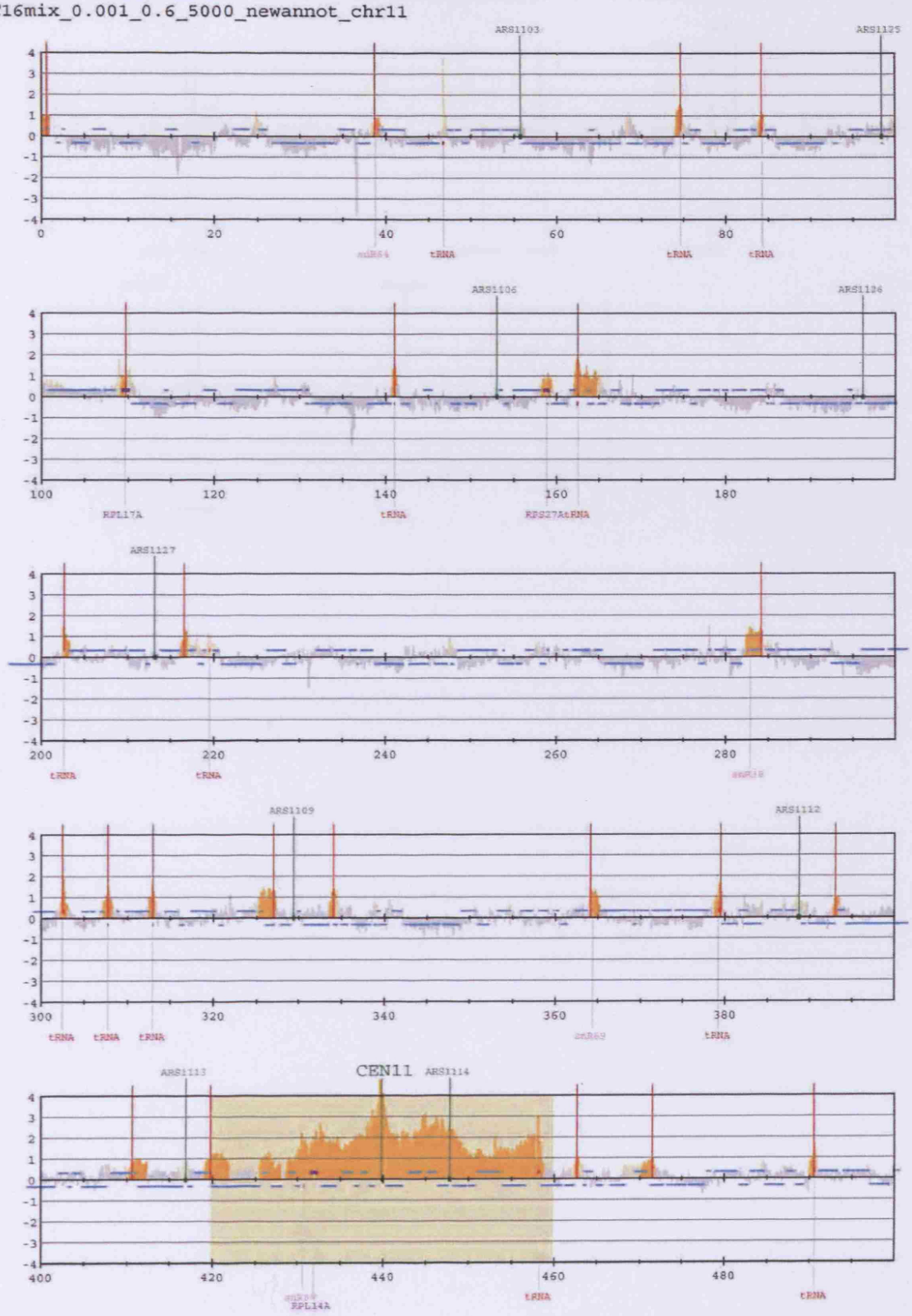

C15C16mix_0.001_0.6_5000_newannot_chr11

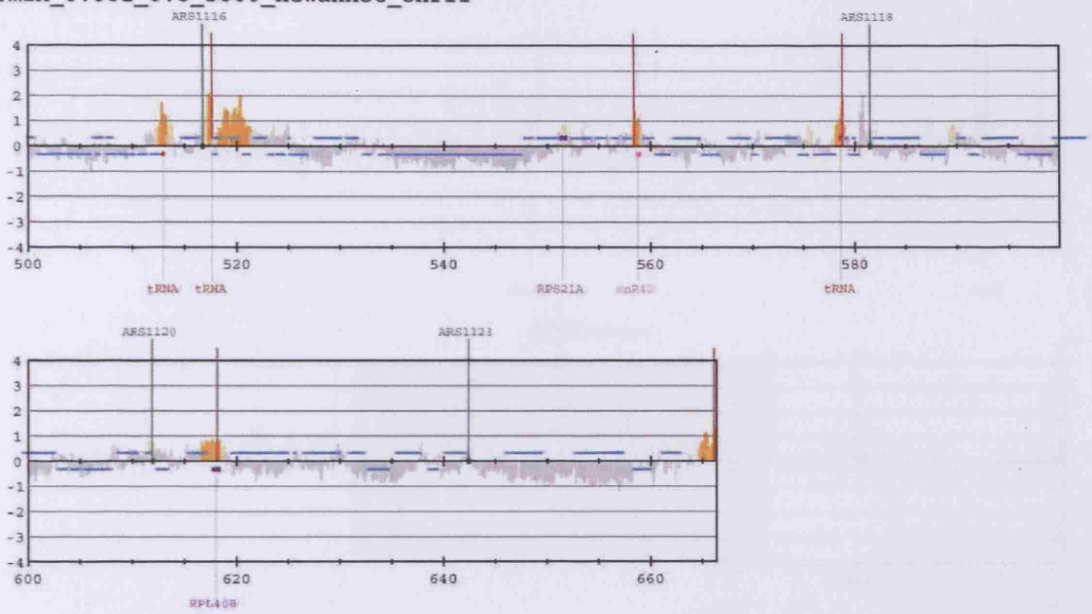

C15C16mix_0.001_0.6_5000_newannot_chr12

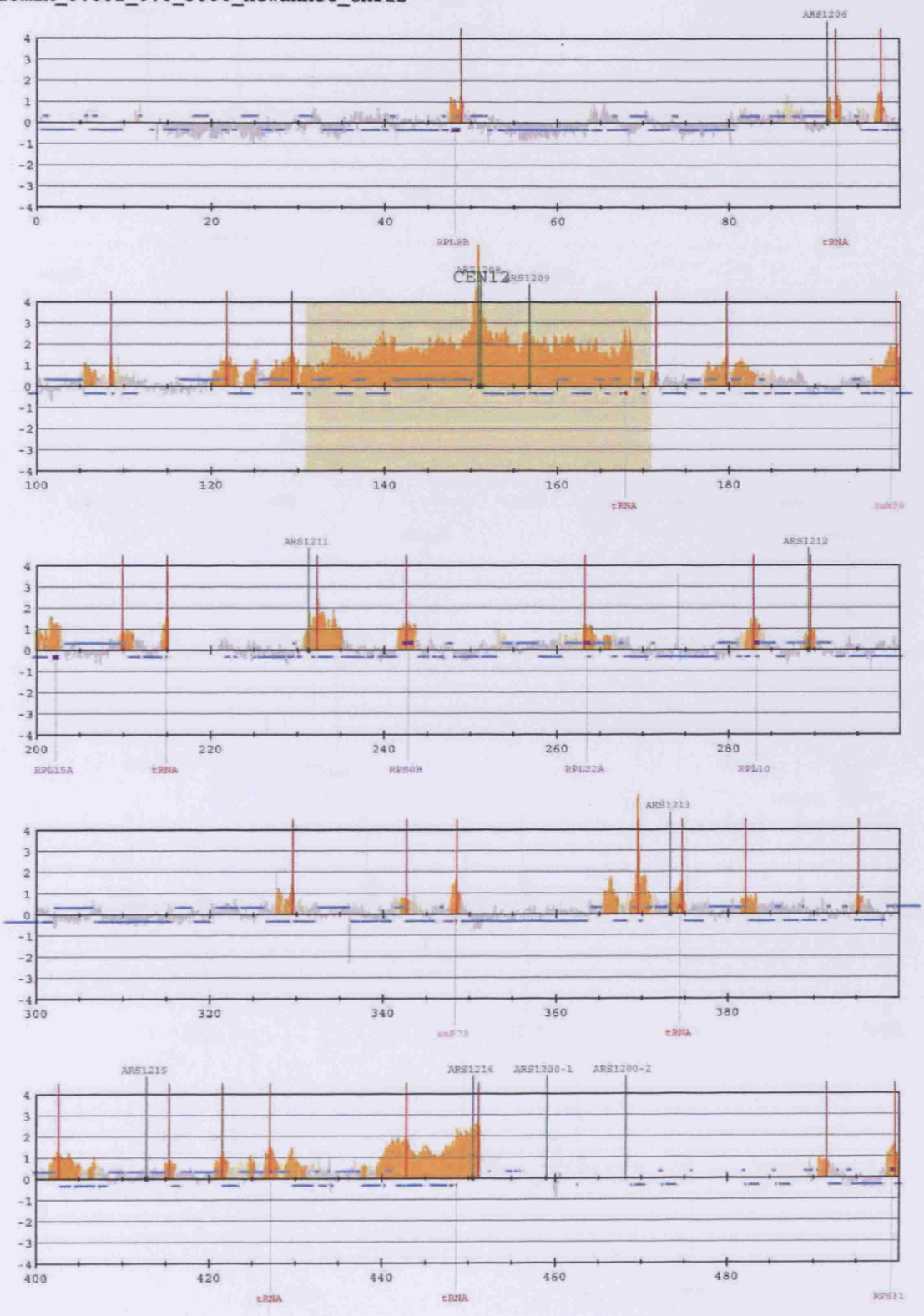

C15C16mix_0.001_0.6_5000_newannot_chr12

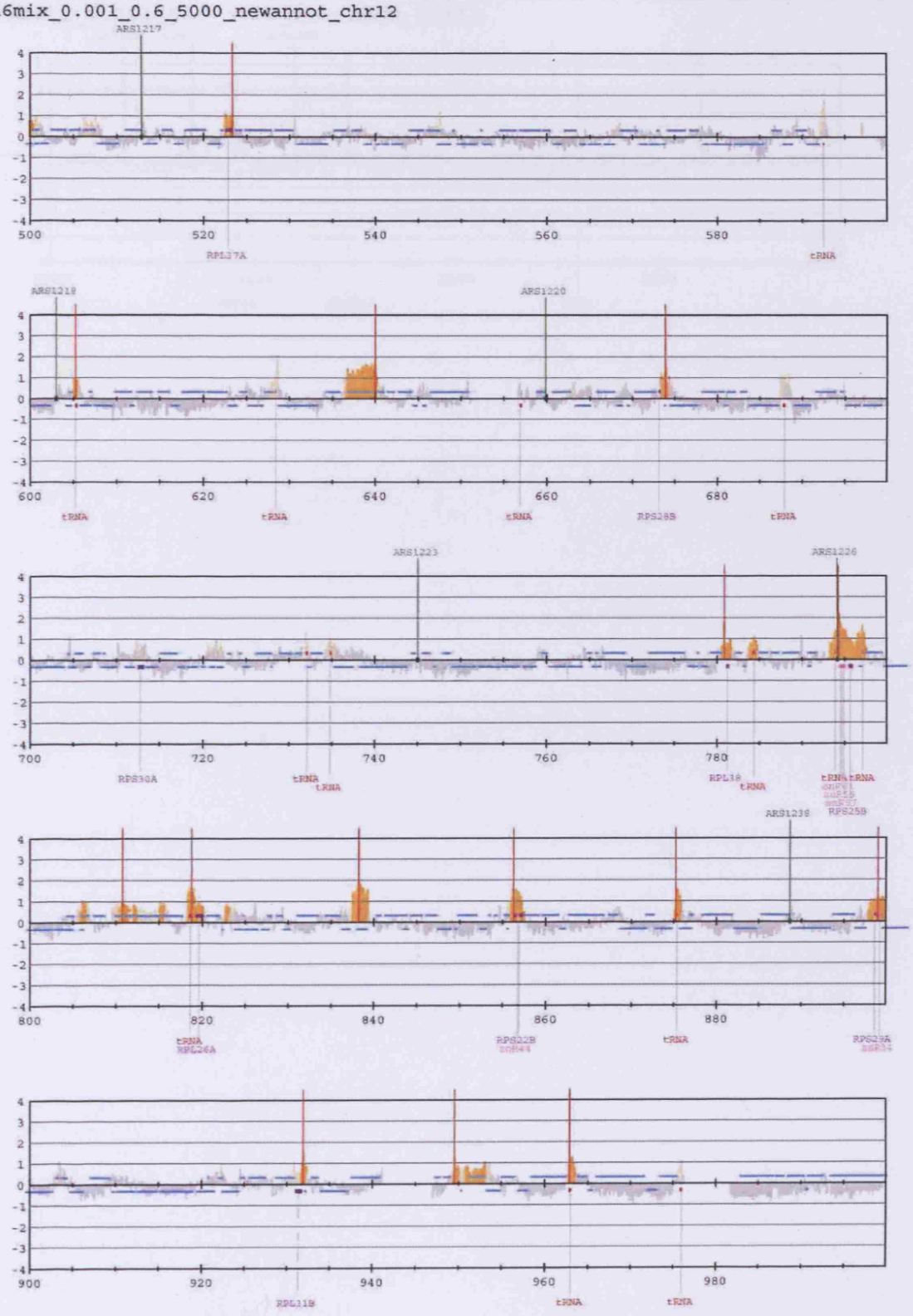

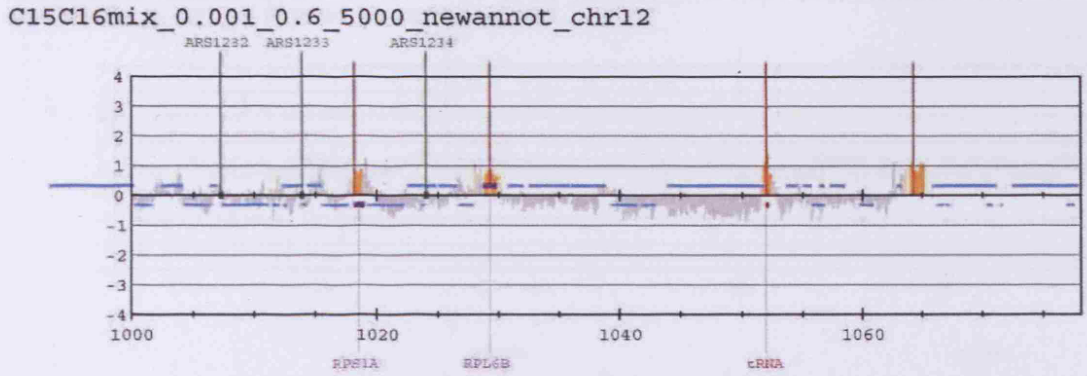
C15C16mix_0.001_0.6_5000_newannot_chr12
ARS1232
ARS1233
ARS1234
4
3
2
1
0
-1
-2
-3
-4
1000
1020
1040
1060
RPS1A
RPL6B
tRNA

C15C16mix_0.001_0.6_5000_newannot_chr13

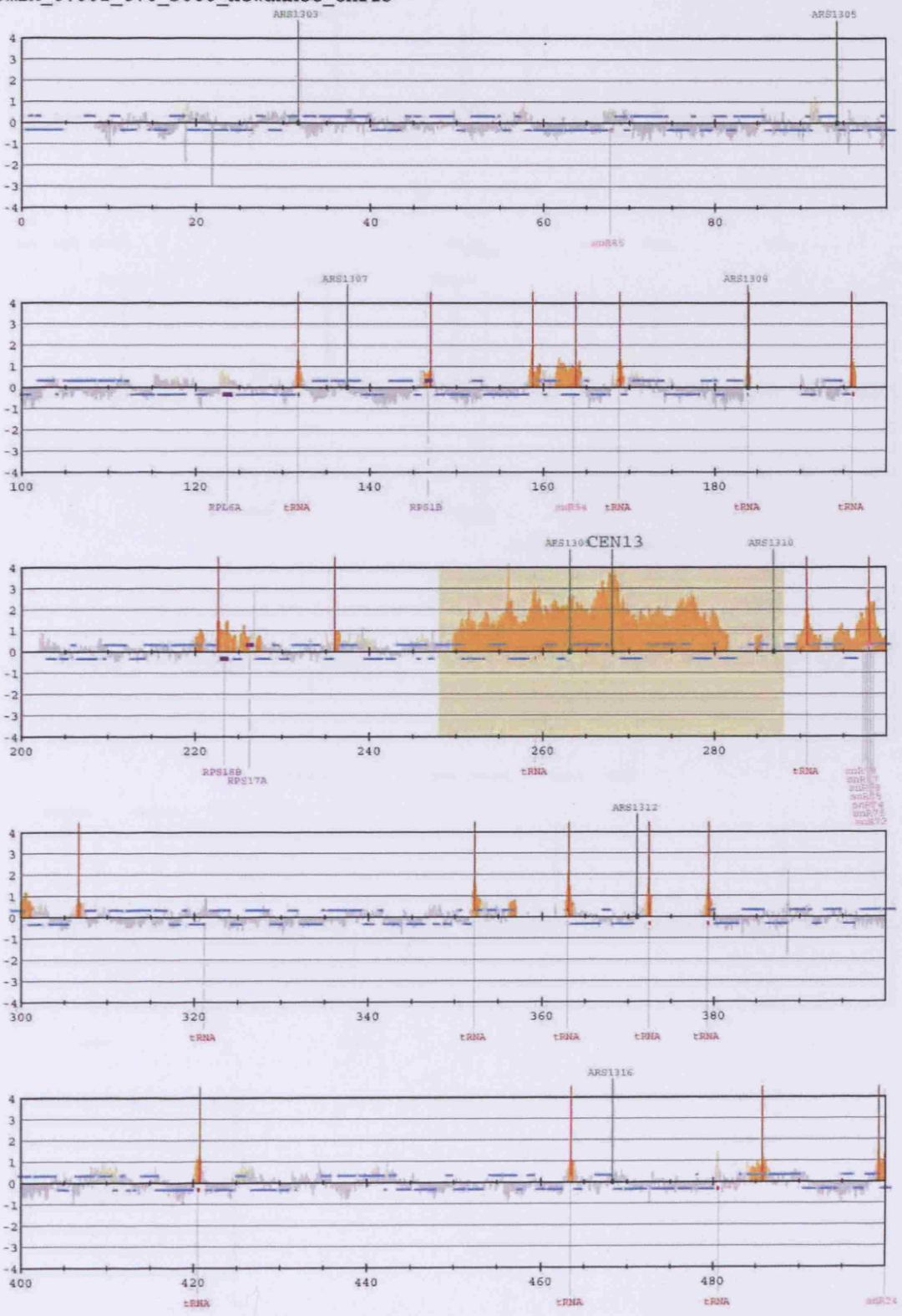

C15C16mix_0.001_0.6_5000_newannot_chr13

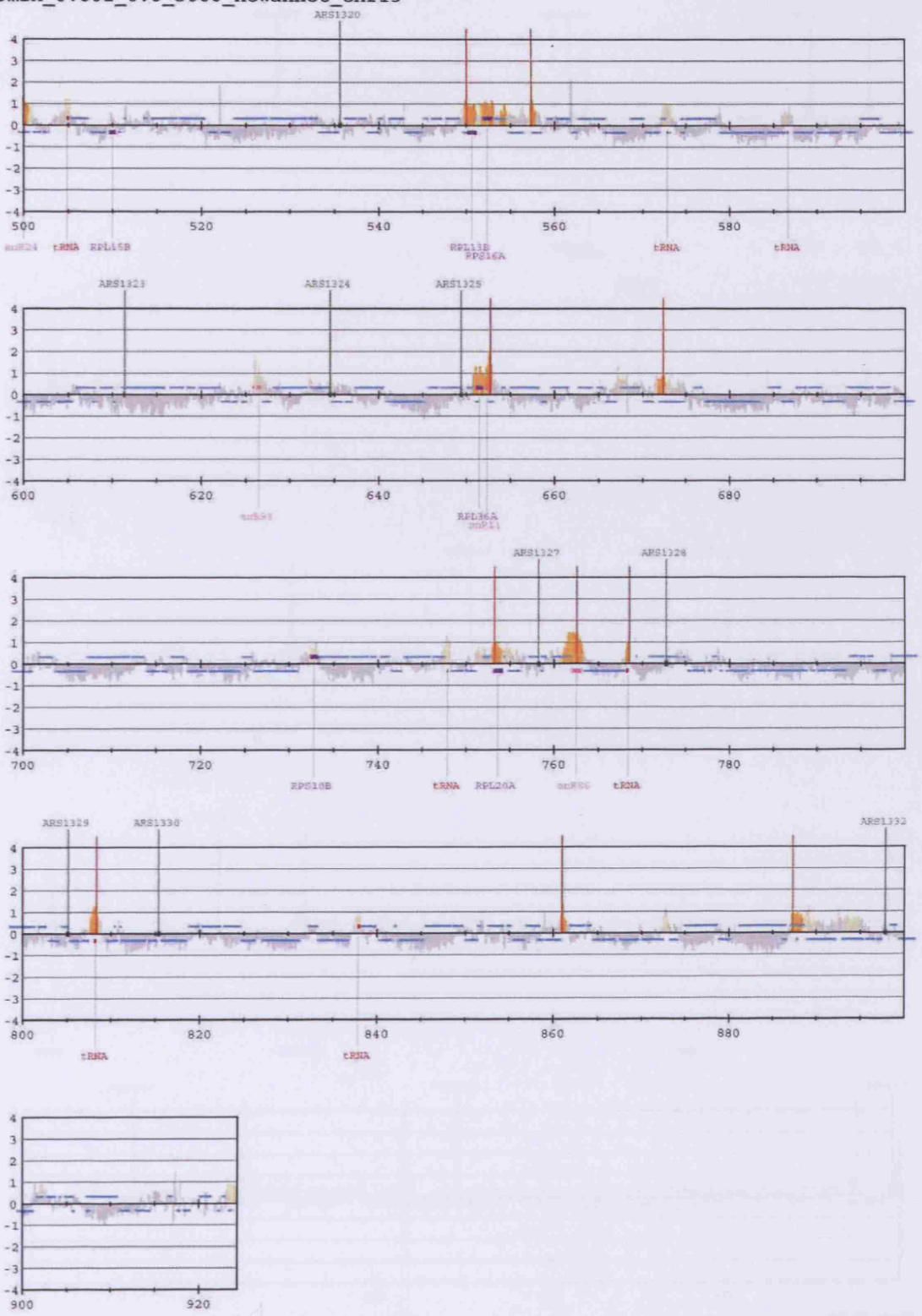

C15C16mix_0.001_0.6_5000_newannot_chr14

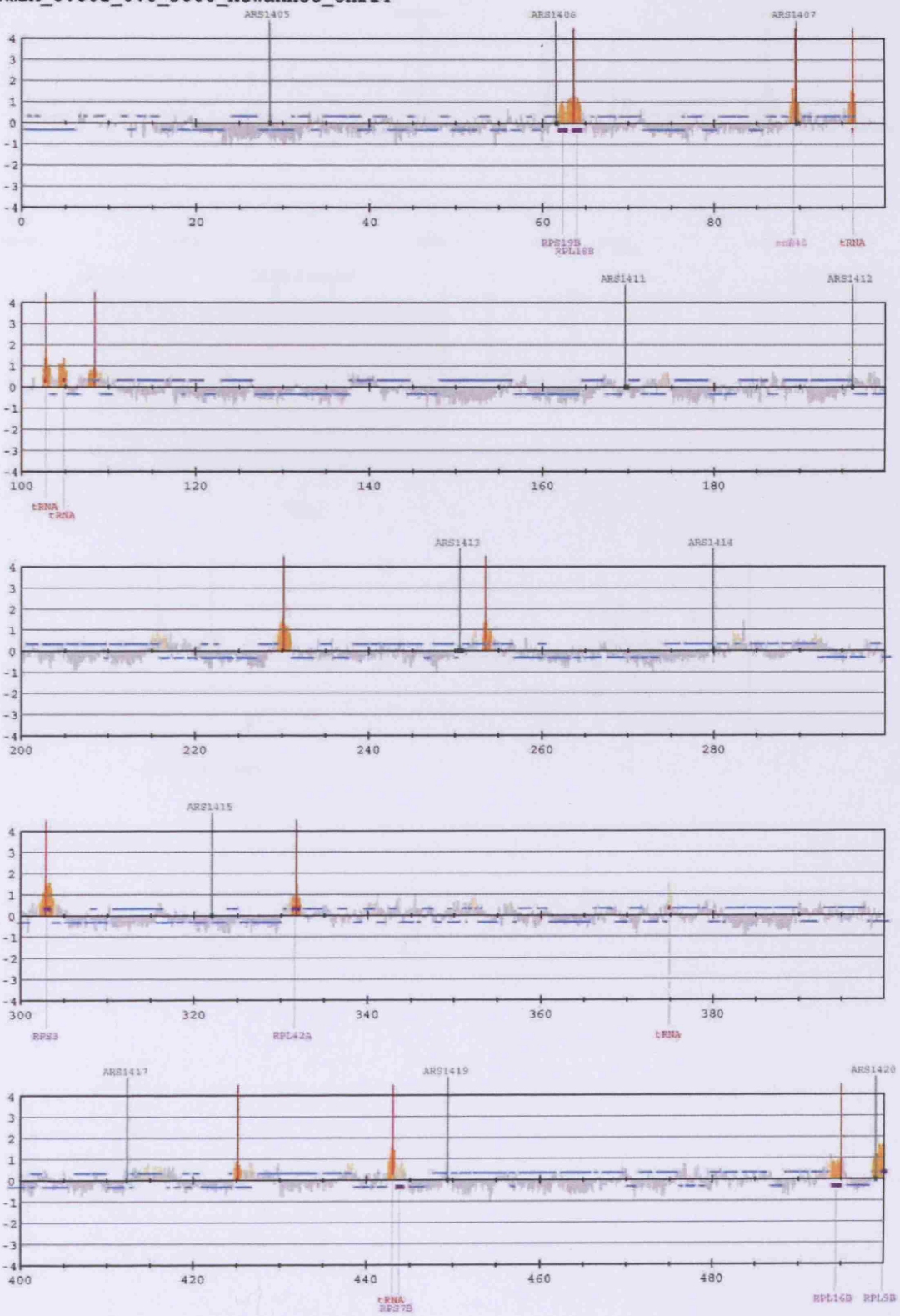

C15C16mix_0.001_0.6_5000_newannot_chr14

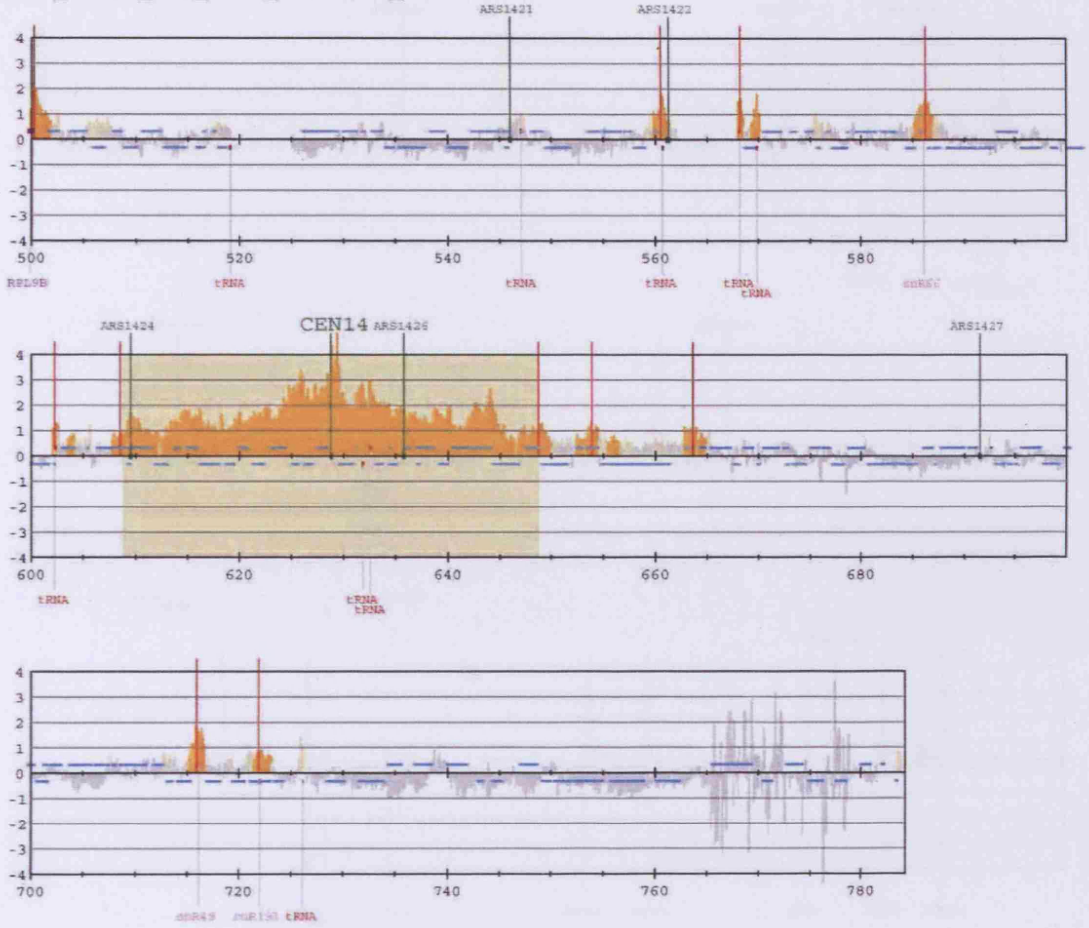

C15C16mix_0.001_0.6_5000_newannot_chr15

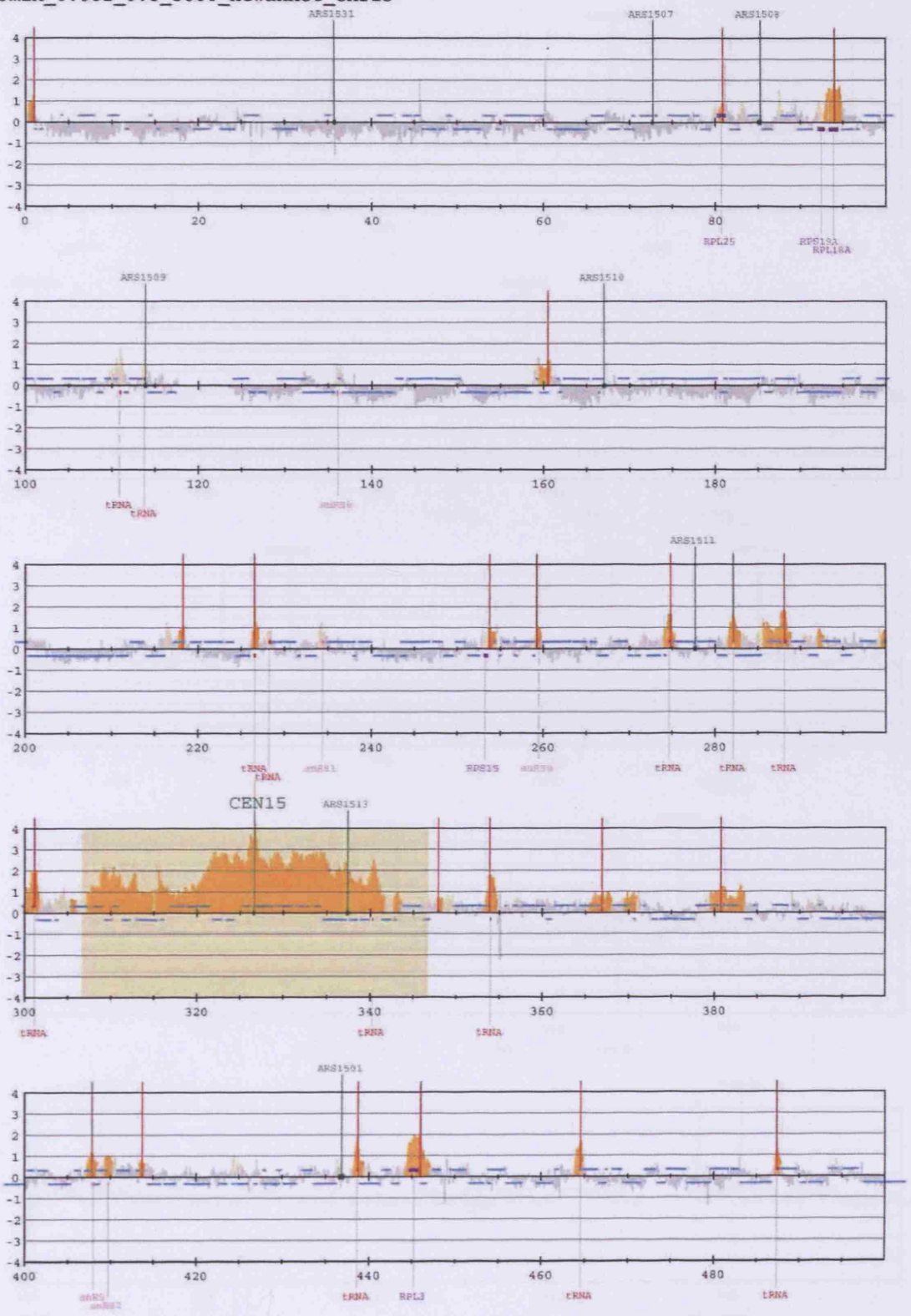

C15C16mix_0.001_0.6_5000_newannot_chr15

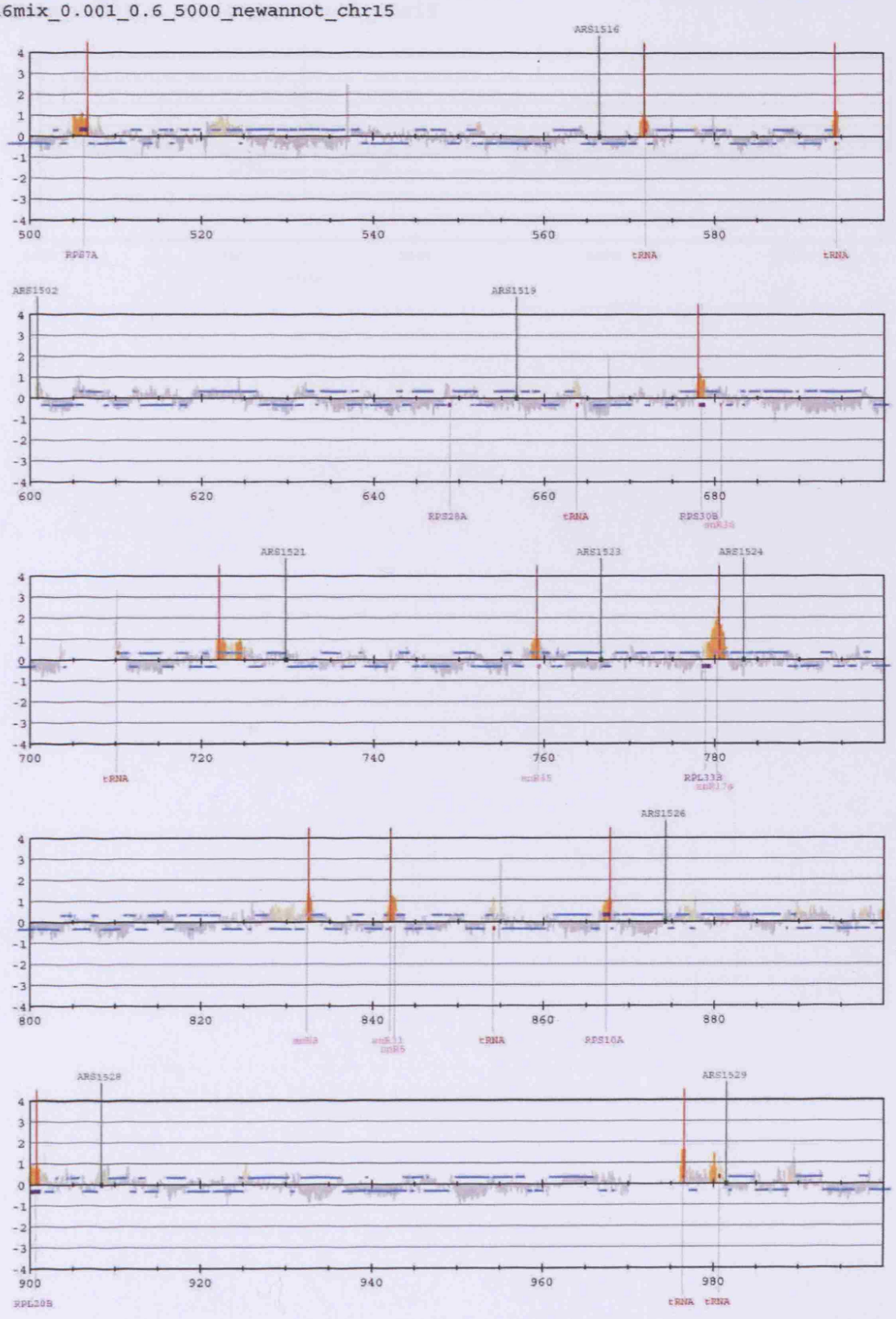

C15C16mix_0.001_0.6_5000_newannot_chr15

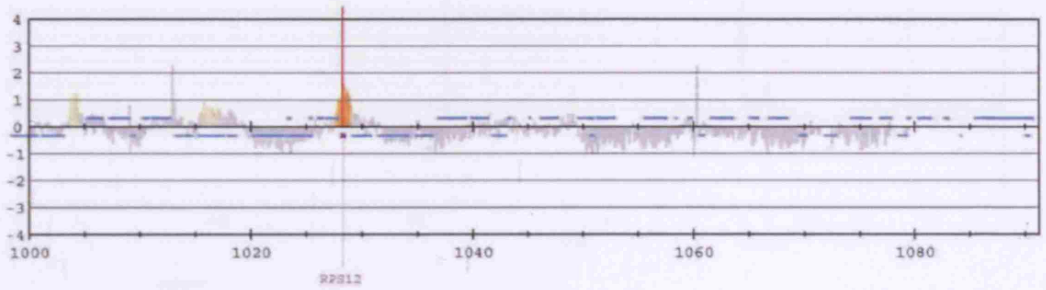

C15C16mix_0.001_0.6_5000_newannot_chr16

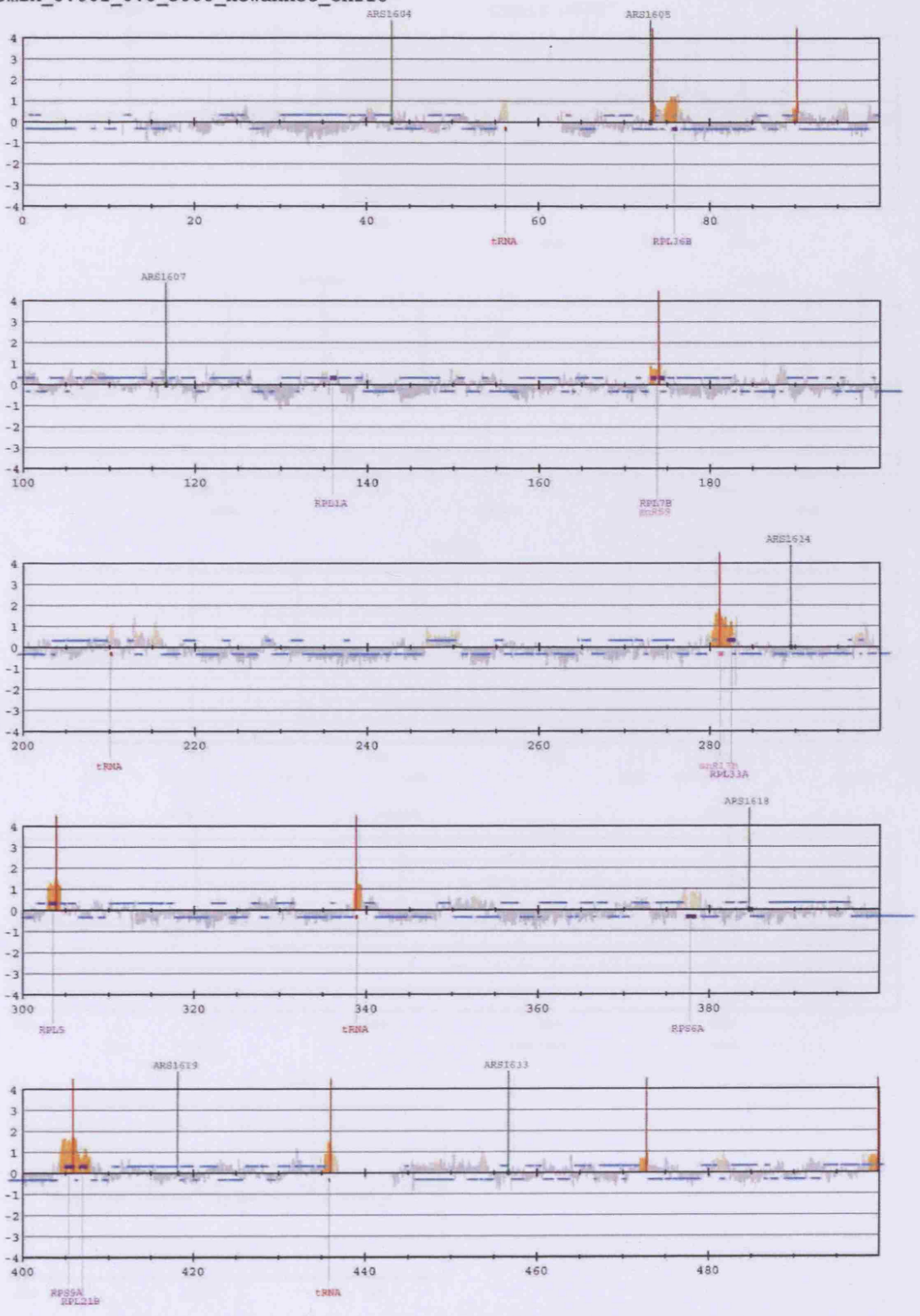

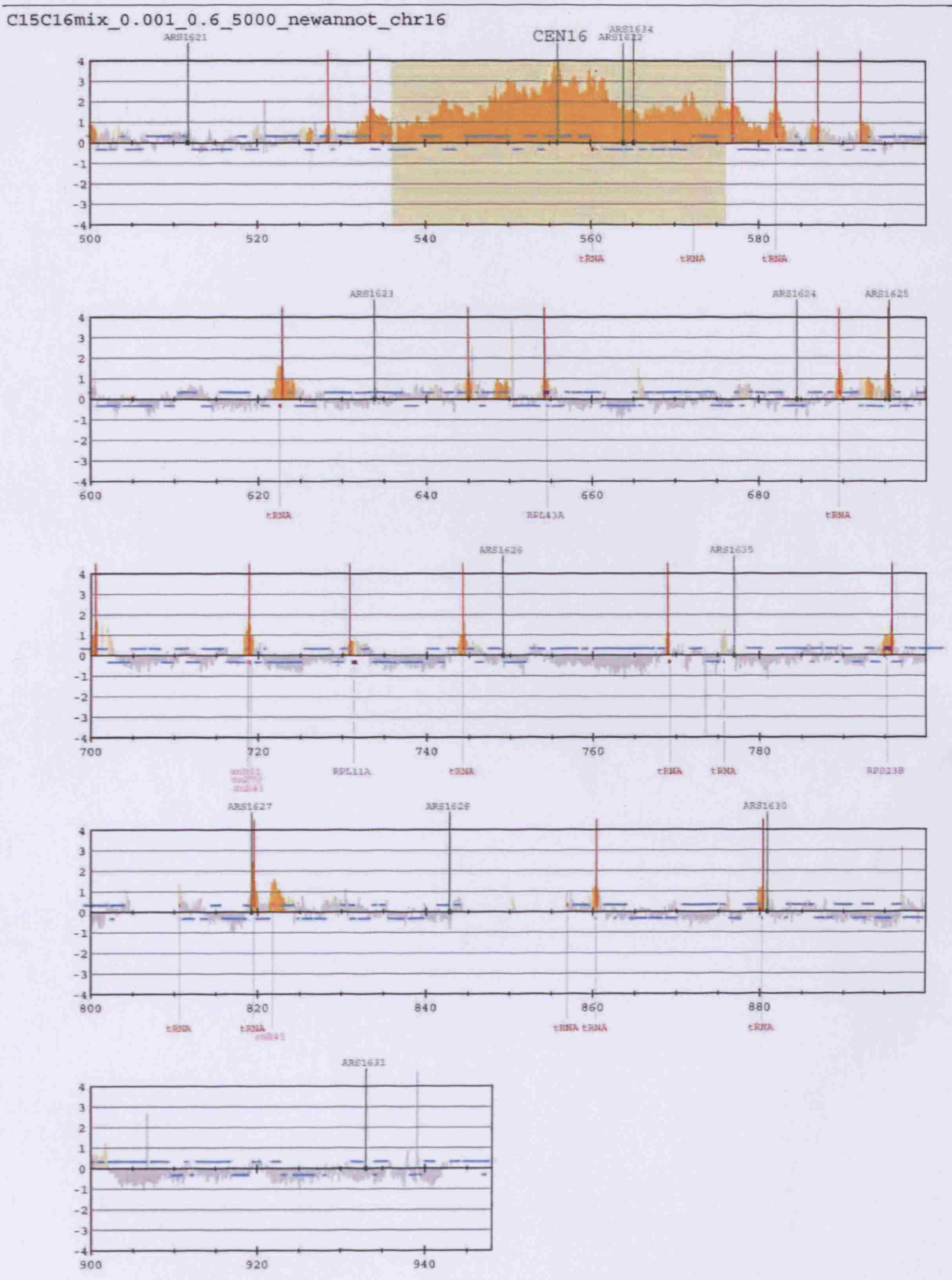
C15C16mix_0.001_0.6_5000_newannot_chr16
CEN16
ARS1621
ARS1634
ARS1622
ARS1623
ARS1624
ARS1625
ARS1626
ARS1635
ARS1627
ARS1628
ARS1630
ARS1631
tRNA
RPL43A
RPL11A
RPS23B